

Chapter 6. Review of Heat Flow Data ¹

WILLIAM H. K. LEE

*Institute of Geophysics and Planetary Physics
University of California, Los Angeles*

SEIYA UYEDA ²

Department of Geophysics, Stanford University, Stanford, California

Abstract. All available heat flow data (about 2000 observations) are reviewed and analyzed. Statistical methods are used to summarize the data, and numerical techniques are developed to find their essential features. Analysis of nearby and repeated measurements suggests that regional heat flow variations $>0.2 \mu\text{cal}/\text{cm}^2 \text{ sec}$ are significant. At the 95% confidence level, the world's mean heat flow is $1.5 \pm 10\% \mu\text{cal}/\text{cm}^2 \text{ sec}$, and the average over the continents does not differ significantly from that over the oceans. Heat flow results are well correlated with major geological features. On land, the average and standard deviation of heat flow values are 0.92 ± 0.17 from Precambrian shields, 1.23 ± 0.4 from Paleozoic orogenic areas, 1.54 ± 0.38 from post-Precambrian non-orogenic areas, and 1.92 ± 0.49 from Mesozoic-Cenozoic orogenic areas. At sea, they are 0.99 ± 0.61 from trenches, 1.28 ± 0.53 from basins, and 1.82 ± 1.56 from ridges. On a large scale, a negative correlation between heat flow and gravity is found.

1. INTRODUCTION

The outflow of heat from the Earth's interior by *conduction* is, energy-wise, the most impressive terrestrial phenomenon. Its present rate of about 2×10^{20} cal/year is orders of magnitude greater than the energy dissipation of earthquakes or heat loss from volcanic eruptions. The study of terrestrial heat flow is fundamental in Earth sciences. It is the most direct observation of the thermal state of the Earth, and geothermal processes play an important role in all theories of the Earth's origin, constitution, and behavior.

Surface heat flow from the Earth's interior is the rate of heat transferred across the Earth's surface per unit area per unit time. The unit of heat flow is $\mu\text{cal}/\text{cm}^2 \text{ sec}$ and will be omitted in this chapter whenever convenient.

All heat flow data reviewed in this chapter are measurements of surface heat flow by *thermal conduction*. The neglect of thermal convection and radiation is justified for most areas of the world, since the upper crust is solid and at a rather low temperature. On land, heat flow observations from geothermal areas are ignored

in the data analysis, because convection and radiation may play an important role (see chapter 8 by Elder, in this volume). At sea, this rejection of data is not possible because the nature of oceanic geothermal areas is poorly known.

Heat flow by conduction, \mathbf{q} , in a solid is found *experimentally* to be proportional to the temperature gradient ∇T :

$$\mathbf{q} = -K \cdot \nabla T \quad (1a)$$

where K is called the 'thermal conductivity.' In general, the thermal conductivity is a second-rank tensor quantity, but it is a constant for a *homogeneous* and *isotropic* solid. The *surface* heat flow by *conduction*, q , is therefore the product of thermal conductivity and vertical temperature gradient:

$$q = K(\partial T/\partial z) \quad (1b)$$

where the flow is vertically outward.

To determine surface heat flow by conduction at a location, we measure (1) temperatures through some finite interval of depth and (2) conductivities of the same interval either in situ or in a laboratory on an appropriate number of samples. Techniques for heat flow measurements on land and at sea have been reviewed in chapters 3 and 4 by Beck and Langseth, respectively.

To obtain meaningful values of heat flow from the Earth's interior, measurements of undis-

¹ Publication 409, Institute of Geophysics and Planetary Physics, University of California, Los Angeles.

² On leave from Geophysical Institute, University of Tokyo, Tokyo, Japan.

turbed temperatures and representative thermal conductivities are essential. These requirements are difficult to meet in practice, and consequently reliable heat flow values are obtained only through laborious efforts. Modern measurements on land were first made in 1939 by E. C. Bullard and A. E. Benfield, and at sea in 1952 by E. C. Bullard, R. Revelle, and A. E. Maxwell. More than 90% of all existing heat flow measurements were published only after 1960 by R. P. Von Herzen, M. G. Langseth, and many others. Recently *Lee* [1963] has summarized the data up to early 1963. Statistical analyses of data have also been attempted by *Lee* [1963] and *Lee and MacDonald* [1963].

In this chapter we will briefly review and analyze all available heat flow data. Local details are often omitted because abundant literature on heat flow is available (more than 100 papers and theses). Statistical methods are used to summarize the data, and numerical techniques are developed to find their essential features. The chapter closes with a brief summary of the most important results of the investigation. An up-to-date listing of heat flow data with extensive references is given in the appendix. The next chapter, by MacDonald, in this volume, in which geophysical deductions from heat flow observations are presented, is a continuation of the present one.

2. HEAT FLOW DATA

As of the end of 1964, about 2000 individual heat flow observations were available (approximately 50% of them published, 30% in press, and 20% unpublished). Excluding unpublished values, preliminary results, very crude estimates, and observations published prior to 1939, over 1300 of the available data have been catalogued by us. Almost all plottings and computations in this chapter have been based entirely on these catalogued data. They are listed as 1162 entries in the Appendix, after values from closely-spaced stations (usually less than 10 km apart) have been averaged.

In the computations, locally anomalous or questionable values have also been discarded, so that only 1043 values were analyzed. In a few cases, some values from the unpublished data were also used, bringing the total number of analyzed data to 1150 values. Criteria for select-

ing data for the analysis will be discussed later at the beginning of sections 3 and 4.

2.1 *Geographical Distribution of Heat Flow Observations*

It is obvious (see Figure 1) that the geographical distribution of heat flow data is very uneven. There are many more oceanic heat flow values than continental ones: 89% versus 11%. Since the oceans occupy some 71% of the Earth's surface, we have about 3 times more data per unit area at sea than on land. Although observations are fairly well distributed over the oceans, measurements tend to be concentrated over anomalous regions, such as the East Pacific Rise. The large gaps are in the massive continental and high latitude regions; there are no measurements in South America, Antarctica, and most of Asia and Africa. The sites of heat flow stations at sea can be randomly chosen along the ship tracks. However, existing measurements have usually been made where the ocean bottom is relatively flat to ensure penetration of the probe. The land stations are mostly in pre-existing oil wells and mines which may not be representative of the continents in general. Locations of heat flow stations are therefore selective, and consequently data analysis is extremely difficult.

2.2 *Application of Statistics in Summarizing Data*

Statistical methods deal with the presentation, analysis, and interpretation of numerical data. A useful statistical manual is *Crow et al.* [1960], which defines the terms we used.

Histogram, modes, mean, and standard deviation are most useful for summarizing a set of numerical data $\{x_1, x_2, \dots, x_n\}$. A histogram gives a visual picture of all the data of $\{x\}$, and the modes (because there is often more than one peak in the histogram) give the most likely occurring intervals of x . By using Tchebyshev's inequality [*Alexander*, 1961, p. 64] with the mean (\bar{x}) and standard deviation (s), we can easily specify the *center* and *dispersion* of $\{x\}$: at least $(1 - 1/k^2) \times 100\%$ of the data fall within the interval $(\bar{x} \pm ks)$ for any value of k and for *any* distribution of x . In the text, the mean and standard deviation is given in the form

$$\bar{x} \pm s \text{ s.d.} \quad (2a)$$

where s.d. indicates that the value s preceding it is the standard deviation of x_i , $i = 1, \dots, n$, from the sample mean \bar{x} .

In the following sections, a histogram and a few statistics of each set of data will be presented in summarizing numerical values. Although *weighted statistics* can be introduced, every value of $\{x\}$ is usually considered to be of equal importance, because a weighting factor is hard to assign. Most plottings and all computations are programmed on an IBM 7094 computer in Fortran language.

The set of data $\{x_1, x_2, \dots, x_n\}$ is usually a *sample* drawn from a *population* $\{x_1, x_2, \dots, x_m\}$, where $m \gg n$. We are obviously interested in estimating the population characteristics from the sample. If the sample is chosen in such a way that every individual in the population has an equal chance of being chosen, then the sample is called a *random sample* and statistical methods are applicable. In particular, if the population is also *normally distributed*, then at $100(1 - p)\%$ confidence level, the population mean is

$$\bar{X} = \bar{x} \pm t(p,f)s/\sqrt{n} \quad (2b)$$

where $t(p,f)$ is the student t deviate from $f = n - 1$ degrees of freedom, the probability of exceeding which is p ; and s/\sqrt{n} is the standard error.

Suppose we wish to determine the mean heat flow for a region A defined by

$$\bar{q} = \int_A q da / \int_A da \quad (2c)$$

from a sample of heat flow observations $\{x_1, x_2, \dots, x_n\}$. If it is a random sample, then we can generally claim that at 95% confidence level

$$\bar{q} = \bar{x} \pm 2s/\sqrt{n} \quad (2d)$$

by using (2b). Normality is, of course, assumed for the population, but it is not critical because deviation from normality will not greatly invalidate (2d); n is preferably greater than 20, but $t \approx 2$, unless n is less than 5.

Because heat flow stations are selective and heat flow values are not exact (due to measurement errors), there are *additional* error terms in equation 2d. Cochran [1953, pp. 7-10] has considered the effect of a bias in the sampling

procedure. Assuming normality, he found that the effect of bias on the accuracy of an estimate is negligible if the bias (B) is less than one-tenth of the standard deviation of the estimate (σ); and at $B = \sigma$, the total probability of error is 0.17, about 3 times the value of 0.05 given in equation 2d. Unfortunately, the amount of bias cannot be properly estimated from the existing heat flow data. A statistically designed heat flow survey over a given region will be useful in estimating the bias and should be made in the future. Furthermore, measurement errors (discussed in the next section) may be even more serious than the sampling bias. For these reasons, we cannot assign confidence limits of heat flow means by equation 2d. Although standard error is usually computed for each set of data and tabulated together with other statistics, one must be cautious in interpreting its significance.

2.3 Reliability of Heat Flow Data

In general, *instrumental* errors of heat flow measurements seldom exceed $\pm 10\%$. Most observers are careful in testing their equipment, but have little control over effects of the environment. Instruments employed for measurements on land differ widely. Therefore it is difficult to give a comprehensive review of instrumental errors in land observations. Instrumental errors for measurements at sea have been reviewed by *Von Herzen and Langseth* [1965]. They conclude that the error of individual heat flow measurements at sea varies with the geothermal gradient, the sediments covering the bottom, and the techniques used. When the geothermal gradient is average (6×10^{-4} °C/cm) and the bottom sediment is uniform with depth, the error is no more than 10% for a good station. Otherwise, errors up to 20% are possible.

To ascertain the significance of a heat flow value, measurement errors (due to instrumentation and local effects) must be known. Such errors can be estimated if repeated measurements have been made under the same conditions. Unfortunately repeated observations were very seldom made at the same heat flow station. However, a general estimate of the measurement errors can be obtained by analyzing repeated and closely spaced observations.

Table 1 summarizes the statistics of $\{x_i - y_i\}$,

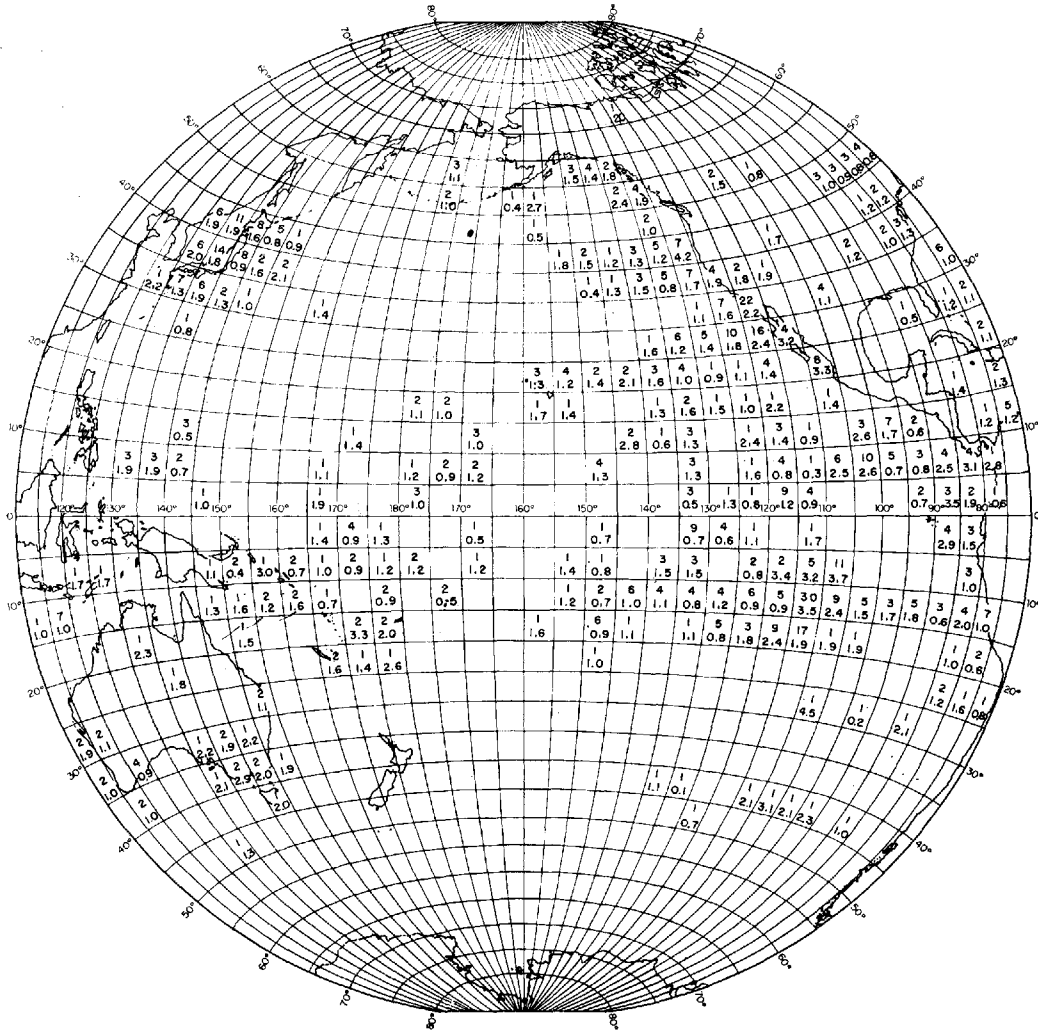


Fig. 1a. Number and arithmetic mean of analyzed heat flow data in 5° by 5° grid.

$i = 1, 2, \dots, n$, for pairs of heat flow stations that are less than 10 km apart and have heat flow values of x_i and y_i . At sea, pairs of such stations are almost indistinguishable in position, and thus they may be considered as pairs of repeated observations. On land, if heat flow variations within 10 km are due to some geological effects (e.g. volcanism), these stations have been excluded from the analysis. It is therefore not surprising that $\{x - y\}$ is less scattered on land than at sea (see Figure 2). Because land measurements have not usually been repeated by different research groups, some additional systematic errors may be present, and thus $\{x - y\}$ on land may actually be more

scattered than is shown. For simplicity, we will consider the case at sea as applicable to both land and sea and will estimate the measurement errors as follows.

If V_x and V_y are the variances due to measurement errors for $\{x\}$ and $\{y\}$ respectively, then the variance of $\{x - y\}$ is

$$V_{x-y} = V_x + V_y \quad (2e)$$

Let us assume that the measurement errors are essentially the same for x and y , so that $V_x = V_y$. Then

$$\sigma_x = \pm (1/\sqrt{2}) \sigma_{x-y} \quad (2f)$$

where σ 's denote standard deviations.

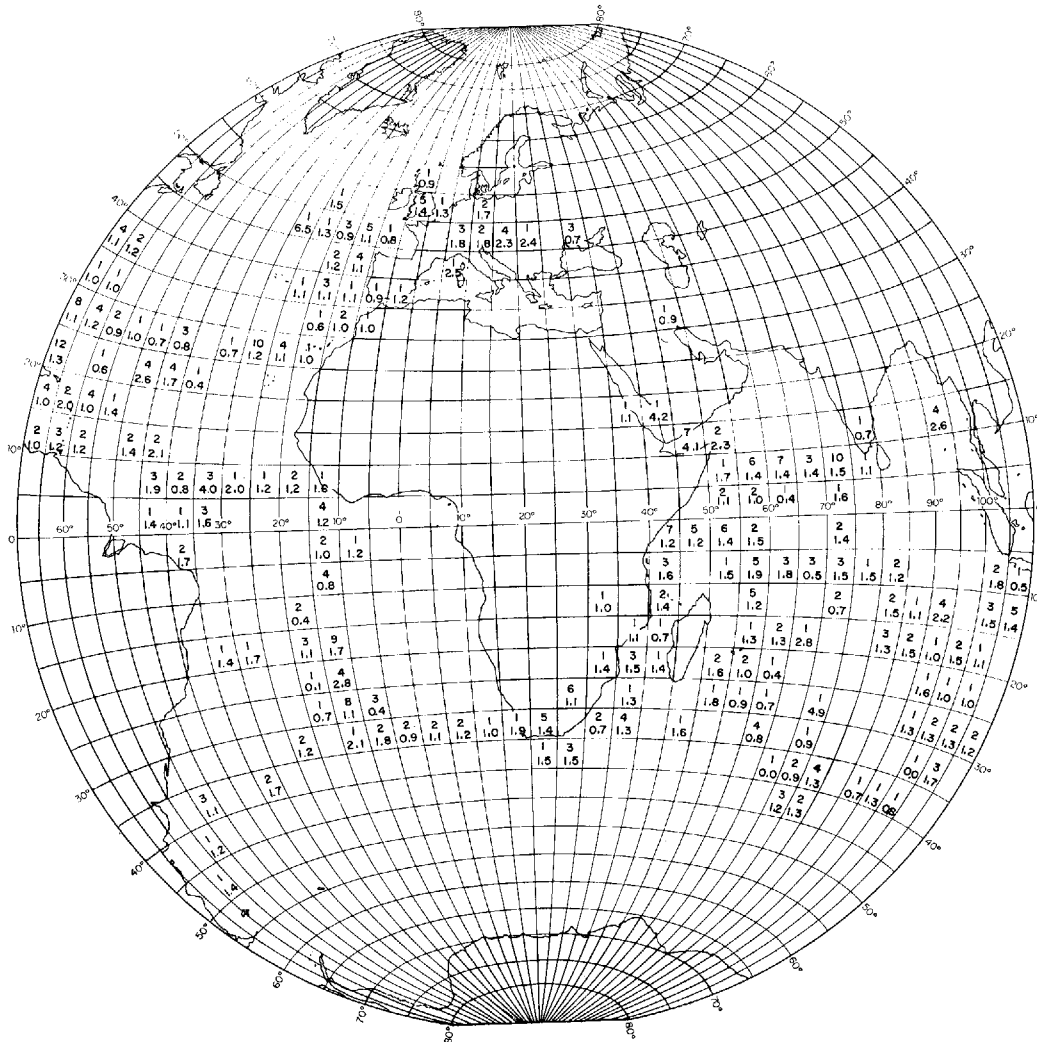


Fig. 1b. Number and arithmetic mean of analyzed heat flow data in 5° by 5° grid.

From Table 2

$$\sigma_x = \pm (1/\sqrt{2}) 0.47 = \pm 0.33 \quad (2g)$$

and hence

$$\sigma_{\bar{x}} = \sigma_x/\sqrt{n} = \pm 0.33/\sqrt{n} \quad (2h)$$

In other words, because of measurement errors the mean heat flow value for a region determined from n observations can be in error by $\pm 0.66/\sqrt{n}$ at a 95% confidence level (assuming normality). For $n = 10$, this error is about 0.2 $\mu\text{cal}/\text{cm}^2 \text{ sec}$. Therefore, it is reasonable to assume that regional heat flow variations $> 0.2 \mu\text{cal}/\text{cm}^2 \text{ sec}$ are significant. Here regional heat flow variations refer to differences in re-

gional mean heat flow values, each of which is determined from a sufficient number (> 10) of observations.

As remarked in section 2.2, we cannot simply apply equation 2d because of biased sampling and measurement errors. The standard error calculated from a biased sample of measured values may have already included some of the measurement errors and biased sampling errors. However, we have no sure way of knowing from the existing heat flow data. For this reason, we seldom consider the variations of heat flow means in terms of their computed standard errors.

TABLE 1. Statistics of $\{x_i - y_i\}$ for Pairs of Heat Flow Stations Less Than 10 km Apart with Heat Flow Values x_i and y_i in $\mu\text{cal}/\text{cm}^2 \text{ sec}$

	Number of Pairs	Arithmetic Mean	Standard Deviation	Standard Error
Land	74	-0.01	0.15	0.02
Ocean	49	0.04	0.47	0.07

3. REVIEW OF HEAT FLOW DATA ON LAND

Measuring heat flow on land is rather difficult. Temperature disturbances which affect the heat flow include effects of drilling the hole, variations of surface temperature, past climatic changes, uplift and erosion, topographic and conductivity irregularities, water circulation, and volcanic activity. Knowledge of the local geology is needed to determine some of these disturbances, and, to avoid most of them, it is essential that holes for measurements be deep (>300 meters) and preferably through hard rocks. These disturbances, of which water circulation is the most troublesome, vary from location to location and may require corrections of magnitude comparable to the actual heat flow value. When corrections are large, the data are considered to be unreliable in this chapter. When corrections are small, uncorrected values are adopted, unless the corrected values are favored by the original investigators.

Determining a representative conductivity in the laboratory presents even greater problems because of the difficulty in selecting and preparing adequate samples. Furthermore, conductivity may vary tens of per cent from rock to rock or even from sample to sample of an apparently uniform rock. Techniques of measuring conductivity in situ are in a state of development, and the accuracy of the results obtained from them is still uncertain.

Techniques of heat flow measurement have been reviewed in chapter 3, by Beck, in this volume, and mathematical treatments for various corrections have been given in chapter 2 by Jaeger. The quality of heat flow data on land varies from crude estimates to elaborate determinations. The data have been classified into categories A, B, and C. Category A data are derived from 'good' stations, where temperature and conductivity were well measured and disturbances were minor. Category B stations are

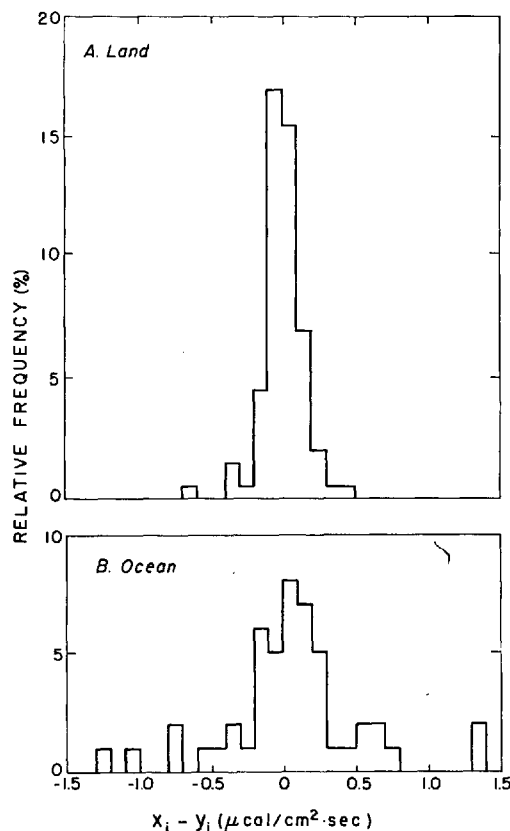


Fig. 2. Histograms of $\{x_i - y_i\}$ for pairs of heat flow stations less than 10 km apart with heat flow values x_i and y_i : (a) for land data and (b) for oceanic data.

'fair' ones because conductivity may have been measured from rock samples nearby, and/or some disturbances may have affected the results. Category C data are questionable; they may have been considered to be unreliable by original investigators, may lack conductivity measurements, and/or disturbances may have greatly affected the results. All category C data have been rejected from the analysis.

We wish to emphasize, however, that this classification of data is rather subjective, and some data have been classified as lower in quality because of lack of information.

Heat flow data on land are reviewed geographically according to continents. For each region, the literature is briefly reviewed and the data are summarized and discussed with respect to the major features of the continents. Heat flow values are plotted in maps with generalized geology and topography and are alphabetically

TABLE 2. Heat Flow Values in Africa

MD, maximum depth in meters; *N*, conductivity samples; *q*, heat flow; *q**, corrected heat flow; *DC*, data class

Data No.	Station	Type	<i>MD</i>	<i>N</i>	<i>q</i>	<i>q*</i>	<i>DC</i>	Remarks	Reference
Nyasaland									
0018	Lake Nyasa	Lake			~1		<i>B</i>	About 20 measurements using oceanic techniques; disturbances suspected for some measurements	Von Herzen, 1964b
South Africa									
Cape of Good Hope									
0011	Bothadale	Borehole	1457	85	1.28	1.34	<i>A</i>	In southern limit of Karroo system; heat flow increases with depth; climatic correction applied	Gough, 1963
0004	Dubbeldevlei	Borehole	1496	4	1.52		<i>A</i>	From 'old granite' section (lower 670 m) only	Bullard, 1939
0012	Kalkkop	Borehole	300	24	1.21	1.31	<i>A</i>	See Bothadale; hole too shallow to indicate heat flow increase with depth	Gough, 1963
0010	Koegelfontein	Borehole	851	59	1.45	1.57	<i>A</i>	See Bothadale	Gough, 1963
0009	Sambokkraal	Borehole	1760	102	1.39	1.44	<i>A</i>	See Bothadale	Gough, 1963
Orange Free State									
0001	Jacoba-Doornhoutrivier				0.96		<i>A</i>	Average value of 0001A and 0001B; in South African Shield	Bullard, 1939
	A. Jacoba	Borehole	2230	14	0.95		<i>A</i>	Sections were mainly lavas	
	B. Doornhoutrivier	Borehole	1830		0.97		<i>B</i>	Conductivities from Jacoba (5 km away) were used; sections were mainly lavas	
0008	Kestell	Borehole	1402	22	1.29		<i>A</i>	Borehole through bands of sandstone, dolerite, and shale; outside the shield	Carte, 1954
Transvaal									
0002	Gerhardminnebron-Doornkloof				1.24		<i>A</i>	Average value of 0002A and 0002C; in South African Shield	Bullard, 1939
	A. Gerhardminnebron	Borehole	3022	31	1.28		<i>A</i>	Temperature data in dolomite section (upper 1270 m) were discarded because of water circulation; lower sections consisted mainly of quartzite	
	B. Driefontein	Borehole through dolomite	587		0.75		<i>C</i>	Conductivities from Gerhardminnebron were used; heat flow value was discarded by author because of water circulation	
	C. Doornkloof	Borehole	1915		1.20		<i>B</i>	Conductivities from Gerhardminnebron were used; temperature data in dolomite section (upper 1237 m) were discarded because of water circulation	
0005	HB 15	Borehole	1996	32	1.05		<i>A</i>	Temperature data in dolomite section (upper 600 m) were discarded because of water circulation; lower sections were Precambrian lava and quartzite	Carte, 1954
0007	Messina	Borehole	395	13	1.37		<i>A</i>	Borehole in Northern Transvaal through narrow bands of granite, dyke and quartzite; isolated from other heat flow stations; in low-lying area outside the South African plateau	Carte, 1954
0003	Reef-Nigel	Borehole	1430		1.03		<i>B</i>	Conductivities from Jacoba and Gerhardminnebron, about 130 km west, were used; in South African Shield	Bullard, 1939
0006	Roodeport	Borehole	1762	15	0.86		<i>A</i>	Heat flow varied with depth: 0.80 at 400 m, 0.92 at 1380 m	Carte, 1954

tabulated according to geographical location. Numerical data arranged according to the published papers are given in the appendix.

3.1 Africa

Reliable heat flow measurements were first made in South Africa and in Great Britain. The classic study by Bullard [1939] in South Africa

has been extended by Carte [1954] and Gough [1963]. Except for attempts to measure heat flow in Lake Nyasa using oceanic techniques (R. P. Von Herzen, private communication), the rest of the African continent remains unexplored. Heat flow values are more numerous in South Africa than in most areas of comparable size; those from South Africa are summarized in Table 2 and in Figure 3.

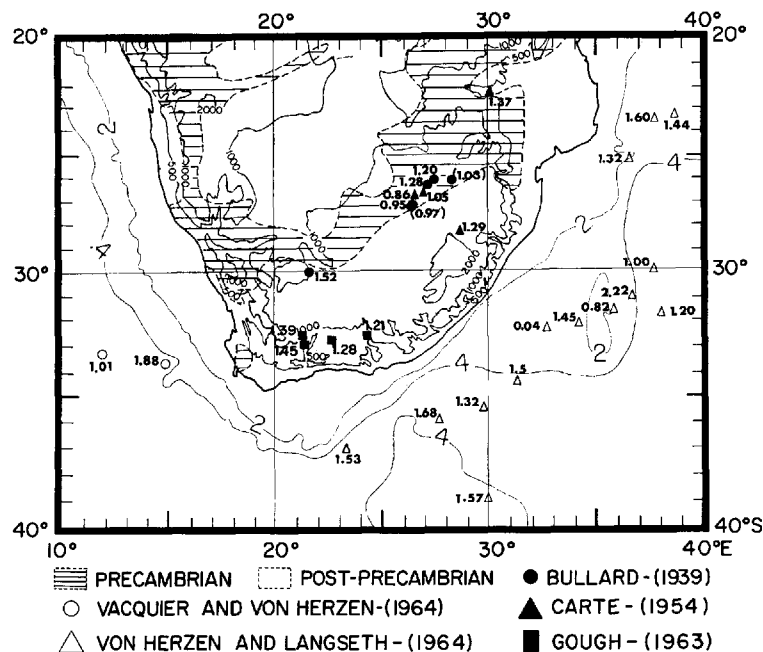


Fig. 3. Heat flow values in South Africa. Topographic contours in meters and bathymetric contours in kilometers. Values in parentheses are fair data (category B).

General geology. Geological formations in South Africa extend from Archaozoic to Recent. The oldest rocks include granite, gneiss, and ancient metamorphosed sediments. These are succeeded by the later Precambrian systems (Witwatersrand, Ventersdorp, Transvaal), which have been locally disturbed by Earth movements and by igneous intrusions. Among the systems overlying the Precambrian, the Paleozoic Cape system is strongly folded, forming an orogenic belt in the south. Overlying the Cape system, the Paleozoic-Mesozoic Karroo system consists of about 7500 meters of sediments, mostly sandstones and shales, injected with much dolerite. Except locally, the Karroo beds have not been disturbed by folding and are almost horizontal, forming more than half the surface of South Africa. Post-Karroo formations cover comparatively small coastal areas and synclinal valleys in the Cape folded area.

South African Shield. Six of Bullard's [1939] stations were holes drilled relatively close to one another for searching gold-bearing reefs of the Witwatersrand system. They all gave low heat flow values (0.75 to 1.28 $\mu\text{cal}/\text{cm}^2 \text{ sec}$), as did two nearby stations of Carte [1954], which have values of 1.05 and 0.86 (see Figure 3).

Both authors discarded results in the dolomite sections because of water circulation in the fissures. The average of the remaining 5 values is 1.03 ± 0.13 s.d. (s.d. is standard deviation from the mean).

South African non-shield areas. Bullard [1939] observed a heat flow of 1.52 at Dubbeldevlei bore, which is about 800 km southwest of his shield stations and is drilled through Karroo sandstones and shales and 'old granite.' Outside the shield, Carte [1954] obtained values of 1.37 and 1.29. Gough [1963] measured heat flow from four exploratory boreholes (in search of oil, but no oil was found) in the Southern Karroo system, obtaining values ranging from 1.21 to 1.45 (1.31 to 1.57 when corrected for climatic change). The average of 7 uncorrected heat flow values lying outside the shield is 1.36 ± 0.10 s.d., which is slightly higher (by 0.3 $\mu\text{cal}/\text{cm}^2 \text{ sec}$) than the average in the shield.

Carte [1954, p. 671, Table 5] also reported additional heat flow results from other boreholes in Transvaal and Orange Free State. Since the temperature measurements are of low precision, the heat flow values are much less reliable than those reviewed above. Further-

more, the lack of information about these results has prevented us from cataloging them in Table 2 and in the appendix.

Bullard [1939] considers that variation of his heat flow values is due both to thermal refraction caused by nonuniform thermal conductivity near the surface and to nonuniform heat generation in the crust. *Carte* [1954] states that both his and Bullard's measurements show little heat flow variation in South Africa. *Gough* [1963] concludes provisionally that the heat flow is appreciably higher in the Southern Karroo than in the shield. Since seismic and gravity studies do not indicate any abnormal crustal thickness in the Southern Karroo region, Gough suggests that attention should be paid to the mantle in seeking an explanation.

R. P. Von Herzen (private communication) measured the heat flow on Lake Nyasa utilizing oceanic techniques. His results show rather large variations in the lake, probably due to rapid local sedimentation or thermal instability of bottom water. Oceanic heat flow values around South Africa [*Vacquier and Von Herzen*, 1964; *Von Herzen and Langseth*, 1965] generally agree with land values in non-shield areas, as shown in Figure 3.

3.2 Americas

In North and South America, heat flow measurements have been carried out only in Canada, Puerto Rico, and the United States. Heat flow observations in the United States were initiated by F. Birch in the 1940's, and almost all the measurements were made by Birch and his associates. A. D. Misener and his associates began heat flow measurements in Canada in the early 1950's. At present, extensive programs of measuring heat flow are underway in many areas of the United States and Canada, but most of the results are not yet available.

The results of heat flow observations in North America are summarized in Table 3 and plotted in Figure 4. We shall briefly outline the general geology of North America and then review the heat flow observations in various general geological provinces.

General geology. In the north-central part of North America is the *Canadian Shield*, which is made up of ancient Precambrian rocks, mostly granites and gneisses, but including various

kinds of old folded sediments and lavas. This shield has been worn down into a low rolling surface which passes southward and southwestward beneath post-Precambrian sedimentary rocks of the Interior Lowlands. Around the Canadian Shield and Interior Lowlands are various mountain systems which have been formed at different times since the Precambrian. To the southeast is the Paleozoic Appalachian system, extending from Newfoundland to Alabama. To the west is the post-Paleozoic Cordilleran system, extending the entire length of the continent along the Pacific Ocean. Far to the north, there are systems of folded mountains along the oceanward sides of the Arctic Islands and Greenland. Lastly, to the south is the coastal plain of the Gulf of Mexico, where a great thickness of dominantly Tertiary sedimentary rocks marks the edge of the continent.

The Canadian Shield. Heat flow measurements have been made in the Canadian Shield by *Misener et al.* [1951] and *Leith* [1952] in the mining regions of Ontario and Quebec; by *Birch* [1954a] in mines and boreholes in Calumet, Michigan; by *Beck* [1962] in a copper mine near Flin Flon, Manitoba; by *Beck and Logis* [1963] in a drill hole at Brent Crater, Ontario; and by *Roy* [1963] in boreholes at Delaware and White Pine, Michigan (see Figure 4). These observations are summarized in Table 3A and in the appendix.

Heat flow values in the Canadian Shield are fairly uniform: 0.69 to 1.07 $\mu\text{cal}/\text{cm}^2 \text{ sec}$, 50% of the values falling within 0.9 ± 0.1 . The average of 10 values in the shield is 0.88 ± 0.13 s.d., in good agreement with results from shield areas elsewhere.

The Interior Lowlands. Heat flow measurements have been made in the Interior Lowlands by *Herrin and Clark* [1956] in oil wells of West Texas and eastern New Mexico; by *Garland and Lennox* [1962] in oil wells at Redwater and Leduc, Alberta; and by *Roy* [1963] in mining exploration holes at Boss and Bourbon, Missouri. Heat flow estimates have also been made by *Birch and Clark* [1945] for an oil well in the West Texas Permian Basin and by *Birch* [1950] in Syracuse, Kansas (see Figure 4). These observations are summarized in Table 3B and in the appendix.

Heat flow values in the Interior Lowlands are slightly higher than those in the Canadian

TABLE 3. Heat Flow Values in North America

MD, maximum depth in meters; *N*, conductivity samples; *q*, heat flow; *q**, corrected heat flow; *DC*, data class

Data No.	Station	Type	<i>MD</i>	<i>N</i>	<i>q</i>	<i>q*</i>	<i>DC</i>	Remarks	Reference
A. THE CANADIAN SHIELD									
Canada									
Manitoba									
0059	Flin Flon	Copper mine	412	?	0.7- 0.9		<i>B</i>	Water flows suspected for lowering observed heat flow in upper section; number of rock samples for conductivity not specified	<i>Beck</i> , 1962
Ontario									
0060	Brent Crater	Borehole	400	8	0.75		<i>A</i>	In a Cambrian crater; temperature measured in three consecutive years; conductivities measured in situ	<i>Beck and Logis</i> , 1963
0048	Kirkland Lake	3 mines	2200	40	1.00		<i>A</i>	Samples mostly syenite porphyry; in Superior Province	<i>Misener et al.</i> , 1951
0050	Larder Lake	Mine	1000	6	0.88		<i>A</i>	Samples mostly carbonate; in Superior Province	<i>Misener et al.</i> , 1951; <i>Leith</i> , 1952
0045	Sudbury	Mine	1500	6	1.01		<i>A</i>	Samples mostly norite; in Superior Province	<i>Misener et al.</i> , 1951
0051	Timmis	2 mines	1500	10	0.73		<i>A</i>	Samples mostly rhyolite; in Superior Province	<i>Misener et al.</i> , 1951
Quebec									
0047	Calumet Island	Mine	400	4	1.32		<i>C</i>	Large probable error was assigned by authors; in Grenville Province	<i>Misener et al.</i> , 1951
0049	Malartic	Gold mine	450	9	0.69		<i>A</i>	Samples mostly diorite and schist; in Superior Province	<i>Misener et al.</i> , 1951
United States									
Michigan									
0028	Calumet	Mine and borehole	2490	90	0.9	0.93	<i>A</i>	In Keweenaw peninsula; topographic correction applied; no definite thermal effect related to past climatic change was found	<i>Birch</i> , 1954a
0036	Delaware	Borehole	270	65	0.85	0.95	<i>A</i>	Near end of Keweenaw peninsula; topographic correction and refraction by heterogeneous conductivity were taken into account; 40 km east of Calumet	<i>Roy</i> , 1963
0037	White Pine	3 nearby boreholes	1000 650 600	156	1.01	1.07	<i>A</i>	Topographic correction applied to temperature gradient; water saturation applied to samples for conductivity measurement; 120 km west of Calumet	<i>Roy</i> , 1963
B. THE INTERIOR LOWLANDS									
Canada									
Alberta									
0056	Leduc	Nonproductive oil well	900		1.6		<i>B</i>	Estimated conductivity from Redwater (80 km SW)	<i>Garland and Lennox</i> , 1962
0057	Redwater	Oil well	900	44	1.46		<i>A</i>	Rock samples (shales and sandstones) for conductivity from nearby wells	<i>Garland and Lennox</i> , 1962
United States									
Kansas									
0024	Syracuse	Oil well			1.4- 1.7		<i>C</i>	Estimated conductivity	<i>Birch</i> , 1950
Missouri									
0034	Boss	Borehole through Cambrian and Precambrian rocks	550	102	1.29		<i>A</i>	Cambrian sections were discarded because of no core and water movement; Precambrian sections consisted of rhyolite (upper half) and andesite (lower half); rhyolite section was taken to be representative of the region because andesite was considered to be a dike	<i>Roy</i> , 1963
0035	Bourbon	Borehole	600	28	1.22		<i>A</i>	160 km north of Boss; geology is similar except the Precambrian is about 250 m deeper	<i>Roy</i> , 1963

TABLE 3. Heat Flow Values in North America (continued)

MD, maximum depth in meters; *N*, conductivity samples; *g*, heat flow; *g**, corrected heat flow; *DC*, data class

Data No.	Station	Type	<i>MD</i>	<i>N</i>	<i>g</i>	<i>g*</i>	<i>DC</i>	Remarks	Reference
<i>B. THE INTERIOR LOWLANDS (continued)</i>									
New Mexico									
0021	Eddy County	5 oil wells			1.1		<i>B</i>	Reliable temperature gradient from 3 of 5 oil wells; only temperature data in salt section were used; conductivity of rock salt was estimated	<i>Herrin and Clark, 1956</i>
0022	Lea County	Oil well			1.2		<i>C</i>	Estimated conductivity of rock salt was used; temperature gradient was considered not reliable by authors	<i>Herrin and Clark, 1956</i>
Texas									
0016	Big Lake No. 1-B	Oil well	2523	4	2.0		<i>C</i>	In West Texas Permian Basin; conductivities were measured on samples from nearby wells; see text	<i>Birch and Clark, 1945</i>
0020	Midland County	Oil well			1.2		<i>C</i>	Estimated conductivity of rock salt was used; temperature gradient was considered not reliable by authors	<i>Herrin and Clark, 1956</i>
0017	Reeves County	Oil well			1.1		<i>B</i>	Estimated conductivity of rock salt was used	<i>Herrin and Clark, 1956</i>
0018	Regan County	12 oil wells			1.1		<i>B</i>	Reliable temperature gradient from 6 of 12 oil wells; estimated conductivity of rock salt was used	<i>Herrin and Clark, 1956</i>
0019	Upton County	Oil well			1.1		<i>B</i>	Estimated conductivity of rock salt was used	<i>Herrin and Clark, 1956</i>
<i>C. THE APPALACHIAN SYSTEM</i>									
Canada									
Ontario									
0044	Toronto	Oil well	300	6	1.03		<i>A</i>	Limestone samples; in foreland of Appalachians	<i>Misener et al., 1951</i>
Quebec									
0055	Loupan-Cartier	2 boreholes through alternating sandstone and shale	250	?	0.82		<i>A</i>	Temperature measured by probe-contained oscillator transmitting temperature-dependent frequency signal; number of samples for conductivity measurement not specified	<i>Saull et al., 1962</i>
0053	Montreal	Borehole	340	?	0.74		<i>A</i>	See Loupan-Cartier; borehole through sandstone, dolomite, and conglomerate	<i>Saull et al., 1962</i>
0054	Ste. Rosalie	Borehole	450	?	0.81		<i>A</i>	See Loupan-Cartier; borehole through beds dipping steeply and having slaty cleavage	<i>Saull et al., 1962</i>
0046	Thetford	Mine	300	8	1.05		<i>A</i>	In metamorphosed zone of Appalachians; samples mostly serpentinized peridotite	<i>Misener et al., 1951</i>
United States									
District of Columbia									
0033	Washington	3 closely spaced boreholes	1058 875 843	35	1.12		<i>A</i>	Borehole through quartz-mica schist in metamorphosed zone of Appalachians	<i>Diment and Werre, 1964</i>
Georgia									
0025	Georgia	2 shallow wells			~1		<i>C</i>	Estimated conductivity; Birch estimated heat flow to be 1.4; later Diment and associates re-estimated heat flow from corrected temperature gradient given by Spicer [1942]	<i>Birch, 1950; Diment and Robertson, 1963; Diment and Werre, 1964</i>
	A. Griffin		213		0.97		<i>C</i>		
	B. LaGrange		188		1.02		<i>C</i>		
Pennsylvania									
0029	Butler County	Oil well in Devonian shales	1500		1.2		<i>B</i>	Conductivity estimated; in Foreland of Appalachians	<i>Joyner, 1960</i>
0030	Potter County	2 oil wells in Devonian shales	1500		1.4		<i>B</i>	Conductivity estimated; in Valley and Range Province of Appalachians	<i>Joyner, 1960</i>
South Carolina									
1134	Aiken	6 boreholes	600		1.0		<i>A</i>	Rock types are schists and gneisses	<i>Diment et al., 1965a</i>

TABLE 3. Heat Flow Values in North America (continued)

MD, maximum depth in meters; *N*, conductivity samples; *q*, heat flow; *q**, corrected heat flow; *DC*, data class

Data No.	Station	Type	<i>MD</i>	<i>N</i>	<i>q</i>	<i>q*</i>	<i>DC</i>	Remarks	Reference
C. THE APPALACHIAN SYSTEM (continued)									
Tennessee									
0032	Oak Ridge	Borehole	880	146	0.73		A	Borehole drilled in Valley and Ridge Province of Appalachians, close to the axis of regional gravity low; samples are mostly limestones and shales	<i>Diment and Robertson, 1963</i>
Virginia									
1133	Alberta	Borehole through granite	312	21	1.1- 1.4		A	In metamorphic zone of Appalachians; rock samples from two large pieces of the core and two samples of gneiss from nearby quarry; difficulty in obtaining representative conductivity value; heat flow value 1.4 is preferred by authors	<i>Diment et al., 1965b</i>
West Virginia									
0031	Doddridge, Marin, and Harrison Counties	3 oil wells	2200		1.2		B	Estimated conductivity from well sample log; in Valley and Range Province of Appalachians	<i>Joyner, 1960</i>
D. THE CORDILLERAN SYSTEM									
Canada									
Northwest Territories									
0058	Norman Wells	Nonproductive oil well	410	17	2.14	2.00	A	In permafrost region; rock samples (shales and limestones) for conductivity from nearby wells; heat flow value corrected for the effect of river nearby	<i>Garland and Lennox, 1962</i>
United States									
Arizona									
0027	Sau Manuel	11 churn drill wells	305	3	~1.2		C	Samples not from the same holes; inflections in temperature-depth relations were interpreted as due to past climatic changes and oxidation of sulfides; heat flow was determined from the least disturbed sections	<i>Lovering, 1948</i>
California									
0015	Bakersfield	Nonproductive oil well	2640	32	1.29		A	About 20 km NE from San Andreas Fault; rocks penetrated were all shale	<i>Benfield, 1947</i>
0042	Barstow	2 boreholes	730 360	250	2.1		A	SW portion of Basin and Range Province; fault zone at about 450 m deep caused small disturbance in gradient	<i>Roy, 1963</i>
0014	Grass Valley	Several mines		29		0.69	B	Temperature measured at 21 levels in several mines and corrected for topographic effect; Spicer estimated the heat flow to be 0.57 to 0.81 using estimated conductivity and uncorrected gradient	<i>Clark, 1957; Spicer, 1941</i>
Colorado									
0023	Colorado Springs (Red Creek)	Borehole	850		1.0- 1.4 1.2- 1.6		C	Estimated conductivity was used; small water flow existed in the well	<i>Birch, 1947a, 1950</i>
0026	Front Range (Adams Tunnel)	Tunnel	1200	123		1.7	A	Tunnel 20 km long under Rocky Mountains at a mean altitude of 2500 m; topographic corrections were applied	<i>Birch, 1947b 1950</i>
Nevada									
0041	Yerington	3 boreholes in and near a magnetite deposit	500 290 280	31	2.36		A	Rock types are mainly metamorphosed limestones, garnetites, and felsites of Triassic age, with later igneous intrusives	<i>Roy, 1963</i>

TABLE 3. Heat Flow Values in North America (continued)

MD, maximum depth in meters; *N*, conductivity samples; *q*, heat flow; *q**, corrected heat flow; *DC*, data class

Data No.	Station	Type	<i>MD</i>	<i>N</i>	<i>q</i>	<i>q*</i>	<i>DC</i>	Remarks	Reference
<i>D. THE CORDILLERAN SYSTEM (continued)</i>									
Utah									
0040	Eureka	Borehole into latite of Middle Eocene age	250	21		3.51	<i>C</i>	Terrain correction was applied; questionable significance because of local heat sources: hot springs activity and possibly oxidizing sulfides	<i>Roy</i> , 1963
0089	Government Canyon	Borehole into latite of Middle Eocene age	330	5		1.9	<i>A</i>	9 km SW of Eureka; Basin and Ridge Province; terrain correction was applied	<i>Roy</i> , 1963
1185	Salt Valley	5 boreholes		167	1.2		<i>B</i>	Average of 5 values; conductivity measured on samples not from the same holes	<i>Spicer</i> , 1964
A.	Reeder		900		1.32		<i>B</i>	In graben area of the Salt Valley anticline	
B.	Crescent		600		1.30		<i>B</i>		
C.	Brendell		450		1.33		<i>B</i>		
D.	Balsley		900		1.10		<i>B</i>	In southern area of Salt Valley anticline	
E.	Hyde		1700		1.01		<i>B</i>	To the east and off the Salt Valley anticline	
Washington									
0038	Metaline	4 boreholes	700 650 360 400	29		2.31	<i>A</i>	In Northern Rocky Mountain Province; topographic corrections applied; complex local geology	<i>Roy</i> , 1963
<i>E. OTHER AREAS</i>									
Canada									
Northwest Territories									
0052	Resolute Bay	Borehole	200	15	2.9	1.25	<i>C</i>	In permafrost region; value corrected by Lachenbruch for the effect of ocean nearby	<i>Misener</i> , 1955, <i>Lachenbruch</i> , 1957
Puerto Rico									
0043	Mayaguez	Borehole	305	18		0.6	<i>A</i>	Drill hole into ultrabasic body (serpentine); local terrain and climatic corrections applied	<i>Diment and Weaver</i> , 1964

Shield. The average of 8 values is 1.25 ± 0.18 s.d. This result is consistent with the fact that there are no significant geological differences between these two regions, except a thin cover of Paleozoic and later sediments in the Interior Lowlands. The study of *Herrin and Clark* [1956] covered a fair size area (10^5 km²), and they obtained remarkably uniform heat flow values of 1.1 ± 0.1 μ cal/cm² sec. They remark that the value (2.0) at Big Lake, Texas, estimated by *Birch and Clark* [1945] is probably too large.

The Appalachian system. In the Appalachian area, heat flow has been estimated at Griffin and LaGrange, Georgia, by *Birch* [1947a, 1950], and in Pennsylvania and West Virginia by *Joyner* [1960]; measured in Toronto, Ontario, and Thetford, Quebec, by *Misener et al.* [1951]; in the St. Lawrence lowland by *Saull et al.* [1962]; at Oak Ridge, Tennessee, by *Diment and Robertson* [1963]; near Washington, D.C., by *Diment*

and *Werre* [1964]; near Alberta, Virginia, by *Diment et al.* [1965b]; and near Aiken, South Carolina, by *Diment et al.* [1965a] (see Figure 4). These observations are summarized in Table 3C and in the appendix.

Heat flow values in the Appalachian system show small variations (0.73 to 1.4 μ cal/cm² sec) despite great diversity in rock type and geological history. The average of 12 values is 1.04 ± 0.23 s.d., which is slightly higher than that of the Canadian Shield, but the difference is not significant. Why the average heat flow value from the Appalachian region is similar to that from the Canadian Shield and the Interior Lowland is not quite apparent, especially when there is a marked difference in geology between these regions.

The Cordilleran system. In the Cordilleran system, heat flow measurements have been made by *Spicer* [1941] and *Clark* [1957] at Grass Valley, California; by *Benfield* [1947] near

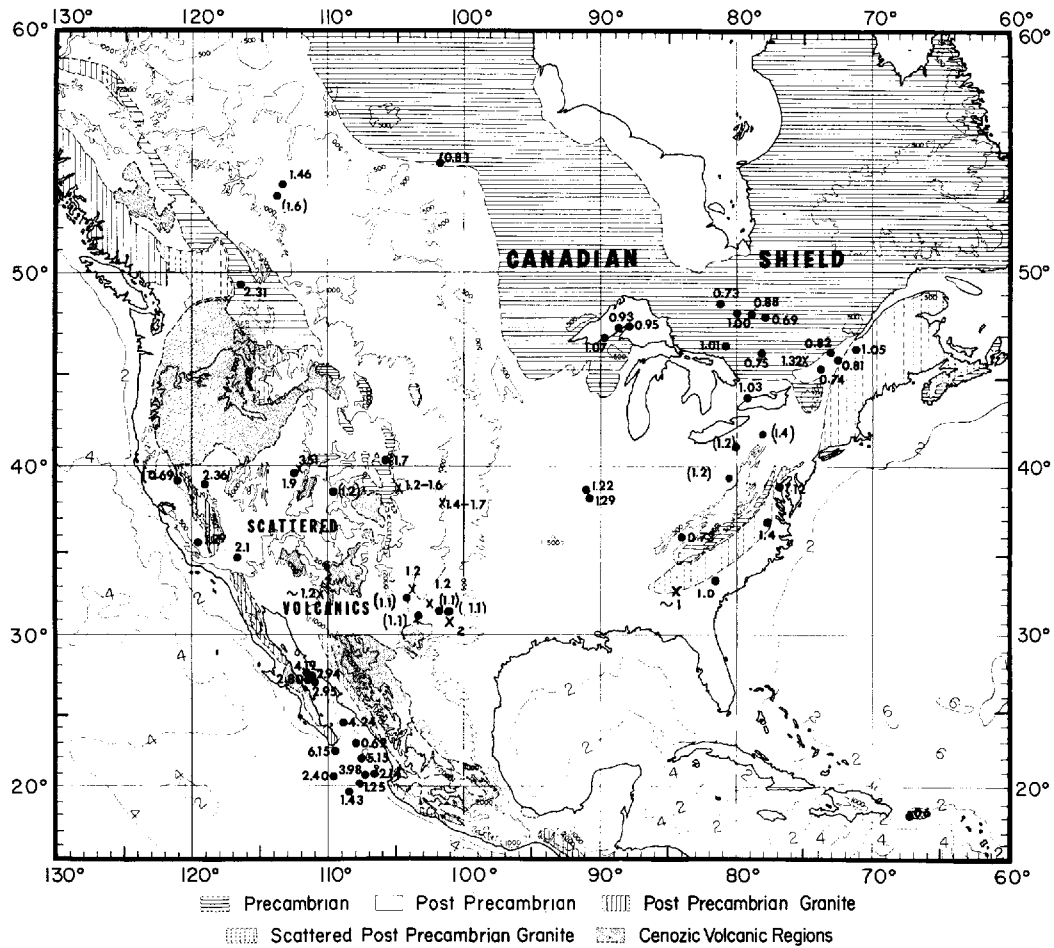


Fig. 4. Heat flow values in North America. Topographic contours in meters and bathymetric contours in kilometers. X is rejected station (category C), and values in parentheses are fair data (category B).

Bakersfield, California; by *Lovering* [1948] in San Manuel, Arizona; by *Birch* [1947a] near Colorado Springs, Colorado; by *Birch* [1947b, 1950] at Front Range, Colorado; by *Garland and Lennox* [1962] at Norman Well, N.W.T.; by *Roy* [1963] at Government Canyon and Eureka, Utah; Yerington, Nevada; Barstow, California; and Metaline, Washington; and finally by *Spicer* [1964] at Salt Valley anticline, Utah (see Figure 4). These observations are summarized in Table 3D and in the appendix. Very recently, T. S. Lovering (private communication) has measured the heat flow in the East Tintic district, Utah. He found an area of about 20 km² where the heat flow is anomalous and ranges from 3 to 7 $\mu\text{cal}/\text{cm}^2$ sec; farther

west, however, where the heat flow is normal, it amounts to from 1.7 to 2.2 $\mu\text{cal}/\text{cm}^2$ sec.

Heat flow varies greatly in the Cordillera (0.69 to 2.36 $\mu\text{cal}/\text{cm}^2$ sec, discarding the value 3.51 at Eureka, Utah, as not representative). Values are generally lower in the west and in the east. *Menard* [1960] suggests that the region of high heat flow along the crest of the East Pacific Rise may continue through the Gulf of California into western North America (see Figures 22 and 23). Indeed, heat flow values are high (≥ 2 $\mu\text{cal}/\text{cm}^2$ sec) in the Basin and Range Province. Furthermore, widespread hot spring activities, higher electrical conductivity [*Schmucker*, 1964], and lower seismic velocity in the Basin and Range Province also seem to

favor higher subsurface temperature and consequently higher heat flow. We need more observations, however, to define the extent of the high heat flow region in the Cordillera. The average of 9 values in the Cordillera is 1.73 ± 0.53 s.d., which is considerably greater than averages from other North American areas.

Other areas. Misener [1955] reports a heat flow of $2.9 \mu\text{cal}/\text{cm}^2 \text{ sec}$ at Resolute Bay, Cornwallis Island, Northwest Territories, Canada. However, Lachenbruch [1957] argues that heat flow from such permafrost areas is affected by the unfrozen ocean nearby and suggests a corrected value of 1.25. The value obtained by Diment and Weaver [1964] at Mayaguez, Puerto Rico, will be discussed in section 4.1. These two measurements are summarized in Table 3E and in the appendix.

3.3 Asia

Asia occupies 30% of the world's land area, but has only a few heat flow measurements. Extensive heat flow studies have been carried out in Japan, which occupies only 0.9% of Asia's area and geologically is not characteristic of the Asian continent. Elsewhere in Asia, one preliminary determination in India and 18 measurements in Iran have been made. Asian observations are summarized in Table 4 and also in the appendix.

India. Verma and Rao [1965] report a preliminary heat flow determination in South India at the Kolar Gold Fields. The heat flow obtained is $0.66 \mu\text{cal}/\text{cm}^2 \text{ sec}$, which agrees quite well with values in shield areas elsewhere.

Iran (Persia). Coster [1947] determined the heat flow from 18 wells in the Masjid-i-Sulaiman (Masjed Soleyman) oil field in southwest Persia. The study covers a region of about 30 km by 5 km where stratigraphy is complicated and where recent tectonic movements have occurred. Representative sampling of rocks for conductivity was not available, and some temperatures were measured after oil production in some wells. The measured heat flows range from 0.53 to $1.22 \mu\text{cal}/\text{cm}^2 \text{ sec}$, with an arithmetic mean of 0.87 ± 0.04 s.e. (s.e. is standard error). A substantial part of the largest regional variation of heat flow may be accounted for by the influence of geological structure. Recent climatic changes may have

decreased the heat flow by about 30% throughout the region. Topographic irregularities, recent tectonic movement, and denudation are found to have insignificant effect on the heat flow. The average of heat flow values corrected for climatic changes is 1.18 ± 0.04 s.e.

Japan. In Japan, heat flow work was initiated in 1957 by the Earthquake Research Institute, and to date 39 land observations and 19 measurements in the surrounding seas have been published [Horai, 1959, 1963a, b, c; Uyeda and Horai, 1960, 1963a, b; Uyeda et al., 1958, 1962; Yasui et al., 1963]. Recently, Horai and Uyeda [1963], Uyeda and Horai [1964], and Horai [1964] have presented comprehensive summaries of these results. Of the land stations, 26 are in various metal mines, 4 in coal mines, 2 in oil fields, 3 in natural gas fields, and 4 at other types of sites. Oceanic measurements are conducted under a joint project with the Japan Meteorological Agency and the Hydrographic Department.

All the Japanese results, including 38 new sea measurements [Yasui and Watanabe, 1965], are plotted in Figure 5 (Table 4 contains published land data only, and the appendix contains all data). Because of complex geology, the accuracy at some individual stations may be lower than the average. However, the distribution of heat flow in Figure 5 shows a definite pattern: (I) the basin of the Japan Sea has moderately high heat flow (1.84 ± 0.6 s.d.); (II) regions of high heat flow (2.01 ± 0.38 s.d.) also exist in the Japan Sea side of the island arc and branch off toward the Izu-Marianne arc, through the central part of Honshu; (III) most regions of Mesozoic metamorphism have normal heat flow (1.58 ± 0.47 s.d.); (IV) the Pacific side of northeastern Japan has low heat flow (0.70 ± 0.15 s.d.); and (V) the Kurile and Japan Trenches also have low heat flow (0.99 ± 0.38 s.d.). These heat flow zones are labeled in Figure 6 with the relevant geological and topographical features of the Japanese area. The land region of high heat flow coincides precisely with the region of Cenozoic volcanic activity. The zone of low heat flow is just inside the Japan and Kurile Trenches, and in the zones of Mesozoic metamorphism the heat flow is rather normal. Assuming a steady state, Uyeda and Horai [1964] calculate the temperature distribution in the crust under various

TABLE 4. Heat Flow Values in Asia

MD, maximum depth in meters; *N*, conductivity samples; *q*, heat flow; *q**, corrected heat flow; *DC*, data class

Data No.	Station	Type	<i>MD</i>	<i>N</i>	<i>q</i>	<i>q*</i>	<i>DC</i>	Remarks	Reference
India									
0083	Kolar	Mine	2000	10	0.66		A	Temperature measured at 12 levels in gold field in South India; samples are hornblende schists	Verma and Rao, 1965
Iran (Persia)									
0084	Masjid-i-Sulaiman	18 oil wells	1200	35	0.87	1.18	A	Climatic correction applied; other corrections are small; local variations explained by geological structure, using an electrical analog model	Coster, 1947
Japan									
Central Japan									
0101	Ashio	Cu mine	800	2	2.23		B	Temperature measured at 10 levels in mine; geology is a simple rhyolite mass	Uyeda and Horai, 1964;
0103	Chichibu	Fe mine	400	3	1.34		A	2 underground drill holes (120, 180 m deep) in mine; rocks are limestones, little magnetite, and pyrite	Uyeda and Horai, 1964;
0096	Hitachi	Cu mine	550	36	0.71		A	Temperature measured at 65 localities (9 levels) in mine; rocks are mainly granites, schists, and pyrite	Uyeda and Horai, 1964;
0105	Kamioka	Pb, Zn mine	720	4	1.80		A	2 underground boreholes (400 and 200 m deep) and a level in mine; rocks are mainly gneiss, limestone, and skarn	Uyeda and Horai, 1964;
0098	Kashima	Borehole	900	3	0.76		A	Nonproductive gas well into silt	Uyeda and Horai, 1964;
0097	Katsuta	Borehole	900	3	0.91		A	Nonproductive gas well into silt	Uyeda and Horai, 1964;
0107	Kune	Cu mine	560	4	1.60		C	Temperature measured at 13 depths and an underground borehole in mine; rocks are crystalline schists	Uyeda and Horai, 1964;
0102	Kusatsu-Shirane	Borehole	250	5	10.8		C	Exploration hole in geothermal area on flank of an active volcano; andesites	Uyeda and Horai, 1964;
0109	Minenosawa	Cu mine	190	4	1.79		B	2 underground drill holes (80, 100 m deep); 80 m deep hole under drilling operation; 5 km south of Nako; crystalline schists	Uyeda and Horai, 1964;
0099	Mobara	Borehole	1900	6	0.54		A	5 gas exploration drill holes into sandstone and siltstone (470, 450, 275, 1300, 1900 m deep)	Uyeda and Horai, 1964;
0106	Nakatatsu	Zn, Pb mine	640	4	1.95		A	1 underground drill hole (180 m deep) and 2 levels in mine; rocks are skarn and porphyrite	Uyeda and Horai, 1964;
0108	Nako	Cu mine	640	7	1.44		A	Temperature measured at 6 depths in mine; 5 km SE of Kune; rocks are crystalline schists	Uyeda and Horai, 1964;
0104	Sasago	Tunnel	480	2	2.06		B	Tunnel 4647 m long through hornfels and quartz diorite; temperature-depth relation needs correction for topography	Uyeda and Horai, 1964;
0100	Tokyo	Borehole	885	3	0.74		A	Research hole at Tokyo Univ., into sand and clay	Uyeda and Horai, 1964;
Hokkaido									
0088	Akabira	Coal mine	700	4	1.07		A	2 drill holes (35, 73 m deep) and 5 points in 2 levels in coal mine; rocks are sandstones and schists	Uyeda and Horai, 1964;
0089	Ashibetsu	Borehole	500	6	1.35		A	Coal-prospecting bore into shale and sandstone	Uyeda and Horai, 1964;
0085	Haboro	Borehole	350	5	1.87		B	Coal-prospecting bore; cores for conductivity from a bore 3 km away were used; sandstones and mudstones	Uyeda and Horai, 1964;
0087	Konomai	Au, Ag mine	520	9	2.54		A	17 boreholes (3 nearly vertical, 14 horizontal) in mine; rocks are shales, tuffs, liparites, and propylites	Uyeda and Horai, 1964;
0086	Shimokawa	Cu, Fe mine	530	7	1.71		A	Temperature measured at 7 levels in mine; spilitic samples were used for conductivity	Uyeda and Horai, 1964;

TABLE 4. Heat Flow Values in Asia (continued)

MD, maximum depth in meters; *N*, conductivity samples; *q*, heat flow; *q**, corrected heat flow; *DC*, data class

Data No.	Station	Type	<i>MD</i>	<i>N</i>	<i>q</i>	<i>q*</i>	<i>DC</i>	Remarks	Reference
Hokkaido (continued)									
0090	Toyoha	Zn, Pb mine	400		5.		<i>C</i>	Mine in geothermal area; estimated conductivity	<i>Uyeda and Horai, 1964; Horai, 1964</i>
Kyushu									
0120	Izuhara	Borehole, Pb, Zn mine	480	8	2.17		<i>B</i>	3 boreholes (250, 480, 450 m deep) from ground surface and 4 shorter boreholes in mine; in Tsushima Island; rocks are sandstones, shales, and porphyry	<i>Uyeda and Horai, 1964; Horai, 1964</i>
0123	Makimine	Cu, Fe mine	845	6	1.79		<i>A</i>	Temperature measured at 40 localities at 11 depths in mine; rocks are phyllites, sandstones, and greenstones	<i>Uyeda and Horai, 1964; Horai, 1964</i>
0122	Taio	Ag, Au mine	560	11	1.05		<i>B</i>	Temperature measured at 39 localities in mine; temperatures scattered probably because of water movement; rocks are propylites	<i>Uyeda and Horai, 1964; Horai, 1964</i>
0121	Takamatsu	Coal mine	1000	8	1.92		<i>A</i>	Temperature measured at 11 levels in coal mine; rocks are sandstones and shales	<i>Uyeda and Horai, 1964; Horai, 1964</i>
Northeastern Japan									
0092	Innai	Borehole	1050	4	1.49		<i>B</i>	Gradient obtained from bottom temperature of more than 100 oil wells; water saturated silt for conductivity	<i>Uyeda and Horai, 1964; Horai, 1964</i>
0095	Kamaishi	Cu, Fe mine	530	12	0.52		<i>B</i>	Temperature measured at 4 boreholes and 9 depths in mine; temperatures found disturbed probably by water movement; rocks are limestone, skarn, slate, and intrusives	<i>Uyeda and Horai, 1964; Horai, 1964</i>
1136	Matsukawa	Borehole			15		<i>C</i>	Geothermal area	<i>Uyeda and Horai, 1964; Horai, 1964</i>
0094	Nodatamagawa	Mn mine	400	6	1.14		<i>A</i>	Temperature measured at 6 depths in mine; rocks are cherts, sandstones, and shales	<i>Uyeda and Horai, 1964; Horai, 1964</i>
0093	Osarizawa	Au, Ag mine, borehole	300	14	2.24		<i>A</i>	Temperature measured at 1 borehole from surface (300 m deep) and 11 levels in mine; rocks are tuffs, shales, and propylites	<i>Uyeda and Horai, 1964; Horai, 1964</i>
0091	Yabase	Borehole	1700	2	2.01		<i>B</i>	Gradient obtained from bottom temperatures of more than 200 oil wells in shale	<i>Uyeda and Horai, 1964; Horai, 1964</i>
Southwestern Japan									
0119	Besshi	Cu mine	1600	8	1.22		<i>A</i>	3 underground boreholes (150, 530, 705 m deep) in mine; crystalline schists	<i>Uyeda and Horai, 1964; Horai, 1964</i>
0117	Hidaka	Borehole	310	4	2.12		<i>A</i>	Hot-spring exploration borehole into sandstone; nonproductive	<i>Uyeda and Horai, 1964; Horai, 1964</i>
0110	Ikuno	Cu, Zn mine	880	6	1.38		<i>A</i>	Temperature measured at 15 depths in mine; rocks are liparite, tuffs, and andesite	<i>Uyeda and Horai, 1964; Horai, 1964</i>
0113	Isotake	Borehole	170	3	3.49		<i>C</i>	2 boreholes in Pb, Zn mine; temperature disturbed because of shallow depth of bore into gypsum, clay, and phillite	<i>Uyeda and Horai, 1964; Horai, 1964</i>
0115	Kuwayama	Borehole, Cu mine	520	6	1.00		<i>A</i>	2 boreholes (300, 450 m deep) from surface and 1 underground borehole (300 m) in mine; weakly metamorphosed Paleozoic area	<i>Uyeda and Horai, 1964; Horai, 1964</i>
0118	Kiwa	Cu mine	410	6	1.31		<i>B</i>	3 underground boreholes (100, 150, 290 m deep) in sandstones; temperature scattered	<i>Uyeda and Horai, 1964; Horai, 1964</i>
0116	Naka	Cu mine	640	2	1.79		<i>A</i>	Underground borehole 190 m deep in mine; rocks are entirely schist	<i>Uyeda and Horai, 1964; Horai, 1964</i>
0111	Nakaze	Au, Sb mine	365	9	2.21		<i>A</i>	Temperature measured at 5 depths and an underground borehole (100 m deep) in mine; rocks are andesite tuff and schists	<i>Uyeda and Horai, 1964; Horai, 1964</i>
0114	Tsumo	Cu, Zn mine	310	7	1.09		<i>A</i>	2 underground boreholes (200, 140 m deep) in mine; rocks are mainly hornfels	<i>Uyeda and Horai, 1964; Horai, 1964</i>
0112	Yanahara	Borehole	940	6	1.20		<i>A</i>	2 boreholes (200, 940 m) into slate of Fe mine	<i>Uyeda and Horai, 1964; Horai, 1964</i>

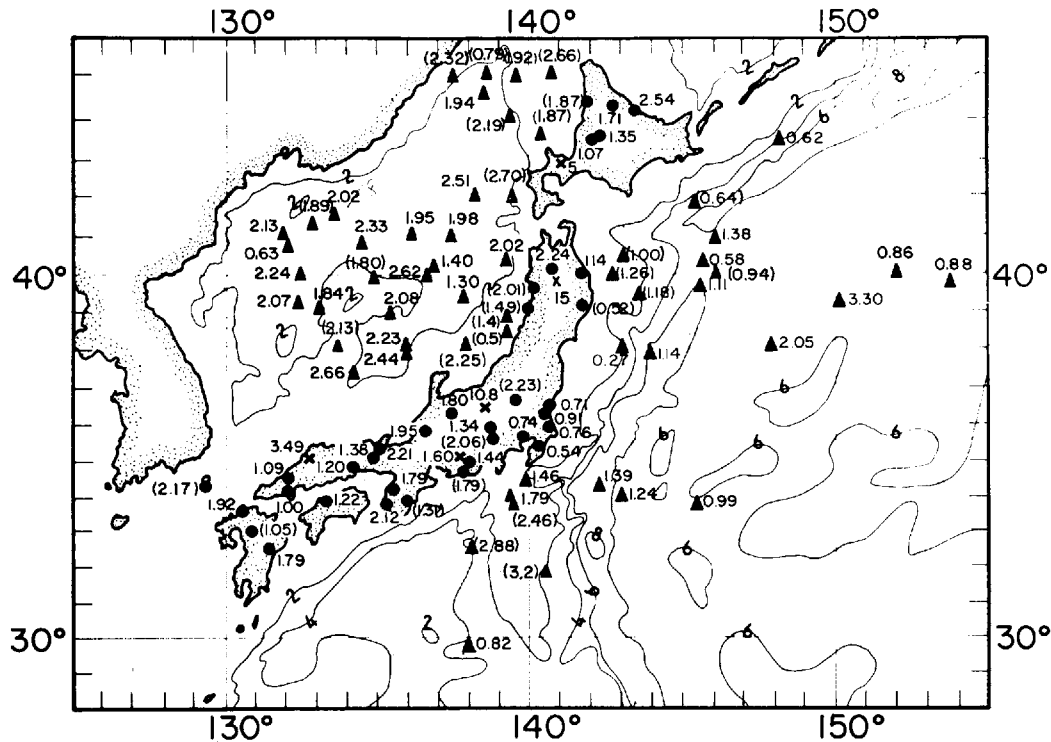


Fig. 5. Heat flow values in and around Japan. Bathymetric contours in kilometers. On land, X is rejected station (category C), and values in parentheses are fair data (category B). At sea, values in parentheses are rejected data.

zones of Japan. Although depending on the assumed radioactivity in the crust, the lateral temperature variation under Japan is shown to be very great: at the Mohorovicic discontinuity, the temperature in the Japan Sea side (high heat flow zone) may be 800°C to 1200°C , whereas it is only about 200°C in the low heat flow zone in the Pacific Ocean side.

Despite pronounced tectonism in island arc areas, the average heat flow in Japan is 1.53 ± 0.57 s.d., which is quite close to the world's average value, 1.58 ± 1.14 s.d. However, the characteristic feature of the heat flow in Japan is the areal distribution of anomalies. *McBirney* [1963] proposes that this distribution is caused by a refraction mechanism due to heterogeneous thermal conductivity. *Uyeda and Horai* [1964] consider, however, that such a pronounced refraction of heat flow is unlikely in Japan.

3.4 Australia

Heat flow measurements in Australia were initiated by J. C. Jaeger in the 1950's. Observa-

tions are relatively well distributed. They are plotted in Figure 7 and summarized in Table 5 and in the appendix. Recently, *Howard and Sass* [1964] have presented a comprehensive study of their heat flow measurements and have also summarized all previous works. Since then *Sass* [1964b] has reported additional heat flow observations in eastern Australia. Some oceanic heat flow measurements have been made near Australia by *Von Herzen and Langseth* [1965] and M. G. Langseth (private communication). These oceanic observations are also shown in Figure 7.

General geology. Australia is of low elevation, moderate relief, and without young mountains. About two-thirds of it consists of Precambrian rocks. The ancient Australian Shield in the west is usually buried under desert sands. In the east, flanking the narrow coastal plain are a series of deeply eroded ranges and table lands which have been raised in relatively recent geological time. Between the eastern highlands and the western shield is a broad depression. It is

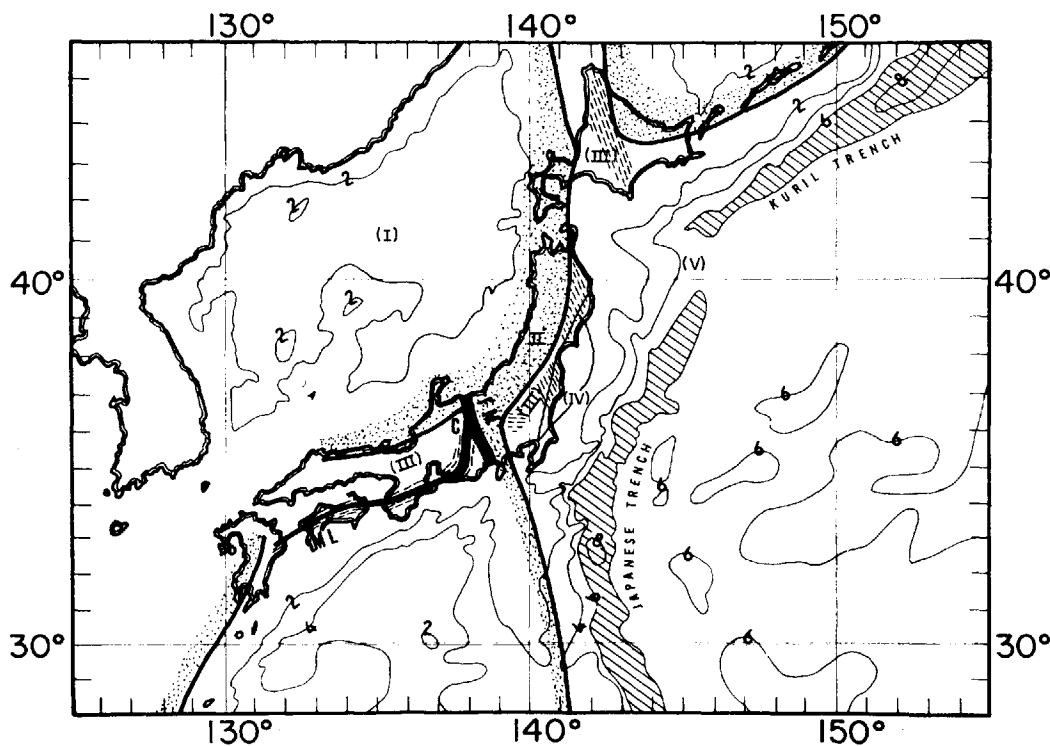


Fig. 6. Map of Japan showing major geological features. Stippled area is late Cenozoic volcanic zone. Dashed area is Mesozoic metamorphic zone. *FM* is Fossa Magna. *ML* is median tectonic line. (I) to (V) correspond to areas described in the text. Bathymetric contours in kilometers.

floored by relatively soft Mesozoic and Cenozoic sedimentary rocks overlying the Paleozoic and Precambrian formations.

Folding had almost ceased in Australia by the end of Paleozoic time, and Australia has remained relatively stable in the last 200 million years. In Miocene time, volcanic activity and lava flows were quite widespread in eastern Australia, and throughout the Cenozoic era Australia was emergent. The generalized geology and the topography of Australia are shown in Figure 7, and radioactive ages from Australian Precambrian rocks and tectonic activities are given in Figure 8.

The Australian Shield. Sass [1964a] measured the heat flow at three quite closely spaced stations in the central Archean Gold Fields province of the shield, and obtained values consistently near $1 \text{ } \mu\text{cal/cm}^2 \text{ sec}$. Later Howard and Sass [1964] not only confirmed the earlier results, but they have also measured the heat flow at four stations to the west, obtaining

similar values (see Figure 7). These observations are summarized in Table 5A and the appendix. The average of 7 values in the Australian Shield is $1.02 \pm 0.15 \text{ s.d.}$

The Australian Interior Lowlands. LeMarne and Sass [1962], Sass and LeMarne [1963], Howard and Sass [1964], and Sass [1964b] obtained 5 fairly uniform heat flow values of about $2 \text{ } \mu\text{cal/cm}^2 \text{ sec}$ in the mining areas of New South Wales and South Australia. Howard and Sass [1964] also observed 3 similar values in northern Australia. Values obtained in Rum Jungle are doubtful because of high local radioactivity and disagreement among themselves. In the eastern edge of the Great Artesian Basin that covers a large part of eastern Australia, Sass [1964b] observed two low values of about $1 \text{ } \mu\text{cal/cm}^2 \text{ sec}$ from oil wells. Whether these low values are representative of the Basin is very uncertain. Observations in the Interior Lowlands (see Figure 7) are summarized in Table 5B and in the appendix. Excluding doubt-

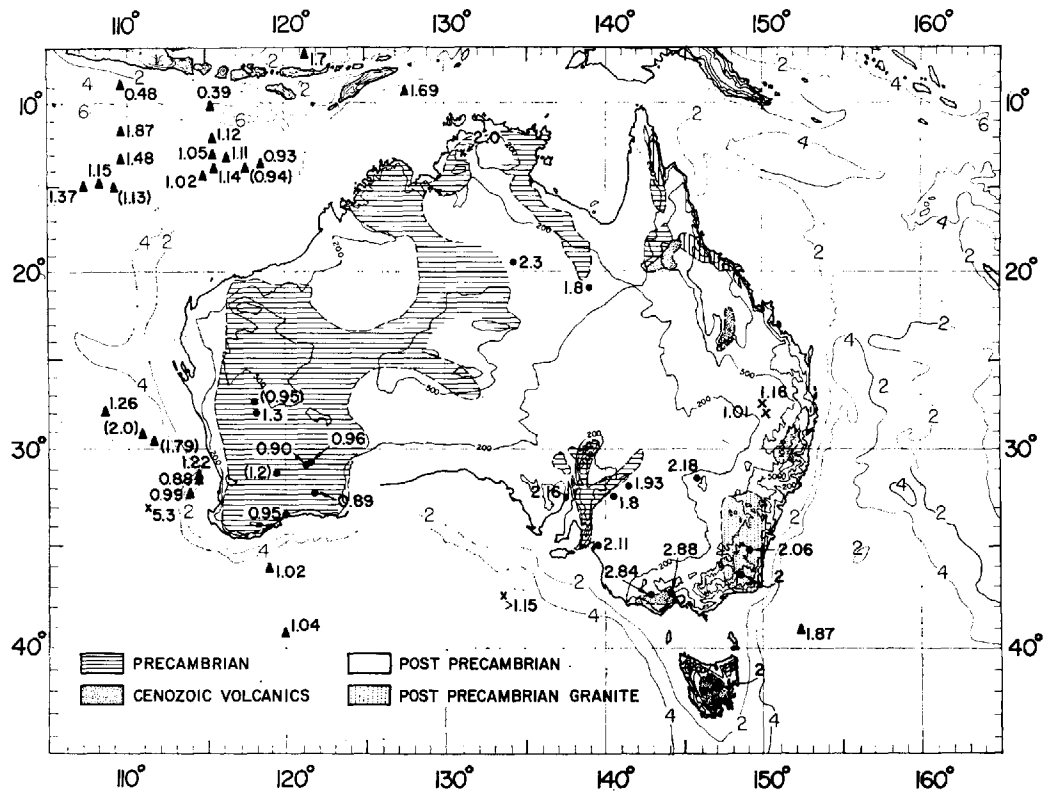


Fig. 7. Heat flow values in and around Australia. Topographic contours in meters. Bathymetric contours in kilometers. X is rejected station (category C), and values in parentheses are fair data (category B).

ful values, the average of 7 values in the Australian Interior Lowlands is 2.04 ± 0.18 s.d., which is much higher than that in the interior lowlands of other continents.

East Australian Highlands. Newstead and Beck [1953] observed quite high heat flow (2.04 to 2.54 $\mu\text{cal}/\text{cm}^2$ sec) in Tasmania, where the geology is extremely complex. Jaeger and Sass [1963] confirmed these results by applying Lees' topographic corrections and also made several new measurements. Beck [1956] observed heat flow values of about 2 $\mu\text{cal}/\text{cm}^2$ sec in the Snowy Mountains, which were confirmed later by Howard and Sass [1964]. Sass [1964b] observed a similar value in a specially drilled hole near Canberra and even higher values of about 3 $\mu\text{cal}/\text{cm}^2$ sec in mines near Stawell and Castlemaine, Victoria, which may be related to Cenozoic volcanism or oxidation of sulfides. All

these observations (see Figure 7) are summarized in Table 5C and in the appendix. The average of 5 values in the East Australian Highlands is 2.36 ± 0.38 s.d.

According to the studies reviewed above, heat flow is low (1.02 ± 0.15 s.d.) in the Western Australian Shield area and high in eastern Australia (2.16 ± 0.33 s.d.). This tendency is again confirmed by oceanic heat flow measurements along the south coast of Australia made by Scripps Institution of Oceanography and by Lamont Geological Observatory: four values of about 1.0 $\mu\text{cal}/\text{cm}^2$ sec off the southwest coast and one value of about 1.9 off the southeast coast (see Figure 7).

On the basis of these observations and some plausible assumptions about the radioactive contents and thermal conductivity of the crust, Howard and Sass [1964] estimate that the tem-

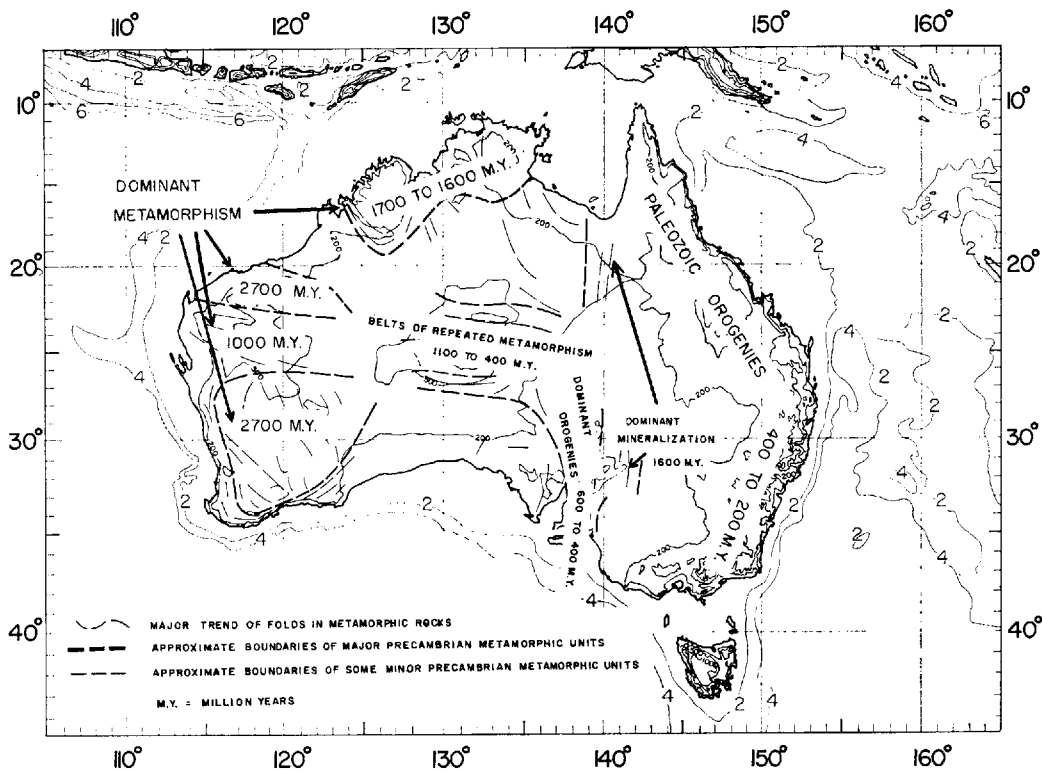


Fig. 8. Radioactive ages from Precambrian rocks and tectonic activities in Australia [after Wilson *et al.*, 1961, Figure 11].

perature difference at the Mohorovicic discontinuity in western and eastern Australia should be at least 200°C.

3.5 Europe

Despite the fact that geology and geophysics are well studied in Europe, heat flow measurements are still few in number. The present data are plotted in Figure 9 and are given in Table 6 alphabetically by nations. Numerical data are listed in the appendix. Because of the lack of data, we shall review heat flow observations by countries.

General geology. Precambrian sequences are widely distributed only in northern and eastern Europe, with a few scattered ones elsewhere. Apart from older orogenies, the building of the core of the European mainland was completed by the later Precambrian. This core, known as the Baltic-Russian Shield, includes the lowland of Sweden, Finland, Russia, and the Baltic Sea.

During the Paleozoic, the Caledonian, and Variscan orogenic episodes profoundly affected the continent. Alpine diastrophism, beginning in the late Mesozoic and continuing to the present, has culminated in folding and faulting of the Alps and their extensions with widespread volcanism, particularly in southern Europe and Asia Minor. Unlike other large continents, geological provinces in Europe are small in extent.

Great Britain. British scientists have pioneered heat flow measurements on land, obtaining some twenty values in Great Britain within an area smaller than 5° by 5°. Benfield [1939] obtained an average heat flow of about 1 $\mu\text{cal}/\text{cm}^2 \text{ sec}$ from five boreholes. Anderson [1940] recalculated some of Benfield's values and also obtained new ones. Plotting these values on a map, Anderson shows that the relatively high heat flows at Glasgow and Durham are in an area coinciding with the southeastern extension of the 'Mull Swarm,' a complex of Tertiary dykes. Since these values are uncertain (see re-

TABLE 5. Heat Flow Values in Australia

MD, maximum depth in meters; *N*, conductivity samples; *q*, heat flow; *q**, corrected heat flow; *DC*, data class

Data No.	Station	Type	<i>MD</i>	<i>N</i>	<i>q</i>	<i>q*</i>	<i>DC</i>	Remarks	Reference
A. THE AUSTRALIAN SHIELD									
Western Australia									
0073	Bullfinch	Mine	370	8	1.2		<i>B</i>	Geology is very complex; mostly dolomitized greenstones; heat flow value 1.2 may be too low because of uncertainty in obtaining a representative conductivity	Howard and Sass, 1964
0066	Coolgardie	2 boreholes 20 km apart	320 300	12	0.90		<i>A</i>	Average of 2 values (1.09 and 0.72); one hole passes through massive granite with about 30 m of greenstone at the top; another penetrates a fine-grained greenstone	Sass, 1964a; Howard and Sass, 1964
0071	Cue	2 boreholes 300 m apart	420 330	19	0.95		<i>B</i>	2 bores gave identical temperature-depth curves; gradient increased with depth; rocks are greenstone	Howard and Sass, 1964
0065	Kalgoorlie	4 boreholes	900 550 300 250	47	0.99	0.96	<i>A</i>	Bores into altered basic and ultrabasic rocks; effect of salt lake is corrected; Howard and Sass from 4 mines to depth of 1100 m and covering 5 km ² obtained heat flow value of 0.89, using conductivity by Sass	Sass, 1964a; Howard and Sass, 1964
0072	Mount Magnet	Mine	480	10	1.3		<i>A</i>	Gold mine in an area of jaspilite and altered greenstone	Howard and Sass, 1964
0067	Norseman				0.95		<i>A</i>	Average of two values	
	A. Norseman	3 boreholes	390 420 600		1.01		<i>A</i>	Conductivities were measured on samples from the deepest hole	Sass, 1964a
	B. Norseman	3 nearby boreholes	480		0.89		<i>A</i>	Bores pass through altered basic rocks with quartz-porphry dikes	Howard and Sass, 1964
0075	Ravensthorpe	Borehole	330	19	0.95		<i>A</i>	Drill hole into quartz-diorites and basic greenstones	Howard and Sass, 1964
B. THE INTERIOR LOWLANDS									
New South Wales									
0064	Broken Hill	Boreholes, mine	1200	118	1.93		<i>A</i>	18 drill holes covering 500 km ² and 32 horizontal holes in mine walls; samples are mostly quartzites and gneisses; 4 holes studied by Howard and Sass gave results in good agreement	Sass and LeMarne, 1963; Howard and Sass, 1964
0063	Cobar	2 boreholes 100 m apart	575 340	16	2.18		<i>A</i>	Bores in western edge of Tasman geosyncline through a fairly uniform slate formation with some mineralized zones	LeMarne and Sass, 1962
Northern Territory									
0068	Rum Jungle	3 boreholes	550 300 400	27	2.0 1.9 1.02		<i>C</i>	Low value (1.02) probably not representative because of measurement through narrow and vertical bodies of low conductive amphibolites; the area is known for high radioactivity	Howard and Sass, 1964
0069	Tennant Creek	Borehole, mine	300	16	2.3		<i>A</i>	4 horizontal holes in mine and 1 borehole; in a large area of Precambrian deep marine sediments containing abundant graywackes interbedded with shales, siltstones, conglomerates, and breccias	Howard and Sass, 1964
Queensland									
0076	Cabawin	Oil well	3000	19	1.16		<i>C</i>	In eastern edge of Great Artesian basin; water flow at depth suspected	Sass, 1964b
0077	Moonie	Oil well	1700		1.01		<i>C</i>	See Cabawin; conductivity estimated from Cabawin, 24 km apart	Sass, 1964b
0070	Mount Isa	Borehole	430	12	1.8		<i>A</i>	Drill hole penetrating a uniform shale formation	Howard and Sass, 1964
South Australia									
0080	Kanmantoo	2 boreholes	250 160	16	2.11		<i>A</i>	Both holes pass through andalusite-biotite schists; topographic correction applied for shorter hole; anisotropic conductivity because of schistosity	Sass, 1964b
0074	Radium Hill	7 boreholes	305	30	1.8		<i>A</i>	Holes penetrated into Precambrian paragneisses consisting mainly of micas, quartz, and feldspars	Howard and Sass, 1964
0079	Whyalla	Borehole	185	8	2.16		<i>A</i>	Drill hole into alternating iron ore and amphibolites	Sass, 1964b

TABLE 5. Heat Flow Values in Australia (continued)

MD, maximum depth in meters; *N*, conductivity samples; *q*, heat flow; *q**, corrected heat flow; *DC*, data class

Data No.	Station	Type	<i>MD</i>	<i>N</i>	<i>q</i>	<i>q*</i>	<i>DC</i>	Remarks	Reference
C. THE EAST HIGHLANDS									
A.C.T.									
0078	Canberra	Borehole	225	7	2.06		A	Specially drilled hole penetrating porphyry	<i>Sass</i> , 1964 <i>b</i>
New South Wales									
0062	Snowy Mountains	Tunnel, boreholes	>300	27		2	A	Average of about 10 values from Encumbene-Tumut tunnel area (80 × 15 km); topographic correction applied later by Howard	<i>Beck</i> , 1956, private communication; <i>Howard and Sass</i> , 1964
Tasmania									
0061	Great Lake	Borehole	314	8	2		A	Drill hole into a tholeiite sill; data from 4 other holes were included as corroborative evidence; further studies by Jaeger and Sass confirmed early results	<i>Newstead and Beck</i> , 1953; <i>Jaeger and Sass</i> , 1963
Victoria									
0082	Castlemaine	Borehole	165	5	2.88		A	Drill hole into interbedded slates and sandstones	<i>Sass</i> , 1964 <i>b</i>
0081	Stawell	Borehole	300	7	2.84		A	Drill hole into a fine-grained slate with inclusions of quartz and pyrite	<i>Sass</i> , 1964 <i>b</i>

marks in Table 6), more measurements are needed to clarify this correlation between heat flow and igneous activity.

Bullard and Niblett [1951] measured the heat flow in six boreholes in Nottinghamshire and two in north Yorkshire. Four Nottinghamshire bores give high values (~2.5) which were possibly caused by the underground water flow over an anticline. We suggest that the values (~1.6) from the two remaining Nottinghamshire bores are more representative of the regional heat flow, as further supported by two similar values obtained by *Mullins and Hinsley* [1958] in the same area. Four other values obtained by the latter authors at the Nottinghamshire-Yorkshire border are moderately high, which may also be caused by underground water movement.

Heat flow at Cambridge is estimated to be small by *Anderson* [1940]. However, *Chadwick* [1956] determined the heat flow there to be 1.28 from a specially drilled hole.

All British heat flow measurements are summarized in Table 6 and in the appendix under the subheading Great Britain. The average heat flow from 7 reliable values is 1.31 ± 0.38 s.d. It is highly desirable to establish the role of water circulation and to extend measurements in Scotland, Wales, and Ireland.

Austria and Switzerland. *Clark and Niblett* [1956] measured the heat flow at three tunnels

in the Swiss Alps: two values (Loetschberg and Simplon) were about 2 $\mu\text{cal}/\text{cm}^2$ sec, and the other (Gotthard) was 1.4. They also estimated the heat flow at tunnels in the eastern Alps (Arlberg and Tauern), but more reliable figures of similar values were obtained later by *Clark* [1961]. In such an area of folded mountains, anisotropy of thermal conductivity due to foliation presents unique problems.

Hungary, Czechoslovakia, and Italy. Intensive thermal studies have been conducted in Hungary by *Boldizsar* and associates [*Boldizsar*, 1956*a, b, c*; 1958*a, b*; 1959; 1964*a, b, c*; *Boldizsar and Gozon*, 1963; *Scheffer*, 1963]. Seven determinations, including one in Czechoslovakia, give high values of about 2.5 $\mu\text{cal}/\text{cm}^2$ sec. In addition to these heat flow values, more than 400 underground temperature measurements have been made to show that the Tertiary Hungarian Basin is characterized by high heat flow.

Within the Hungarian Basin, relatively high heat flows occur where the Paleozoic and Mesozoic bottom rocks are elevated, whereas relatively low ones occur where Tertiary sediments are thick owing to the subsidence. There is no indication of present volcanic activity even in the highest heat flow area. *Boldizsar* [1964*a, c*] considers that the Hungarian basin is an isolated geothermal high, surrounded by normal territories.

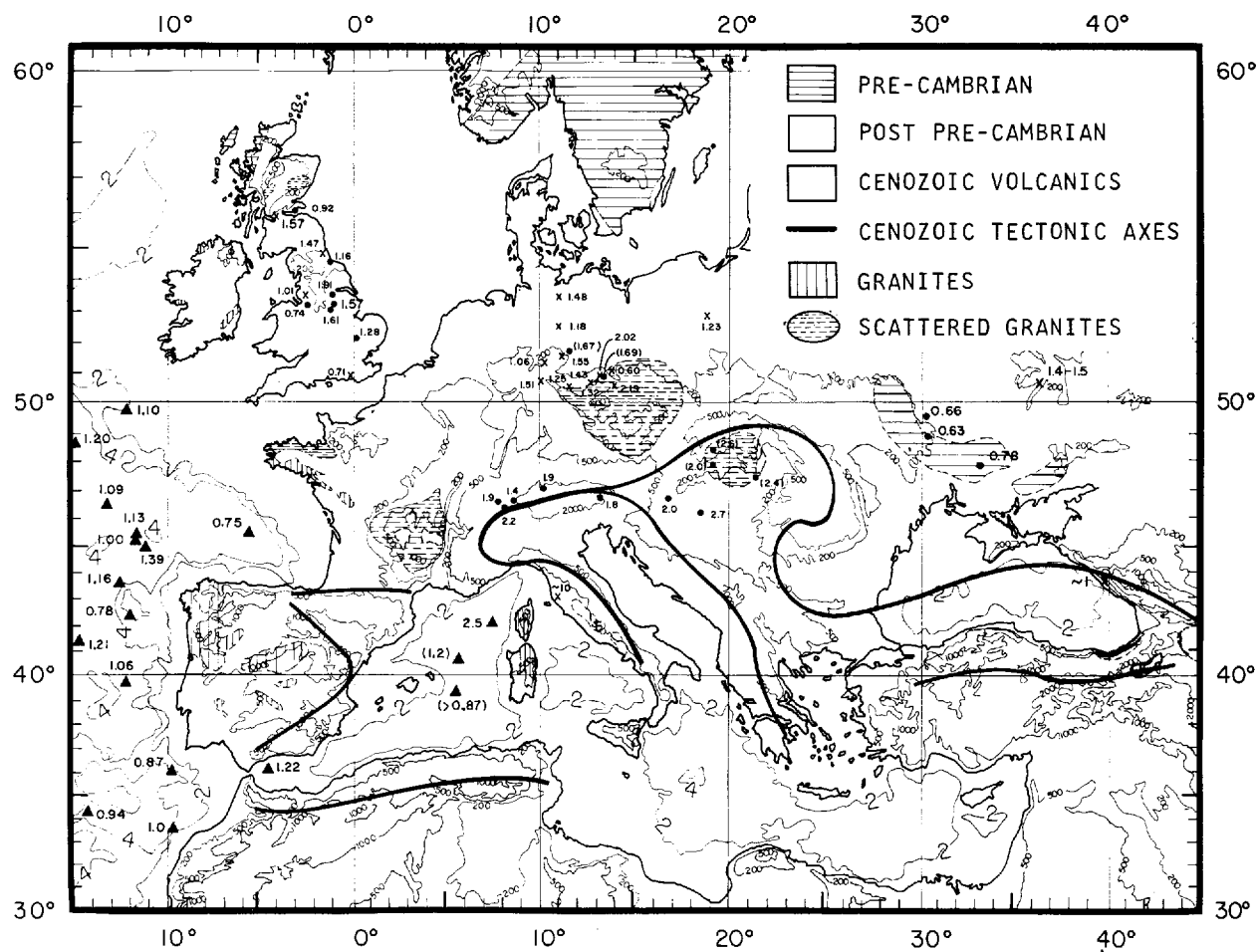


Fig. 9. Heat flow values in Europe. Topographic contours in meters. Bathymetric contours in kilometers. X is rejected station (category C), and values in parentheses are fair data (category B).

TABLE 6. Heat Flow Values in Europe

MD, maximum depth in meters; *N*, conductivity samples; *q*, heat flow; *q**, corrected heat flow; *DC*, data class

Data No.	Station	Type	<i>MD</i>	<i>N</i>	<i>q</i>	<i>q*</i>	<i>DC</i>	Remarks	Reference
Austria									
0188	Arlberg	Tunnel	680	15		1.9	A	Tunnel through gneisses and schists of the pre-Mesozoic basement beneath the Arlberg pass; topographic correction applied; difficulty in sampling for conductivities	Clark, 1961
0189	Tauern	Tunnel	1440	27		1.8	A	Tunnel through granites and granite gneisses; topographic correction applied; 220 km E of Arlberg	Clark, 1961
Great Britain									
0133	Bawtry	4 boreholes	1190 980 970 1140	26	1.91		A	Survey holes in virgin coal areas through sandstone, marls, limestones, and breccia, on Nottinghamshire-Yorkshire border	Mullins and Hinsley, 1958
0130	Cambridge	Borehole	240	>16	1.28	1.48	A	Specially drilled hole; conductivity measured at 16 levels in Paleozoic section (lower half), and external samples were used for Mesozoic section (upper half); climatic correction applied	Chadwick, 1956
0128	Durham	Underground borehole	520		1.47	1.82	C	Estimated conductivity; climatic correction applied	Anderson, 1940
0124	Dysart	2 boreholes			0.92		A	Average value of 0124B and 0124C	Anderson, 1940
	A. Balfore bore		1200		0.68	1.16	B	Conductivities from Boreland bore, 5 km away; climatic correction applied	Benfield, 1939
	B. Balfore bore				0.89	1.20	B	Recalculated value of 0124A; climatic correction applied	Anderson, 1940
	C. Boreland bore		1000	6	0.95	1.28	A	Climatic correction applied	Anderson, 1940
0126	Glasgow	2 boreholes			1.57		C	Average value of 0126C and 0126D	Anderson, 1940
	A. Blythwood bore		100		1.24	1.56	C	Estimated conductivity	Benfield, 1939
	B. South Balfary bore		160		1.53	1.85	C	Estimated conductivity	Benfield, 1939
	C. Blythwood bore				1.41	1.75	C	Recalculated value of 0126A	Anderson, 1940
	D. South Balfary bore				1.73	2.07	C	Recalculated value of 0126B	Anderson, 1940
0127	Hankham	Borehole	235	8	0.71	1.12	C	Uncertainty due to absence of lithological information	Benfield, 1939
0125	Holford	Borehole	295	6	0.74	1.43	A	2 drill holes a few hundred meters apart through marl and rock salt; climatic correction applied	Benfield, 1939
0134	Nottingham	2 boreholes	693 533		1.61		A	Geology similar to Bawtry; same conductivity data as Bawtry	Mullins and Hinsley, 1958
0131	Nottinghamshire		670	60	1.57		A	Average value of 0131E and 0131F; samples mostly sandstones, marls, limestones, and shales	Bullard and Niblett, 1951
	A. Earkring 5		600		2.73		C	} Possibly disturbed by water flow	
	B. Earkring 6		660		2.75		C		
	C. Earkring 64		610		1.97		C		
	D. Earkring 141		605		2.87		C		
	E. Kelham Hill 1		670		1.47		A		
	F. Caunton 11		650		1.67		A		
0132	Yorkshire	2 boreholes	930 900		1.16		A	Some conductivity data from 0131 were also used	Bullard and Niblett, 1951
0129	Wigan	Colliery shaft	730		1.01	1.34	C	Temperature recorded during sinking of shaft in colliery; estimated conductivity; climatic correction applied	Anderson, 1940
Czechoslovakia									
0144	Banska Stiavnica				2.6		B	Tertiary andesite and dacite area; detail to be published	Boldizsar, 1964a, b
East Germany									
0155	Altenberg	Mine	240	?	2.19		C	Reliable temperature only from one level	Schossler and Schwarzlose, 1959
0146	Bleicherode	Mine	470	?	1.06		C	Temperature measured at 2 levels (404, 470 m deep)	Schossler and Schwarzlose, 1959
0153	Brand-Erbisdorf	Mine	?	?	2.02		C	Temperature measured at 2 levels 60 m apart in depth	Schossler and Schwarzlose, 1959

TABLE 6. Heat Flow Values in Europe (continued)

MD, maximum depth in meters ; *N*, conductivity samples ; *q*, heat flow ; *q**, corrected heat flow ; *DC*, data class

Data No.	Station	Type	<i>MD</i>	<i>N</i>	<i>q</i>	<i>q*</i>	<i>DC</i>	Remarks	Reference
East Germany (continued)									
0156	Dorndorf	Mine	400	?	1.51		<i>C</i>	Temperature measured at 3 levels (largest vertical distance 55 m)	<i>Schossler and Schwarzlose, 1959</i>
0154	Freiberg	Mine	690	?	1.69		<i>B</i>	Temperature measured at 4 levels (600, 650, 530, 400 m deep)	<i>Schossler and Schwarzlose, 1959</i>
0152	Freitel	Mine		?	0.60		<i>C</i>	Temperature measured at a pair of 2 levels (75, 294 m in vertical distance)	<i>Schossler and Schwarzlose, 1959</i>
0158	Oebisfelde	Borehole	1350		0.91- 1.46		<i>C</i>	Deep hole into porphyry and quartz ; estimated conductivity	<i>Schossler and Schwarzlose, 1959</i>
0149	Pechtelsgrün	Quarry	430		1.43		<i>C</i>	Temperature measured at 2 levels (250 m in vertical distance, 350 m in horizontal distance)	<i>Schossler and Schwarzlose, 1959</i>
0157	Rehna I	Borehole	890		1.14- 1.83		<i>C</i>	Limestone section between 700 m and ~890 m was used ; estimated conductivity	<i>Schossler and Schwarzlose, 1959</i>
0150	Schmiedfeld	Mine	276	?	1.25		<i>C</i>	2 levels were used for temperature measurement in each of 2 mines 2.5 km apart (131, 176 m deep and 202, 276 m deep)	<i>Schossler and Schwarzlose, 1959</i>
0147	Stassfurt	Mine	614	?	1.67		<i>B</i>	Temperature measured at 4 levels (484, 528, 560, 614 m deep)	<i>Schossler and Schwarzlose, 1959</i>
0148	Strassberg	Quarry	280	?	1.55		<i>C</i>	Temperature measured at 2 levels (190, 280 m deep)	<i>Schossler and Schwarzlose, 1959</i>
0151	Zwickau	Mine	830	?	1.32		<i>C</i>	Temperature measured at 2 levels (730, 830 m deep)	<i>Schossler and Schwarzlose, 1959</i>
Hungary									
0142	Hajduszoboszló				2.2- 2.6		<i>B</i>	In Great Hungarian Plain of Pliocene sediments ; details to be published	<i>Boldizsar, 1964a, b</i>
0141	Nagyenyel	Oil wells			1.9- 2.0			In Western Hungary	<i>Boldizsar, 1964a, b</i>
0143	Szentendre				2.0		<i>B</i>	Edge of mid-Hungarian Mountains of Oligocene sandstone ; details to be published	<i>Boldizsar, 1964a, b</i>
0140	Zobak-Hosszúhetény-Bakonya	Mine	600		2.7		<i>A</i>	Average value of 3 stations in Mecsek Mountains ; earlier value at Zobak [<i>Boldizsar, 1956c</i>] of 3.04 was confirmed ; for other stations, detail to be published	<i>Boldizsar, 1964a, b</i>
Iceland									
1188	Iceland					4-5	<i>C</i>	Estimated conductivity	<i>Bodvarsson, 1955</i>
Italy									
0145	Larderello	9 boreholes	1400	18	6-14		<i>C</i>	In geothermal area	<i>Boldizsar, 1963</i>
Poland									
0159	Ciechocinek	Deep brine well	1300		1.23		<i>C</i>	Estimated conductivity	<i>Stenz, 1954</i>
Switzerland									
0135	Gotthard	Tunnel	1520	15	1.23	1.4	<i>A</i>	Tunnel through Swiss Alps ; topographic correction applied	<i>Clark and Niblett, 1956</i>
0137	Loetschberg	Tunnel	1530	47	1.73	1.9	<i>A</i>	See Gotthard	<i>Clark and Niblett, 1956</i>
0136	Simplon	Tunnel	2050	51	1.98	2.2	<i>A</i>	See Gotthard	<i>Clark and Niblett, 1956</i>
USSR									
0161	Belaya Tserkov	Borehole	120	10	0.63		<i>A</i>	In NW part of Ukrainian Shield ; area of present subsidence (< 2 mm/yr)	<i>Lubimova et al., 1964 ; Lubimova, 1964</i>
0160	Krivoy Rog	3 boreholes	1425 790 360	20	0.78		<i>A</i>	In SE part of Ukrainian Shield ; area of present uplift (< 10 mm/yr)	<i>Lubimova et al., 1964 ; Lubimova, 1964</i>

TABLE 6. Heat Flow Values in Europe (continued)

MD, maximum depth in meters; *N*, conductivity samples; *q*, heat flow; *q**, corrected heat flow; *DC*, data class

Data No.	Station	Type	<i>MD</i>	<i>N</i>	<i>q</i>	<i>q*</i>	<i>DC</i>	Remarks	Reference
USSR (continued)									
0164	Mazesta-Hosta	3 boreholes	2170 1350	15	~1		<i>C</i>	In Black Sea Coast of Caucasus; effect of Black Sea on gradient suspected; rocks obtained from nearby hole for sections above 950 m	<i>Lubimova et al.</i> , 1964; <i>Lubimova</i> , 1964
0162	Uman	Borehole	180	10	0.66		<i>A</i>	In NW part of Ukrainian Shield; 3 other holes (150, 140, 90 m deep) with 8 conductivities gave heat flow values 0.64, 0.63, 0.60 [<i>Lubimova</i> , 1964]	<i>Lubimova et al.</i> , 1964; <i>Lubimova</i> , 1964
0163	Yakovlevski	2 boreholes	820 380	34	1.4- 1.5		<i>C</i>	Bores into iron ore layer; 100 km south of Kursk; temperature disturbed	<i>Lubimova et al.</i> , 1964

Even more pronounced hyperthermal areas are often found in Italy, where many active volcanoes are known. *Boldizsar* [1963] reports heat flows ranging from 6 to 14 $\mu\text{cal}/\text{cm}^2$ sec in Larderello, Tuscany, where geothermal energy is utilized for large-scale power production (see chapter 9 by McNitt).

East Germany and Poland. In the western part of the German Democratic Republic, 13 heat flow determinations in two boreholes and eleven mines have been made [*Schossler and Schwarzlose*, 1959]. Near the Czechoslovakian border, the stations in the Erzgebirge Mountains show high heat flows which have been considered to be related to the relatively strong radioactivity of the granites there.

In Poland, *Stenz* [1954] estimates the heat flow to be 1.23 $\mu\text{cal}/\text{cm}^2$ sec in a deep well at Ciechocinek, which is situated on the border between the old Russian Shield and the folded central Europe.

West Germany. *Creutzburg* [1964] has made 10 heat flow measurements in West Germany and has estimated the average heat flow to be 1.6 $\mu\text{cal}/\text{cm}^2$ sec. Very high heat flow values (up to 4.6) were observed in the salt masses in the Lower Saxony area and were not thought to be representative of the regional heat flow. However, these data have not been catalogued because of lack of information concerning their measurements.

USSR. The Soviet Union covers an area of about 22 million square kilometers (15% of the world's land area), but so far has only five published heat flow stations. *Lubimova et al.* [1961, 1964] measured the heat flow for three boreholes in the Caucasus near the Black Sea. They point out that the heat flow (~ 1 $\mu\text{cal}/\text{cm}^2$

sec) may be disturbed by the cooling effect of the neighboring Black Sea and of the Mazesta's springs.

Lubimova et al. [1964] also describe in detail the heat flow measurements at four other Soviet locations: Krivoi Rog, Uman, and Belaya Tserkov in the Ukrainian Shield and Yakovlevski Iron Ore Deposit. These observations are summarized in Table 6 under USSR.

Lubimova [1964] reviews the above shield measurements and compares them with the data on recent tectonic movements. She postulates that the Krivoi Rog area, which is uplifting, has slightly higher heat flow than the subsiding Kiev area (Uman and Belaya Tserkov). However, *Diment* [1965] suggests that her heat flow values in the Kiev area are about 20% too low and that the heat flow difference between the Kiev and Krivoi Rog areas is not significant.

Miscellany. *Kraskovski* [1961], in discussing heat flow in old shields, quotes heat flow estimates of 0.8 $\mu\text{cal}/\text{cm}^2$ sec at Monche-Tundra, 0.8 at Boliden (Sweden), both in the Baltic Shield area, and 0.88 near Krivoi Rog in the Ukrainian Shield. Details, however, are not given.

Sisoev [1961] measured the heat flow in the Black Sea with reversing thermometers (see section 2.3, Chapter 4, by Langseth). Since the method is doubtful and the assumed conductivity is too high, the results (data no. 0166 in the appendix) are very uncertain.

Scheffer [1964] reviews the European heat flow data and draws a heat flow contour map. As Scheffer notes, Figure 9 seems to suggest that the heat flow is generally high in Central Europe. By comparing this map with the geoid map of Europe [*Heiskanen and Vening-Meinesz*,

1958, p. 286], he maintains that the high heat flow is associated with an elevation of the geoid.

4. REVIEW OF HEAT FLOW DATA AT SEA

In measuring heat flow, we are much more fortunate at sea. The bottom temperature in deep oceans being remarkably constant with space and time, temperature disturbances in the sediment from above are negligible, and the ocean floor sediment is quite easily penetrable by heat flow probes. An important disturbance is the effect of frictional heat generated by the penetration of the probe which has been satisfactorily eliminated by the design of the instrument or by the reduction of the data. The slow sedimentation in deep ocean (normally less than 1 cm per 1000 years) and water circulation in the sediments have negligible effects in disturbing the temperature. Moreover, the conductivity of ocean sediments varies only slightly (see Table 6.5). In early oceanic heat flow measurements, temperature gradients were measured with Bullard-type probes that penetrated a few meters into the sediment, and the conductivities were measured from cores taken at or near the site of temperature measurement. Recently Ewing-type probes have also been introduced. They are less convenient to operate, but they are more reliable because they combine coring (usually piston coring) and temperature gradient measurement into one operation and consequently offer deeper penetration and several temperature-sensing elements. Techniques of measuring heat flow through the ocean floor have been reviewed in chapter 4 by Langseth.

In considering the heat transfer through the ocean bottom, Lubimova et al. in chapter 5 of this volume conclude that to obtain representative heat flow measurements at sea other controls are desirable to determine the effects of environment. Alternatively, large numbers of observations should be made over an area to reduce the effect of random variables. Since measuring heat flow at sea is fast (a few hours per observation) and relatively inexpensive, detailed surveys of heat flow and reduction of data using statistical methods are recommended.

The quality of heat flow data at sea is far more uniform than that on land. We have rejected some oceanic data because of one or more

TABLE 6.5. Statistics of Thermal Conductivity of Oceanic Sediments

Ocean	Number of Values*	Mean	Standard Deviation	Standard Error	Mode
Atlantic	106	2.09	0.19	0.02	2.1
Indian	180	1.98	0.25	0.02	2.1
Pacific	300	1.95	0.20	0.01	2.1
All	586	1.98	0.22	0.01	2.1

* These values are usually the mean conductivities at different locations, each of which is the average determined from a number of sediment core samples by needle probe or water content methods.

of the following reasons: (1) an upper or a lower or a range of heat flow values is given for a station; (2) conductivity values are adopted from nearby stations and temperature probes have partly penetrated the sediment; and (3) measurements were made over shallow water (e.g. ≤ 1 km deep). The oceanic data are reviewed separately for the Atlantic, Indian, Pacific, and Arctic oceans. For each region, the literature is briefly reviewed, and the data are summarized and discussed under major features of the oceans. Heat flow values are plotted on maps and are tabulated in the appendix.

4.1 Atlantic Ocean

The Atlantic is the second largest ocean, covering nearly 20% of the Earth's surface. North of the equator, because of projecting land areas and islands arcs, the Atlantic is characterized by several semi-enclosed seas. Excluding these adjacent seas, the Atlantic Ocean floor can be divided into three major divisions: the continental margins, basins, and the Mid-Atlantic Ridge, each occupying about one-third of the total area. Bathymetric maps for the North and the South Atlantic, with heat flow stations indicated, are given in Figures 10 and 12, respectively.

The pioneering work on heat flow measurements in the Atlantic was carried out by Bullard in 1954. Within a decade, about 250 heat flow values have been obtained (see Figures 11 and 13). The literature includes *Bullard* [1954], *Bullard and Day* [1961], *Reitzel* [1961a, b; 1963], *Gerard et al.* [1962], *Lister* [1962, 1963a, b], *Lister and Reitzel* [1964], *Nason and Lee* [1962, 1964], *Vacquier and Von Herzen* [1964], *Langseth and Grim* [1964], *Birch* [1964], and M. G. Langseth (private communi-

cation). They are summarized in Table 7, and their numerical results are given in the appendix.

General geology. The most striking feature of the Atlantic is the continuous, broad, fractured swell known as the Mid-Atlantic Ridge (Figures 10 and 12). It runs along almost the entire length of the ocean and is almost exactly equidistant from Europe and Africa on one side and the Americas on the other. The Ridge rises about two kilometers above the deep basins on either side. It is very mountainous, and some of the highest parts rise above the sea level, forming islands. The crest zone has extremely rugged relief, and *Heezen and Ewing* [1963] maintain that a continuous central rift valley lies along the axis, coinciding with the belt of mid-oceanic earthquake epicenters. In Figures 11 and 13, the crest of the Mid-Atlantic Ridge is indicated by heavy solid lines, and the extent of the ridge is given by dashed lines. Numerous faults, approximately perpendicular to the ridge crest, have displaced much of the Ridge. Recent seismic and gravity studies over the Mid-Atlantic Ridge reveal normal thickness of the crust, lower seismic velocity under the axial zones, and null free air gravity anomaly over the entire ridge [*Le Pichon et al.*, 1965; *Talwani et al.*, 1965].

On either side of the Mid-Atlantic Ridge, many basins are separated by a series of small transverse ridges and rises that extend from the Mid-Atlantic Ridge or out from the continents. Most basins are more than four kilometers deep, and some parts are deeper than six kilometers. In many places, the basin floors are extremely smooth and slope gently toward the deeper parts, constituting the abyssal plains. In other places, the floors are intensely disrupted and have a finely textured relief; these are the abyssal hills. In addition to the abyssal plains and abyssal hills, there are small asymmetric oceanic rises with moderate relief, but they do not occupy much area.

The Atlantic Ocean has only a few small trenches. The Puerto Rico Trench (maximum depth 9200 meters) has a flat floor and can be traced for only about a thousand kilometers, much shorter and shallower than the Pacific trenches.

Mid-Atlantic Ridge. *Bullard and Day* [1961] observed a high heat flow of $6.52 \mu\text{cal}/\text{cm}^2 \text{ sec}$ in the central valley of the Mid-Atlantic Ridge

(47°N). The area is very rocky, causing great difficulty in attempts to repeat the measurements. *Reitzel* [1961*a, b*] also obtained a high value of >6.2 in a small valley about 50 km northeast of the Ridge (51°N). The temperature gradient at this station exceeded the range of the instrument, and no core for conductivity measurement was taken. A pipe dredge haul brought up yellow mud with large and abundant shards of fresh volcanic glass. Like the value found by *Bullard and Day*, this high heat flow is attributed to recent volcanism. *Lister and Reitzel* [1964] report a line of six stations along 29°N across the crest of the Ridge. These successful stations, out of 13 trials, give low values of about $1 \mu\text{cal}/\text{cm}^2 \text{ sec}$. Rough rocky bottom caused considerable penetration difficulties, so that these stations may not be representative of the crestal zone. Some 700 km south, *Nason and Lee* [1962, 1964] made a profile of 11 stations across the Ridge. Values as low as $0.3 \mu\text{cal}/\text{cm}^2 \text{ sec}$ are found on the flanks, and values as high as $6.5 \mu\text{cal}/\text{cm}^2 \text{ sec}$ at the crest.

Vacquier and Von Herzen [1964] made extensive heat flow and magnetic studies of the Mid-Atlantic Ridge. Fourteen crossings (30°S to 6°S) revealed the presence of a continuous magnetic intensity anomaly characteristic of the crest. Nearly all heat flow values greater than $2 \mu\text{cal}/\text{cm}^2 \text{ sec}$ lie within 100 km of the apex of the magnetic anomaly. Low heat flow values are observed to be predominant between 300 and 600 km from the crest. Many of these low values do not appear to be associated with unusual local topography and are quite uniformly distributed on the ocean floor.

Atlantic Basins. In various Atlantic Basins (including those in the Caribbean Sea), very uniform heat flow values of about $1.1 \pm 0.2 \text{ s.d.}$ have been observed. *Reitzel* [1963] determined heat flow at sixteen stations regularly spaced over the North American Basin. The results show a remarkable uniformity in heat flow ($1.14 \pm 0.06 \text{ s.d.}$) over 10^6 km^2 area, which have been further confirmed by later workers. *Lister* [1963*a*] discusses ten measurements forming a close group in the Canary Basin around the Madeira and the Cape Verde abyssal plains. His values range from 1.03 to 1.39, with a standard deviation of 0.11. *Nason and Lee* [1964] also found similar values in the same region.

Other Atlantic areas. Heat flow values are

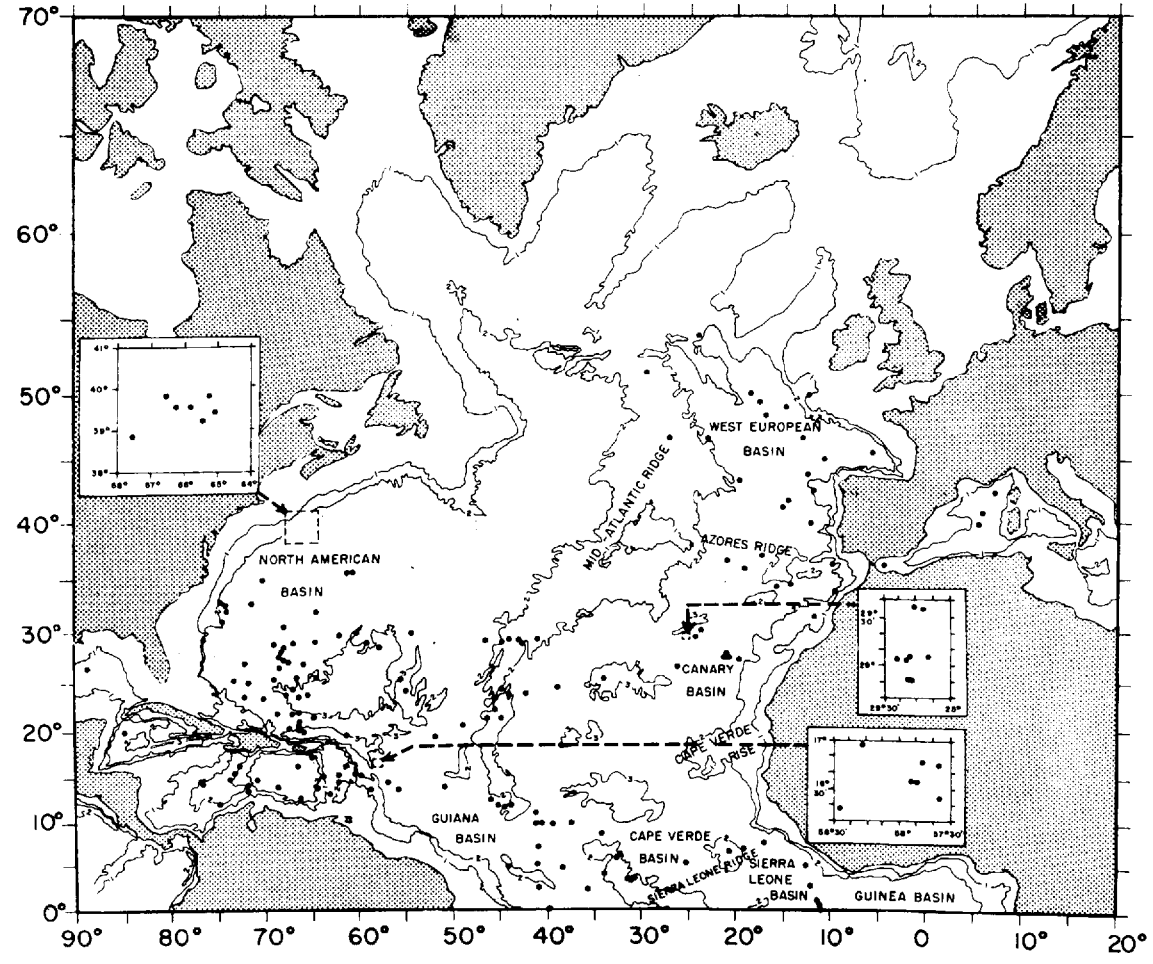


Fig. 10. Bathymetric map of the North Atlantic with locations of heat flow stations. Contours in thousands of fathoms.

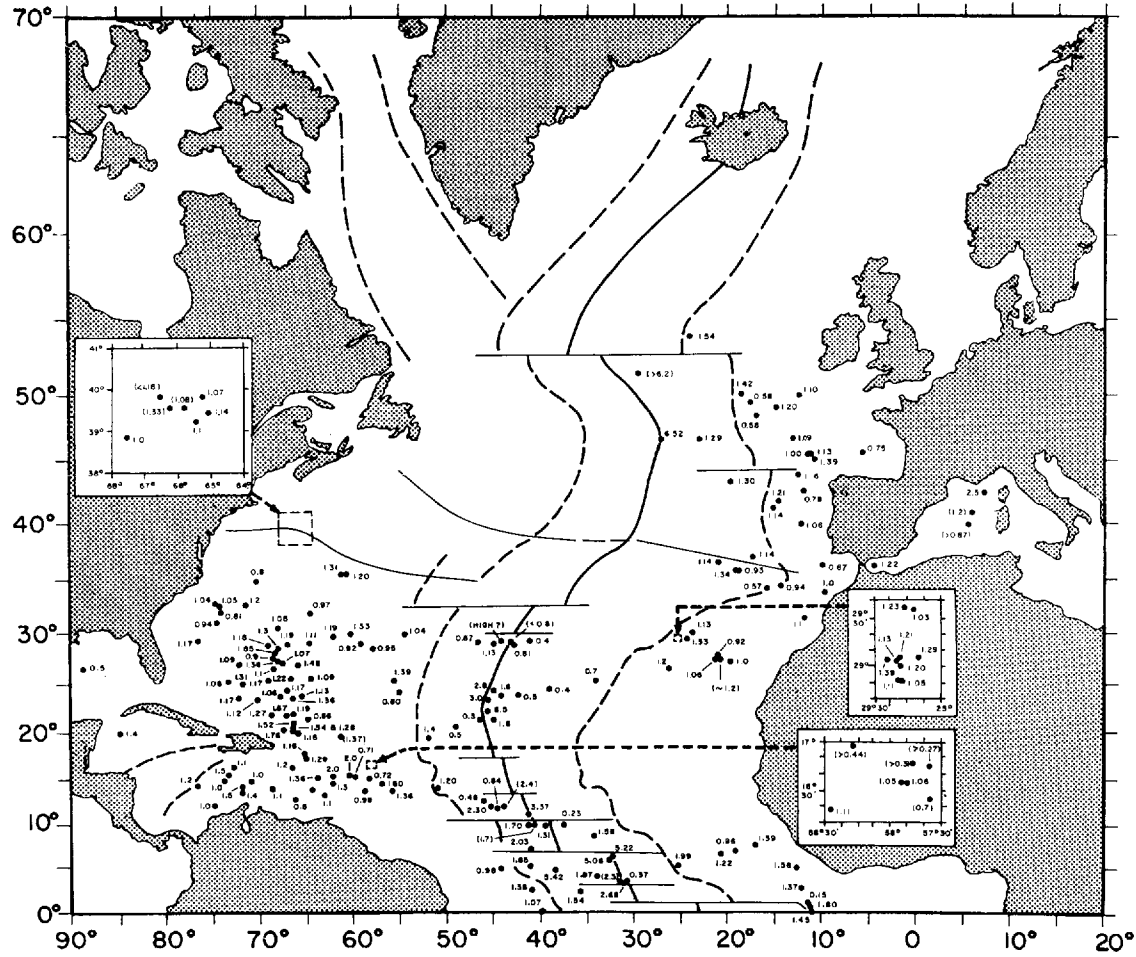


Fig. 11. Heat flow values in the North Atlantic. Values in parentheses are rejected data (category C). Heavy solid lines indicate the crest, and dashed lines the extent of the Mid-Atlantic Ridge (taken from Figure 38).

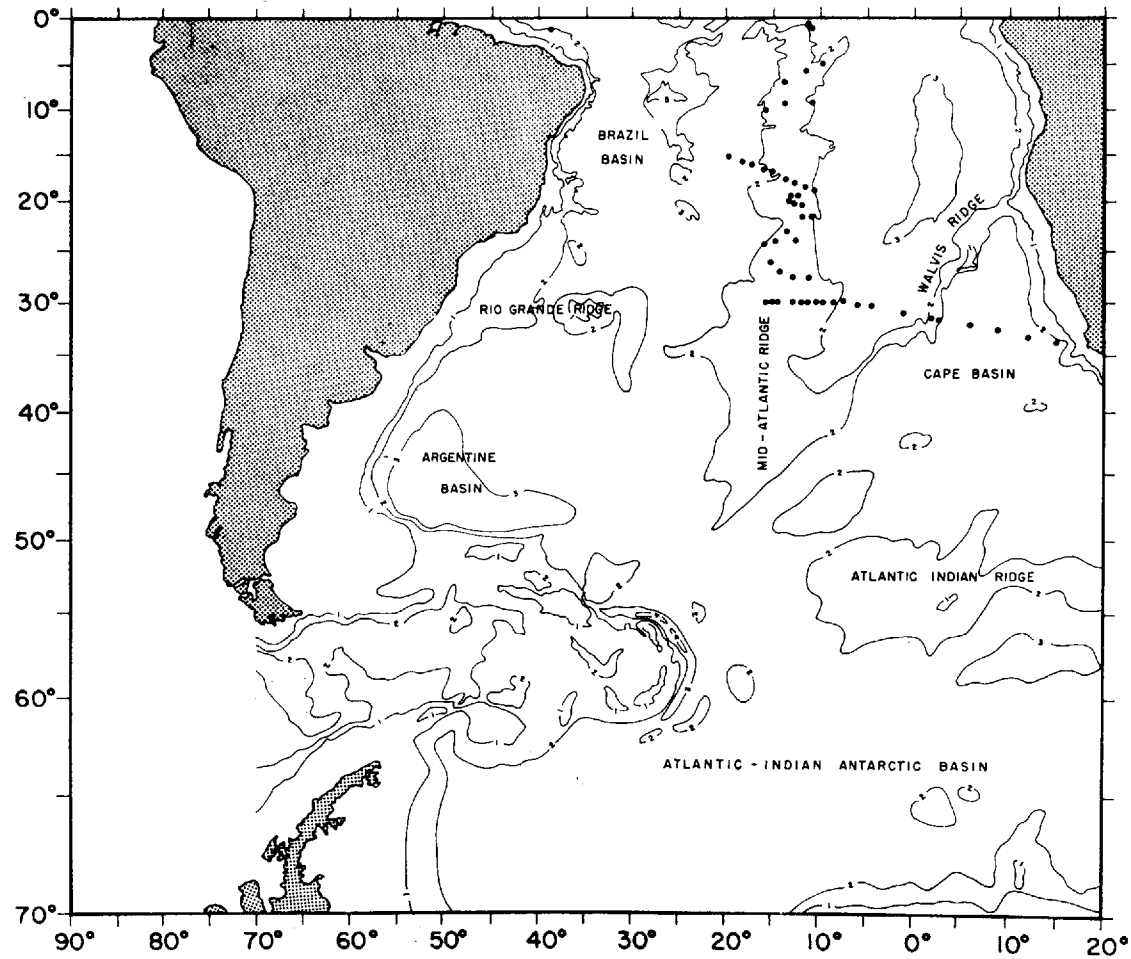


Fig. 12. Bathymetric map of the South Atlantic with locations of heat flow stations. Contours in thousands of fathoms.

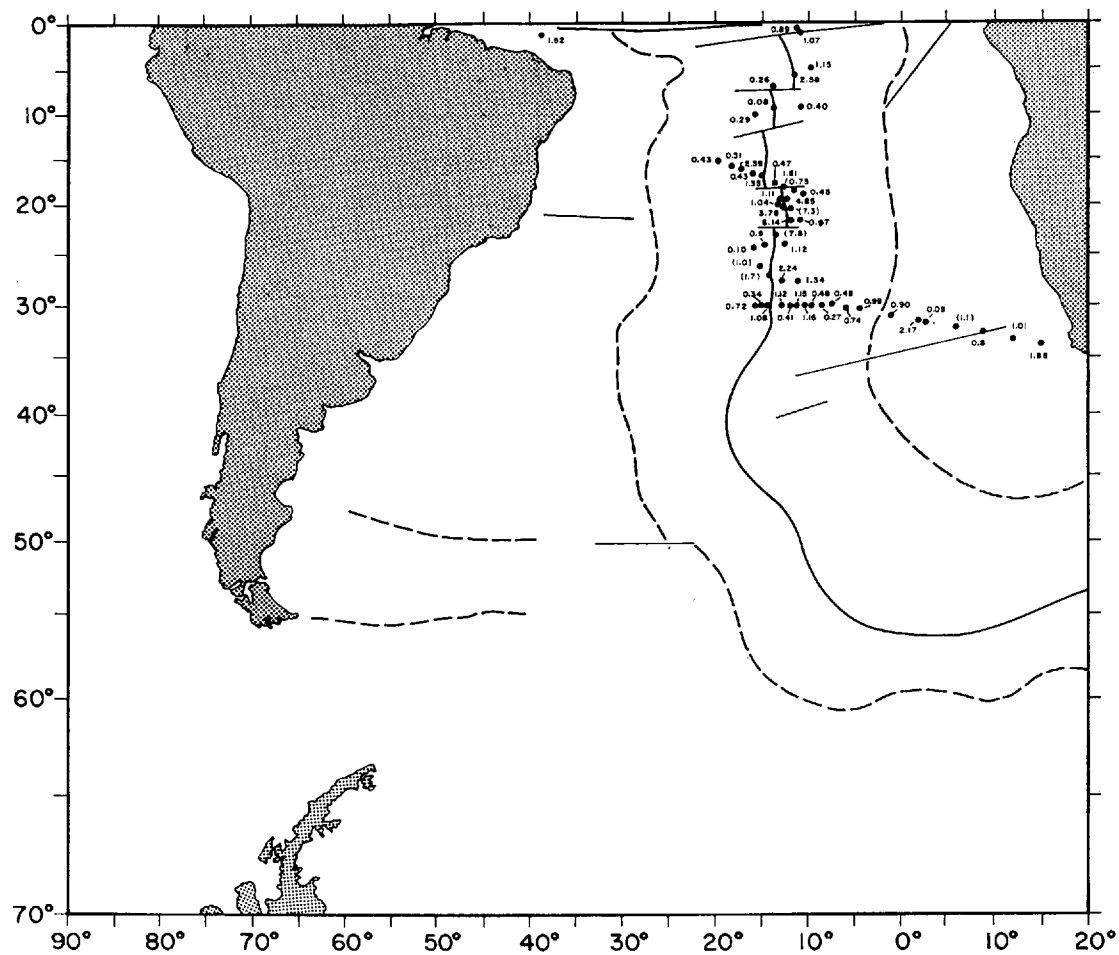


Fig. 13. Heat flow values in the South Atlantic. Values in parentheses are rejected data (category C). Heavy solid lines indicate the crest, and dashed lines the extent of the Mid-Atlantic Ridge (taken from Figure 38).

TABLE 7. Summary of Heat Flow Data in the Atlantic Ocean

Reference	Data No.	No. of Stations	Regions	Remarks on Heat Flow Data
<i>Bullard, 1954</i>	0391-0395	5	West European Basin	First measurements in the Atlantic; average value is 0.98 ± 0.35 s.d.
<i>Bullard and Day, 1961</i>	0214-0229	16	West European Basin, Mid-Atlantic Ridge, and Mediterranean Sea	Fairly uniform (0.78 to 1.89) values in the Basin and the east flank of the Mid-Atlantic Ridge; high value (6.52) in the central valley of the Ridge; difficult to repeat this measurement because of rocky bottom
<i>Reitzel, 1961a</i>	0230-0233	4	North American Basin and Mid-Atlantic Ridge	Two stations (10 km apart) in the Basin gave similar values (1.20 and 1.31); high value (> 6.2) in a small valley about 50 km NE of the crest of the Mid-Atlantic Ridge
<i>Reitzel, 1961b</i> <i>Gerard et al., 1962</i>	0234-0247	14	Various Atlantic Basins, Mid-Atlantic Ridge, and Puerto Rico Trench	Ph.D. thesis; detailed account of <i>Reitzel</i> [1961a] Values are: continental rise off Brazil (1.52 & 1.07), Ceara abyssal plain (1.38), edge of Guiana abyssal plain (1.85), western flank of Mid-Atlantic Ridge (2.08), transverse trough in the Ridge axis (3.37), SE extension of Puerto Rico Trench (1.60), Antilles outer ridge (1.52), Nares abyssal plain (1.86), crest of Antilles outer ridge (1.67), floor of Puerto Rico Trench (1.16), continental rise off U.S. (1.03 & 1.04); conductivity estimated from chlorine content
<i>Lister, 1962</i>				Ph.D. thesis; source material for <i>Lister</i> [1963a, b] and <i>Lister and Reitzel</i> [1964]
<i>Lister, 1963a</i>	0348-0357	10	Around Madeira and Cape Verde abyssal plains (Madcap) in west Canary Basin	Closely spaced ($\sim 1^\circ \times 1^\circ$) stations giving very uniform values: 1.20 ± 0.11 s.d.; Madcap caldera causes a reduction in heat flux at its summit as expected from the effect of topographic relief
<i>Lister, 1963b</i>	168, 170, 171, 174, 0348-0370	27	Various Atlantic Basins, Mid-Atlantic Ridge, and Mediterranean Sea	Brief summary of values obtained in <i>Lister</i> [1962]
<i>Lister and Reitzel, 1964</i>	0167-174	8	A profile along 29°N over Mid-Atlantic Ridge; a pair on the outer ridge north of Puerto Rico Trench	6 successful stations out of 13 trials on the ridge have rather low values (0.8-1.1); difficult for the probe to penetrate sediments because of rocky bottom; a pair of stations (< 4 km apart) by two different techniques are 1.28 and 1.54
<i>Nason and Lee, 1962</i>		14	A profile across the Mid-Atlantic Ridge from Martinique to Canary Islands	Preliminary results of some part of <i>Nason and Lee</i> [1964]
<i>Nason and Lee, 1964</i>	0328-0347	20	A profile from Panama to Nice, France, across the Caribbean, various Atlantic Basins, Mid-Atlantic Ridge, and the Mediterranean	Values of ~ 1.2 in various basins; low values in the flanks of Mid-Atlantic Ridge and high values in the crest; values obtained in the east of Antilles and the Mediterranean are questionable because of possible thermal disturbances in the sediment
<i>Reitzel, 1963</i>	0175-0194	20	North American Basin; near Puerto Rico Trench; continental slope off U.S.	16 regularly spaced stations over North American Basin between Bermuda and the Bahama Banks show a remarkable uniformity in heat flow (1.14 ± 0.06 s.d.); value at southern edge of the above area near the Puerto Rico Trench is 1.76; rather low values (~ 1) close to continental slope off U.S.
<i>Vacquier and Von Herzen, 1964</i>	0248-0327	81	14 crossings of the crest of the Mid-Atlantic Ridge between 30°S and 6°S ; a long profile from Freetown, Africa, to the Caribbean	Nearly all heat flow values > 2 are within 100 km of the apex of the magnetic anomaly which is characteristic of the crest; between 300 and 600 km from the crest, low values are predominant, and most of them do not seem to be associated with unusual local topography and are systematically distributed on the ocean floor; a somewhat high value (2.7) in the center of Walvis Ridge and low values over its flanks; six values from deep sea to the inside of the Lesser Antilles arc showed higher values near the central part of the island arc
<i>Birch, 1964</i>	0195-0213	19	Barracuda Fault Zone, New England Seamounts, and abyssal hills SE of Bermuda	M.Sc. thesis; details not available to us
<i>Langseth and Grim, 1964</i>	0371-0390	20	Western Atlantic, Caribbean Sea and Gulf of Mexico	Preliminary report; details not available

few over the Puerto Rico Trench and do not indicate any significant feature, except that values on its outer ridge are slightly higher (about 1.5) than the value (1.2) measured on the floor of the trench [*Gerard et al.*, 1962]. *Diment and Weaver* [1964] obtained a low

value of 0.6 from a hole 300 meters deep in a serpentinized ultrabasic body (see Table 3E) near Mayaguez, Puerto Rico.

Around the Antilles island arc, heat flow values are fairly variable (0.3 to 2.0). Because of disturbance observed in the sediment cores,

heat flow values observed over this area are probably not representative of the regional heat flow [Nason and Lee, 1964].

The Mediterranean Sea and the Gulf of Mexico have only a few measurements, and hence no definite conclusions can be drawn.

Heat flow results. Histograms of heat flow values from the Atlantic ridges (almost all from the Mid-Atlantic Ridge) and basins are given in Figures 14 and 16. The arithmetic mean for 87 ridge values is 1.48 ± 1.48 s.d., whereas that for 74 basin values is 1.13 ± 0.24 s.d. (see Table 14). Heat flow values in the Mid-Atlantic Ridge are plotted versus distance from the crest in Figure 15. Values exceeding 2.5 are found only within 100 km of the ridge crest. The average of 32 measurements within 100 km of the crestal zone is 3 ± 2 s.d. $\mu\text{cal}/\text{cm}^2 \text{ sec}$, which is twice the world average. 75-, 50-, and 25-percentile lines are also given for heat flow values from the Mid-Atlantic Ridge and the Atlantic basins in Figure 15. (For example, the 75-percentile line separates the data into two groups: 75% of the data points are above it, and 25% of the data points below it. In drawing the percentile lines, the horizontal axis is divided into small intervals. Within each interval, a horizontal line separating the number of data points into different percentiles is drawn. Each set of these horizontal lines is then connected smoothly to form the percentile line.) The contrast is obvious: whereas values from the Mid-Atlantic Ridge are widely scattered, those from the Atlantic basins are very uniform. Furthermore, the percentile lines for the values from the Mid-Atlantic Ridge indicate two subgroups: (1) within 100 km of the ridge crest heat flow values are extremely scattered, and (2) beyond 100 km the values become less scattered as the distance from the ridge crest increases.

4.2 Indian Ocean

The Indian Ocean is the second smallest of the four oceans and covers about 15% of the Earth's surface. The major topographic features and locations of heat flow stations are shown in Figure 17. Figure 18 gives the heat flow values and morphologic divisions.

Heat flow measurements were first made in the Indian Ocean by R. P. Von Herzen, and within a few years about 220 heat flow values

have been obtained by four research groups (Cambridge, Lamont, Scripps, and USCGS). (See Figure 18.) The literature includes Von Herzen [1963], Burns [1964], Von Herzen and Langseth [1965], and J. Selater (private communication). They are summarized in Table 8, and their numerical results are given in the appendix. Very recently, V. Vacquier and associates (private communication) have made extensive heat flow measurements in the Indian Ocean. However, the results are too late to be catalogued in this chapter.

General geology. The Indian Ocean has a well developed basin and ridge structure [Stocks, 1960]. The Mid-Indian Ocean Ridge system is believed to be part of the seismically active worldwide rift system [Heezen and Ewing, 1963]. It begins in the north as the Carsberg Ridge and extends from the Gulf of Aden southeastward to the equator. It then runs nearly due south, passing to the east of the Seychelles-Mauritius Ridge and branches into two separate ridges at about 25°S. The southwest branch runs around the southern tip of Africa to join the Mid-Atlantic Ridge. The southeast branch runs south of Australia and is continuous with the ridge of the southwestern Pacific Ocean. This ridge system divides the Indian Ocean into three units, western, eastern, and southern. The last unit has hardly been explored.

The three major units of the Indian Ocean are further divided into various basins by minor ridges; e.g., the Laccadive Ridge and Ninety-East Ridge. For the most part these ridges are seismically inactive and extend from the Mid-Indian Ridge system toward the continents, varying in width from 150 to 300 km. Most of the Indian Ocean basins are more than 3.5 km deep, and some parts are deeper than 5 km. The deepest basins and the only trench (Java-Sumatra Trench off the Indonesian arc) occur in the east. In the west the sediments are chiefly globigerina ooze, whereas in the east red clay predominates.

Extensive study of the Indian Ocean is still in progress. The International Indian Ocean Expedition (1960-1965) has yielded much valuable information, but most of it is not yet published.

Heat flow results. The most extensive heat flow study of the Indian Ocean is given by Von Herzen and Langseth [1965]. Besides giv-

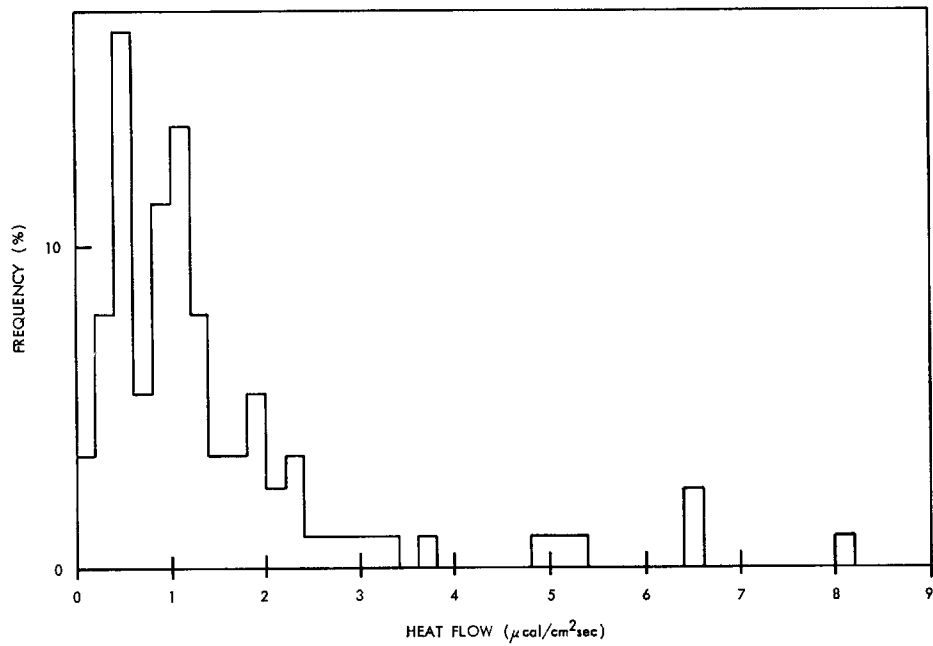


Fig. 14. Histogram of heat flow values from Atlantic ridges.

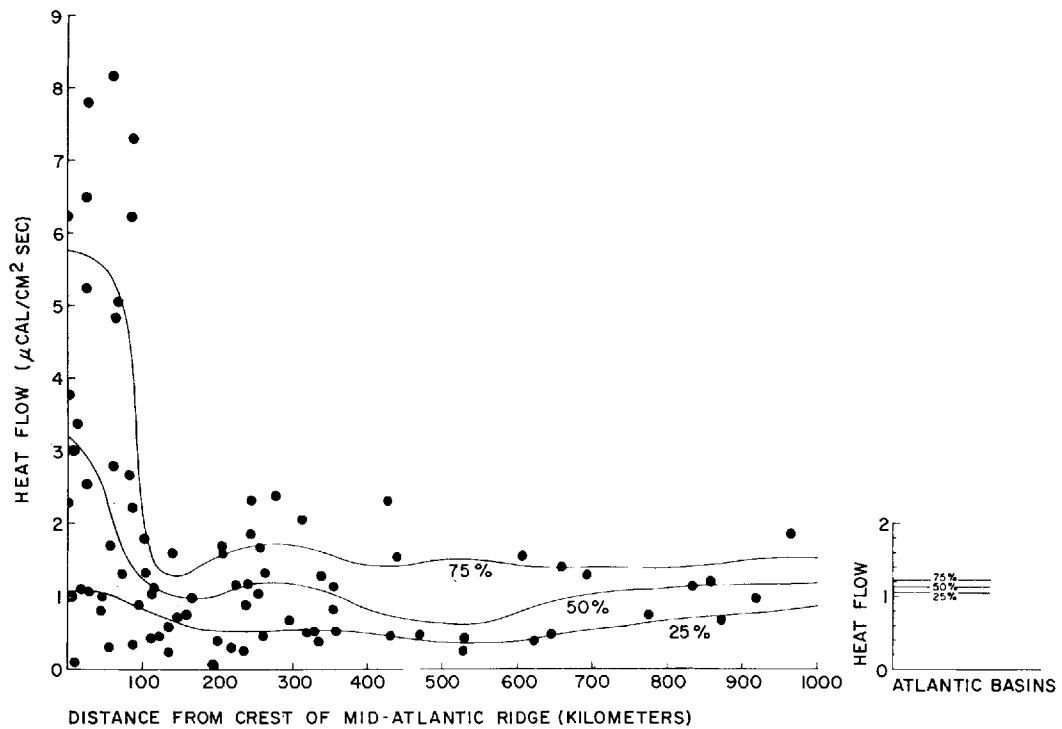


Fig. 15. Heat flow values versus distance from the crest of the Mid-Atlantic Ridge; 75-, 50-, and 25-percentile lines are given for values from the Mid-Atlantic Ridge and the Atlantic basins. For example, the 50-percentile line separates half the data points above and half the data points below it.

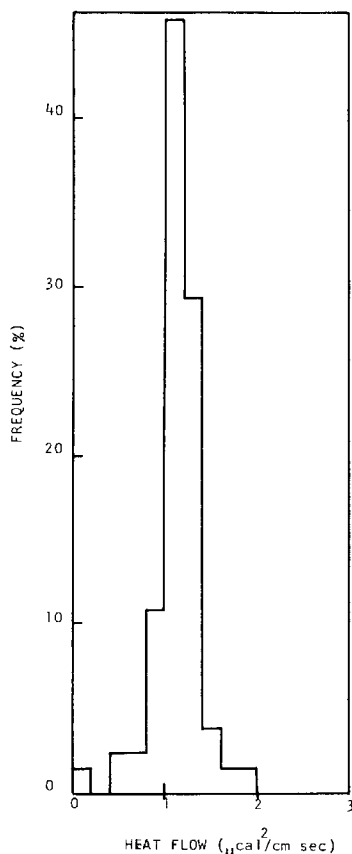


Fig. 16. Histogram of heat flow values from the Atlantic basins.

ing an excellent review of oceanic heat flow measurements in general, they also present a comprehensive account of their heat flow observations in the Indian Ocean. The measurements by Scripps Institution of Oceanography using Bullard-type probes, and those by the Lamont Geological Observatory utilizing the Ewing technique, have been made independently of one another. The authors give a critical

evaluation of measurements by different techniques, and they summarize and discuss their results under major physiographic features.

Histograms of heat flow values from the Indian Ocean ridges and basins are given in Figures 19 and 21. The arithmetic mean of 85 ridge values is 1.57 ± 1.17 s.d., whereas the mean of 90 basin values is 1.39 ± 0.42 s.d. (see Table 14). Heat flow values in the Mid-Indian Ocean Ridge are plotted versus distance from the crest in Figure 20. As for the Mid-Atlantic Ridge (Figure 15), values exceeding 2.5 are found only within about 100 km of the crestal zone. In Figure 20, 75-, 50-, and 25-percentile lines are also given for heat flow values from the Mid-Indian Ocean Ridge and the basins. Although the contrast is not as great as in the Atlantic Ocean, the picture is similar. The percentile lines fall to a minimum at about 300 to 400 km from the crest of the Mid-Indian Ocean Ridge and then increase (Figure 20).

A few measurements from the Java Trench suggest that the inner trench may be a region of low heat flow, whereas the outer trench may have moderately high heat flow. Recently *Vacquier and Taylor* [1965] have made a detailed survey in the trench area off Sumatra. They obtained a mean value of 1.23 ± 0.88 s.d. from 20 measurements in the deep trench and a mean value of 1.57 ± 0.84 s.d. from 37 measurements outside the trench. However, these data were too late to be catalogued.

4.3 Pacific Ocean

The Pacific is the largest ocean and covers about 35% of the Earth's surface. *Menard* [1964] provides an excellent account of the general geology and geophysics of the Pacific. Bathymetric maps for the Pacific and locations

TABLE 8. Summary of Heat Flow Data in the Indian Ocean

Reference	Serial No.	No. of Stations	Regions	Remarks on Heat Flow Data
<i>Von Herzen</i> , 1963	0424-0428	5	Gulf of Aden	High values (2.5 to 6) were obtained; see <i>Von Herzen and Langseth</i> [1964]
<i>Turns</i> , 1964	0587-0590	4	Volcanic trend of the primary arc enclosing the Adaman Sea	Widely different values (0.9 to 5.3) over a nearly straight north-south profile of about 300 km length
<i>Von Herzen and Langseth</i> , 1965	0396-0586	191	Fairly well distributed over the whole Indian Ocean	See text
clater, private communication	0591-0617	27	Red Sea, Gulf of Aden, West Indian Ocean	High values observed in Red Sea and Gulf of Aden; details not available

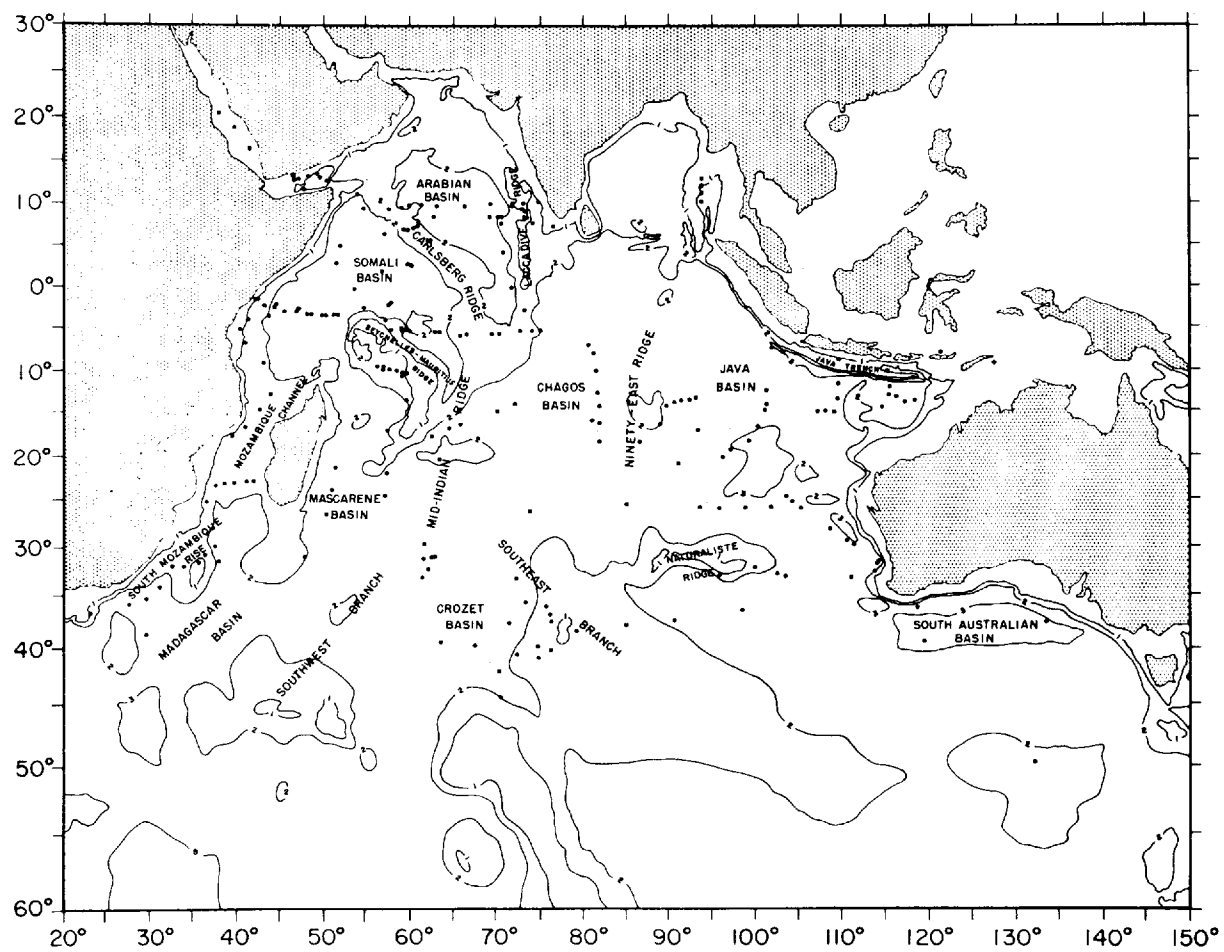


Fig. 17. Bathymetric map of the Indian Ocean with locations of heat flow stations; contours in thousands of fathoms.

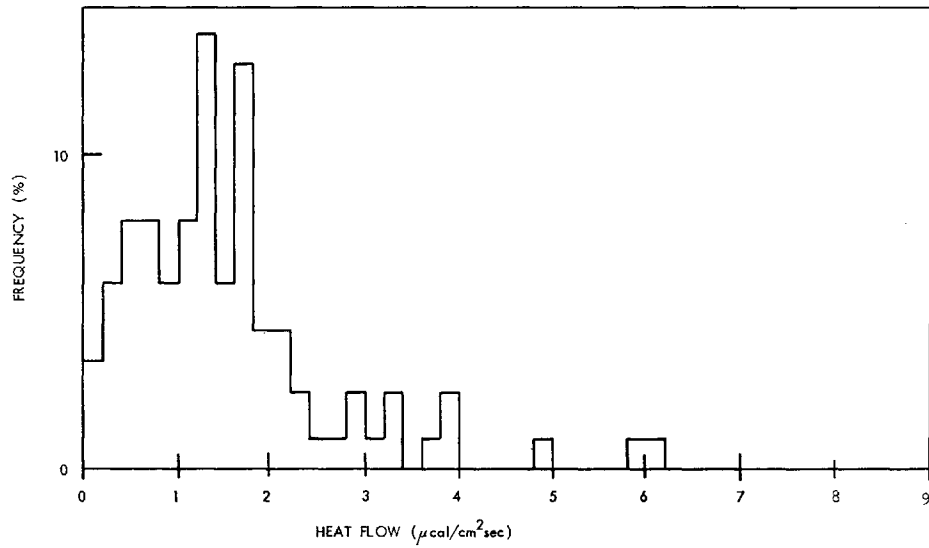


Fig. 19. Histogram of heat flow values from the Indian Ocean ridges.

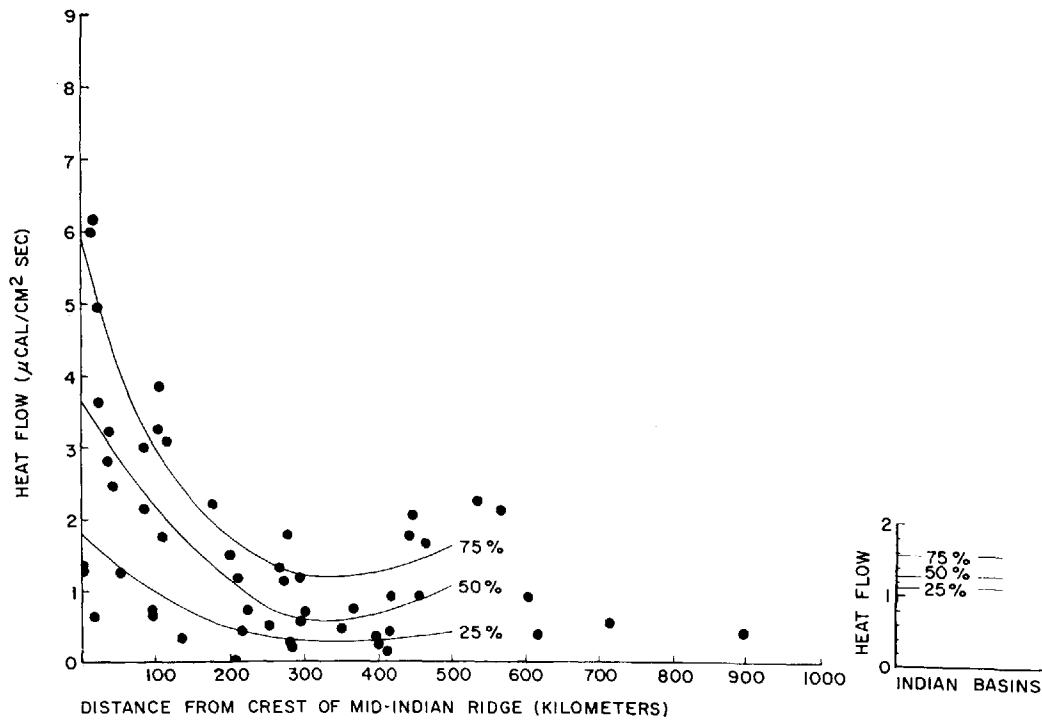


Fig. 20. Heat flow values versus distance from the crest of the Mid-Indian Ocean Ridge; 75-, 50-, and 25-percentile lines are given for values from the Mid-Indian Ocean Ridge and the Indian Ocean basins. For example, the 50-percentile line separates half the data points above and half the data points below it.

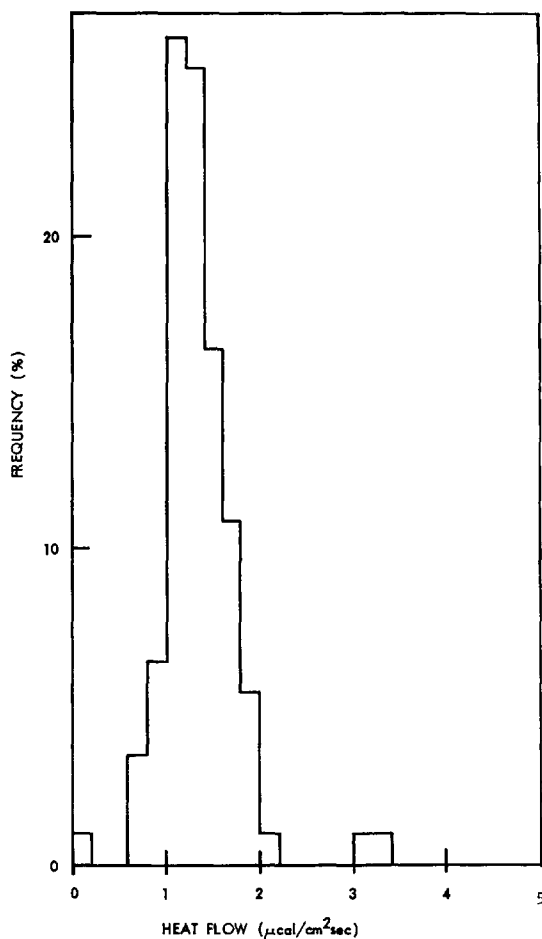


Fig. 21. Histogram of heat flow values from the Indian Ocean basins.

of heat flow stations are given in Figures 22, 24, 26, and 27.

E. C. Bullard, R. Revelle, and A. E. Maxwell pioneered the heat flow measurements in the Pacific in the early 1950's. Since then about 500 heat flow values have been published (see Figures 23, 25, 26, and 27). Unfortunately most data are centered around the central east Pacific. The literature includes *Revelle and Maxwell* [1952], *Bullard et al.* [1956], *Maxwell and Revelle* [1956], *Maxwell* [1958], *Von Herzen* [1959, 1960, 1963, 1964, and private communication], *Uyeda et al.* [1962], *Foster* [1962], *Von Herzen and Uyeda* [1963], *Von Herzen and Maxwell* [1964], *Rhea et al.* [1964], *Uyeda and Horai* [1964], *Langseth et al.* [1965], P. Grim (private communication), and *Yasui and*

Watanabe [1965]. They are summarized in Table 9 and their numerical results are given in the appendix.

General geology. The northwestern half of the Pacific is relatively deep compared with the southeastern half and is relatively normal: water depth of 5 to 6 km, crustal thickness of about 5 to 6 km, and aseismic. Clusters of volcanoes are common and usually occur along very long faults. The southeastern half is 3 to 5 km deep and has been deformed into a system of elongated, broad rises.

The most prominent of the rises is the East Pacific Rise, a vast, low bulge of the sea floor 2 to 3 km high, 2000 to 4000 km wide, and about 15,000 km long [*Menard*, 1964, p. 118]. Its size is comparable to North and South America, which it roughly parallels and in part overlaps. Both ends are ill-defined, and its boundaries are rather vague (Figures 23 and 25). The southern end may be at about 60°S and 160°W and can be traced as a continuous feature trending northeast, although the crest is offset between 25 and 30°S. The general trend of the rise changes to northwest at the equator, and it is so close to land that the eastern flank begins to be obscured. The crest disappears as an identifiable topographic feature at the southern end of the Gulf of California, and *Menard* suggests that it continues under the Gulf of California and reappears off Oregon. North of the Mendocino fracture zone, the crest of the rise reappears as a belt of ridges and troughs, but again vanishes, because of transverse faulting, at about 50°N. The western flank butts into Alaska, and the crest has not been identified farther north. Seismic refraction studies indicate that the depth to the Mohorovicic discontinuity under the crest of the East Pacific Rise is shallow and upper mantle velocities are low. Shallow earthquakes are also common along the crest.

Most Pacific basins are to the west of the East Pacific Rise. They are usually 5 to 6 km deep and mostly not mountainous. A series of deep ocean trenches almost surrounds the Pacific at the margin. The circum-Pacific margin including these trenches is the most active geological structure on Earth. Special features are the greatest ocean depths, largest gravity anomalies, most extensive volcanism, most intense

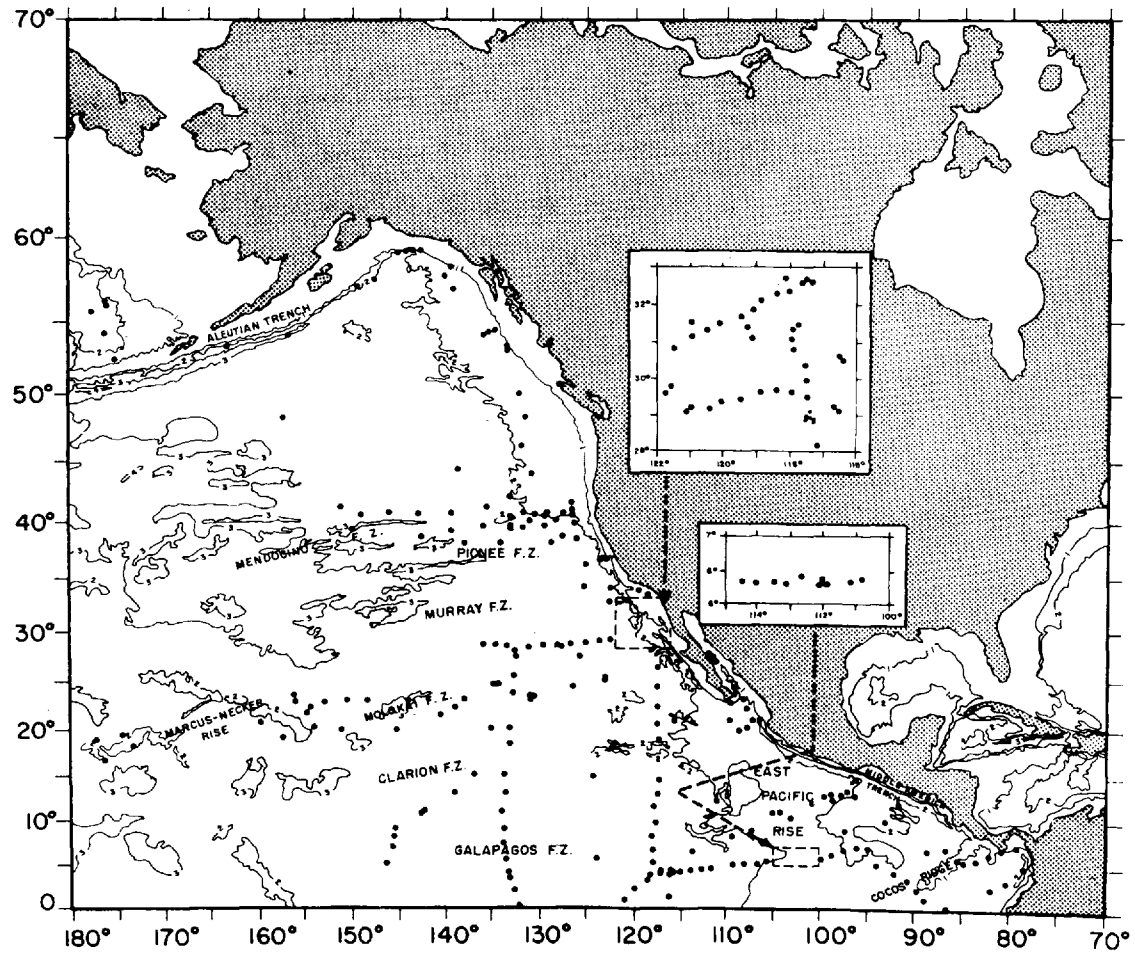


Fig. 22. Bathymetric map of the northeast Pacific with locations of heat flow stations, contours in thousands of fathoms.

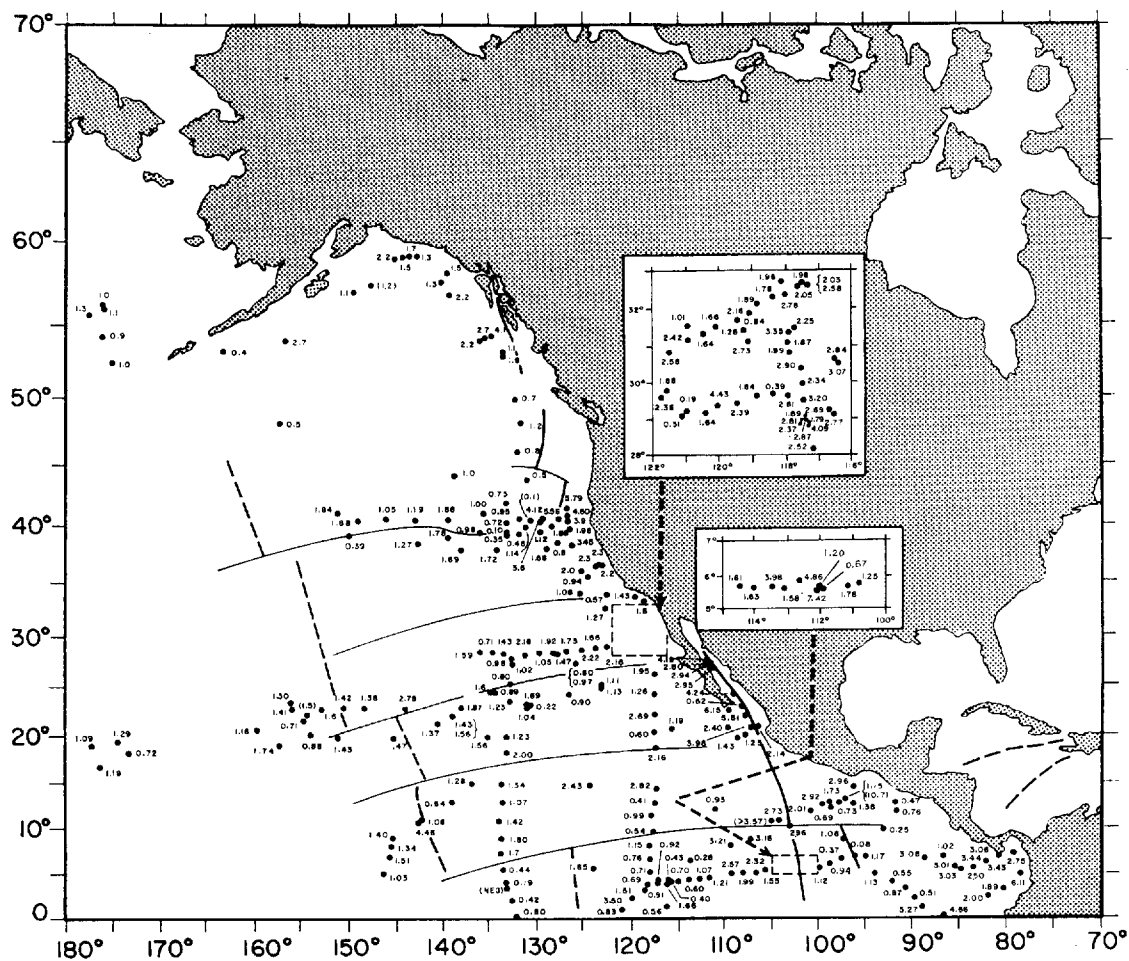


Fig. 23. Heat flow values in the northeast Pacific. Values in parentheses are rejected data (category C). Heavy solid lines indicate the crest and dashed lines the extent of the East Pacific Rise (taken from Figure 38).

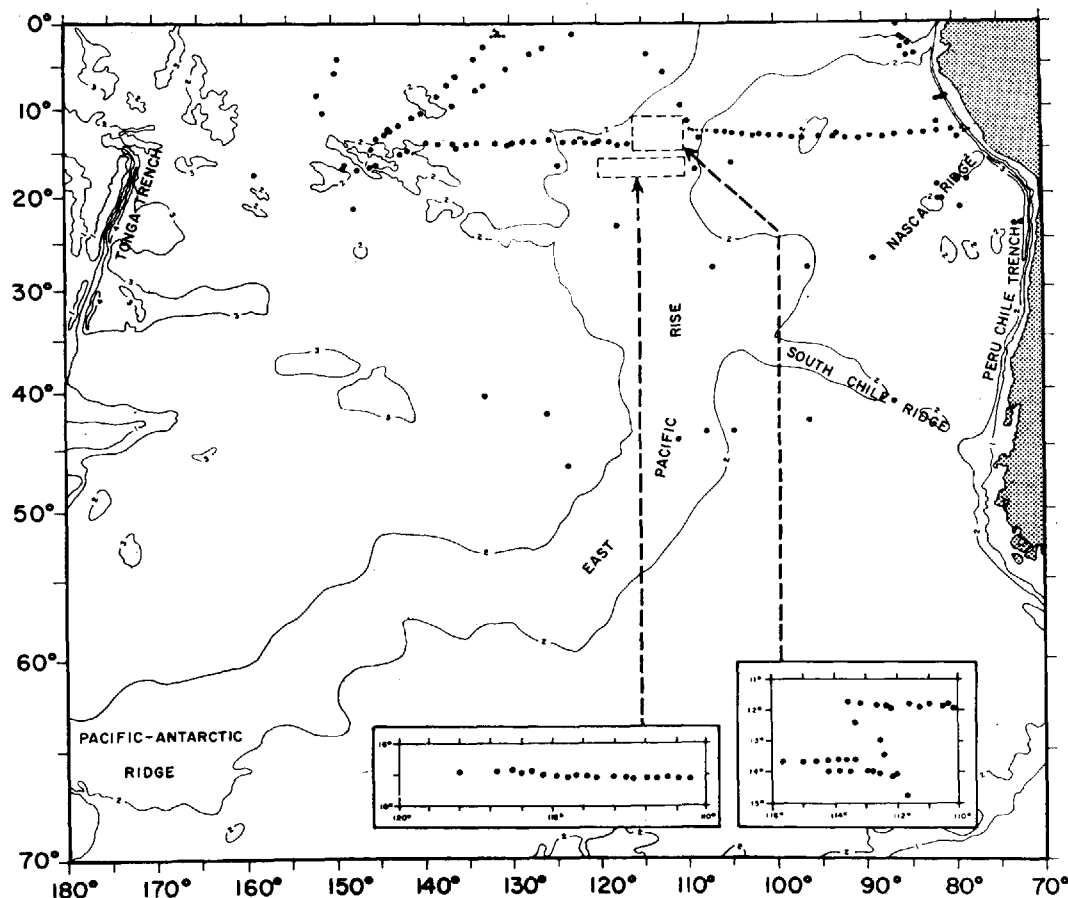


Fig. 24. Bathymetric map of the Southeast Pacific with locations of heat flow stations; contours in thousands of fathoms.

shallow seismicity, and almost all the known deeper earthquakes.

East Pacific Rise. Bullard *et al.* [1956] first observed three high heat flow values in the East Pacific Rise. Von Herzen [1959] observed a relatively narrow band of high heat flow in the crest and areas with low heat flow roughly on each side. Von Herzen and Uyeda [1963] made extensive heat flow studies over the Rise and concluded that it is systematically associated with high values, a strip 200 to 300 km wide at the crest having an average heat flow of about $3 \mu\text{cal}/\text{cm}^2 \text{ sec}$. Within this strip, the highest values occur in two narrower zones which seem to be parallel and symmetrically oriented to the crest. The source of high heat flow is thought to be a region of unusually high temperature, a few tens of kilometers wide, located about

10 km beneath the ocean. One-fourth of their measurements give low heat flow values (≤ 0.8). They find two approximately equidimensional regions near the equator and to each side of the rise showing generally low heat flow. In many areas, isolated low heat flow values are correlated with flat topography, suggesting a local environmental effect. Langseth *et al.* [1965] also found broad variations of heat flow similar to previous findings. A broad heat flow maximum of about $3 \mu\text{cal}/\text{cm}^2 \text{ sec}$ is found near the East Pacific Rise at 10°N , while three singular peaks of high heat flow of 3.3, 3.5, and $7.1 \mu\text{cal}/\text{cm}^2 \text{ sec}$ have been measured over the rise at 17°S . Another high heat flow area is found to extend from the East Pacific Rise to the Gulf of Panama.

Other areas. Extensive heat flow studies have

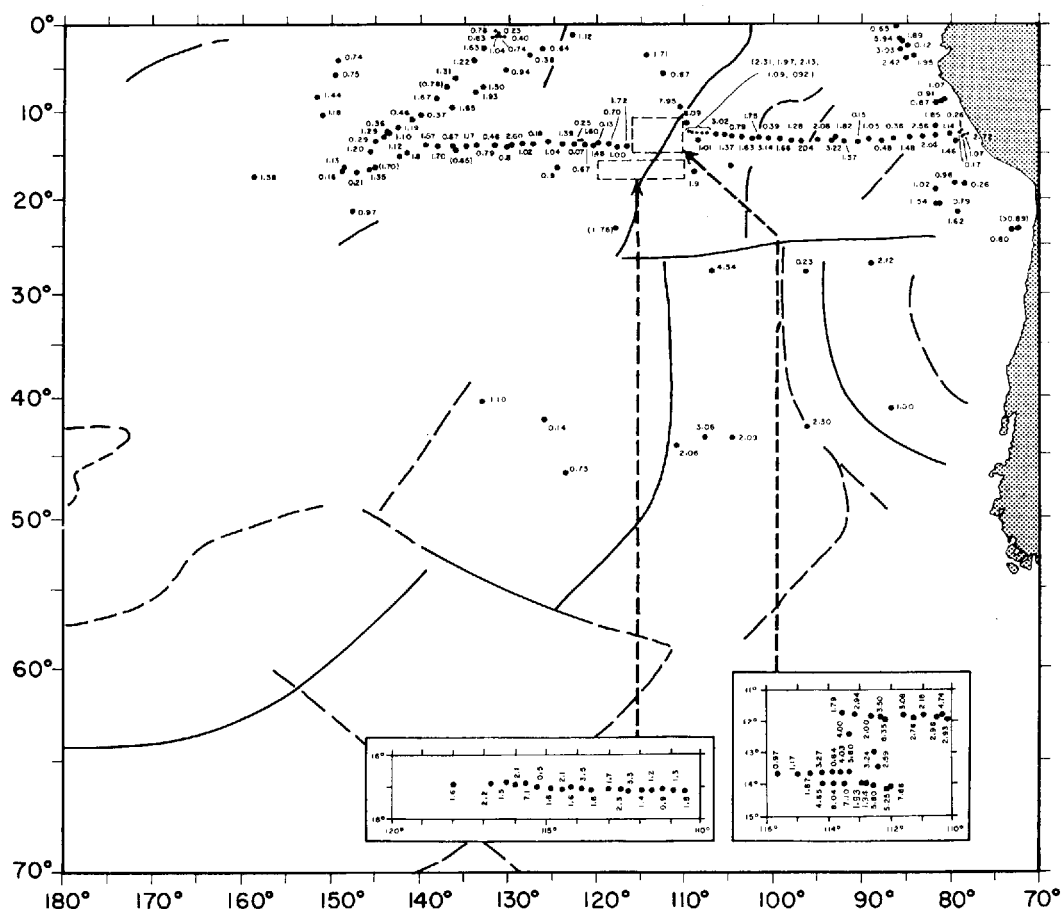


Fig. 25. Heat flow values in the southeast Pacific. Values in parentheses are rejected data (category C). Heavy solid lines indicate the crest and dashed lines the extent of the East Pacific Rise (taken from Figure 38).

been made off the Pacific Coast of the United States and Baja California [Von Herzen, 1964]. Most measurements at the same location have been repeated reasonably well. High heat flow values are observed near the coast, three or four times normal north of the Mendocino fault, and twice normal in the borderland off southern and Baja California. Values observed west of North America range from 0.1 to 6 $\mu\text{cal}/\text{cm}^2$ sec. Some of the large anomalies seem to have wavelengths ranging from about 250 km off Baja to 1000 km off northern California. For the most part the anomalies appear to be uninterrupted across the Mendocino fracture zone.

Between North America and the Hawaiian Islands, Rhea et al. [1964] observed heat flow

values which range from 0.80 to 2.78 and average 1.4 $\mu\text{cal}/\text{cm}^2$ sec. No significant heat flow differences between recognized topographic provinces, including the Hawaiian Ridge and the Molokai fracture zone, are observed.

Foster [1962] observed a low value of 0.4 on the bench just north of the Aleutian Trench off Unimak Pass, whereas a moderately high value of 2.7 was found in the Aleutian Trench proper. Measurements over the Japan and Kurile Trenches and nearby areas have been discussed in section 3.3.

Finally, heat flow has been measured at the preliminary Mohole site, 75 km east of Guadalupe Island [Von Herzen and Maxwell, 1964]. The technique used is different from usual prac-

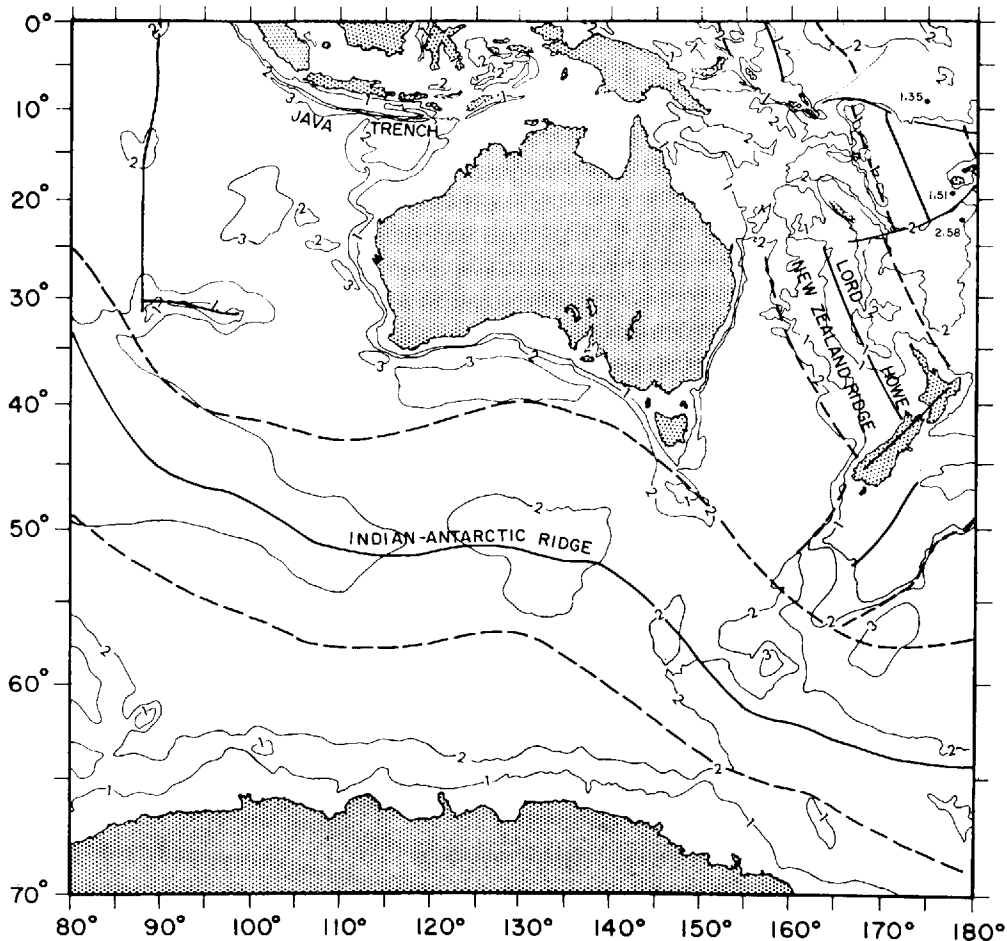


Fig. 27. Bathymetric map of the southwest Pacific with heat flow values. Contours in thousands of fathoms. Geological features are taken from Figure 38. Heat flow values in Indian Ocean are not shown here because they have been plotted in Figure 18.

of the crestal zone. In Figure 29, 75-, 50-, and 25-percentile lines are also given for heat flow values from the East Pacific Rise and the Pacific Ocean basins. The contrast is very obvious, as in the case for the Atlantic and the Indian oceans. The percentile lines drop to a minimum at about 300 km from the crest of the East Pacific Rise (similar to the Mid-Indian Ocean Ridge), increase, and drop again at about 600 to 700 km (Figure 29).

Although heat flow values from Pacific basins are more scattered (Figure 30) than those from the Atlantic and Indian oceans (Figures 16 and 21), their averages (1.18, 1.13, and 1.34 $\mu\text{cal}/\text{cm}^2 \text{ sec}$) are similar.

A histogram of heat flow values from the Pacific trenches is shown in Figure 31. The average of 16 trench values is 0.94 ± 0.6 s.d.; modes are 0.9 and 1.1. It appears that the heat flow is low over the trenches, but this conclusion cannot be fully substantiated yet.

4.4 Arctic Ocean

The Arctic Ocean is the smallest ocean, and its features are relatively unknown. Heat flow measurements using a Ewing-type probe have been made by *Lachenbruch and Marshall* [1964] and *Lachenbruch et al.* [1965]. Their measurements are unique in that a drifting ice-island

TABLE 9. Summary of Heat Flow Data in the Pacific Ocean

Reference	Data No.	No. of Stations	Regions	Remarks on Heat Flow Data
<i>Revelle and Maxwell</i> , 1952	1027-1031	6	1 near the base of the main ridge of the Hawaiian Island, 4 in the vicinity of the sunken Mid-Pacific Mountains, and 1 in the deep water off the coast of Southern California	First successful measurements of heat flow through the ocean floor; values (from 0.9 to 1.3) were revised and discussed in detail in <i>Maxwell</i> [1958]. E. C. Bullard has a brief note added after this article
<i>Maxwell and Revelle</i> , 1956 <i>Bullard et al.</i> , 1956				See <i>Bullard et al.</i> [1956]
<i>Maxwell</i> , 1958	1027-1051	25	Values fairly well distributed over the Pacific	Review of all oceanic heat flow values available in 1956; see <i>Maxwell</i> [1958] Ph.D. thesis; detailed account of every station; average value is 1.44 ± 1 s.d. and the average of 16 values obtained within the deep Pacific Basin is 1.27 ± 0.4 s.d.
<i>Von Herzen</i> , 1959	0759-0794	36	Southeastern Pacific	Results (together with Maxwell's) indicated: (1) a narrow band of high heat flow over the crest of the East Pacific Rise and areas of low heat flow on each side, and (2) low values over axes of trenches bordering the eastern Pacific Ocean
<i>Von Herzen</i> , 1960				Ph.D. thesis; detailed account of <i>Von Herzen</i> [1959] and <i>Von Herzen</i> [1963]
<i>Von Herzen</i> , 1963	0746-0758	18	Gulf of California	10 high values (2.4-6.2) and 3 rather low values (0.6-1.4) were observed
<i>Uyeda et al.</i> , 1962	0618-0620	3	Profile along 38°N across the Japan Trench	Very low value (0.27) on the inner side of the arc, moderately low (1.14) in the trench, and moderately high (2.05) farther to the east
<i>Foster</i> , 1962	0795-0830	36	Northeast Pacific, Bering Sea, and Aleutian Trench	A low value of 0.4 on the bench just north of the Aleutian Trench off Unimak Pass; a fairly high value of 2.7 in the Aleutian Trench proper; large difference in heat flow (0.1 to 3.6) at station 90 km apart over the extension of the crest of the East Pacific rise off the coast of Oregon
<i>Von Herzen and Uyeda</i> , 1963	0831-1026	196	Eastern Pacific	A strip 200-300 km wide having high heat flow values (~3) at the crest of East Pacific Rise, the highest values being in two narrow zones parallel and symmetrically oriented to the crest; two large areas of low heat flow values near the equator on each side of the Rise; many isolated low values were correlated with topography, suggesting an effect of local environment
<i>Von Herzen and Maxwell</i> , 1964	0745	1	Preliminary Mohole site, 75 km E of Guadalupe Is.	Heat flow almost constant to a depth of 154 meters; the average value, 2.81, agreed well with other measurements nearby using Bullard-type probes penetrating only a few meters
<i>Von Herzen</i> , 1964a	0672-0744	78	West of U.S. and Baja California	High heat flow values near the N. American west coast: 3 or 4 times normal north of Mendocino fault and 2 times normal in the borderland of southern and Baja California; heat flow seems to be uninterrupted across the Mendocino fracture zone
<i>Rhea et al.</i> , 1964	1114-1132	23	Between North America and the Hawaiian Is.	Values ranged from 0.8 to 2.8 and averaged 1.4; no significant differences in heat flow were recognized over various topographic provinces, including the Hawaiian ridge and the Molokai fracture zone
<i>Uyeda and Horai</i> , 1964	0621-0636	16	Pacific off Japan	Low heat flow (<1) prevailed in the oceanic area directly east of northeastern Japan
<i>Yasui and Watanabe</i> , 1965	0637-0671 1140-1142	38	Japan Sea	Moderately high heat flow (<2) in most parts of Japan Sea Basin
<i>Langseth et al.</i> , 1965	1052-1113	62	East Pacific	A broad heat flow maximum (~3) near the East Pacific Rise at 10°N and 3 singular peaks of high heat flow at 17°S; area of high heat flow seems to extend from the East Pacific Rise to the Gulf of Panama

station is used instead of a vessel. Slow drifting of the ice-island permits some twenty closely spaced stations. Remarkably uniform heat flow values (1.41 ± 0.06 s.d. $\mu\text{cal}/\text{cm}^2 \text{ sec}$) are observed in the abyssal plain of the Canada Basin and lower values (1.15 ± 0.25 s.d.) over the Alpha Rise. This variation is thought to be caused by nonuniform thermal conductivity.

Heat flow data from the Arctic Ocean have

been catalogued in the Appendix but were received too late to be included in the analysis.

5. GLOBAL REVIEW OF HEAT FLOW DATA

Heat flow data that have been regionally reviewed in the last two sections are now synthesized, with simple generalizations, on a worldwide basis. We shall proceed from large-scale regions to smaller ones.

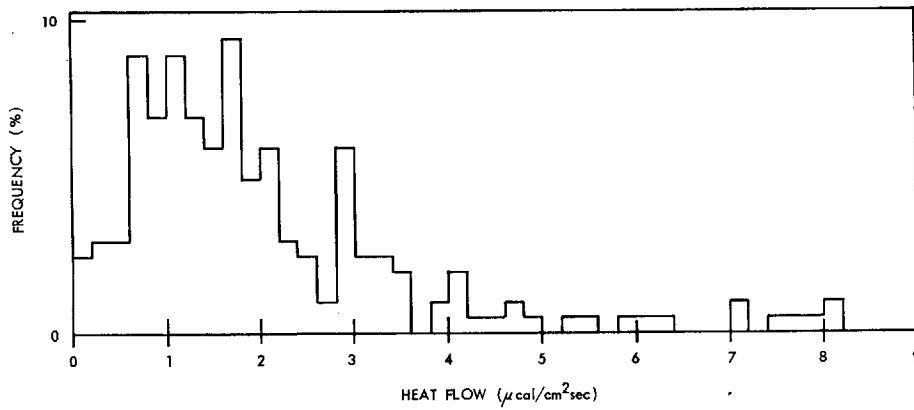


Fig. 28. Histogram of heat flow values from Pacific ridges.

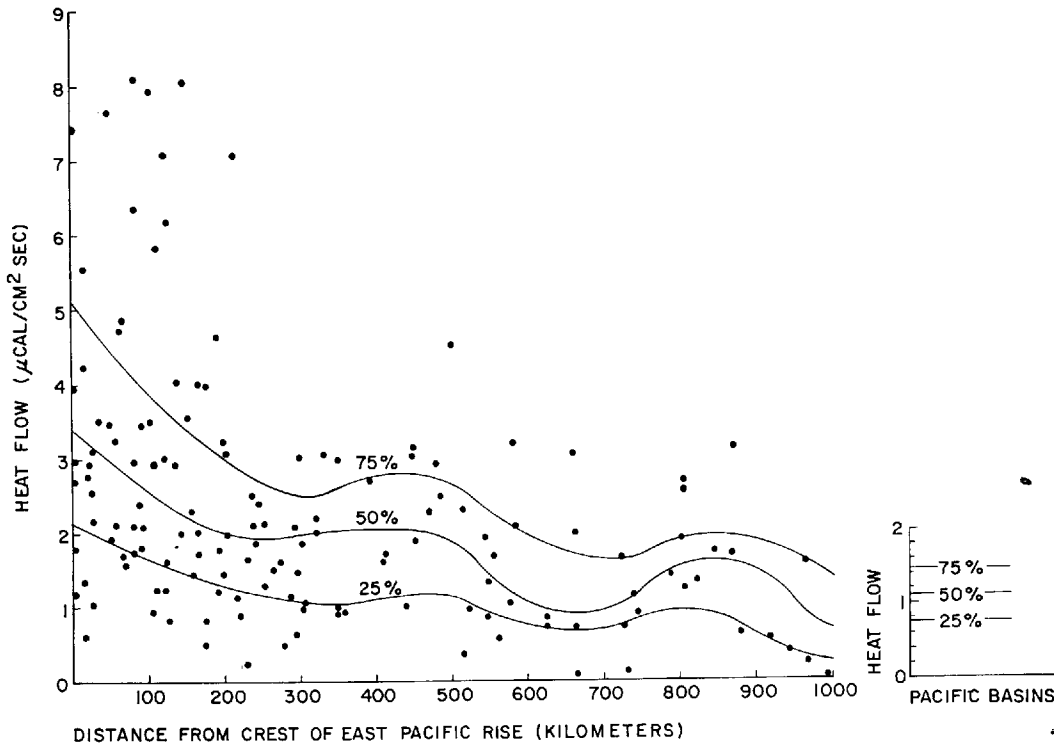


Fig. 29. Heat flow values versus distance from the crest of the East Pacific Rise (50°S to 20°N). 75-, 50-, and 25-percentile lines are given for values from the East Pacific Rise and the Pacific basins. For example, the 50-percentile line separates half the data points above and half the data points below it.

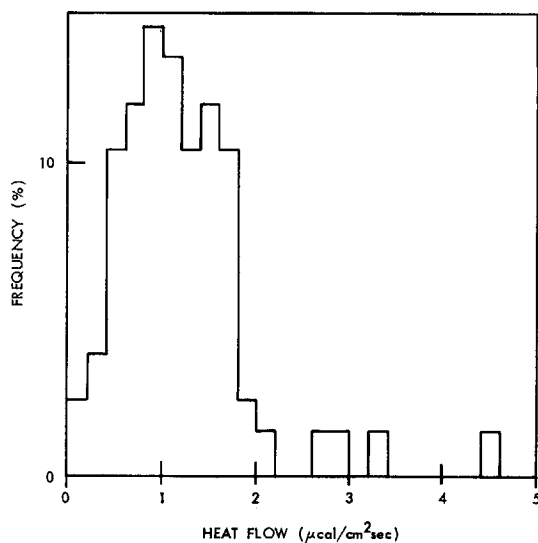


Fig. 30. Histogram of heat flow values from Pacific basins.

5.1 World

The global heat flow data have been shown in Figures 1a and 1b, where the number and arithmetic mean of analyzed data in 5° by 5° grid are given.

Statistics. A histogram of the world's heat flow values is given in Figure 32a. The mode occurs at $1.1 \mu\text{cal}/\text{cm}^2 \text{ sec}$, and the number of data drops off rather rapidly and symmetrically on both sides of this value to 0 and about $2.5 \mu\text{cal}/\text{cm}^2 \text{ sec}$, with a long 'tail' toward high values. The slight skewness of the distribution causes the average heat flow to exceed the most frequently observed value. The arithmetic mean of 1043 'published' heat flow values is $1.58 \pm 1.12 \text{ s.d.}$; that for 1150 values including 'unpublished' ones is essentially the same: $1.58 \pm 1.14 \text{ s.d.}$ For comparison, these results and previous ones are given in Table 10.

Heat flow values greater than $3 \mu\text{cal}/\text{cm}^2 \text{ sec}$ are uncommon and may not be representative of the conducted heat flow. If these values are excluded, the arithmetic mean of 951 published values (0 to $3 \mu\text{cal}/\text{cm}^2 \text{ sec}$ only) is $1.33 \pm 0.63 \text{ s.d.}$ However, we can also argue that a fair amount of low heat flow values (about 120 values are less than $0.6 \mu\text{cal}/\text{cm}^2 \text{ sec}$) are also not representative of the conducted heat flow.

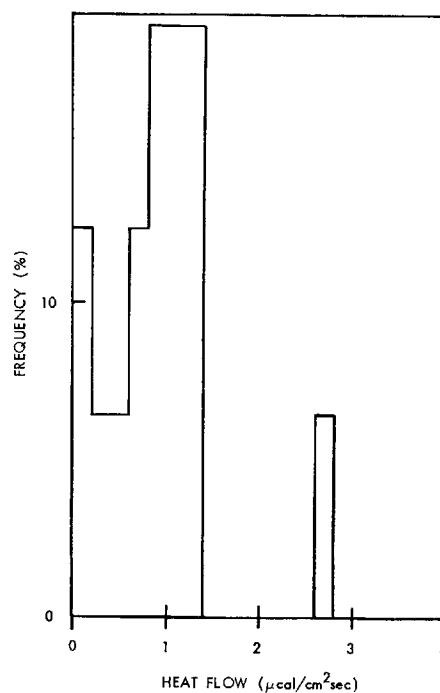


Fig. 31. Histogram of heat flow values from Pacific trenches.

If these low values are excluded, then the arithmetic mean will increase again.

Weighted statistics. Because of uneven geographical distribution of observations, Lee [1963] introduced successive averaging weighted according to areas of the grids (bounded by meridians and parallels) chosen. The advantage is in reducing sampling bias, but there is also a danger of over-weighting isolated values. Since grids formed by latitudes and longitudes have unequal area, the averaging process by Lee [1963] does not give an unbiased sample of grid averages. To avoid this difficulty, averages for grids of equal area are computed (for convenience, we take an area of 300 by 300 square nautical miles, i.e., 5° by 5° at the equator). A histogram of these equal-area averages is given in Figure 32b. The arithmetic mean for 389 such averages is $1.43 \pm 0.75 \text{ s.d.}$ Smoothing of data is indicated by the decrease of the standard deviation, and sampling bias toward too high a value is reduced by the decrease of the mean.

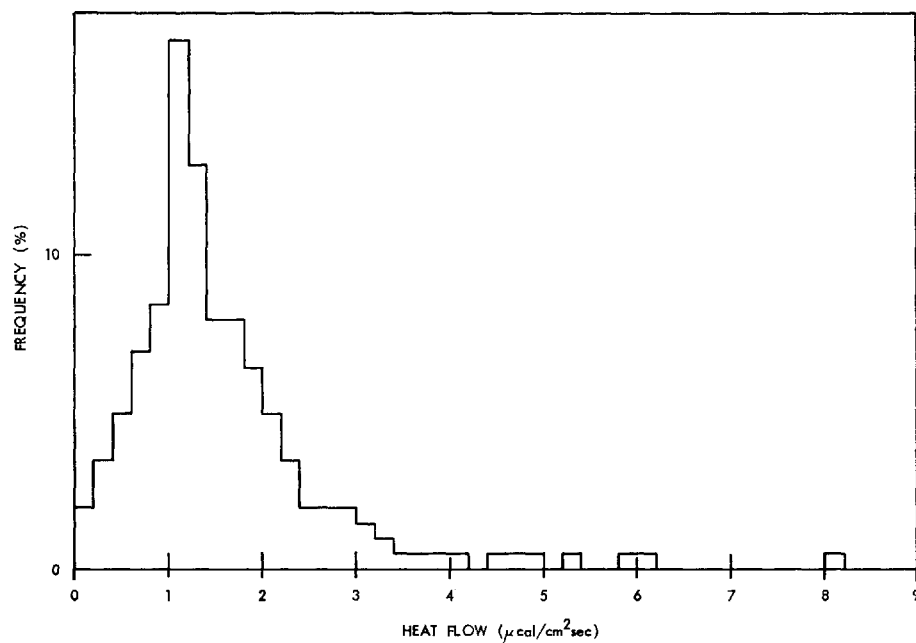


Fig. 32a. Histogram of world's heat flow values.

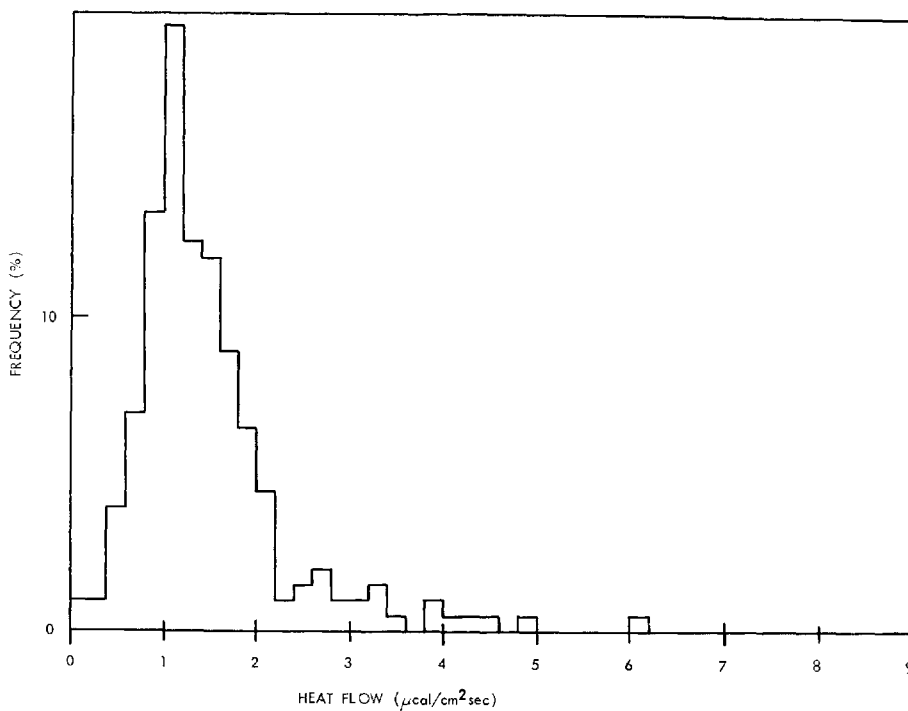


Fig. 32b. Histogram of world's heat flow grid averages (9×10^4 square nautical miles per grid).

TABLE 10. Statistics of World's Heat Flow Values

Date	Number of Values	Mean	Standard Deviation	Standard Error	Mode	Reference
Jan. 1963	634	1.62	1.21	0.05	1.1	Lee [1963]
June 1963	757	1.61	1.16	0.04	1.1	Lee and MacDonald [1963]
Feb. 1964	987	1.58	1.16	0.04	1.1	Lee [1965]
Dec. 1964	1043 *	1.58	1.12	0.04	1.1	This article
Dec. 1964	1150 †	1.58	1.14	0.03	1.1	This article
Dec. 1964	389 ‡	1.43	0.75	0.04	1.1	This article

* Published values.

† Published and unpublished values.

‡ Grid (300 by 300 square nautical miles) averages derived from 1150 individual values.

Mean heat flow. The world's mean heat flow by conduction is defined as

$$\bar{q} = \int_{\sigma} q d\sigma / \int_{\sigma} d\sigma \quad (3)$$

where the integration is over the entire surface of the Earth. Lee [1963] has estimated \bar{q} from spherical harmonic analysis and concludes that at the 95% confidence level

$$\bar{q} = 1.5 \pm 10\% \text{ ucal/cm}^2 \text{ sec} \quad (4)$$

Current analysis with twice the amount of data confirms this result.

Heat loss from the Earth's interior. The amount of heat losses from the Earth's interior is an important geophysical quantity in considering its origin, constitution, and behavior. The total heat loss by conduction Q through the Earth's surface can be estimated from the world's mean heat flow and the surface area of the Earth ($5.1 \times 10^{18} \text{ cm}^2$) as

$$Q = 7.7 \times 10^{12} \pm 10\% \text{ cal/sec} \quad (5)$$

To this value of conducted heat, we must add heat loss transported by hot mobile constituents, such as volcanic ash and lavas, steam, and hot water. Lotze [1927] estimates the heat loss from volcanic eruptions to be of the order of $2 \times 10^{10} \text{ cal/sec}$ for the Earth, and Verhoogen [1946] estimates that the heat escaped during volcanic activity since the Precambrian is of the order of $3 \times 10^9 \text{ cal/sec}$. Although these estimates are crude, they are orders of magnitude less than the conducted heat. Hence the amount of heat loss from the Earth's interior is essentially given by the conducted heat: $7.7 \times 10^{12} \text{ cal/sec}$.

Sources of heat. Radioactivity is probably the main source of heat, and other sources, such as tidal dissipation, initial heat, etc., are believed to be small [Bullard *et al.*, 1956; Gutenberg, 1959]. The observed heat losses from the Earth's interior can be completely accounted for if we assume that the entire Earth has the same potassium, thorium, and uranium content as chondritic meteorites and that the heat arrives at the Earth's surface at the same rate as that at which it is generated. Since the thermal conductivity of solid rock is rather low, it can be shown that the heat generated below a few hundred kilometers has not been conducted to the surface even in billions of years [Slichter, 1941]. To explain the observed heat flow by radioactive decay in a chondritic Earth model, either one or both of the following are required: the radioactive elements are concentrated in the outer few hundred kilometers, or there are other mechanisms to transfer heat more quickly than by the assumed conduction alone. Recently the validity of a chondritic Earth model has been questioned because the K/U ratio for terrestrial rocks is about 1×10^4 , whereas that for the meteoritic materials is about 7×10^4 [Wasserburg *et al.*, 1964]. The main difficulty is our present ignorance of the radioactivity at depth, and the observed heat flow does not uniquely determine the internal concentration of radioactivity.

5.2 Continents and Oceans

The first-order feature of the Earth's surface is its division into continents and oceans by the sea level. Although many shallow water areas

have continental structure, we shall ignore this modification because current oceanic heat flow techniques cannot safely be applied in shallow water.

Statistics. Histograms of continental and oceanic heat flow are shown in Figures 33a and 34a, respectively. These two histograms are very different. The continental values do not extend beyond $3 \mu\text{cal}/\text{cm}^2 \text{ sec}$ because values from geothermal areas on land have been excluded from the analysis. Thus we probably should compare only the part of the histogram from 0 to $3 \mu\text{cal}/\text{cm}^2 \text{ sec}$. In this part the land values seem to be divided into two subgroups—around 1 and $2 \mu\text{cal}/\text{cm}^2 \text{ sec}$ —whereas at sea there is only one group. The modes for both land and sea values are the same: 1.1. The arithmetic mean for 131 continental values is $q_c = 1.43 \pm 0.56$ s.d., whereas for 793 oceanic values (excluding those $>3 \mu\text{cal}/\text{cm}^2 \text{ sec}$), the mean is $q_o = 1.31 \pm 0.65$ s.d. (the arithmetic mean for all 913 oceanic values is $q_o = 1.60 \pm 1.18$ s.d.). Since $|q_o - q_c| < 0.2 \mu\text{cal}/\text{cm}^2 \text{ sec}$ in both cases, the difference between the heat flow averages on land and at sea is *not* significant (see section 2.3). This conclusion is further supported by considering the weighted statistics.

Weighted statistics. As we remarked in section 5.1, averages over grids of equal area tend to reduce sampling bias and hence are more representative values. Histograms for continental and oceanic grid averages (9×10^4 square nautical miles) are given in Figures 33b and 34b, respectively. The arithmetic mean for 51 continental grid averages is 1.41 ± 0.52 s.d., whereas that for 340 oceanic ones is 1.42 ± 0.78 s.d. The difference is clearly insignificant.

Equality of heat flow. The equality of heat flow between oceans and continents suggests that radioactivity is roughly the same beneath land and sea. Since the continental and oceanic crusts are very different in thickness and probably in composition, this further suggests that there are differences between the upper mantle under the continents and that under the oceans. Most of the continental heat flow (about 70%) can be easily accounted for by the radioactivity of the continental crust, assuming it has intermediate composition (e.g. granodiorite). Since the continental crust is about 35 km thick, and since some heat must come from below the Mohorovicic discontinuity, the difficulty is not

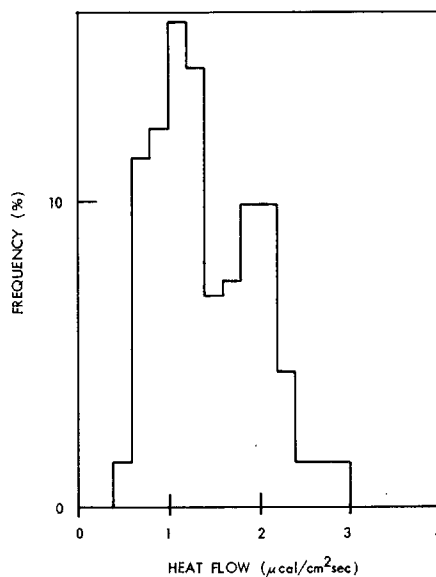


Fig. 33a. Histogram of continental heat flow values.

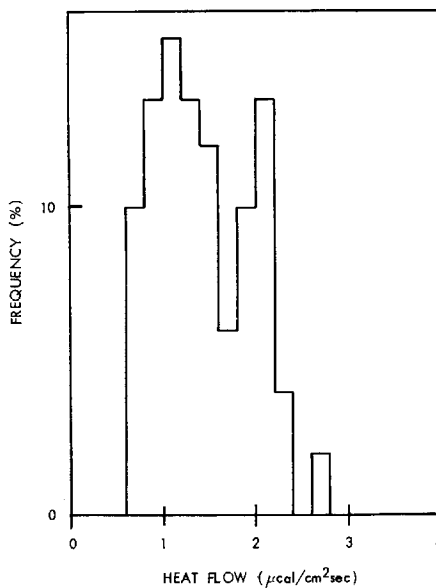


Fig. 33b. Histogram of continental heat flow grid averages (9×10^4 square nautical miles per grid).

the lack of a heat source but to explain why the continental heat flow is not greater than it is. A simple explanation may be that the radioactivity of the continental crust is much less than that of granodiorite. On the other hand,

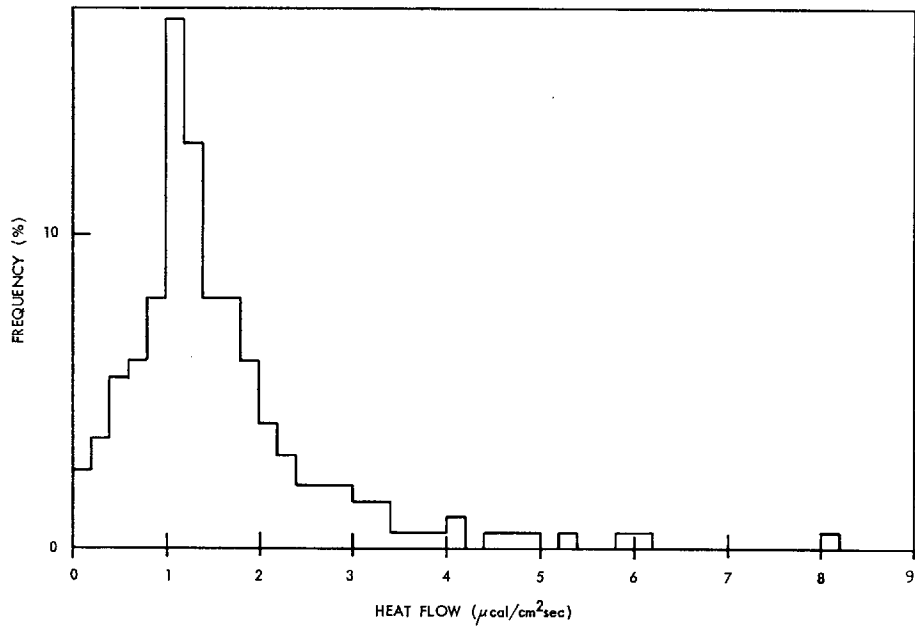


Fig. 34a. Histogram of oceanic heat flow values.

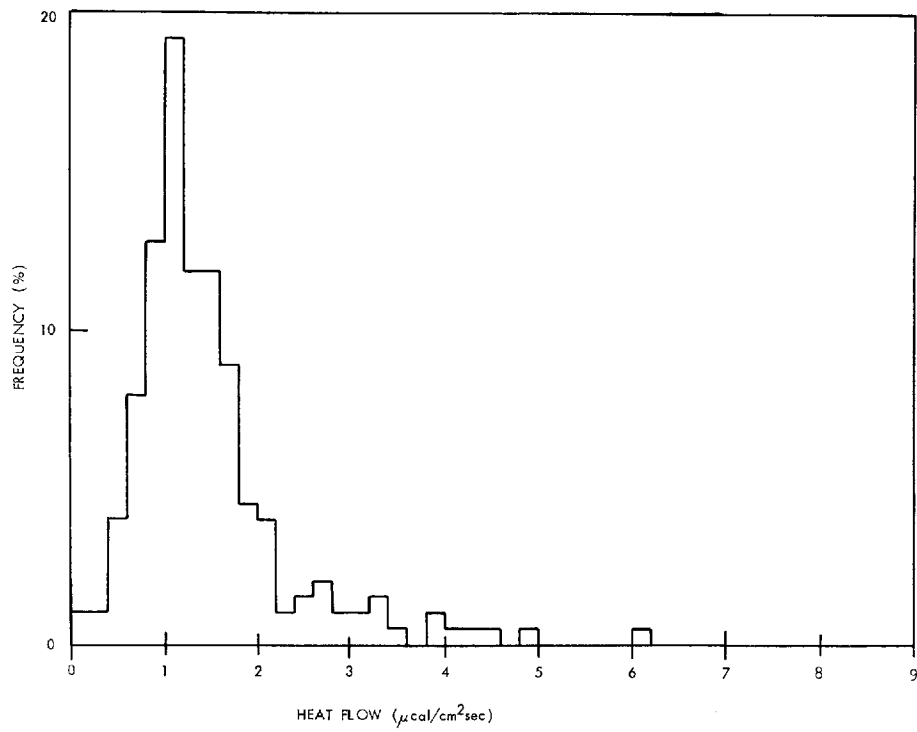


Fig. 34b. Histogram of oceanic heat flow grid averages (9×10^4 square nautical miles per grid).

TABLE 11. Statistics of Heat Flow Values for Various Continents

Continent	Number of Values	Mean	Standard Deviation	Standard Error	Modes	Remark
Africa	13	1.20	0.20	0.06	1.3	Almost all data from South Africa
Asia	37	1.49	0.58	0.10	1.1 and 1.3	Almost all data from Japan
Australia	19	1.75	0.62	0.14	2.1	
Europe	22	1.62	0.60	0.13	0.7 and 1.9	
North America	40	1.19	0.44	0.07	1.1	
All continents	131	1.43	0.56	0.05	1.1	
Grid averages of all continents	51	1.41	0.52	0.07	1.1	9×10^4 square nautical miles per grid

the oceanic crust is thin (about 7 km) and may be of basaltic composition, which contains about 30% of the radioactivity of granodiorite. Thus, if the oceanic crust is basaltic, most of the oceanic heat flow (about 90%) must come from below the Mohorovicic discontinuity. The main problem is then to find a source for the heat and a way of getting it to the oceanic surface without invoking a temperature above the melting point at a depth of a few hundred kilometers or contradicting other geophysical evidence. MacDonald in Chapter 7 of this volume shows that a variety of concentrations of radioactive elements within the Earth is consistent with the observed heat flow and with the estimated melting gradient, provided that radiative transfer is effective.

Various continents. Statistics of heat flow values for various continents are summarized in Table 11. Since heat flow values are few for individual continents and their distributions are uneven, no definite conclusion can be drawn.

Various oceans. Statistics of heat flow values for various oceans are summarized in Table 12 with histograms shown in Figures 35*a* and *b*, 36*a* and *b*, and 37*a* and *b*. Although all oceans have values extending to higher values, the main parts (0 to 3 $\mu\text{cal}/\text{cm}^2 \text{ sec}$) of the histograms are quite different. The mean and scattering of values increases from the Atlantic to the Indian Ocean and to the Pacific. These differences may be related to their different structures and histories. However, they may also be caused by nonuniform sampling of measure-

TABLE 12. Statistics of Heat Flow Values for Various Oceans

	Number of Values	Mean	Standard Deviation	Standard Error	Modes
A. Individual values					
Atlantic	206	1.29	1.00	0.07	1.1
Indian	210	1.47	0.89	0.06	1.3
Pacific	497	1.79	1.31	0.06	1.1
All Oceans	913	1.60	1.18	0.04	1.1
B. Grid averages (9×10^4 square nautical miles per grid)					
Atlantic	65	1.21	0.64	0.08	1.1
Indian	94	1.35	0.67	0.07	1.3
Pacific	181	1.53	0.87	0.06	1.1
All Oceans	340	1.42	0.78	0.04	1.1

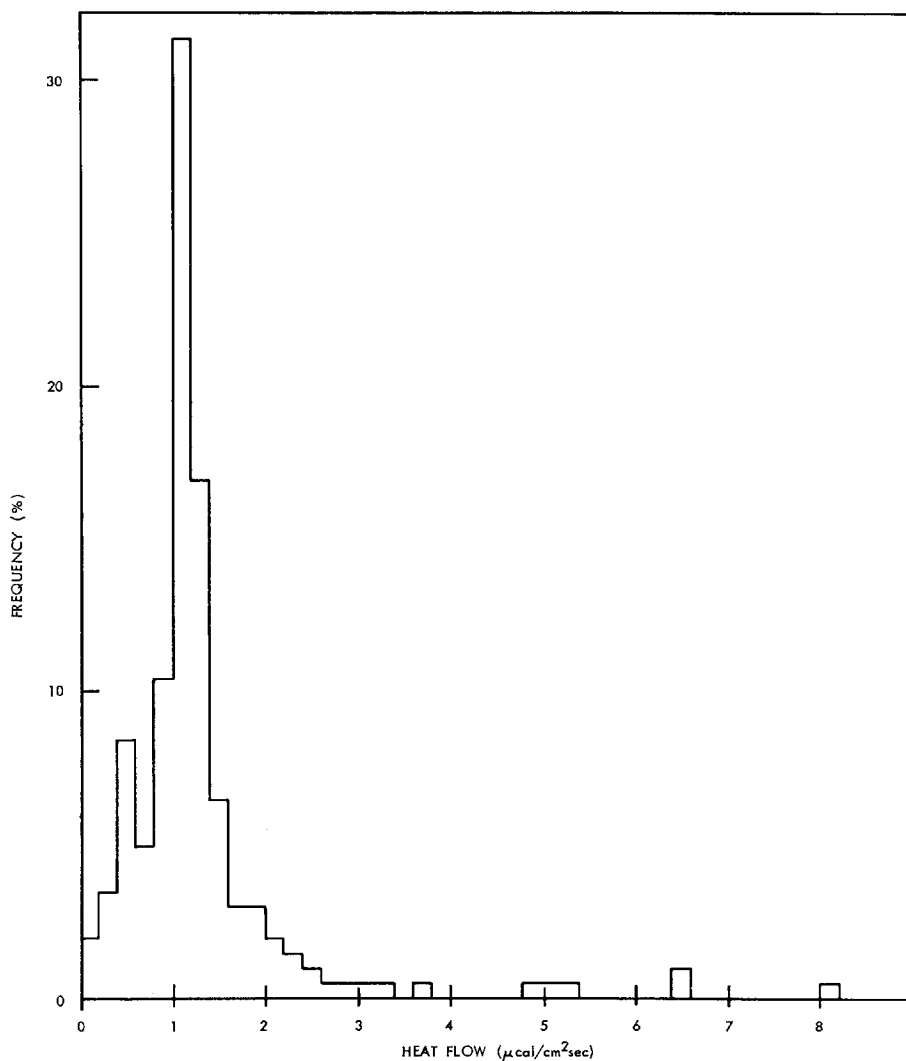


Fig. 35a. Histogram of Atlantic heat flow values.

ments (ratio of number of values from ridges to that from basins varies from about 1:1 in the Atlantic and the Indian oceans to about 2:1 in the Pacific). When grid averages are compared (see Table 12, section *B*), heat flow values are approximately the same for various oceans.

5.3 Major Geological Features

Figure 38 shows a *gross* picture of the major geological features of the Earth's surface, and statistics of heat flow values corresponding to these features on land are summarized in Table 13 and those at sea in Table 14.

5.3.1 Land

Shields and non-shields. About 80% of the land surface is covered by post-Precambrian rocks. When Precambrian rocks are exposed in large continental areas, they are called *shields*. The shields are generally areas of low relief and have been very stable since the Precambrian. Heat flow results bear witness to their stability. A histogram of shield values is given in Figure 39a, and statistics for them are summarized in section 1 of Table 13. Heat flow values are very uniform in all shield areas, and the average is 0.92 ± 0.17 s.d. On the other hand, heat flow

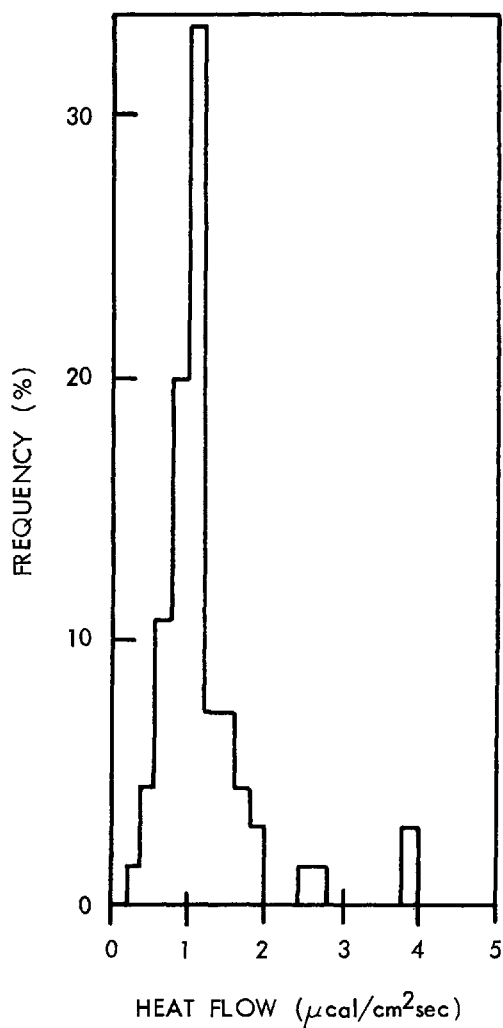


Fig. 35b. Histogram of Atlantic heat flow grid averages (9×10^4 square nautical miles per grid).

values outside the shields are usually higher and have greater variation, as seen in sections 2, 3, and 4 of Table 13.

Post-Precambrian orogenic and non-orogenic areas. In areas covered by the post-Precambrian rocks, interior lowlands and mountain belts are generally recognized. The former are little disturbed and underlain by Precambrian formations; the latter have been severely deformed during orogenesis. Sections 2 and 3 in Table 13 and Figures 39b and 39c summarize the results of the heat flow values in these two areas. Their averages are essentially the same, but

heat flow values in the orogenic areas are more scattered. The average heat flow undoubtedly will be higher in the orogenic areas if we include data from Cenozoic volcanic areas.

Heat flow values from the Interior Lowlands of Australia are much higher than those of North America's Interior Lowlands and may be related to Cenozoic volcanism.

With the exception of the East Australian Highlands, the Paleozoic orogenic areas have much smaller heat flow values than later orogenic areas. The Alpine and Cordilleran systems are characterized by relatively high heat flow. Cenozoic volcanic areas are associated with high heat flow, as is expected (see Table 13).

Among island arc areas (Figure 39d), extensive heat flow studies have only been carried out in Japan (see section 3.3).

5.3.2 Oceans

The ocean floor consists of three major morphological divisions: (1) continental margin, (2) ocean-basin floor, and (3) mid-oceanic ridge, each occupying about one-third the area [Heezen and Menard, 1963]. For heat flow studies, major features of the oceans are basins, ridges, and trenches (see Figure 38). Basins are characterized by relatively smooth bottom, deep water, normal thickness of oceanic crust, and aseismicity. Trenches are usually associated with island arcs, very deep water, and strong seismicity. Ridges have rugged relief and shallow water, and can be further divided into two groups according to seismicity. The seismic active mid-ocean ridge system is a spectacular feature [Heezen and Ewing, 1963], whereas aseismic ridges are small and occupy little area. Since heat flow data are few over aseismic ridges, we have not made this distinction. For convenience, any stations that do not clearly fall into the three categories of basins, ridges, and trenches are grouped under 'other areas.'

Statistics of heat flow values in basins, ridges, trenches, and other areas are summarized in Table 14, and corresponding histograms are given in Figures 40, 41, 42, and 43. Heat flow values in the ocean basins are fairly uniform and rather low, whereas those in the ridges and 'other areas' are higher and more scattered. The average of the trench values is rather low ($\sim 1 \mu\text{cal}/\text{cm}^2 \text{ sec}$). However, the trench data

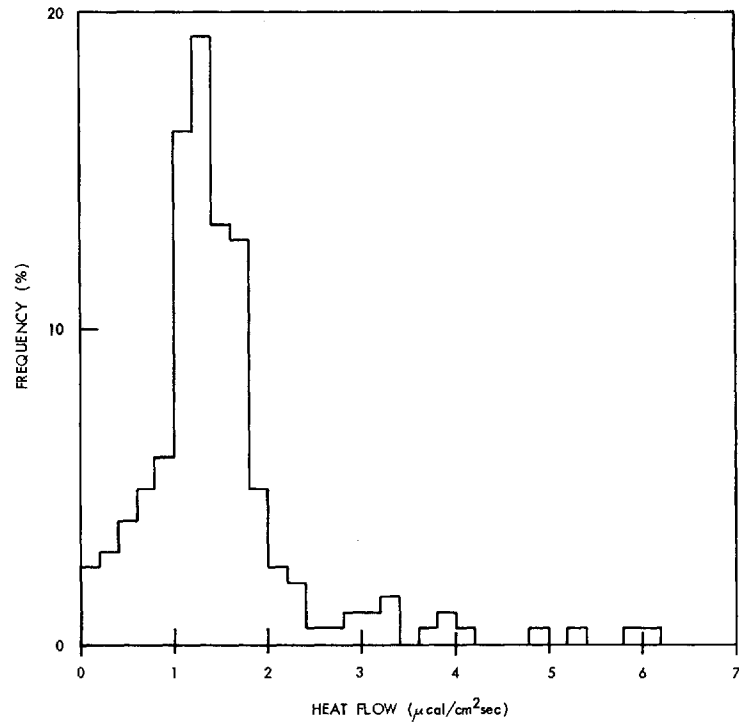


Fig. 36a. Histogram of Indian Ocean heat flow values.

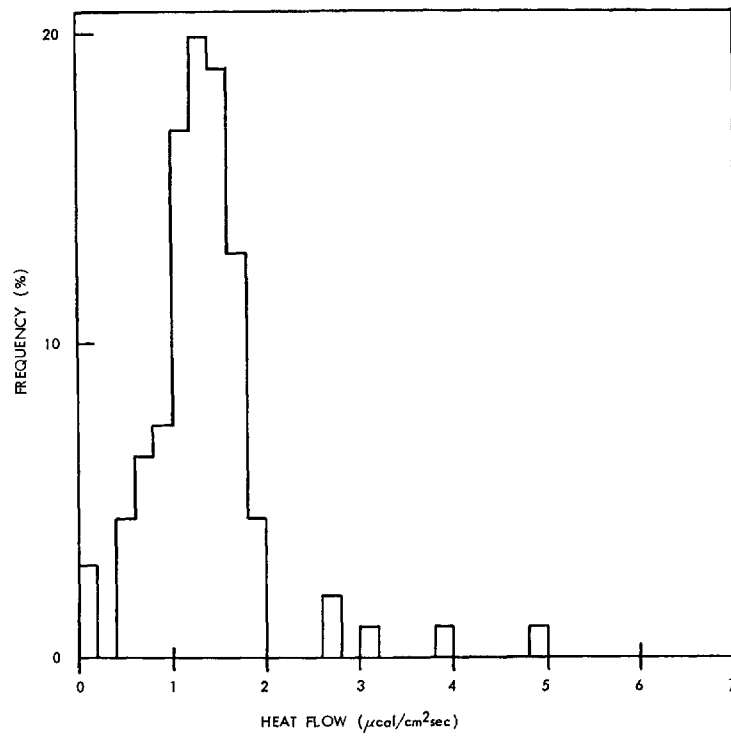


Fig. 36b. Histogram of Indian Ocean heat flow grid averages (9×10^4 square nautical miles per grid).

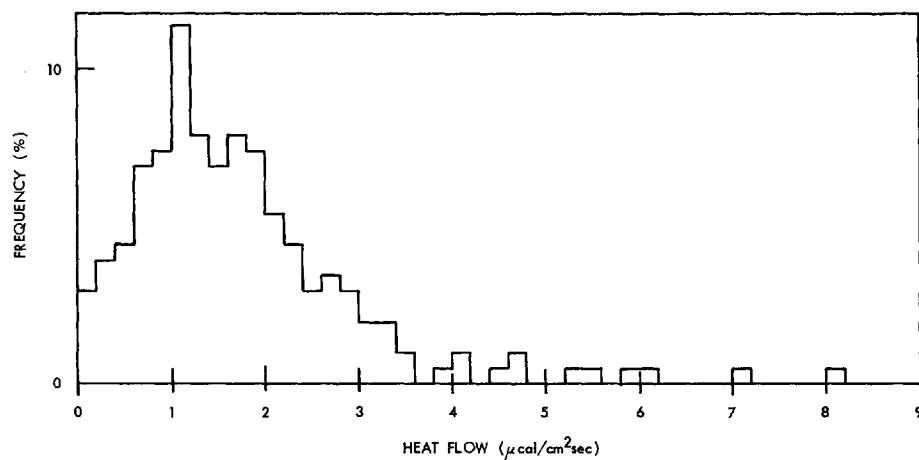


Fig. 37a. Histogram of Pacific heat flow values.

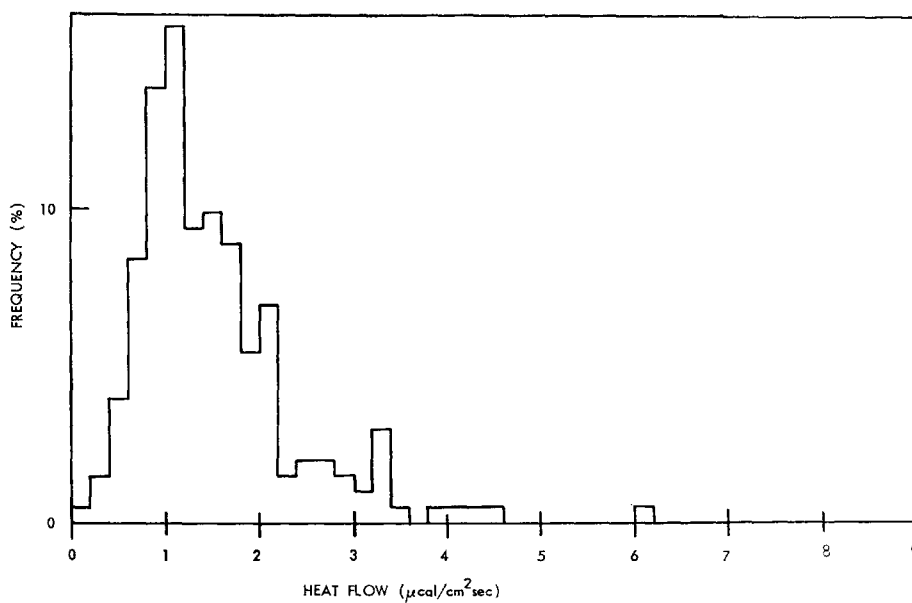


Fig. 37b. Histogram of Pacific heat flow grid averages (9×10^4 square nautical miles per grid).

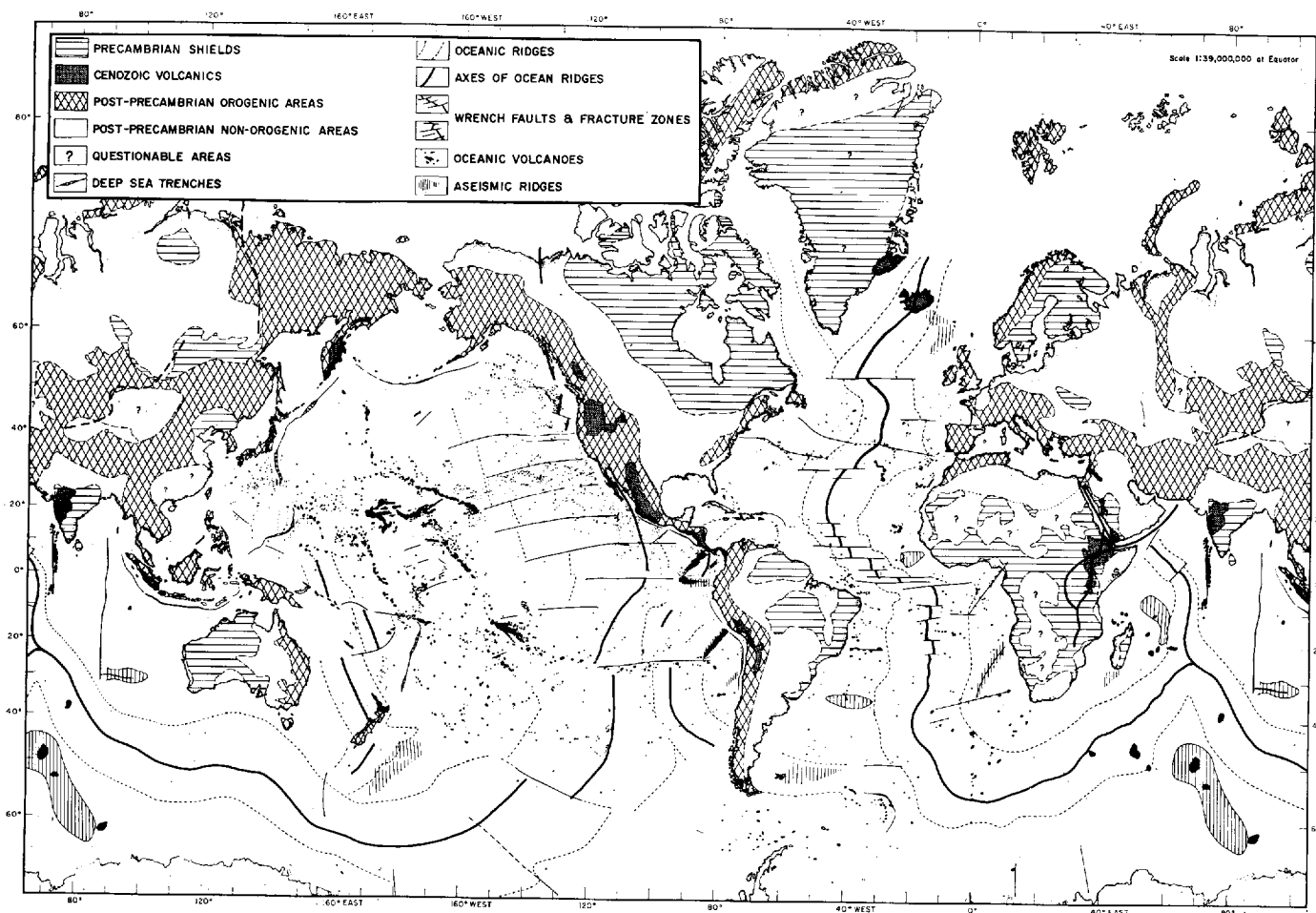


Fig. 38. Major geological features of the Earth. Most oceanic geological features are taken from *Menard* [1965], with a few additional data taken from *Fisher and Hess* [1963], *Heezen* [1962], *Heezen and Ewing* [1963]. Geological features on land are compiled from various geological maps.

TABLE 13. Statistics of Heat Flow Values for Major Geological Features on Land

Geological Feature	Number of Values	Mean	Standard Deviation	Standard Error	Modes
1. Precambrian shields	26	0.92	0.17	0.03	0.9
Australian Shield	7	1.02	0.15	0.06	0.9
Ukrainian Shield	3	0.69	0.07	0.04	0.7
Canadian Shield	10	0.88	0.13	0.04	0.9
Indian Shield	1	0.66			
South African Shield	5	1.03	0.13	0.06	0.9
2. Post-Precambrian non-orogenic areas	23	1.54	0.38	0.08	1.3
Europe	1	1.67			
Interior Lowlands of Australia	7	2.04	0.18	0.07	1.9 and 2.1
Interior Lowlands of N. America	8	1.25	0.18	0.06	1.1
South Africa	7	1.36	0.10	0.04	1.5
3. Post-Precambrian orogenic areas *	68	1.48	0.56	0.07	1.1
Paleozoic orogenic areas	21	1.23	0.40	0.09	1.1
Appalachian system	12	1.04	0.23	0.07	1.1
East Australian Highlands	2	2.03	0.03	0.02	2.0
Great Britain	7	1.31	0.38	0.14	no mode
Mesozoic-Cenozoic orogenic areas	19	1.92	0.49	0.11	1.9 and 2.1
Alpine system	10	2.09	0.38	0.12	1.9 and 2.1
Cordilleran system	9	1.73	0.53	0.18	1.3, 2.1, 2.3
Island Arc areas	28	1.36	0.54	0.10	1.1
4. Cenozoic volcanic areas (excluding geothermal areas)	11	2.16	0.46	0.14	2.1

* Excluding Cenozoic volcanic areas.

TABLE 14. Statistics of Heat Flow Values for Major Geological Features at Sea

Geological Feature	Number of Values	Mean	Standard Deviation	Standard Error	Modes
1. Ocean basins	273	1.28	0.53	0.03	1.1
Atlantic Ocean	74	1.13	0.24	0.03	1.1
Indian Ocean	90	1.34	0.42	0.04	1.1
Pacific Ocean	75	1.18	0.69	0.08	0.9
Mediterranean seas	8	1.20	0.22	0.08	1.5
Marginal seas	26	1.83	0.60	0.12	1.9
2. Ocean ridges	338	1.82	1.56	0.09	1.1
Atlantic Ocean	87	1.48	1.48	0.16	0.5
Indian Ocean	85	1.57	1.17	0.13	1.3
Pacific Ocean	166	2.13	1.70	0.13	1.7
3. Ocean trenches	21	0.99	0.61	0.13	1.1
4. Other areas	281	1.71	1.05	0.06	1.1
Atlantic Ocean	24	1.16	0.33	0.07	1.1
Indian Ocean	27	1.53	0.85	0.16	1.5
Pacific Ocean	209	1.80	1.13	0.08	1.1
Mediterranean seas	14	1.50	0.87	0.23	1.1
Marginal seas	7	1.71	0.57	0.21	1.7

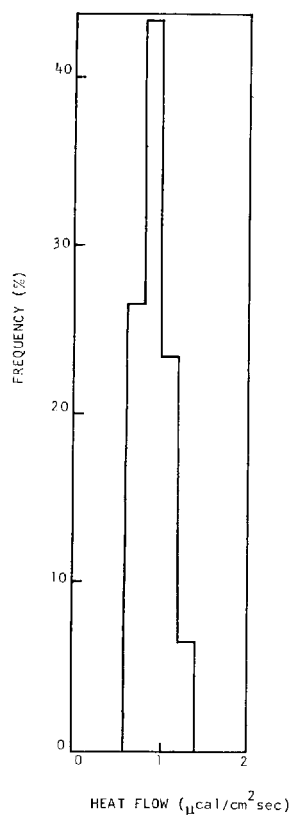


Fig. 39a. Histogram of heat flow values from Precambrian shields.

(21 in number) are still too few to be of great significance.

Basins. Heat flow values from basins of various oceans are similar (Figures 16, 21, and 30), although the average is highest for the Indian Ocean and the scattering is greatest for the Pacific (section 1 of Table 14). For basins in adjacent seas, data are still insufficient to draw definite conclusions. The relatively high average for marginal seas is mainly due to moderately high values obtained in the Japan Sea (see section 3.3).

Ridges. The crestal zones of ridges are usually characterized by high heat flow and large variations, whereas relatively low values are observed over the flanks. Details for each ocean have been discussed previously. Section 2 in Table 14 summarizes the statistics. High values observed in the crest are undoubtedly related to recent volcanisms, but the low ones are difficult to explain [Von Herzen and Uyeda, 1963].

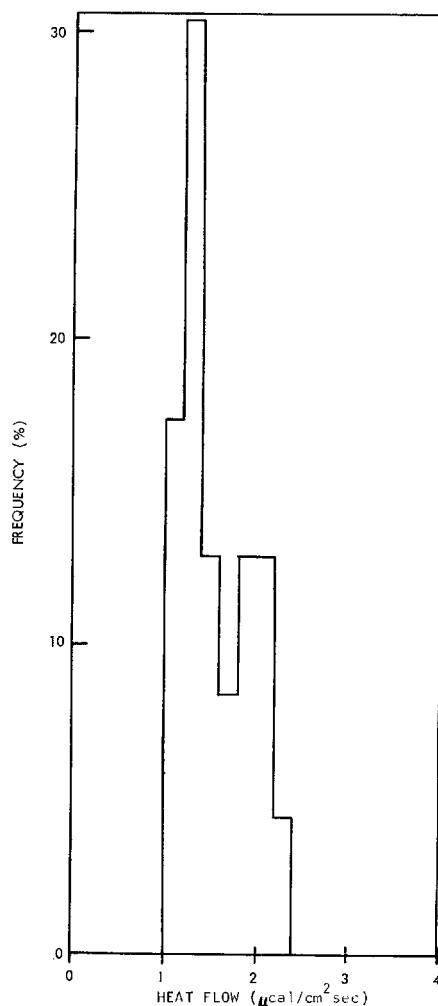


Fig. 39b. Histogram of heat flow values from post-Precambrian non-orogenic areas.

(See section 3.7, chapter 8, by Elder for a suggested explanation.)

6. GLOBAL ANALYSIS OF HEAT FLOW OBSERVATIONS

6.1 Global Representation

Having a set of heat flow observations, it is desirable to construct a contour map of isoflux that best fits the observations. It is hoped that some general picture of the heat flow pattern will appear in such a contour map, and that explanations for it will be found. Contouring is usually done by 'eye,' but it can be done more

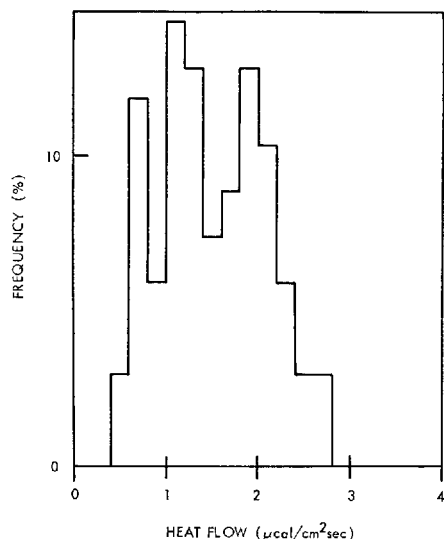


Fig. 39c. Histogram of heat flow values from post-Precambrian orogenic areas.

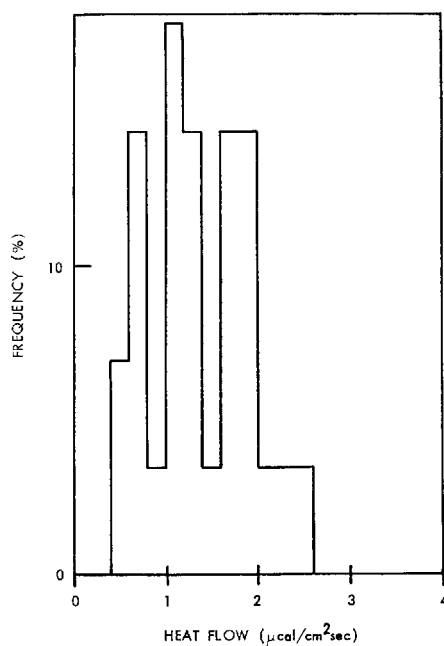


Fig. 39d. Histogram of heat flow values from island arc areas.

objectively by numerical methods using electronic computers. A set of heat flow data $q(\theta_i, \varphi_i)$, $i = 1, 2, \dots, N$, where θ_i is the colatitude, and φ_i the east longitude of the i th station, can

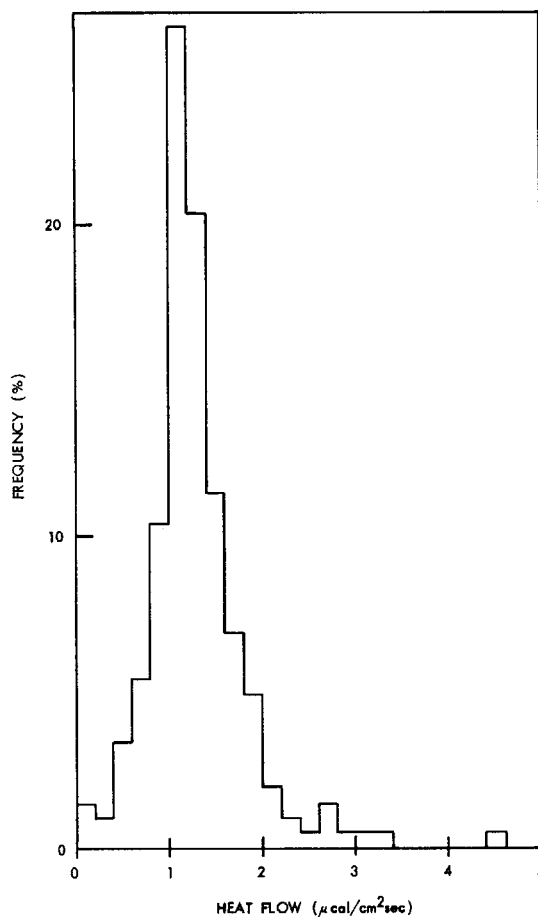


Fig. 40. Histogram of heat flow values from ocean basins.

be fitted by a least squares method to a spherical harmonic expansion of order M :

$$q(\theta, \varphi) = \sum_{n=0}^M \sum_{m=0}^n [A_n^m P_n^m(\mu) \cos(m\varphi) + B_n^m P_n^m(\mu) \sin(m\varphi)] \quad (6)$$

$$\equiv \sum_{j=1}^k t_j T_j(\theta, \varphi), \quad k \equiv (M+1)^2$$

where $\mu \equiv \cos(\theta)$, and the $P_n^m(\mu)$ are the normalized associated Legendre functions. The coefficients t_j (and hence A_n^m and B_n^m) are determined from the normal equations:

$$\sum_{j=1}^k t_j \sum_{i=1}^N T_l(\theta_i, \varphi_i) T_j(\theta_i, \varphi_i) = \sum_{i=1}^N q(\theta_i, \varphi_i) T_l(\theta_i, \varphi_i) \quad (7)$$

$l = 1, 2, \dots, k$

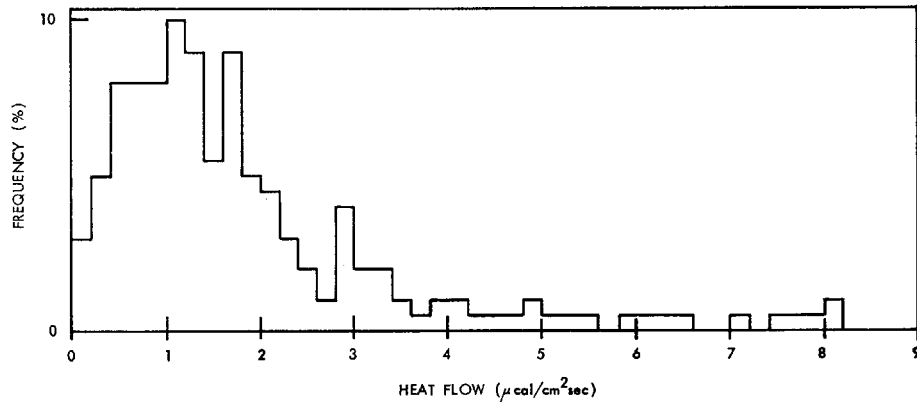


Fig. 41. Histogram of heat flow values from ocean ridges.

For observing stations on a regular grid, (7) is greatly simplified to:

$$t_j = \frac{\sum_{i=1}^N q(\theta_i, \varphi_i) T_j(\theta_i, \varphi_i)}{\sum_{i=1}^N T_j^2(\theta_i, \varphi_i)} \quad (8)$$

$j = 1, 2, \dots, k$

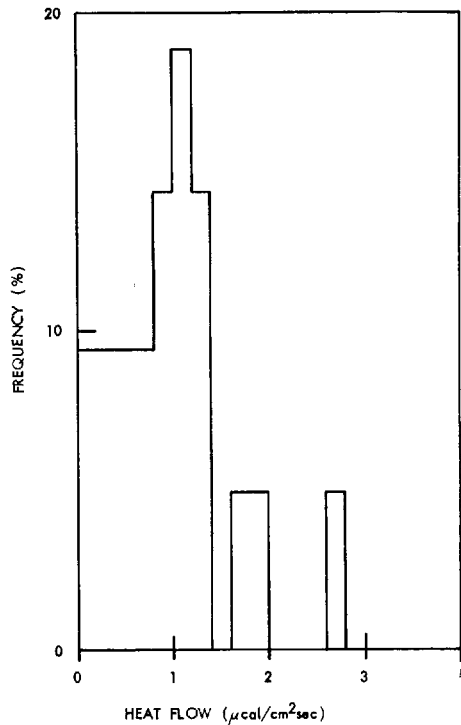


Fig. 42. Histogram of heat flow values from ocean trenches.

Although the geophysical stations are usually irregularly distributed, it is still possible to average over grid squares and use these regularly spaced averages to obtain the spherical harmonic representation. This is essentially the classical method of Gauss. The averaging smooths the values and lowers the 'energy' at wavelengths that are short compared with the intergrid distance. Such a procedure is difficult when the data are limited, for it requires judgment as to the area over which the smoothing should take place. Further, there is the problem of extrapolation into regions where no data exist. However, *Lee* [1963] did not extrapolate in this manner, but solved the set of normal equations 7 directly for t_j via matrix inversion by Jordan's method. A better computing scheme is to expand the heat flow field in functions orthogonal to the observing stations and to determine the maximum order of spherical harmonic expansion by an objective statistical test of significance [*Lee and MacDonald*, 1963].

A global representation of the heat flow field has been constructed by *Lee and MacDonald* [1963], and a revised one up to third order spherical harmonics is shown in Figure 44. Contour lines over regions where no data exist are dashed. Spherical harmonic coefficients of the heat flow field based on 987 observations are given in Table 15. A recent analysis based on all available observations gives essentially the same picture.

The main features of the heat flow field are highs over the eastern Pacific and east Africa, and lows over the Atlantic and central Pacific. However, it should be emphasized that *the*

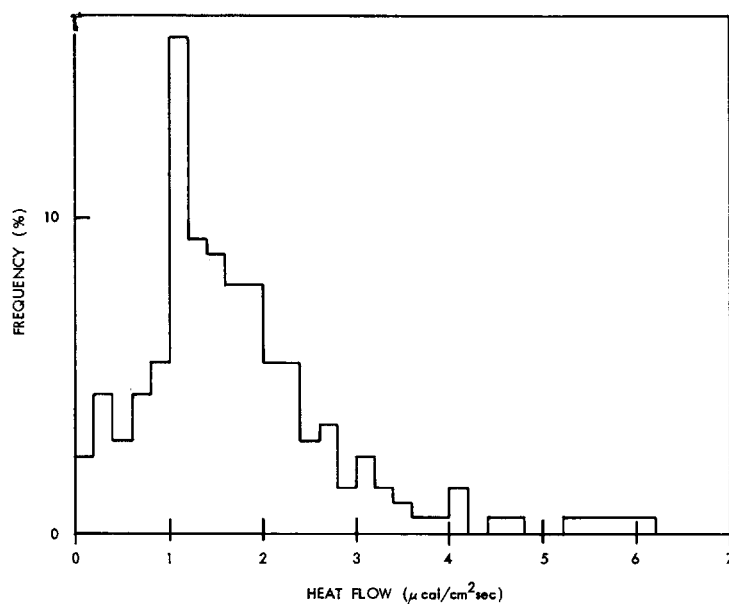


Fig. 43. Histogram of heat flow values from oceanic 'other areas.'

analysis averages out the small-scale variations in the heat flow field, and there is also a possibility that the anomalies in the heat flow field are actually much smaller-scale phenomena than those that can be represented by the low-order harmonics [Lee and MacDonald, 1963]. The resolution of third-order spherical harmonic analysis is about 2000 km; i.e., variations of a scale less than 2000 km will not appear. Nevertheless, on the average and over a large area, the heat flow is high in the eastern Pacific and low in the central Pacific and in the Atlantic. The east African high is uncertain, because there are very few measurements there.

6.2 Comparison with the Gravitational Field

Lee and MacDonald [1963] suggest that the contour representation of the heat flow shows

certain similarities to the geoid (see Figures 44 and 45). The correlation is that where gravity is high the heat flow is low and vice versa. Wang [1963, 1964] reaches similar conclusions independently by using mostly Lee's [1963] data and finds a large negative correlation coefficient of -0.82 between Izsak's [1964] satellite geoid and Lee and MacDonald's [1963] heat flow distribution. Kaula [1965] made a cross-covariance analysis of the gravity and heat flow data, the results of which are shown in Figure 46. The horizontal axis is the angular distance between stations in degrees. The vertical axis is the covariance, i.e. the mean product of heat flow and free-air gravity anomaly pairs adjusted to zero mean product as a function of distance. If heat flow and gravity were not correlated, then the points would all

TABLE 15. Spherical Harmonic Coefficients of the Heat Flow Field

$$\text{The normalization is } \int_0^\pi \int_0^{2\pi} \left[P_n^m(\mu) \begin{Bmatrix} \cos(m\varphi) \\ \sin(m\varphi) \end{Bmatrix} \right]^2 \sin \theta \, d\theta \, d\varphi = 4\pi$$

n	0	1		2		3				
m	0	0	1	0	1	2	0	1	2	3
A_n^m	1.475	0.118	0.064	-0.107	0.107	-0.044	0.037	-0.162	0.043	0.110
B_n^m			-0.018		0.085	0.133		-0.009	0.089	0.219

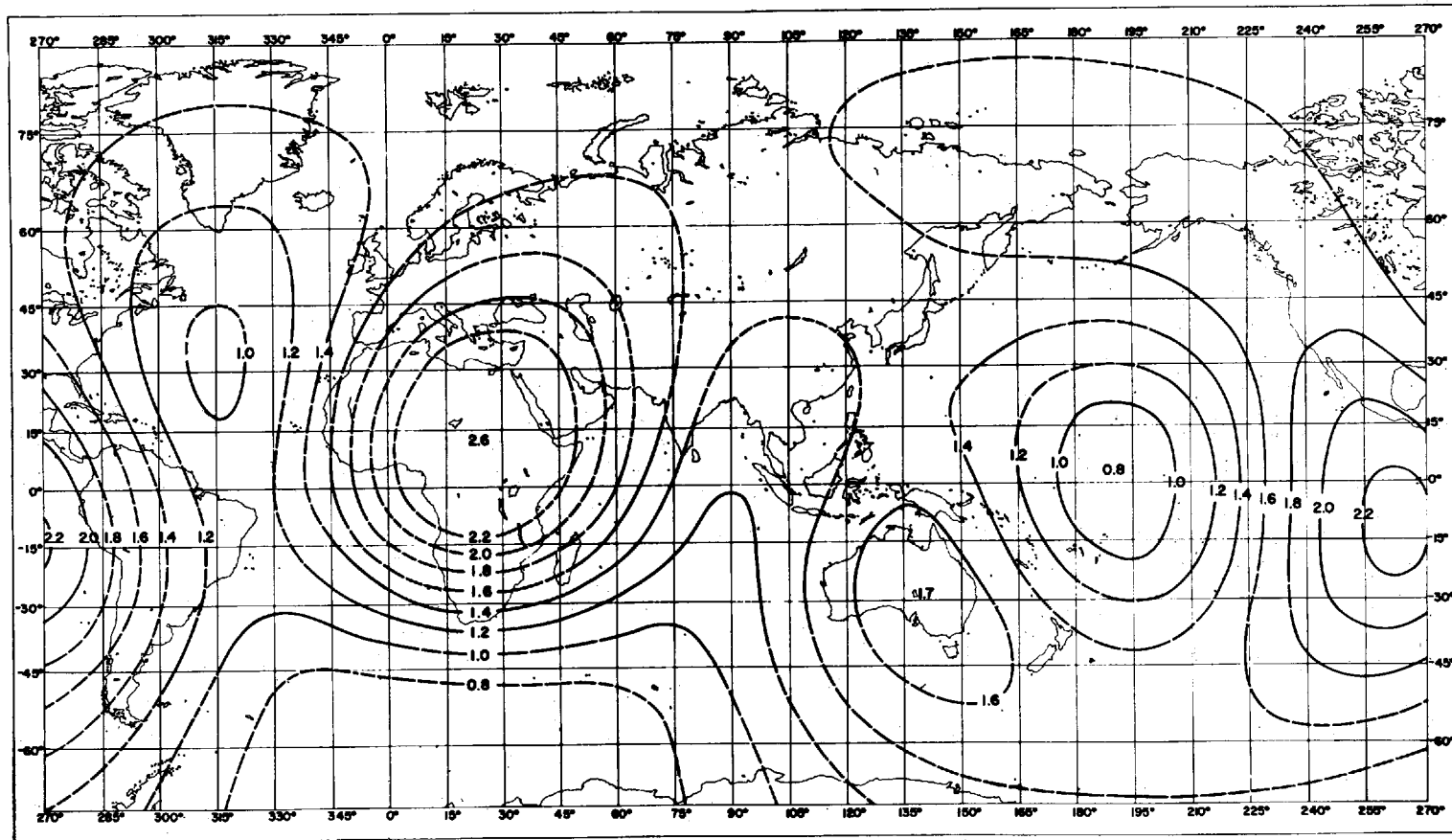


Fig. 44. Orthogonal function representation (to third-order spherical harmonics) of 987 heat flow values. Contour lines are in $\mu\text{cal}/\text{cm}^2 \text{ sec}$ and are dashed over regions where no data exist.

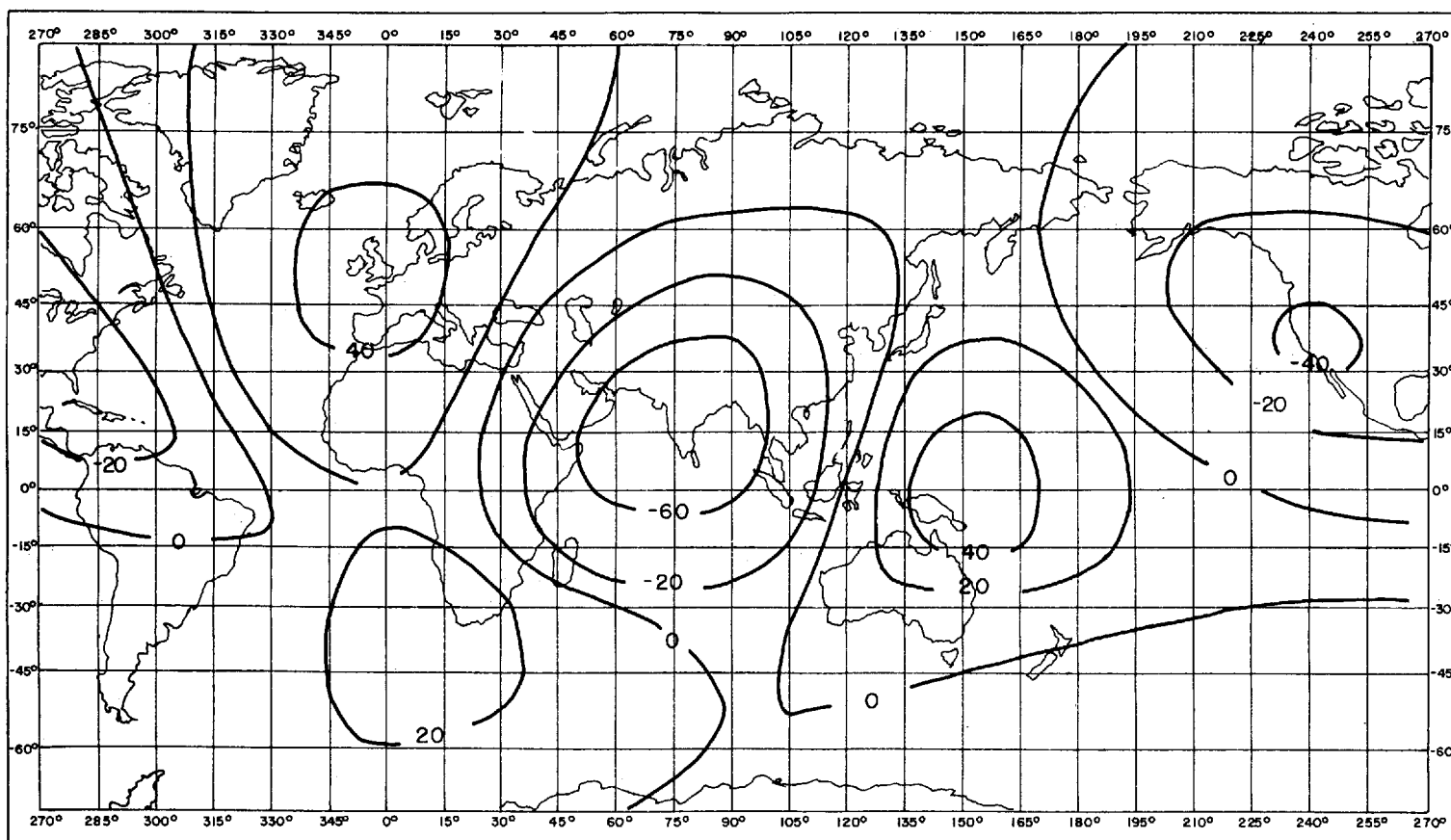


Fig. 45. Geoid heights (in meters, referring to the ellipsoid with a flattening of $1/298.37$) constructed from spherical harmonics up to third order from analysis up to eighth order of the latest artificial satellite data [Guier, 1965].

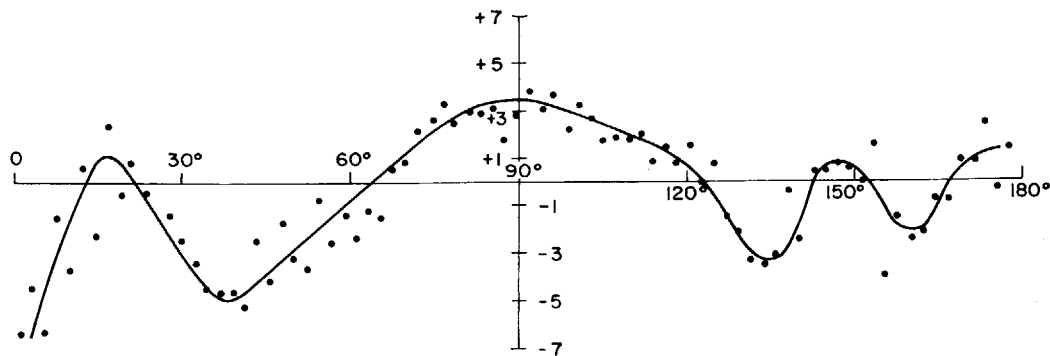


Fig. 46. Cross covariance of heat flow and free-air gravity anomalies (in units of milligal $\mu\text{cal}/\text{cm}^2 \text{ sec}$; taken from *Kaula* [1965, Figure 31]; see text.

fall close to the zero covariance and show no marked pattern. Figure 46 shows negative covariance at 0° —corroborating the negative correlation between heat flow and gravity—but also shows an interesting variation in covariance with extrema at about 17° , 38° , and 90° . The peak at 17° and the trough at 38° may be produced by convection cells of a wavelength of 38° (i.e., about 4000 km).

The correlation between heat flow and gravity is not yet well established because of the uncertainties of (1) our knowledge of both the heat flow and gravity fields, and (2) their interrelationships. The gravity field reflects the present mass distribution, whereas the surface heat flow field (because of slow thermal conduction) may lag millions of years in indicating the temperature distribution of the corresponding depth in the Earth's interior. A very strong negative correlation between heat flow and gravity would imply that (1) the density irregularities are near the surface and are due to thermal expansion and contraction, rather than chemical variation, and (2) thermal properties are uniform.

Because of the slowness of thermal conduction process, the negative correlation between heat flow and gravity may be more easily explained by convection motions within the mantle. A hot, rising column represents a deficiency in mass and carries an excess of heat, whereas a descending column contains a greater mass and less heat. *Lee and MacDonald* [1963] have demonstrated by an order of magnitude calculation that the anomalies in the gravitational and heat flow fields are consistent with convection currents having velocities of the order of a few centimeters per year. Inhomogeneity in heat sources and in other physical and chemical properties of the Earth's interior may also explain the negative correlation.

genity in heat sources and in other physical and chemical properties of the Earth's interior may also explain the negative correlation.

6.3 Heat Flow and Topography

Lee and MacDonald [1963] have investigated the distribution of heat flow values with ocean depth. They note that there is some tendency for high values to be associated with a 3000-meter depth (oceanic rises), but on the whole there is a low linear correlation (correlation coefficient = -0.33) of the heat flow in oceans with topography.

Figure 47 shows the distribution of heat flow with station elevation or depth. The oceanic part is essentially the same as noted by *Lee and MacDonald*. The land part is too scattered to draw any definite conclusion. On the whole, the linear correlation of heat flow with topography is insignificant (correlation coefficient = -0.1).

7. SUMMARY

Surface heat flow by conduction is determined as the product of thermal conductivity and vertical temperature gradient. At present, about 2000 observations are available; however, their geographical distribution is extremely uneven, with three times more data per unit area at sea than on land. Analysis of nearby and repeated measurements suggests that in general regional heat flow variations $>0.2 \mu\text{cal}/\text{cm}^2 \text{ sec}$ are significant.

From spherical harmonic analysis, the global mean heat flow is $1.5 \pm 10\% \mu\text{cal}/\text{cm}^2 \text{ sec}$ at 95% confidence level. The heat arriving at the Earth's surface is believed to be produced

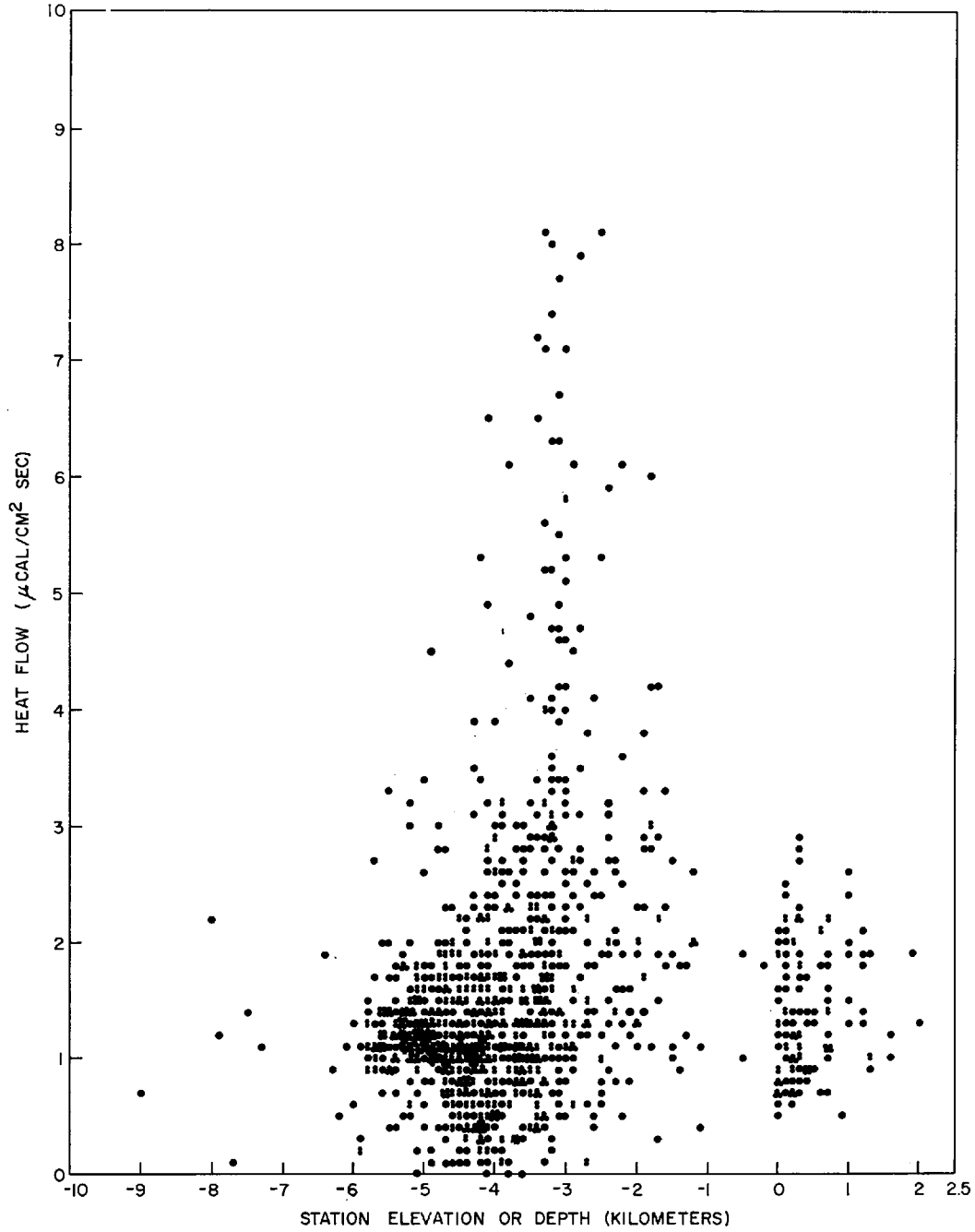


Fig. 47. Distribution of heat flow values with station elevation or depth. Each dot, regardless of its size, represents one data point.

mainly by radioactivity within the Earth [Birch, 1954b]. The average heat flow over the continents does not differ significantly from that over the oceans. This equality of heat flow suggests that radioactivity is approximately the same beneath land and sea, and further implies that there are differences between the upper mantle under the continents and that under the oceans.

Heat flow values are well correlated with major geological features. On land, the average and standard deviations of heat flow values are 0.92 ± 0.17 from Precambrian shields, 1.23 ± 0.4 from Paleozoic orogenic areas, 1.54 ± 0.38 from post-Precambrian non-orogenic areas, and 1.92 ± 0.49 from Mesozoic-Cenozoic orogenic areas. At sea, they are 0.99 ± 0.61 from trenches, 1.28 ± 0.53 from basins, and 1.82 ± 1.56 from ridges.

Global analysis of heat flow data has indicated that the main features of the heat flow field are highs over the eastern Pacific and east Africa and lows over the Atlantic and central Pacific. On a large scale, heat flow seems to be inversely correlated with gravity: where gravity is high, the heat flow is low, and vice versa. The correlation between heat flow and gravity is not yet well established because of uncertainties in the determination of both fields and in their relationships. Moreover, the gravity field reflects the present mass distribution, whereas the surface heat flow field may lag millions of years in indicating the temperature distribution of the corresponding depth in the Earth's interior.

The origin of continents and oceans has long been the object of speculation and debate (see, for example, Hess [1962], Kennedy [1962], and Engel [1963]). A common hypothesis is that the original crust of the Earth is oceanic and that continents are originated and have grown by differentiation of the mantle through geologic time [Menard, 1964, p. 234]. As noted above, heat flow observations are consistent with this theory. It may also be noted that heat flow variations over short distances are most pronounced over active areas (e.g., the crest of the oceanic ridges, and island arc and trench areas). Recently, Ramberg [1964] suggested a model of early-formed global crust of sialic composition. However, postulating an early differentiation over the whole Earth may have difficulty in

explaining the equality of heat flow over land and sea.

In a little more than 25 years, heat flow has become one of the leading topics in geophysical research and has greatly influenced our thought about the Earth's interior. Although progress is accelerating, much remains to be done: development of new experimental techniques, correlation with other geophysical and geological parameters, as well as global and regional surveys. It is extremely important to extend observations to areas where there are no data: most land areas and high-latitude seas. Greater efforts should be made in measuring heat flow around island arc and trench areas, where large heat flow variations occur over short distances. Investigations should also be made to find the reasons for extremely low heat flow values and the role of water circulation from high areas of intake to low areas of discharge.

Note added in proof. To keep this review as up-to-date as possible, a brief summary of the heat flow data that came to our knowledge after the completion of the manuscript will be made.

Using the oceanic heat flow technique, Law *et al.* [1965] have made 3 heat flow measurements from sea ice in the northwestern part of the Arctic Archipelago of Canada. They obtained a weighted mean heat flow of 0.84 ± 0.09 s.e. $\mu\text{cal}/\text{cm}^2 \text{ sec}$, which has not provided evidence to support the suggestion that the structure responsible for the magnetic variation anomaly at nearby Mould Bay is of thermal origin.

Von Herzen and Vacquier [1965] obtained 60 heat flow values along nine profiles across the Mid-Indian Ocean Ridge. They found results similar to those of the south Mid-Atlantic Ridge reported in Vacquier and Von Herzen [1964].

Several heat flow papers were presented at the 46th Annual Meeting of the American Geophysical Union. The abstracts of these papers were published in the *Transactions, American Geophysical Union*, vol. 46, pp. 174-176, 1965. The following researchers have reported some new data:

Roy and Decker reported 7 preliminary heat flow values (1.2 to 2.2 $\mu\text{cal}/\text{cm}^2 \text{ sec}$) in the White Mountains, New England. Three high values (>1.9) were interpreted as due to high radioactivity of Conway granite.

Diment, Ortiz, Silva, and Ruiz made the first land measurements in the South American continent in seven boreholes (maximum depth 800 m) at two locations near Vallenar, Chile. Heat flow values are between 0.7 and 1.0 $\mu\text{cal}/\text{cm}^2 \text{ sec}$. Some uncertainty was associated with the degree of alteration and amount of magnetite in the strata concerned.

Diment, Werre, Baldwin and Saunders made studies on the thermal state in Green Lake, near Fayetteville, N. Y., and found that the computed heat flow is higher than would be expected for the region. Similar attempts in Seneca Lake, N.Y., were reported by Steinhart and Hart. Sub-bottom temperature gradient was measured to a depth of 7 meters, and the heat flow value of 1.7 was obtained.

F. S. Birch (private communication) has revised some of his heat flow values. Data number and revised heat flow values are as follows: 0195, 1.00; 0196, 1.03; 0198, >0.4; 0199, 1.07; 0200, 1.03; 0201, >0.47; 0202, 1.13; 0204, 1.34-1.65; 0205, 1.02; 0206, 1.12; 0207, 1.14; 0209, 1.22-1.56.

APPENDIX

A LISTING OF HEAT FLOW DATA

The following compilation covers all available heat flow observations up to the end of 1964. It includes many observations in press which have been made available before publication through the kind cooperation of many colleagues. The quality of data ranges from crude estimates to elaborate determinations. When the same data appear in several sources, or when data are modified in later publications, only the latest values are given, and references to the most easily accessible sources (in America) are quoted. Although care has been taken to insure accuracy, errors undoubtedly will occur because of large amounts of data being processed. We will be grateful if readers will inform us about these errors.

The data are arranged in geographical divisions with the following notations:

1. Data number: An arbitrary number is assigned to each heat flow station as it is processed. If several measurements are made or several values are given by different authors, these data are further tabulated under the

given station using letters *A, B, C*, etc., and the average or 'best' value is assigned to the given station.

2. Code: A six digit number is used for classification of each heat flow station.

First digit is geographical code.

- 0 Africa
- 1 Americas
- 2 Australia
- 3 Eurasia
- 4 other lands and Arctic Ocean
- 5 Atlantic Ocean
- 6 Indian Ocean
- 7 Pacific Ocean
- 8 mediterranean seas
- 9 marginal seas

Second digit is geological code.

- 0 post-Precambrian orogenic area
- 1 Precambrian shield
- 2 post-Precambrian non-orogenic area
- 3 Cenozoic volcanic area
- 4 land area where geology is little known
- 5 ocean basin
- 6 oceanic ridge or rise
- 7 ocean trench
- 8 other oceanic area
- 9 complicated area

Third digit indicates type of temperature measurement.

- 0 no measurement
- 1 in borehole
- 2 in mine
- 3 in tunnel
- 4 in other
- 5 using Bullard-type probe
- 6 Bullard-type probe partly penetrating sediments
- 7 using Ewing-type probe
- 8 using other probe
- 9 in boreholes and in mines

Fourth digit indicates type of conductivity measurement.

- 0 no measurement
- 1 using divided bar method
- 2 using transient method
- 3 measured in situ
- 4 using other method
- 5 using needle probe method
- 6 using method of water content

- 7 using method of chlorine content
 8 using other method
 9 measurement made on nearby samples
- Fifth digit indicates type of corrections applied.
- 0 no particular correction applied
 1 water circulation
 2 climatic changes
 3 topographic correction
 4 uplift and erosion
 5 sedimentation
 6 effects of nearby lakes, or river, or ocean
 8 corrections for composite effects
- Sixth digit indicates the quality of data.
- 0 heat flow value not reliable
 1 lower limit of heat flow value
 2 upper limit of heat flow value
 3 average value of a given range of heat flow values
 4 station located in geothermal area
 5 no location available
 6 heat flow disturbed
 7 'fair' value
 8 'good' value
3. Station name: first eight characters are used if station name exceeds eight characters.
4. Station latitude in degrees and minutes: S = south, and N = north.
5. Station longitude in degrees and minutes: E = east, and W = west.
6. Station elevation or depth in meters.
7. Temperature gradient (∇T) in 10^{-3} °C/cm.
8. Thermal conductivity (K) in mcal/cm sec °C.
9. Heat flow (Q) in $\mu\text{cal}/\text{cm}^2$ sec.
10. Number of heat flow values available for the station (NO).
11. Reference number (REF); see below.
12. Year of Publication (YR), e.g. 39=1939.
- Reference number (REF) refers to the list below. Complete citations are given in the Reference section of this article.
1. *Von Herzen and Langseth*, 1965
 2. *Burns*, 1964
 3. *Lister and Reitzel*, 1964
 4. *Reitzel*, 1963
 5. *Birch*, 1964
 6. *Bullard and Day*, 1961
 7. *Reitzel*, 1961a
 8. *Gerard et al.*, 1962
 9. *Vacquier and Von Herzen*, 1964
 10. *Nason and Lee*, 1964
 11. *Lister*, 1963a
 12. *Lister*, 1963b
 13. *Langseth and Grim*, 1964
 14. *Nason and Lee*, 1962
 15. *Bullard*, 1954
 16. *Bullard et al.*, 1956
 17. *Reitzel*, 1961b
 18. *Uyeda and Horai*, 1964
 19. *Von Herzen*, 1964a
 20. *Von Herzen and Maxwell*, 1964
 21. *Von Herzen*, 1963
 22. *Von Herzen*, 1959
 23. *Foster*, 1962
 24. *Von Herzen and Uyeda*, 1963
 25. *Maxwell*, 1958
 26. *Revelle and Maxwell*, 1952
 27. *Von Herzen*, 1960
 28. *Langseth et al.*, 1965
 29. *Rhea et al.*, 1964
 30. *Lister*, 1962
 31. *Horai and Uyeda*, 1963
 32. *Maxwell and Revelle*, 1956
 33. *Birch*, 1947b
 34. *Uyeda et al.*, 1962
 35. *Lachenbruch et al.*, 1965
 36. *Yasui et al.*, 1963
 37. *Bullard*, 1939
 38. *Carte*, 1954
 39. *Gough*, 1963
 40. *Von Herzen*, 1964b
 41. *Spicer*, 1941
 42. *Clark*, 1957
 43. *Benfield*, 1947
 44. *Birch and Clark*, 1945
 45. *Herrin and Clark*, 1956
 46. *Birch*, 1947 a, b
 47. *Birch*, 1950
 48. *Lovering*, 1948
 49. *Birch*, 1954a
 50. *Joyner*, 1960
 51. *Diment and Robertson*, 1963
 52. *Diment and Werre*, 1964
 53. *Roy*, 1963
 54. *Diment and Weaver*, 1964
 55. *Lachenbruch and Marshall*, 1964
 56. *Misener et al.*, 1951

57. *Leith*, 1952
58. *Misener*, 1955
59. *Lachenbruch*, 1957
60. *Saull et al.*, 1962
61. *Garland and Lennox*, 1962
62. *Beck*, 1962
63. *Beck and Logis*, 1963
64. *Newstead and Beck*, 1953
65. *Jaeger and Sass*, 1963
66. *Beck*, 1956
67. *Howard and Sass*, 1964
68. *Le Marne and Sass*, 1962
69. *Sass and Le Marne*, 1963
70. *Sass*, 1964a
71. *Sass*, 1964b
72. *Bodvarsson*, 1955
73. *Benfield*, 1939
74. *Anderson*, 1940
75. *Bullard and Niblett*, 1951
76. *Chadwick*, 1956
77. *Mullins and Hinsley*, 1957
78. *Clark and Niblett*, 1956
79. *Clark*, 1961
80. *Boldizar*, 1964a, c
81. *Boldizar*, 1963
82. *Schossler and Schwarzlose*, 1959
83. *Stenz*, 1954
84. *Langseth*, 1964
85. *Grim*, 1964
86. *Yasui and Watanabe*, 1965
87. *Sisoev*, 1961
88. *Sclater*, 1964
89. *Coster*, 1947
90. *Verma and Rao*, 1965
91. *Boldizar*, 1964b
92. *Boldizar and Gozon*, 1963
93. *Boldizar*, 1959
94. *Lubimova et al.*, 1964
95. *Birch*, 1956
96. *Kraskovski*, 1961
97. *Diment et al.*, 1965a
98. *Diment et al.*, 1965b
99. *Spicer*, 1964
100. *Lubimova et al.*, 1961

Note added in proof. Note the following changes in heat flow values given on page 166: Data No. 0161 should read 0.63 (instead of 0.66); Data No. 0162 should read 0.66 (instead of 0.63).

DATA NUMBER	STATION CODE	STATION NAME	LATI- TUDE	LONGI- TUDE	ELE./ DEPTH	V.T	K	Q	NO	REF	YR	
AFRICA--SOUTH AFRICA												
0001	011108	JACO-DOH	27-18S	26-24E	+1310	.130	7.43	0.96	2	37	39	
	A	011108	JACOBA	27-18S	26-24E	+1310	.128	7.46	0.95	1	37	39
	B	011907	DOORNHOU	27-18S	26-24E	+1300	.131	7.40	0.97	1	37	39
0002	011108	GERH-DOK	26-24S	27-21E	+1590	.092	13.5	1.24	3	37	39	
	A	011108	GERHARDM	26-30S	27-12E	+1520	.095	13.5	1.28	1	37	39
	B	011900	DRIEFONT	25-52S	29-11E	+1000	.070	10.8	0.75	1	37	39
	C	011907	DOORNKLO	26-18S	27-30E	+1660	.089	13.5	1.20	1	37	39
0003	011907	REEF-NIG	26-18S	28-18E	+1565	.103	10.0	1.03	1	37	39	
0004	021108	DUBBELDE	30-30S	21-30E	+ 990	.223	6.80	1.52	1	37	39	
0005	011108	HB15	26-48S	26-54E	+1310	.105	10.0	1.05	1	38	54	
0006	011108	ROODEPOR	26-54S	26-36E	+1300	.119	7.2	0.86	1	38	54	
0007	021108	MESSINA	22-18S	30-06E	+ 518	.269	5.1	1.37	1	38	54	
0008	021108	KESTELL	28-18S	28-42E	+1980	.248	5.2	1.29	1	38	54	
0009	021128	SAMBOKKR	32-42S	21-18E	+ 737	.183	7.6	1.39	1	39	63	
0010	021128	KOEGELFO	33-00S	21-18E	+ 726	.182	7.9	1.45	1	39	63	
0011	021128	BOTHADAL	32-48S	22-36E	+ .952	.178	7.1	1.28	1	39	63	
0012	021128	KALKKOP	32-42S	24-24E	+ .654	.196	6.1	1.21	1	39	63	
AFRICA--LAKE NYASA												
0013	045507	L.NYASA	11-27S	34-29E	- 460	.62	1.6	1.0	20	40	65	
AMERICA--UNITED STATES												
0014	102137	GRASS VA	39-12N	121-03W	+ 667	.095	7.2	0.69	1	42	57	
	A	102137	GRASS VA	39-12N	121-03W	+ 667	.095	7.2	0.69	1	42	57
	B	102000	GRASS VA	39-12N	121-03W	+ 667	.095	7.2	0.69	1	41	41
0015	101108	BAKERSFI	35-28N	119-45W	+ 207	.350	3.7	1.29	1	43	47	
0016	121900	BIG LAKE	31-12N	101-29W	+ 500	.25	8.	2.0	1	44	45	
0017	121907	REEVES C	31-10N	103-14W	+ 700	.083	13.	1.1	1	45	56	
0018	121907	REGAN CO	31-15N	101-28W	+ 700	.083	13.	1.1	12	45	56	
	A	121907	BLU 103	31-15N	101-28W	+ 700	.090	13.	1.2	1	45	56
	B	121900	BLU 106	31-15N	101-28W	+ 700	.088	13.	1.1	1	45	56
	C	121900	BLU 110	31-15N	101-28W	+ 700	.098	13.	1.3	1	45	56
	D	121900	BLU 112	31-15N	101-28W	+ 700	.092	13.	1.2	1	45	56
	E	121907	BLU 115	31-15N	101-28W	+ 700	.076	13.	1.0	1	45	56
	F	121907	BLU 118	31-15N	101-28W	+ 700	.079	13.	1.0	1	45	56
	G	121907	BLU 119	31-15N	101-28W	+ 700	.083	13.	1.1	1	45	56
	H	121900	BLU 124	31-15N	101-28W	+ 700	.085	13.	1.1	1	45	56
	I	121900	BLU 125	31-15N	101-28W	+ 700	.083	13.	1.1	1	45	56
	J	121907	BLU 126	31-15N	101-28W	+ 700	.083	13.	1.1	1	45	56
	K	121907	BLU 127	31-15N	101-28W	+ 700	.086	13.	1.1	1	45	56
	L	121900	UNIV 1	31-15N	101-28W	+ 700	.097	13.	1.3	1	45	56
0019	121907	UPTON CO	31-23N	101-48W	+ 700	.083	13.	1.1	1	45	56	
0020	121900	MIDLAND	31-39N	102-15W	+ 700	.094	13.	1.2	1	45	56	
0021	121907	EDDY COU	32-29N	104-03W	+ 700	.085	12.6	1.1	5	45	56	
	A	121907	SM-1	32-38N	104-14W	+ 700	.103	11.8	1.2	1	45	56
	B	121900	S-1C	32-14N	104-07W	+ 700	.101	11.8	1.2	1	45	56
	C	121900	NMPR 1B	32-24N	104-16W	+ 700	.073	13.	0.9	1	45	56
	D	121907	M-O-1W	32-18N	103-45W	+ 700	.077	13.	1.0	1	45	56
	E	121907	G-7D	32-31N	104-09W	+ 700	.080	13.	1.0	1	45	56
0022	121900	LEA CNTY	32-47N	103-48W	+1000	.092	13.	1.2	1	45	56	
0023	101013	COLORADO	38-49N	104-49W	+1885	.2	7.	1.4	1	47	50	

REVIEW OF HEAT FLOW DATA

161

DATA NUMBER	STATION CODE	STATION NAME	LATI- TUDE	LONGI- TUDE	ELE./ DEPTH	VT	K	Q	NO	REF	YR	
AMERICA--UNITED STATES (CONTINUED)												
0024	121003	SYRACUSE	37-57N	101-45W	+1051	.28	5.5	1.55	1	47	50	
0025	101000	GEORGIA	33- N	84- W	+ 300	.143	7.	1.0	3	51	63	
	A	101000	GEORGIA	33- N	84- W	+ 300	.2	7.	1.4	1	47	50
	B	101000	GRIFFIN	33- N	84- W	+ 300	.139	7.	0.97	1	51	63
	C	101000	LAGRANGE	33- N	84- W	+ 300	.146	7.	1.02	1	51	63
0026	103138	FRONT RA	40-15N	105-40W	+2500	0.22	7.8	1.7	1	47	50	
0027	101983	SAN MANU	32-37N	110-39W	+ 970	.15	8.	1.2	1	48	48	
0028	119138	CALUMET	47-17N	88-28W	+ 360	.186	5.0	0.93	1	49	54	
0029	101007	1-BUTLER	40-59N	80-08W	+ 200	.29	4.2	1.2	1	50	60	
0030	101007	POTTER	41-54N	77-56W	+ 200	.37	3.8	1.4	2	50	60	
	A	101007	3-POTTER	41-56N	77-51W	+ 500	.39	3.7	1.47	1	50	60
	B	101007	4-POTTER	41-52N	78-00W	+ 500	.35	3.7	1.31	1	50	60
0031	101007	DO-MA-HA	39-20N	80-32W	+ 200	.33	3.6	1.2	3	50	60	
	A	101007	2-DODDRI	39-17N	80-46W	+ 200	.29	4.2	1.22	1	50	60
	B	101007	5-MARIO	39-25N	80-05W	+ 200	.34	3.5	1.20	1	50	60
	C	101007	6-HARRIS	39-18N	80-14W	+ 200	.37	3.4	1.26	1	50	60
0032	101108	OAK RIDG	35-55N	84-19W	+ 240	.12	6.1	0.73	1	51	63	
0033	101108	WASHINGT	39- N	77- W	+ 30	.157	7.13	1.12	1	52	64	
0034	121108	BOSS	37-39N	91-10W	+ 375	.17	7.6	1.29	1	53	63	
0035	121108	BOURBON	38-09N	91-15W	+ 290	.15	8.1	1.22	1	53	63	
0036	111138	DELAWARE	47-24N	88-01W	+ 389	.16	5.3	0.95	1	53	63	
0037	111138	WHITE PI	46-44N	89-34W	+ 281	.16	6.7	1.07	3	53	63	
	A	111138	DDH-N-55	46-45N	89-34W	+ 279	.16	6.7	1.07	1	53	63
	B	111138	DDH-N-65	46-44N	89-34W	+ 305	.16	6.6	1.06	1	53	63
	C	111138	DDH-E-27	46-44N	89-36W	+ 260	.16	6.9	1.10	1	53	63
0038	101138	METALINE	48-54N	117-21W	+ 686	.20	11.6	2.31	4	53	63	
	A	101138	DDH-CS-2	48-55N	117-20W	+ 671	.24	11.	2.67	1	53	63
	B	101138	DDH-CS-9	48-53N	117-21W	+ 734	.21	11.	2.31	1	53	63
	C	101138	DDH-R-1	48-54N	117-21W	+ 664	.20	12.	2.38	1	53	63
	D	101138	DDH-R-4	48-54N	117-20W	+ 675	.19	12.	2.25	1	53	63
0039	101138	GOVERNME	39-52N	112-04W	+1860	.40	4.7	1.9	1	53	63	
0040	131134	EUREKA	39-57N	112-03W	+1702	.80	4.4	3.51	1	53	63	
0041	101138	YERINGTO	38-55N	119-04W	+1034	.27	8.7	2.36	3	53	63	
	A	101138	DDH-L-2	38-55N	119-04W	+1459	.27	8.4	2.26	1	53	63
	B	101138	DDH-L-5	38-56N	119-04W	+1410	.28	8.5	2.39	1	53	63
	C	101137	DDH-L-13	38-56N	119-04W	+1434	.21	9.1	1.9	1	53	63
0042	101138	BARSTOW	34-39N	116-21W	+1245	.24	8.8	2.1	2	53	63	
	A	101106	DDH-M-10	34-39N	116-41W	+1246	.24	6.6	1.59	1	53	63
	B	101138	DDH-M-11	34-39N	116-21W	+1245	.24	8.8	2.10	1	53	63
1133	101108	ALBERTA	36-52N	77-54W	+ 116	.18	7.8	1.4	1	98	65	
1134	101108	AIKEN SC	33-17N	81-40W	+ 100	.15	6.7	1.0	6	97	65	
1135	101907	SALT VLY	38-55N	109-50W	+1500	.385	3.43	1.2	5	99	64	
	A	101907	REEDER 1	38-55N	109-50W	+1500	.374	3.54	1.32	1	99	64
	B	101907	CRESCENT	38-55N	109-50W	+1500	.386	3.38	1.30	1	99	64
	C	101907	BRENDELL	38-55N	109-50W	+1500	.394	3.38	1.33	1	99	64
	D	101907	BALSLEY	38-46N	109-38W	+1500	.314	3.51	1.10	1	99	64
	E	101907	HYDE	38-51N	109-30W	+1500	.194	5.23	1.01	1	99	64

AMERICA--PUERTO RICO

0043	101188	MAYAGUEZ	18-09N	67-10W	+ 30	.10	6.0	0.6	1	54	64
------	--------	----------	--------	--------	------	-----	-----	-----	---	----	----

DATA NUMBER	STATION CODE	STATION NAME	LATI- TUDE	LONGI- TUDE	ELE./ DEPTH	∇T	K	Q	NO	REF	YR
AMERICA--CANADA											
0044	101108	TORONTO	43-42N	79-25W	+ 100	.160	6.4	1.03	1	56	51
0045	112108	SUDBURY	46-30N	81-01W	+ 200	.158	6.4	1.01	1	56	51
0046	102108	THETFORD	46-06N	71-18W	+ 200	.157	6.7	1.05	1	56	51
0047	112100	CALUMET	45-49N	74-41W	+ 50	.156	8.5	1.32	1	56	51
0048	112108	KIRKLAND	48-10N	80-02W	+ 200	.130	7.7	1.00	3	56	51
A	112108	KL-LS	48-10N	80-02W	+ 200	.130	7.5	0.97	1	56	51
B	112108	KL-TH	48-10N	80-02W	+ 200	.130	7.9	1.03	1	56	51
C	112108	KL-WH	48-10N	80-02W	+ 200	.130	7.7	0.99	1	56	51
0049	112108	MALARTIC	48-09N	78-09W	+ 200	.101	6.8	0.69	1	56	51
0050	112108	LARDER L	48-06N	79-44W	+ 200	.097	9.1	0.88	1	56	51
0051	112108	TIMMINIS	48-30N	81-20W	+ 200	.091	8.0	0.73	2	56	51
A	112108	TIMMIN-D	48-30N	81-20W	+ 200	.092	8.0	0.73	1	56	51
B	112107	TIMMIN-M	48-30N	81-20W	+ 200	.090	8.0	0.73	1	56	51
0052	101180	RESOLUTE	74-41N	94-54W	+ 0	.395	7.3	2.9	1	58	55
0053	101108	MONTREAL	45-15N	073-57W	+ 50	.062	12.0	0.74	1	60	62
0054	101108	STE-ROSA	45-38N	072-40W	+ 49	.159	5.06	0.81	1	60	62
0055	101108	LOUN-CAR	46-05N	073-08W	+ 22	.269	3.03	0.82	1	60	62
0056	121907	LEDUC	53-23N	113-48W	+ 700	.43	3.7	1.6	1	61	62
0057	121908	REDWATER	53-59N	113-07W	+ 700	.30	4.9	1.46	1	61	62
0058	101988	NORMAN W	65-18N	126-51W	+ 100	.65	3.1	2.00	1	61	62
0059	112107	FLIN FLO	54-47N	101-51W	+ 200	.12	6.7	0.8	1	62	62
0060	111308	BRENT CR	46-05N	78-29W	+ 335	.133	5.6	0.75	1	63	63
AUSTRALIA											
0061	231138	GT.LAKE	41-58S	146-11E	+1027	.4	5.	2.	8	65	63
A	231108	NO.1 G.L	41-58S	146-11E	+1027	.43	4.7	2.04	1	64	53
B	231100	NO.2 DTL	41-58S	146-11E	+ 733	.43	4.8	2.06	1	64	53
C	231900	NO.3 DTL	41-58S	146-11E	+ 714	.43	4.8	2.07	1	64	53
D	231100	NO.4 ROS	41-46S	145-34E	+ 198	.30	8.2	2.47	1	64	53
E	231100	NO.5 ROS	41-46S	145-34E	+ 263	.28	9.0	2.54	1	64	53
F	231138	GT.LAKE	41-58S	146-11E	+1000	.338	5.4	1.9	1	65	63
G	231136	STOREY C	42- S	146- E	+ 900	.308	12.2	3.8	1	65	63
H	231186	ROSBERY	41-46S	145-34E	+ 320	.29	8.6	2.5	1	65	63
0062	203108	SNOWY MT	36-30S	148- E	+1000	.226	8.6	2.	2	67	64
A	201108	E-5010	36-30S	148- E	+1000	.213	8.8	1.9	1	66	56
B	203108	EUCUMBEN	36-30S	148- E	+1000	.239	8.4	2.0	1	67	64
0063	221108	COBAR	31-32S	145-50E	+ 300	.205	10.6	2.18	1	68	62
0064	229108	BROKEN H	31-57S	141-28E	+ 300	.199	9.70	1.93	18	69	63
A	221108	BH-1205	31-57S	141-28E	+ 300	.197	9.87	1.94	1	69	63
B	221908	BH-1126	31-57S	141-28E	+ 300	.200	9.53	1.91	1	69	63
C	221108	BH-1093	31-57S	141-28E	+ 300	.196	9.84	1.93	1	69	63
D	221908	BH-1040	31-57S	141-28E	+ 300	.193	10.4	2.01	1	69	63
E	221108	BH-950	31-57S	141-28E	+ 300	.198	10.5	2.07	1	69	63
F	221908	BH-W-1	31-57S	141-28E	+ 300	.187	10.3	1.93	1	69	63
G	221908	BH-305	31-57S	141-28E	+ 300	.199	9.49	1.89	1	69	63
H	221908	BH-678	31-57S	141-28E	+ 300	.198	9.51	1.88	1	69	63
I	221908	G-969	31-57S	141-28E	+ 300	.200	10.1	2.03	1	69	63
J	221908	P-814	31-57S	141-28E	+ 300	.188	9.61	1.81	1	69	63
K	221908	P-820	31-57S	141-28E	+ 300	.193	9.93	1.92	1	69	63
L	221908	P-831	31-57S	141-28E	+ 300	.198	9.58	1.90	1	69	63
M	221908	P-835	31-57S	141-28E	+ 300	.189	9.84	1.86	1	69	63
N	221908	C-834	31-57S	141-28E	+ 300	.202	9.61	1.94	1	69	63

REVIEW OF HEAT FLOW DATA

163

DATA NUMBER	CODE	STATION NAME	LATI-TUDE	LONGI-TUDE	ELE./DEPTH	▽T	K	Q	NO	REF	YR
AUSTRALIA (CONTINUED)											
O	221908	57-LBH-1	31-57S	141-28E	+ 300	.211	9.47	2.00	1	69	63
P	221908	57-LBH-6	31-57S	141-28E	+ 300	.203	9.61	1.95	1	69	63
Q	221908	59-P-8	31-57S	141-28E	+ 300	.206	9.61	1.98	1	69	63
R	221108	55-C-6	31-57S	141-28E	+ 300	.216	8.40	1.81	1	69	63
0065	211168	KALGOORL	30-45S	121-30E	+ 380	.093	10.1	0.96	2	67	64
A	212108	KALGOORL	30-45S	121-30E	+ 380	.088	10.1	0.89	1	67	64
B	211168	KALGOORL	30-55S	121-33E	+ 380	.098	10.1	0.96	4	70	64
BA	211168	SE-10	30-55S	121-33E	+ 380	.107	9.7	1.04	1	70	64
BB	211168	SE-12	30-55S	121-33E	+ 380	.105	10.4	1.09	1	70	64
BC	211168	SE-6	30-55S	121-33E	+ 380	.084	9.9	0.83	1	70	64
BD	211168	SE-4	30-55S	121-33E	+ 380	.096	9.2	0.83	1	70	64
0066	211108	COOLGARL	30-57S	121-10E	+ 423	.124	7.3	0.90	2	67	64
A	211108	BV-1	30-57S	121-10E	+ 423	.142	7.7	1.09	1	70	64
B	211108	MLS-1	30-57S	121-10E	+ 423	.105	6.9	0.72	1	70	64
0067	211108	NORSEMAN	32-20S	121-37E	+ 305	.131	7.3	0.89	2	67	64
A	211108	NORSEMAN	32-20S	121-37E	+ 305	.119	7.5	0.89	1	67	64
B	210107	NORSEMAN	32-20S	121-37E	+ 305	.143	7.1	1.01	3	70	64
BA	210107	C-79	32-20S	121-37E	+ 305	.151	6.9	1.04	1	70	64
BB	210107	C-80	32-20S	121-37E	+ 305	.154	6.8	1.05	1	70	64
BC	210107	PRS-105	32-20S	121-37E	+ 305	.125	7.5	0.94	1	70	64
0068	241106	RUM JUNG	13- S	131- E	+ 60	.19	10.5	2.0	3	67	64
A	241106	RJ-337	13- S	131- E	+ 60	.148	6.9	1.02	1	67	64
B	241106	RJ-B35	13- S	131- E	+ 60	.174	11.7	2.0	1	67	64
C	241106	RJ-B40	13- S	131- E	+ 60	.201	9.4	1.9	1	67	64
0069	222108	TENNANT	19-34S	134-13E	+ 328	.225	10.2	2.3	1	67	64
0070	221108	MT. ISA	21- S	139- E	+ 300	.189	9.5	1.8	1	67	64
0071	211107	CUE	27-27S	117-52E	+ 454	.108	8.8	0.95	1	67	64
0072	212108	MT. MAGN	28- S	118- E	+ 460	.113	11.4	1.3	1	67	64
0073	212107	BULLFINC	31-14S	119-19E	+ 360	.139	8.8	1.2	1	67	64
0074	221108	RADIUM H	32-30S	140-30E	+ 305	.230	7.8	1.8	1	67	64
0075	211108	RAVENSTH	33-40S	120- E	+ 180	.116	8.2	0.95	1	67	64
0076	221106	CABAWIN	27-30S	150-12E	+ 300	.25	4.6	1.16	1	71	64
0077	221906	MOONIE	27-44S	150-13E	+ 300	.22	4.6	1.01	1	71	64
0078	201108	CANBERRA	35-17S	149-08E	+ 560	.252	8.15	2.06	1	71	64
0079	221108	WHYALLA	33-10S	137-30E	+ 60	.21	10.3	2.16	1	71	64
0080	221108	KANMANTO	35-05S	139-15E	+ 150	.194	10.9	2.11	1	71	64
0081	231108	STAWELL	37-03S	142-47E	+ 300	.271	10.5	2.84	1	71	64
0082	231108	CASTLEMA	37-03S	144-13E	+ 165	.242	11.9	2.88	1	71	64
ASIA--INDIA											
0083	312108	KOLAR	12-55N	78-15E	+ 600	.104	6.28	0.66	1	90	65
ASIA--IRAN											
0084	341128	MASJID-I	31-59N	49-18E	+ 413	.151	5.8	0.87	18	89	47
A	341128	MIS-T171	31-59N	49-18E	+ 580	.164	6.2	1.01	1	89	47
B	341128	MIS-T230	31-59N	49-18E	+ 565	.147	4.4	0.65	1	89	47
C	341128	MIS-K178	31-59N	49-18E	+ 550	.123	6.5	0.80	1	89	47
D	341128	MIS-SH95	31-59N	49-18E	+ 440	.113	4.7	0.53	1	89	47
E	341128	MIS-B162	31-59N	49-18E	+ 350	.133	4.8	0.64	1	89	47
F	341128	MIS-B187	31-59N	49-18E	+ 310	.114	7.3	0.83	1	89	47
G	341128	MIS-B212	31-59N	49-18E	+ 335	.128	7.2	0.93	1	89	47

DATA NUMBER	CODE	STATION NAME	LATI-TUDE	LONGI-TUDE	ELE./DEPTH	VT	K	Q	NO	REF	YR
ASIA--IRAN (CONTINUED)											
H	341128	MIS-T232	31-59N	49-18E	+ 440	.125	6.4	0.80	1	89	47
I	341128	MIS-CS23	31-59N	49-18E	+ 435	.127	8.9	1.13	1	89	47
J	341128	MIS-B211	31-59N	49-18E	+ 335	.106	6.2	0.66	1	89	47
K	341128	MIS-Q250	31-59N	49-18E	+ 555	.180	5.1	0.92	1	89	47
L	341128	MIS-Q225	31-59N	49-18E	+ 420	.214	5.7	1.22	1	89	47
M	341128	MIS-C209	31-59N	49-18E	+ 335	.181	5.2	0.94	1	89	47
N	341128	MIS-C229	31-59N	49-18E	+ 315	.166	5.4	0.90	1	89	47
O	341128	MIS-C222	31-59N	49-18E	+ 320	.155	6.0	0.92	1	89	47
P	341128	MIS-C240	31-59N	49-18E	+ 335	.150	5.7	0.85	1	89	47
Q	341128	MIS-A244	31-59N	49-18E	+ 305	.186	5.2	0.96	1	89	47
R	341128	MIS-C235	31-59N	49-18E	+ 510	.198	5.3	1.05	1	89	47

ASIA--JAPAN

0085	301907	HABORO	44-21N	141-52E	+ 100	0.45	4.12	1.87	1	18	64
0086	302108	SHIMOKAW	44-14N	142-41E	+ 350	0.30	5.63	1.71	1	18	64
0087	339108	KONOMAI	44-08N	143-21E	+ 100	0.40	6.41	2.54	1	18	64
0088	302108	AKABIRA	43-32N	142-02E	+ 100	0.25	4.31	1.07	1	18	64
0089	301108	ASHIBETS	43-33N	142-12E	+ 100	0.30	4.38	1.35	1	18	64
0090	332004	TOYOHA	42-54N	141-05E	+ 500	1.13	5.	5.6	1	18	64
0091	331907	YABASE	39-44N	140-06E	+ 10	0.48	4.19	2.01	1	18	64
0092	331907	INNAI	39-16N	139-58E	+ 10	0.48	3.11	1.49	1	18	64
0093	339108	OSARIZAW	40-11N	140-45E	+ 300	0.33	6.70	2.24	1	18	64
0094	302108	NODA-TAM	40-04N	141-50E	+ 0	0.14	8.28	1.14	1	18	64
0095	302107	KAMAISHI	39-16N	141-42E	+ 770	0.09	5.66	0.52	1	18	64
0096	302108	HITACHI	36-38N	140-38E	+ 350	0.11	6.62	0.71	1	18	64
0097	301108	KATSUTA	36-24N	140-30E	+ 0	0.30	3.02	0.91	1	18	64
0098	301108	KASHIMA	35-57N	140-41E	+ 0	0.21	3.57	0.76	1	18	64
0099	301108	MOBARA	35-24N	140-20E	+ 0	0.18	2.94	0.54	1	18	64
0100	301108	TOKYO	35-42N	139-46E	+ 20	0.22	3.36	0.74	1	18	64
0101	332107	ASHIO	36-39N	139-27E	+ 700	0.36	6.25	2.23	1	18	64
0102	331104	KUSATSU-	36-37N	138-34E	+1600	2.47	4.48	10.8	1	18	64
0103	331108	CHICHIBU	36-01N	138-48E	+1020	0.19	7.06	1.34	1	18	64
0104	333907	SASAGO	35-37N	138-48E	+ 650	0.27	7.61	2.06	1	18	64
0105	309108	KAMIOKA	36-21N	137-19E	+ 650	0.28	6.49	1.80	1	18	64
0106	309108	NAKATATS	35-52N	136-35E	+ 600	0.29	6.71	1.95	1	18	64
0107	302100	KUNE	35-05N	137-50E	+ 262	0.20	8.14	1.60	1	18	64
0108	302108	NAKO	35-03N	137-52E	+ 285	0.22	6.65	1.44	1	18	64
0109	301107	MINENOSAX	35-00N	137-51E	+ 300	0.29	6.13	1.79	1	18	64
0110	302108	IKUNO	35-10N	134-50E	+ 370	0.19	7.33	1.38	1	18	64
0111	309108	NAKAZE	35-21N	134-57E	+ 300	0.34	6.51	2.21	1	18	64
0112	301108	YANAHARA	34-57N	134-04E	+ 100	0.20	5.89	1.20	1	18	64
0113	331100	ISOTAKE	35-11N	132-26E	+ 100	0.40	8.65	3.49	1	18	64
0114	301108	TSUMO	34-34N	132-00E	+ 350	0.18	6.08	1.09	1	18	64
0115	301108	KAWAYAMA	34-15N	132-59E	+ 350	0.17	5.85	1.00	1	18	64
0116	301108	NAKA	34-15N	135-25E	- 197	0.30	5.90	1.79	1	18	64
0117	301108	HIDAKA	33-57N	135-05E	+ 0	0.29	7.40	2.12	1	18	64
0118	301107	KIWA	33-50N	135-53E	+ 80	0.18	7.06	1.31	1	18	64
0119	301108	BESSHI	34-01N	133-09E	+ 160	0.25	4.89	1.22	1	18	64
0120	331107	IZUHARA	34-13N	129-14E	+ 150	0.29	7.41	2.17	1	18	64
0121	302108	TAKAMATS	33-52N	130-43E	- 450	0.31	6.27	1.92	1	18	64
0122	302107	TAIO	33-07N	130-52E	+ 600	0.17	6.16	1.05	1	18	64
0123	302108	MAKIMINE	32-38N	131-27E	+ 120	0.26	6.95	1.79	1	18	64
1136	331104	MATSUKAW	40- N	141- E	+ 500			15.	1	18	64

REVIEW OF HEAT FLOW DATA

165

DATA NUMBER	CODE	STATION NAME	LATI- TUDE	LONGI- TUDE	ELE./ DEPTH	▽T	K	Q	NO	REF	YR
EUROPE--GREAT BRITAIN											
0124	301127	DYSART	56-08N	3-07W	+	0 .22	4.2	0.92	3	74	40
	A 301927	BALFOUR	56-08N	3-07W	+	0 .23	3.0	0.68	1	73	39
	B 301127	BORELAND	56-08N	3-07W	+	0 .20	4.7	0.95	1	74	40
	C 301927	BALFOUR	56-08N	3-07W	+	0 .24	3.7	0.89	1	74	40
0125	301128	HOLFORD	53-20N	2-30W	+	30 .13	5.7	0.74	1	73	39
0126	301020	GLASGOW	55-53N	4-22W	+	20 .41	3.8	1.57	4	74	40
	A 301020	BLYTHSWO	55-53N	4-20W	+	20 .36	3.4	1.24	1	73	39
	B 301020	SOUTH BA	55-53N	4-20W	+	20 .46	3.3	1.53	1	73	39
	C 301020	BLYTHSWO	55-53N	4-24W	+	20 .36	3.9	1.41	1	74	40
	D 301020	SOUTH BA	55-53N	4-24W	+	20 .46	3.8	1.73	1	74	40
0127	301120	HANKHAM	50-55N	0-15W	+	20 .234	3.0	0.71	1	73	39
0128	301020	DURHAM	54-45N	1-38W	+	20 .306	4.8	1.47	1	74	40
0129	304020	WIGAN	53-30N	2-20W	+	20 .327	3.2	1.01	1	74	40
0130	301128	CAMBRIDG	52-12N	0-00E	+	30 .13	9.8	1.28	1	76	56
0131	301108	NOTTINGH	53-08N	0-53W	+	70 .38	4.1	1.57	6	75	51
	A 301106	EAKR-5	53-09N	0-59W	+	83 .743	3.7	2.73	1	75	51
	B 301106	EAKR-6	53-09N	1-00W	+	86 .786	3.5	2.75	1	75	51
	C 301106	EAKR-64	53-08N	0-59W	+	91 .573	3.4	1.97	1	75	51
	D 301106	EAKR-141	53-09N	1-00W	+	79 .718	4.0	2.87	1	75	51
	E 301108	KH-1	53-07N	0-52W	+	52 .364	4.0	1.47	1	75	51
	F 301108	CAUN-11	53-08N	0-54W	+	30 .391	4.2	1.67	1	75	51
0132	301108	YORKSHIR	54-34N	1-03W	+	39 .24	4.9	1.16	2	75	51
	A 301108	KIRK-1	54-35N	1-05W	+	21 .209	5.5	1.15	1	75	51
	B 301108	TOCK-1	54-33N	1-01W	+	57 .277	4.3	1.18	1	75	51
0133	301108	BAWTRY	53-25N	1-00W	+	50 .36	5.3	1.91	4	77	57
	A 301108	MISSON	53-25N	1-00W	+	50 .38	5.3	2.03	1	77	57
	B 301108	RANBY CA	53-25N	1-00W	+	50 .36	5.5	1.98	1	77	57
	C 301108	RANBY HA	53-25N	1-00W	+	50 .34	5.4	1.84	1	77	57
	D 301108	SCAFTWOR	53-25N	1-00W	+	50 .35	5.1	1.79	1	77	57
0134	301108	NOTTINGH	53-00N	1-10W	+	50 .32	5.0	1.61	2	77	57
	A 301108	GOOSE DAG	53-00N	1-10W	+	50 .31	4.9	1.52	1	77	57
	B 301108	PAPPLEWI	53-00N	1-10W	+	50 .34	5.0	1.69	1	77	57
EUROPE--SWITZERLAND											
0135	303988	GOTTHARD	46-25N	8-35E	+1154	.209	6.70	1.4	1	78	56
0136	303988	SIMPLON	46-25N	8-05E	+705	.328	6.70	2.2	1	78	56
0137	303988	LOETSCHB	46-35N	7-45E	+1243	.244	7.77	1.9	1	78	56
EUROPE--AUSTRIA											
0138	303988	ARLBERG	46-55N	10-10E	+1300	.173	11.0	1.9	1	79	61
0139	303988	TAUERN	46-50N	13-05E	+1200	.230	7.83	1.8	1	79	61
EUROPE--HUNGARY											
0140	302108	ZO-HQ-BA	46-10N	18-14E	+300	.43	6.3	2.7	3	80	64
	A 302108	HOSSZUHE	46-10N	18-22E	+270	.41	6.1	2.49	2	80	64
	B 302108	KO-ZORAK	46-12N	18-18E	+300	.45	7.3	3.31	2	80	64
	C 30 7	BAKONYA	46-07N	18-04E	+300			2.4	1	80	64
0141	301108	NAGYLENG	46-46N	16-45E	+200	.46	4.4	1.9	1	80	64
0142	30 7	HAJDUSZO	47-26N	21-23E	+100			2.4	1	80	64
0143	30 7	SZENTEND	47-41N	19-05E	+200			2.0	1	80	64

DATA NUMBER	STATION CODE	STATION NAME	LATI- TUDE	LONGI- TUDE	ELE./ DEPTH	VT	K	Q	NO	REF	YR
EUROPE--CZECHOSLOVIA											
0144	30	7 BANSKA S	48-27N	18-53E	+1000			2.6	1	80	64
EUROPE--ITALY											
0145	331104	LARDEREL	43-12N	10-54E	+ 300	3.4	3.2	10.6	9	81	63
EUROPE--EAST GERMANY											
0146	322400	BLEICHER	51-30N	10-10E	+ 228	0.14	7.60	1.06	1	82	59
0147	322407	STASSFUR	51-40N	11-30E	+ 76	0.22	7.60	1.67	1	82	59
0148	322400	STRASSBE	51-35N	11-00E	+ 340	0.33	4.69	1.55	1	82	59
0149	342400	PECHTELS	50-30N	12-25E	+ 500	0.25	5.70	1.43	1	82	59
0150	342400	SCHMIEDE	50-30N	11-25E	+ 740	0.23	5.56	1.25	1	82	59
0151	342400	ZWICKAU	50-40N	12-35E	+ 328	0.45	2.8	1.32	1	82	59
0152	342400	FREITAL	51-05N	13-40E	+ 250	0.16	3.7	0.60	1	82	59
0153	342400	BRAND ER	51-00N	13-00E	+ 250	0.34	5.95	2.02	1	82	59
0154	342407	FREIBERG	51-00N	13-30E	+ 427	0.31	5.5	1.69	1	82	59
0155	342400	ALTENBER	50-30N	13-50E	+ 790	0.31	7.09	2.19	1	82	59
0156	322400	DORNDORF	50-50N	10-00E	+ 250	0.15	10.3	1.51	1	82	59
0157	321000	REHNA I	53-20N	11-00E	+ 50	0.23	6.5	1.48	1	82	59
0158	321000	OEBISFEL	52-30N	11-00E	+ 50	0.18	6.6	1.18	1	82	59
EUROPE--POLAND											
0159	321000	CIECHOCI	52-53N	18-47E	+ 100	.23	5.3	1.23	1	83	54
EUROPE--U.S.S.R.											
0160	311208	KRIVOI R	48-02N	33-20E	+ 100	.104	7.5	0.78	3	94	64
A	311208	KR-7554	48-02N	33-20E	+ 100	.104	7.13	0.74	1	94	64
B	311000	KR-8123	47-55N	33-20E	+ 100	.091	8.53	0.78	1	94	64
C	311000	KR-8500	47-55N	33-20E	+ 100	.10	7.1	0.71	1	94	64
0161	311208	BELAYA T	49-50N	30-10E	+ 100	.092	7.2	0.66	1	94	64
0162	311208	UMAN	48-45N	30-13E	+ 200	.11	5.8	0.63	1	94	64
0163	321206	YAKOVLEV	50-30N	36-30E	+ 300	.15	9.7	1.45	1	94	64
0164	341906	MAZESTA	43-35N	39-48E	+ 500	.15	6.7	1.	2	94	64
EUROPE--ICELAND											
1138	431000	ICELAND						4.5	1	72	55
EUROPE--BALTIC SHIELD											
1137	319000	BALTIC S				.15	5.	0.8	3	96	61
PACIFIC ISLAND											
0165	741090	ENIWETOK	11-30N	162-15E	+ 0	0.18	5.	0.9	1	95	56

REVIEW OF HEAT FLOW DATA

167

DATA NUMBER	CODE	STATION NAME	LATI- TUDE	LONGI- TUDE	ELE./ DEPTH	∇T	K	Q	NO	REF	YR
BLACK SEA											
0166	888000	BLACK S.	-	-	-2269	.48	4.0	1.9	7	87	61
A	888000	4742	-	-	-2179	.30	4.0	1.2	1	87	61
B	888000	4745	-	-	-1714	.45	4.0	1.8	1	87	61
C	888000	4751	-	-	-2216	.55	4.0	2.2	1	87	61
D	888000	4750	-	-	-2170	.65	4.0	2.6	1	87	61
E	888000	4752	-	-	-2197	.45	4.0	1.8	1	87	61
F	888000	4753	-	-	-1840	.50	4.0	2.	1	87	61
G	888000	4754	-	-	-1300	.45	4.0	1.8	1	87	61
ATLANTIC OCEAN											
0167	557608	CH21-1	29-51N	54-36W	-5610	0.50	2.08	1.04	1	3	64
0168	567608	CH21-4	28-56N	46-44W	-4370	0.30	2.24	0.67	1	3	64
0169	567608	CH21-5	28-47N	44-55W	-3940	0.51	2.22	1.13	1	3	64
0170	567602	CH21-10	29-04N	43-12W	-3080	0.4	1.96	0.8	1	3	64
0171	567608	CH21-12	28-51N	42-49W	-3520	0.38	2.11	0.81	1	3	64
0172	567607	CH21-13	29-02N	41-10W	-4060	0.2	1.94	0.4	1	3	64
0173	585508	CH19-C	20-13N	66-35W	-5810	0.56	2.27	1.28	1	3	64
0174	587608	CH19-7-1	20-14N	66-35W	-5770	0.75	2.05	1.54	1	3	64
0175	557608	A-282-3	23-20N	70-02W	-5480	0.54	2.09	1.12	1	4	63
0176	557608	A-282-5	23-28N	72-18W	-5300	0.66	1.77	1.17	1	4	63
0177	557608	A-282-6	25-14N	73-16W	-5310	0.53	2.03	1.08	1	4	63
0178	557608	A-282-7	26-59N	72-13W	-5150	0.58	1.86	1.09	1	4	63
0179	557608	A-282-9	25-18N	69-01W	-5580	0.55	2.11	1.17	1	4	63
0180	557608	A-282-10	23-37N	67-54W	-5650	0.53	2.00	1.06	1	4	63
0181	557608	A-282-11	21-47N	68-51W	-5560	0.61	2.10	1.27	1	4	63
0182	587608	A-282-12	20-22N	67-23W	-5410	0.87	2.01	1.76	1	4	63
0183	557608	A-282-13	21-54N	66-37W	-5640	0.61	1.94	1.19	1	4	63
0184	557608	A-282-14	23-40N	65-37W	-5800	0.59	1.92	1.13	1	4	63
0185	557608	A-282-15	25-29N	64-34W	-5680	0.57	1.92	1.09	1	4	63
0186	557608	A-282-17	25-26N	66-40W	-5580	0.64	1.90	1.22	1	4	63
0187	557608	A-282-18	27-05N	67-56W	-5200	0.57	1.88	1.07	1	4	63
0188	557608	A-282-20	28-44N	69-05W	-5330	0.58	2.06	1.18	1	4	63
0189	557608	A-282-21	28-51N	66-50W	-5240	0.62	1.93	1.19	1	4	63
0190	557608	A-282-22	28-54N	64-39W	-4900	0.61	1.80	1.11	1	4	63
0191	557608	A-282-23	30-27N	67-58W	-5230	0.55	1.91	1.05	1	4	63
0192	587607	AII-1-1	32-02N	74-09W	-4870	0.40	2.05	0.81	1	4	63
0193	587607	AII-1-3	30-56N	74-36W	-3430	0.47	1.99	0.94	1	4	63
0194	587608	AII-1-5	29-10N	76-22W	-4990	0.46	2.51	1.17	1	4	63
0195	557608	C-36-1	21-08N	65-02W	-5696	0.53	1.82	0.96	1	5	64
0196	557603	C-36-3	19-24N	61-30W	-5468	0.73	1.89	1.37	1	5	64
0197	557601	C-36-5	16-45N	57-38W	-5853	0.12	2.28	0.27	1	5	64
0198	557601	C-36-6	16-47N	57-49W	-5853	0.15	2.0	0.3	1	5	64
0199	557608	C-36-7	16-34N	57-52W	-4330	0.54	1.96	1.06	1	5	64
0200	557608	C-36-8	16-35N	57-54W	-4330	0.54	1.93	1.05	1	5	64
0201	557601	C-36-9	16-57N	58-24W	-5890	0.22	2.01	0.44	1	5	64
0202	557608	C-36-10	16-18N	58-37W	-5599	0.60	1.86	1.11	1	5	64
0203	587601	ATS296-4	39-32N	65-50W	-4330	0.47	2.29	1.08	1	5	64
0204	587601	ATS296-6	39-33N	66-17W	-4325	0.56	2.37	1.33	1	5	64
0205	587608	ATS296-7	39-47N	65-16W	-4467	0.48	2.22	1.07	1	5	64
0206	587608	ATS296-8	39-26N	65-09W	-4757	0.54	2.10	1.14	1	5	64
0207	587602	ATS296-9	39-46N	66-28W	-3922	0.56	2.11	1.18	1	5	64
0208	557608	C-39-1	29-00N	59-11W	-5811	0.47	1.96	0.92	1	5	64

DATA NUMBER	CODE	STATION NAME	LATI- TUDE	LONGI- TUDE	ELE./ DEPTH	∇T	K	Q	NO	REF	YR
ATLANTIC OCEAN (CONTINUED)											
0209	557603	C-39-2	25-18N	55-44W	-5932	0.72	1.93	1.39	1	5	64
0210	557608	C-39-3	24-04N	55-14W	-5984	0.33	1.82	0.60	1	5	64
0211	557608	C-39-5	28-30N	57-59W	-5800	0.48	1.98	0.95	1	5	64
0212	557608	C-39-6	29-56N	60-33W	-5715	0.72	1.84	1.33	1	5	64
0213	557608	C-39-7	29-47N	62-12W	-4865	0.66	1.81	1.19	1	5	64
0214	586607	B-D-6	39-36N	12-13W	-3020	0.46	2.30	1.06	1	6	61
0215	585608	B-D-7	35-59N	9-59W	-4534	0.37	2.31	0.87	1	6	61
0216	885608	B-D-8	35-58N	4-34W	-1251	0.57	2.13	1.22	1	6	61
0217	555608	B-D-9	45-28N	5-47W	-4592	0.33	2.26	0.75	1	6	61
0218	555608	B-D-10	46-32N	13-04W	-4413	0.50	2.17	1.09	1	6	61
0219	565608	B-D-11	46-30N	22-58W	-4084	0.57	2.25	1.29	1	6	61
0220	566607	B-D-12	46-37N	27-18W	-4109	3.15	2.07	6.52	1	6	61
0221	565608	B-D-13	36-20N	21-00W	-4844	0.54	2.12	1.14	1	6	61
0222	566607	B-D-14	35-36N	19-02W	-5375	0.67	2.01	1.34	1	6	61
0223	566607	B-D-15	35-34N	18-56W	-5380	0.46	2.01	0.93	1	6	61
0224	565608	B-D-16	36-39N	17-21W	-5146	0.53	2.13	1.14	1	6	61
0225	555608	B-D-17	44-55N	10-45W	-4844	0.64	2.18	1.39	1	6	61
0226	556607	B-D-18	40-59N	15-09W	-5305	0.49	2.32	1.14	1	6	61
0227	585608	B-D-19	42-18N	11-53W	-3063	0.36	2.18	0.76	1	6	61
0228	556607	B-D-20	41-27N	14-40W	-5260	0.55	2.18	1.21	1	6	61
0229	555608	B-D-21	43-42N	12-39W	-5030	0.51	2.29	1.16	1	6	61
0230	555808	CHAIN-1	35-35N	61-08W	-4590	0.62	1.92	1.20	1	7	61
0231	555808	CHAIN-2	35-35N	61-15W	-4680	0.68	1.92	1.31	1	7	61
0232	565801	CHAIN-3	51-18N	29-35W	-3260	3.7	1.7	6.2	1	7	61
0233	555808	CHAIN-4	53-53N	24-05W	-3350	0.73	2.10	1.54	1	7	61
0234	587708	V-15-3	00-59S	38-10W	-4137	0.66	2.31	1.52	1	8	62
0235	587708	V-15-4	00-12N	39-54W	-4111	0.48	2.23	1.07	1	8	62
0236	557708	V-15-5	02-30N	40-55W	-4285	0.63	2.19	1.38	1	8	62
0237	567708	V-15-6	05-04N	41-01W	-4544	0.83	2.23	1.85	1	8	62
0238	567708	V-15-7	06-59N	41-04W	-4636	0.90	2.25	2.03	1	8	62
0239	567708	V-15-8	10-45N	41-21W	-5002	1.51	2.23	3.37	1	8	62
0240	557707	V-15-10	14-14N	57-06W	-5002	0.73	2.19	1.60	1	8	62
0241	587708	V-15-12	17-21N	65-11W	-4169	0.52	2.23	1.16	1	8	62
0242	587708	V-15-13	20-49N	66-25W	-5227	0.68	2.23	1.52	1	8	62
0243	557708	V-15-14	23-14N	66-36W	-5605	0.61	2.23	1.36	1	8	62
0244	587708	V-15-16	21-34N	67-06W	-5115	0.75	2.23	1.67	1	8	62
0245	577708	V-15-19	19-50N	65-53W	-7934	0.52	2.23	1.16	1	8	62
0246	587708	V-15-23	32-35N	74-24W	-4521	0.46	2.23	1.03	1	8	62
0247	587708	V-15-24	32-47N	74-49W	-4462	0.47	2.22	1.04	1	8	62
0248	555508	LSDA-55	33-45S	15-00E	-4170	0.77	2.45	1.88	1	9	64
0249	555907	LSDA-56	33-15S	11-59E	-4630	0.43	2.37	1.01	1	9	64
0250	556507	LSDA-57	32-30S	09-01E	-5040	0.40	2.01	0.8	1	9	64
0251	556900	LSDA-58B	32-00S	06-06E	-5210	0.55	2.01	1.1	1	9	64
0252	565907	LSDA-59	31-37S	02-47E	-4215	0.04	2.18	0.09	1	9	64
0253	565508	LSDA-60	31-21S	01-58E	-4190	1.00	2.18	2.17	1	9	64
0254	565907	LSDA-61	30-52S	00-56W	-3810	0.41	2.18	0.90	1	9	64
0255	565508	LSDA-63	30-16S	04-21W	-4890	0.46	2.15	0.99	1	9	64
0256	565907	LSDA-64	30-06S	05-45W	-4340	0.34	2.19	0.74	1	9	64
0257	565508	LSDA-65	29-43S	07-16W	-4150	0.22	2.23	0.48	1	9	64
0258	565907	LSDA-66	29-48S	08-24W	-4155	0.12	2.23	0.27	1	9	64
0259	565508	LSDA-67	29-51S	09-25W	-3940	0.21	2.32	0.48	1	9	64
0260	565907	LSDA-68	29-49S	10-18W	-3735	0.51	2.28	1.16	1	9	64
0261	565907	LSDA-69	29-51S	11-07W	-3690	0.50	2.28	1.15	1	9	64

REVIEW OF HEAT FLOW DATA

169

DATA NUMBER	CODE	STATION NAME	LATI- TUDE	LONGI- TUDE	ELE./ DEPTH	∇T	K	Q	NO	REF	YR
ATLANTIC OCEAN (CONTINUED)											
0262	565907	LSDA-70	29-55S	11-54W	-3400	0.18	2.28	0.41	1	9	64
0263	565508	LSDA-71	29-51S	12-46W	-3200	0.50	2.24	1.12	1	9	64
0264	565907	LSDA-72	29-45S	14-11W	-3385	0.48	2.24	1.08	1	9	64
0265	565907	LSDA-73	29-50S	14-51W	-3735	0.15	2.24	0.34	1	9	64
0266	565907	LSDA-74	29-50S	15-33W	-3405	0.32	2.24	0.72	1	9	64
0267	565907	LSDA-75	27-22S	12-34W	-3520	0.99	2.27	2.24	1	9	64
0268	565508	LSDA-76	27-27S	10-56W	-3580	0.59	2.27	1.34	1	9	64
0269	566900	LSDA-77	26-47S	13-54W	-2480	0.78	2.27	1.7	1	9	64
0270	566900	LSDA-78	25-58S	14-51W	-3785	0.44	2.27	1.0	1	9	64
0271	565508	LSDA-79	24-03S	15-32W	-4100	0.05	2.18	0.10	1	9	64
0272	565907	LSDA-80	23-47S	14-27W	-4000	0.41	2.18	0.9	1	9	64
0273	565907	LSDA-81	23-42S	12-12W	-3580	0.51	2.18	1.12	1	9	64
0274	566900	LSDA-82	22-43S	13-07W	-3605	3.44	2.27	7.8	1	9	64
0275	565508	LSDA-83	21-21S	11-35W	-2515	3.58	2.27	8.14	1	9	64
0276	565907	LSDA-85	21-15S	10-39W	-3535	0.45	2.18	0.97	1	9	64
0277	566900	LSDA-86	20-10S	11-30W	-2925	3.35	2.18	7.3	1	9	64
0278	565907	LSDA-87	19-53S	12-26W	-2710	1.73	2.18	3.78	1	9	64
0279	565508	LSDA-88	19-44S	12-55W	-3500	0.48	2.18	1.04	1	9	64
0280	565907	LSDA-89	18-58S	12-49W	-3125	0.51	2.18	1.11	1	9	64
0281	565907	LSDA-90	18-58S	12-00W	-2510	2.14	2.27	4.85	1	9	64
0282	565508	LSDA-91	18-32S	10-15W	-3395	0.21	2.15	0.45	1	9	64
0283	565907	LSDA-92	18-08S	11-15W	-3305	0.34	2.18	0.75	1	9	64
0284	565907	LSDA-93	17-39S	12-22W	-3440	0.74	2.18	1.61	1	9	64
0285	565907	LSDA-94	17-15S	13-20W	-3340	0.22	2.18	0.47	1	9	64
0286	565907	LSDA-95	16-46S	14-30W	-3455	0.62	2.18	1.35	1	9	64
0287	565907	LSDA-96	16-15S	15-45W	-3435	0.20	2.18	0.43	1	9	64
0288	565907	LSDA-97	15-48S	16-50W	-3820	1.07	2.18	2.33	1	9	64
0289	565907	LSDA-98	15-23S	17-54W	-4390	0.23	2.18	0.51	1	9	64
0290	565508	LSDA-99	14-55S	19-22W	-4230	0.19	2.24	0.43	1	9	64
0291	565508	LSDA-100	10-00S	15-26W	-3595	0.13	2.23	0.29	1	9	64
0292	565508	LSDA-101	09-11S	13-20W	-2690	0.04	2.16	0.08	1	9	64
0293	565907	LSDA-102	09-03S	10-29W	-3550	0.18	2.23	0.40	1	9	64
0294	565907	LSDA-103	06-43S	13-27W	-3245	0.12	2.18	0.26	1	9	64
0295	565508	LSDA-104	05-41S	11-12W	-2905	1.18	2.18	2.58	1	9	64
0296	565907	LSDA-105	04-57S	09-28W	-3500	0.53	2.18	1.15	1	9	64
0297	565907	LSDA-106	00-56S	10-37W	-4040	0.50	2.12	1.07	1	9	64
0298	565907	LSDA-107	00-28S	10-51W	-4350	0.42	2.12	0.89	1	9	64
0299	565508	LSDA-108	00-03N	11-02W	-4125	0.68	2.12	1.45	1	9	64
0300	565907	LSDA-109	00-26N	11-14W	-4215	0.85	2.12	1.80	1	9	64
0301	555907	LSDA-110	00-52N	11-28W	-4950	0.07	2.12	0.15	1	9	64
0302	555508	LSDA-111	02-38N	12-12W	-4735	0.76	1.81	1.37	1	9	64
0303	555508	LSDA-112	05-01N	12-45W	-4390	0.82	1.91	1.56	1	9	64
0304	555508	LSDA-113	07-24N	17-08W	-4800	0.71	1.95	1.39	1	9	64
0305	565508	LSDA-114	06-47N	19-18W	-4360	0.46	2.09	0.96	1	9	64
0306	565907	LSDA-115	06-21N	20-49W	-3590	0.58	2.12	1.22	1	9	64
0307	565508	LSDA-116	05-07N	25-15W	-4360	0.92	2.16	1.99	1	9	64
0308	565508	LSDA-117	03-21N	30-52W	-2590	0.16	2.34	0.37	1	9	64
0309	565907	LSDA-118	03-18N	31-00W	-2820	1.16	2.31	2.68	1	9	64
0310	566900	LSDA-119	03-15N	31-35W	-2415	1.00	2.31	2.3	1	9	64
0311	565508	LSDA-120	03-57N	34-04W	-3340	0.82	2.28	1.87	1	9	64
0312	565907	LSDA-121	05-42N	32-51W	-2955	2.23	2.28	5.08	1	9	64
0313	565907	LSDA-122	05-59N	32-28W	-3300	2.26	2.31	5.22	1	9	64
0314	565508	LSDA-124	08-26N	34-23W	-4790	0.76	2.04	1.56	1	9	64

DATA NUMBER	CODE	STATION NAME	LATI- TUDE	LONGI- TUDE	ELE./ DEPTH	VT	K	Q	NO	REF	YR	
ATLANTIC OCEAN (CONTINUED)												
0315	565907	LSDA-125	09-39N	37-40W	-4045	0.11	2.16	0.23	1	9	64	
0316	565907	LSDA-126	09-34N	39-32W	-3340	0.57	2.28	1.31	1	9	64	
0317	566900	LSDA-127	09-41N	40-49W	-2315	0.74	2.28	1.7	1	9	64	
0318	565907	LSDA-128	09-45N	41-18W	-3295	0.74	2.28	1.70	1	9	64	
0319	566900	LSDA-130	11-35N	44-03W	-2755	1.05	2.28	2.4	1	9	64	
0320	565508	LSDA-131	11-34N	44-48W	-3830	0.40	2.12	0.84	1	9	64	
0321	565907	LSDA-132	11-34N	45-33W	-4105	1.11	2.08	2.30	1	9	64	
0322	565907	LSDA-133	12-17N	46-13W	-4515	0.22	2.08	0.46	1	9	64	
0323	585508	LSDA-134	14-59N	58-19W	-3535	0.32	2.22	0.72	1	9	64	
0324	585508	LSDA-135	15-04N	59-58W	-4480	0.32	2.20	0.71	1	9	64	
0325	586507	LSDA-136	15-04N	60-30W	-2335	0.93	2.15	2.0	1	9	64	
0326	885907	LSDA-137	15-02N	62-15W	-2720	0.93	2.15	2.0	1	9	64	
0327	885508	LSDA-139	15-00N	63-50W	-2082	0.66	2.06	1.36	2	9	64	
	A	885508	LSDA139A	15-00N	63-50W	-2080	0.66	2.06	1.37	1	9	64
	B	885508	LSDA139B	15-00N	63-50W	-2085	0.66	2.06	1.36	1	9	64
0328	855508	ZEP-4	13-36N	71-59W	-4232	0.72	2.0	1.4	1	10	64	
0329	855508	ZEP-5	13-43N	68-38W	-5042	0.53	1.9	1.1	1	10	64	
0330	886507	ZEP-8	14-22N	62-19W	-2877	0.70	1.9	1.3	1	10	64	
0331	555506	ZEP-9	16-24N	57-39W	-4647	0.39	1.8	0.7	1	10	64	
0332	565508	ZEP-11	19-10N	52-03W	-5344	0.81	1.7	1.4	1	10	64	
0333	565508	ZEP-12	20-12N	49-01W	-4632	0.30	1.5	0.5	1	10	64	
0334	865508	ZEP-13	21-06N	46-30W	-3912	0.16	1.9	0.3	1	10	64	
0335	565508	ZEP-14	21-04N	44-57W	-3255	0.84	2.1	1.8	1	10	64	
0336	565508	ZEP-15	21-56N	45-46W	-3372	3.24	2.0	6.5	1	10	64	
0337	565508	ZEP-16	23-06N	45-39W	-3983	1.48	2.0	3.0	1	10	64	
0338	565508	ZEP-17	23-34N	44-14W	-4960	0.81	2.0	1.6	1	10	64	
0339	566507	ZEP-18	23-57N	44-59W	-3493	1.34	2.1	2.8	1	10	64	
0340	566507	ZEP-19	23-36N	42-28W	-4113	0.23	2.1	0.5	1	10	64	
0341	565508	ZEP-20	24-16N	39-06W	-5439	0.19	1.9	0.4	1	10	64	
0342	565508	ZEP-22	25-05N	34-13W	-5602	0.36	1.9	0.7	1	10	64	
0343	555508	ZEP-23	26-14N	26-27W	-5210	0.59	2.0	1.2	1	10	64	
0344	555508	ZEP-25	26-57N	19-58W	-4298	0.46	2.1	1.0	1	10	64	
0345	586507	ZEP-26	31-12N	11-50W	-3210	0.50	2.2	1.1	1	10	64	
0346	585508	ZEP-27	33-35N	9-43W	-4340	0.45	2.2	1.0	1	10	64	
0347	885506	ZEP-32	40-37N	5-50E	-2720	0.56	2.2	1.2	1	10	64	
0348	557608	D 4775	29-02N	25-27W	-5342			1.39	1	11	63	
0349	557608	D 4777	28-60N	25-26W	-5344			1.20	1	11	63	
0350	557608	D 4778	29-03N	25-33W	-5342			1.13	1	11	63	
0351	557608	D 4784	29-04N	25-27W	-5339			1.21	1	11	63	
0352	557608	D 4788	29-05N	25-15W	-5299			1.29	1	11	63	
0353	557608	D 4809	28-51N	25-27W	-4871			1.11	1	11	63	
0354	557608	D 4813	28-50N	25-24W	-4862			1.05	1	11	63	
0355	557608	D 4817	29-34N	25-18W	-5400			1.03	1	11	63	
0356	557608	D 4821	29-35N	25-23W	-5297			1.23	1	11	63	
0357	557608	D 4822	29-08N	24-19W	-5281			1.33	1	11	63	
0358	557607	D 4528	45-19N	11-27W	-4143			1.13	1	12	63	
0359	557608	D 4531	45-19N	11-28W	-4125			1.00	1	12	63	
0360	557608	C19-6-17	31-54N	64-44W	-4262			0.97	1	12	63	
0361	567601	CH21-8	29-04N	44-11W				+	1	12	63	
0362	567608	CH21-14	34-00N	15-51W	-3810			0.57	1	12	63	
0363	567608	CH21-16	34-06N	14-24W	-4315			0.94	1	12	63	
0364	887601	CH21-18	39-31N	05-26E	-2826			0.87	1	12	63	
0365	887607	CH21-19	42-14N	07-09E	-2731			2.5	1	12	63	
0366	557608	D 4790	27-10N	21-06W	-4702			1.06	1	12	63	

REVIEW OF HEAT FLOW DATA

171

DATA NUMBER	STATION CODE	STATION NAME	LATI-TUDE	LONGI-TUDE	ELE./DEPTH	VT.	K	Q	NO	REF	YR
ATLANTIC OCEAN (CONTINUED)											
0367	557603	D 4794	27-10N	21-00W	-4682			1.2	1	12	63
0368	557608	D 4795	27-13N	21-05W	-4707			0.92	1	12	63
0369	557608	D 4805	29-35N	23-52W	-5240			1.13	1	12	63
0370	567608	D 4824	43-06N	19-50W	-5959			1.30	1	12	63
0371	857007	V18-151	19-51N	84-56W	-4564	0.7	2.0	1.4	1	13	64
0372	887508	V18-153	26-35N	88-49W	-2582	0.22	2.3	0.5	1	13	64
0373	557508	V18-155	26-28N	68-25W	-5284	0.55	2.0	1.1	1	13	64
0374	587508	V18-158	38-45N	67-33W	-4184	0.55	1.8	1.0	1	13	64
0375	587007	V18-159	39-11N	65-26W	-4730	0.55	2.0	1.1	1	13	64
0376	557007	V19-1	34-50N	70-15W	-4716	0.42	1.9	0.8	1	13	64
0377	557007	V19-2	32-36N	71-19W	-5392	0.63	1.9	1.2	1	13	64
0378	557508	V19-3	28-20N	68-06W	-5261	0.68	1.9	1.3	1	13	64
0379	557508	V19-4	27-28N	68-27W	-2858	0.47	1.9	0.9	1	13	64
0380	557007	V19-5	24-16N	67-11W	-5562	0.63	1.9	1.2	1	13	64
0381	857508	V19-6	16-06N	66-29W	-4520	0.6	2.0	1.2	1	13	64
0382	887007	C7-2	13-06N	63-09W	-1060	0.55	2.0	1.1	1	13	64
0383	857007	C7-3	12-34N	66-18W	-4529	0.4	2.0	0.8	1	13	64
0384	857007	C7-4	13-59N	71-43W	-3948	0.75	2.0	1.5	1	13	64
0385	887007	C7-5	12-04N	74-54W	-3611	0.5	2.0	1.0	1	13	64
0386	857007	C7-6	14-11N	76-32W	-4087	0.6	2.0	1.2	1	13	64
0387	887007	C7-9	14-50N	73-50W	-3460	0.5	2.0	1.0	1	13	64
0388	887007	C7-10	15-23N	73-17W	-3324	0.75	2.0	1.5	1	13	64
0389	887007	C7-11	16-08N	72-48W	-2893	0.55	2.0	1.1	1	13	64
0390	857007	C7-12	14-36N	70-57W	-3525	0.5	2.0	1.0	1	13	64
0391	555608	BULLARD1	49-46N	12-30W	-2032	0.426	2.59	1.10	1	15	54
0392	555608	BULLARD2	49-58N	18-33W	-4017	0.548	2.58	1.42	1	15	54
0393	555608	BULLARD3	49-09N	17-38W	-4532	0.237	2.43	0.58	1	15	54
0394	555608	BULLARD4	48-14N	16-58W	-4670	0.254	2.28	0.58	1	15	54
0395	555608	BULLARD5	48-52N	15-00W	-4710	0.455	2.64	1.20	1	15	54

INDIAN OCEAN

0396	985508	MSN-12	9-14S	127-30E	-3300	0.81	2.09	1.69	1	1	65
0397	985508	MSN-15	7-46S	121-14E	-4840	0.84	2.02	1.7	1	1	65
0398	655508	MSN-16	11-58S	115-26E	-5010	0.63	1.77	1.12	1	1	65
0399	655508	MSN-17	12-48S	115-24E	-5400	0.64	1.65	1.05	1	1	65
0400	675508	MSN-18	10-11S	115-19E	-4330	0.24	1.63	0.39	1	1	65
0401	655508	MSN-20	13-19S	109-34E	-4630	0.80	1.85	1.48	1	1	65
0402	655508	MSN-21	11-39S	109-35E	-4605	1.00	1.87	1.87	1	1	65
0403	675508	MSN-23	8-49S	109-36E	-3300	0.26	1.88	0.48	1	1	65
0404	655508	MSN-24	12-21S	101-25E	-4745	0.78	1.99	1.56	1	1	65
0405	655508	MSN-28	16-59S	93-29E	-5230	0.61	1.63	1.0	1	1	65
0406	665508	MSN-29	18-14S	86-42E	-4455	0.89	1.83	1.63	1	1	65
0407	655508	MSN-30	15-51S	81-10E	-5000	1.01	1.71	1.73	1	1	65
0408	655508	MSN-32	14-05S	72-15E	-5200	0.77	1.55	1.20	1	1	65
0409	665508	MSN-33	14-56S	70-13E	-4460	0.07	2.06	0.14	1	1	65
0410	665508	MSN-34	16-25S	66-01E	-3660	1.40	1.99	2.78	1	1	65
0411	665907	MSN-35	16-58S	64-46E	-4055	1.10	1.99	2.19	1	1	65
0412	665508	MSN-36	17-48S	62-40E	-3740	0.15	2.26	0.34	1	1	65
0413	665508	MSN-38	26-22S	74-08E	-4130	2.48	1.98	4.91	1	1	65
0414	665508	MSN-40	33-20S	72-37E	-4220	0.42	2.19	0.91	1	1	65
0415	665508	MSN-41	37-44S	71-47E	-4260	0.66	2.08	1.38	1	1	65
0416	665508	MSN-42	42-09S	70-37E	-4200	0.80	2.08	1.67	1	1	65

DATA NUMBER	STATION CODE	STATION NAME	LATI- TUDE	LONGI- TUDE	ELE./ DEPTH	VT	K	Q	NO	REF	YR
INDIAN OCEAN (CONTINUED)											
0417	665800	MSN-43	39-50S	75-03E	-3780	-	2.0	-	1	1	65
0418	665907	MSN-44	38-26S	79-34E	-3410	0.25	2.0	0.5	1	1	65
0419	665907	MSN-45	37-50S	85-22E	-3600	0.35	2.0	0.7	1	1	65
0420	655907	MSN-46	37-18S	90-42E	-3855	0.65	2.0	1.3	1	1	65
0421	655508	MSN-47	36-19S	98-41E	-4375	0.39	1.93	0.76	1	1	65
0422	655508	MSN-48	39-18S	119-52E	-4895	0.58	1.78	1.04	1	1	65
0423	665907	MSN-49	49-31S	132-14E	-3500	0.72	1.8	1.3	1	1	65
0424	665508	Z-1	12-27N	47-07E	-1820	2.95	2.03	5.98	1	1	65
0425	665907	Z-2	12-57N	48-16E	-2205	1.68	1.92	3.62	1	1	65
0426	665508	Z-3	13-17N	49-15E	-2425	1.78	1.81	3.22	1	1	65
0427	665907	Z-4	12-54N	49-38E	-2200	1.29	1.92	2.47	1	1	65
0428	665508	Z-5	12-25N	50-33E	-2420	1.53	2.02	3.09	1	1	65
0429	665508	Z-6	9-08N	54-42E	-3705	0.79	2.11	1.66	1	1	65
0430	665907	Z-7	9-09N	57-30E	-3265	0.68	2.01	1.37	1	1	65
0431	665508	Z-8	9-16N	59-00E	-3200	0.91	1.91	1.74	1	1	65
0432	665907	Z-9	9-34N	59-52E	-3895	0.84	2.01	1.68	1	1	65
0433	665508	Z-10	9-32N	61-24E	-4580	0.45	2.10	0.95	1	1	65
0434	656900	Z-11	9-34N	63-06E	-4505	0.10	2.25	0.23	1	1	65
0435	656507	Z-12	9-40N	66-19E	-4450	0.35	2.30	0.8	1	1	65
0436	655508	Z-13	9-48N	69-15E	-4550	0.69	2.17	1.49	1	1	65
0437	665508	Z-14	9-50N	71-50E	-2370	0.58	2.21	1.29	1	1	65
0438	665508	Z-15	9-56N	73-08E	-1925	0.31	2.09	1.70	1	1	65
0439	665508	Z-16	9-59N	74-50E	-2285	0.82	1.92	1.57	1	1	65
0440	655508	LSDA-1	8-13N	70-39E	-4145	0.71	2.03	1.44	1	1	65
0441	656507	LSDA-2	3-57N	70-49E	-4130	0.84	1.91	1.6	1	1	65
0442	666507	LSDA-3	0-05S	71-50E	-4200	0.51	2.15	1.1	1	1	65
0443	666507	LSDA-4	2-40S	73-16E	-2980	0.79	2.28	1.8	1	1	65
0444	655508	LSDA-5	5-21S	75-08E	-5220	0.92	1.64	1.51	1	1	65
0445	665508	LSDA-6	5-23S	72-47E	-2530	0.84	2.28	1.92	1	1	65
0446	665508	LSDA-7	5-40S	70-17E	-3935	0.30	1.88	0.57	1	1	65
0447	665907	LSDA-8	5-52S	66-36E	-4370	0.16	1.90	0.30	1	1	65
0448	665508	LSDA-9	5-34S	63-42E	-4210	0.87	1.91	1.67	1	1	65
0449	666508	LSDA-10	5-26S	59-14E	-3980	1.19	1.97	2.35	2	1	65
A	666507	LSDA-10A	5-26S	59-14E	-3980	1.93	1.97	3.8	1	1	65
B	665508	LSDA-10B	5-25S	59-13E	-3980	0.82	1.97	1.62	1	1	65
0450	665508	LSDA-11	5-30S	57-56E	-2525	0.61	2.02	1.23	1	1	65
0451	665907	LSDA-12	9-56S	57-07E	-4045	0.76	2.03	1.55	2	1	65
A	665907	LSDA-12A	9-57S	57-07E	-4040	0.76	2.03	1.54	1	1	65
B	665907	LSDA-12B	9-56S	57-07E	-4050	0.77	2.03	1.56	1	1	65
0452	665508	LSDA-13	10-21S	58-31E	-3575	0.46	2.02	0.92	1	1	65
0453	665508	LSDA-14	10-34S	59-51E	-2315	0.71	2.04	1.44	1	1	65
0454	665508	LSDA-15	13-42S	59-42E	-3900	0.50	2.00	1.00	1	1	65
0455	665508	LSDA-16	17-20S	57-42E	-4145	0.60	2.21	1.32	1	1	65
0456	655508	LSDA-17	22-01S	57-34E	-4750	0.51	1.77	0.90	1	1	65
0457	655508	LSDA-18	24-34S	57-26E	-5000	0.77	1.57	1.21	1	1	65
0458	665508	LSDA-19	26-53S	58-12E	-5540	0.58	1.58	0.91	1	1	65
0459	665508	LSDA-20	29-53S	61-52E	-4620	0.41	1.70	0.7	1	1	65
0460	665508	LSDA-21B	31-25S	61-56E	-4420	0.24	1.73	0.42	1	1	65
0461	665508	LSDA-22	32-55S	62-25E	-4745	0.43	1.59	0.68	1	1	65
0462	656900	LSDA-23B	39-44S	63-56E	-4810	1.70	2.18	3.7	1	1	65
0463	665508	LSDA-24	44-36S	70-57E	-3580	0.79	1.89	1.49	1	1	65
0464	665508	LSDA-25	35-47S	73-37E	-4380	0.20	1.93	0.38	1	1	65
0465	665508	LSDA-26	36-52S	76-22E	-3925	0.94	2.17	2.03	1	1	65

REVIEW OF HEAT FLOW DATA

173

DATA NUMBER	CODE	STATION NAME	LATI-TUDE	LONGI-TUDE	ELE./DEPTH	∇T	K	Q	NO	REF	YR
INDIAN OCEAN (CONTINUED)											
0466	685508	LSDA-30	31-28S	114-24E	-3740	0.52	2.04	1.05	2	1	65
	A	685508	LSDA-30A	31-29S	114-25E	-3730	0.43	2.04	0.88	1	1 65
	B	685508	LSDA-30B	31-27S	114-24E	-3750	0.60	2.04	1.22	1	1 65
0467	655907	LSDA-32	29-42S	111-30E	-5340	0.82	2.18	1.79	1	1	65
0468	655508	LSDA-33	25-03S	104-12E	-5100	0.71	1.63	1.15	1	1	65
0469	665508	LSDA-34	16-25S	89-19E	-5625	0.85	1.64	1.39	1	1	65
0470	655508	LSDA-35	13-48S	90-50E	-5200	0.82	1.59	1.30	1	1	65
0471	656507	LSDA-36	13-09S	93-13E	-5230	1.83	1.64	3.0	1	1	65
0472	655508	LSDA-37	14-56S	108-09E	-5580	0.68	1.70	1.15	1	1	65
0473	655508	LSDA-38	13-46S	115-32E	-5680	0.69	1.65	1.14	1	1	65
0474	655508	LSDA-39	13-31S	118-29E	-5680	0.57	1.64	0.93	1	1	65
0475	655508	LSDA-50	30-08S	37-47E	-4990	0.51	1.97	1.00	1	1	65
0476	685907	LSDA-51	31-04S	36-40E	-4535	0.98	2.26	2.22	1	1	65
0477	685508	LSDA-52	31-39S	35-57E	-2545	0.34	2.40	0.82	1	1	65
0478	685907	LSDA-53	32-14S	34-16E	-2660	0.63	2.30	1.45	1	1	65
0479	685508	LSDA-54	32-22S	32-47E	-3560	0.02	2.12	0.04	1	1	65
0480	665508	LSDH-1	9-07N	72-59E	-2135	0.77	2.08	1.61	1	1	65
0481	665508	LSDH-2	9-03N	73-10E	-2110	0.57	2.08	1.18	1	1	65
0482	656507	LSDH-3	7-24N	70-40E	-4110	0.66	2.19	1.44	1	1	65
0483	665508	LSDH-4	5-22S	74-17E	-4780	1.15	1.64	1.88	1	1	65
0484	665508	LSDH-5	5-40S	69-40E	-3815	0.00	2.00	0.00	1	1	65
0485	665508	LSDH-6	5-53S	65-57E	-4260	0.61	1.90	1.16	1	1	65
0486	665907	LSDH-7	5-31S	63-04E	-4255	1.16	1.94	2.26	1	1	65
0487	655907	LSDH-8	5-28S	60-02E	-4100	0.78	1.97	1.54	1	1	65
0488	666507	LSDH-9	5-26S	59-29E	-3952	1.96	2.02	3.95	2	1	65
	A	666507	LSDH-9A	5-26S	59-29E	-3945	2.28	2.02	4.6	1	1 65
	B	666507	LSDH-9B	5-26S	59-29E	-3960	1.63	2.02	3.3	1	1 65
0489	666507	LSDH-11	4-10S	57-15E	-3765	0.94	2.03	1.9	1	1	65
0490	665508	LSDH-13	9-49S	56-28E	-3885	0.13	2.03	0.27	1	1	65
0491	665907	LSDH-14	10-05S	57-53E	-3935	0.64	2.02	1.29	1	1	65
0492	665508	LSDH-15	10-30S	59-23E	-2858	0.66	1.94	1.28	2	1	65
	A	665508	LSDH-15A	10-30S	59-23E	-2870	0.63	1.94	1.22	1	1 65
	B	665508	LSDH-15B	10-30S	59-23E	-2845	0.69	1.94	1.34	1	1 65
0493	665508	LSDH-18	31-14S	62-58E	-5062	0.14	1.60	0.22	2	1	65
	A	665508	LSDH-18A	31-14S	62-57E	-5065	0.15	1.60	0.24	1	1 65
	B	665508	LSDH-18B	31-14S	62-58E	-5060	0.12	1.60	0.19	1	1 65
0494	665508	LSDH-20	33-16S	61-43E	-4695	1.13	1.56	1.77	1	1	65
0495	655508	LSDH-21	39-54S	67-53E	-4065	0.00	2.18	0.00	1	1	65
0496	665508	LSDH-22	40-47S	72-46E	-4000	0.17	2.30	0.40	1	1	65
0497	665508	LSDH-23	40-58S	75-08E	-4030	0.25	2.16	0.54	1	1	65
0498	665508	LSDH-24	40-19S	76-32E	-3020	0.94	2.25	2.12	1	1	65
0499	665907	LSDH-25	36-05S	75-59E	-3290	0.80	2.17	1.74	1	1	65
0500	665508	LSDH-26	37-21S	76-35E	-3380	0.44	2.10	0.92	1	1	65
0501	665907	LSDH-27	32-58S	96-02E	-4030	0.01	2.1	0.01	1	1	65
0502	666507	LSDH-28	32-06S	100-20E	-2450	1.22	2.37	2.9	1	1	65
0503	655508	LSDH-29	32-45S	102-45E	-4760	0.54	1.71	0.93	1	1	65
0504	655508	LSDH-30	32-59S	103-33E	-5130	0.73	1.70	1.27	1	1	65
0505	656900	LSDH-32	33-01S	111-11E	-4390	2.34	2.26	5.3	1	1	65
0506	655508	LSDH-33	32-17S	113-58E	-4190	0.44	2.26	0.99	1	1	65
0507	656507	LSDH-34	29-16S	110-42E	-5550	0.92	2.18	2.0	1	1	65
0508	655907	LSDH-35	25-40S	105-22E	-4830	0.69	1.63	1.13	1	1	65
0509	655907	LSDH-36	24-33S	103-39E	-5400	0.64	1.63	1.04	1	1	65
0510	655508	LSDH-37	20-11S	96-22E	-4910	0.66	1.59	1.05	1	1	65

DATA NUMBER	STATION CODE	STATION NAME	LATI- TUDE	LONGI- TUDE	ELE./ DEPTH	\bar{v}	K	Q	NO	REF
INDIAN OCEAN (CONTINUED)										
0511	655508	LSDH-38	14-12S	89-50E	-5315	0.66	1.63	1.07	1	1 65
0512	655907	LSDH-39	13-39S	91-31E	-5150	0.93	1.59	1.48	1	1 65
0513	655508	LSDH-40	13-23S	92-32E	-5200	1.85	1.73	3.20	1	1 65
0514	655508	LSDH-43	14-06S	101-22E	-5110	1.11	1.63	1.81	1	1 65
0515	655508	LSDH-44	14-56S	107-16E	-5805	0.79	1.74	1.37	1	1 65
0516	655907	LSDH-45	14-58S	109-12E	-5630	0.65	1.74	1.13	1	1 65
0517	655508	LSDH-46	14-13S	114-54E	-5670	0.63	1.62	1.02	1	1 65
0518	655508	LSDH-47	13-09S	116-29E	-5670	0.69	1.60	1.11	1	1 65
0519	655907	LSDH-48	13-41S	117-23E	-5715	0.58	1.62	0.94	1	1 65
0520	657508	V18-54	36-55S	23-24E	-5064	0.63	2.42	1.53	1	1 65
0521	657508	V18-55	38-59S	29-56E	-4202	0.62	2.52	1.57	1	1 65
0522	657508	V18-58	31-12S	48-05E	-4395	0.74	2.23	1.65	1	1 65
0523	657508	V18-59	26-42S	50-28E	-5266	1.08	1.68	1.81	1	1 65
0524	657508	V18-60	23-59S	51-11E	-4928	0.87	1.92	1.67	1	1 65
0525	657508	V18-61	21-26S	51-37E	-4959	0.73	1.99	1.46	1	1 65
0526	667508	V18-63	20-35S	63-32E	-3296	0.16	2.67	0.43	1	1 65
0527	657501	V18-67	25-29S	85-09E	-4559	0.96	2.74	2.64	1	1 65
0528	657508	V18-69	25-47S	93-43E	-4435	0.74	1.75	1.30	1	1 65
0529	657508	V18-70	25-46S	95-58E	-4937	0.75	1.81	1.35	1	1 65
0530	657508	V18-71	25-41S	99-04E	-5365	0.68	1.76	1.20	1	1 65
0531	657507	V18-72	25-41S	101-56E	-4720	0.85	1.82	1.54	1	1 65
0532	657508	V18-73	27-59S	108-40E	-5148	0.63	2.00	1.26	1	1 65
0533	657508	V18-74	36-07S	118-47E	-4590	0.47	2.19	1.02	1	1 65
0534	657501	V18-76	37-27S	133-40E	-5570	0.52	2.22	1.15	1	1 65
0535	677508	V19-54	7-43S	103-15E	-6411	0.96	2.03	1.95	1	1 65
0536	677508	V19-55	7-16S	102-02E	-5663	0.91	1.89	1.72	1	1 65
0537	657508	V19-57	14-31S	101-21E	-5363	0.71	1.69	1.20	1	1 65
0538	657508	V19-58	16-20S	100-33E	-5906	0.60	1.86	1.12	1	1 65
0539	657508	V19-59	18-11S	99-24E	-5754	0.70	1.81	1.26	1	1 65
0540	657508	V19-60	19-02S	97-15E	-5500	0.89	1.91	1.70	1	1 65
0541	657508	V19-61	20-56S	91-12E	-4840	0.83	1.87	1.55	1	1 65
0542	657508	V19-64	18-23S	82-08E	-5224	0.85	1.63	1.38	1	1 65
0543	657508	V19-65	16-11S	82-06E	-5380	0.37	1.77	0.66	1	1 65
0544	657508	V19-66	14-11S	82-08E	-4798	0.74	1.84	1.36	1	1 65
0545	657503	V19-67	12-44S	82-01E	-	1.20	1.68	2.02	1	1 65
0546	657507	V19-68	10-13S	81-37E	-5107	0.97	1.63	1.58	1	1 65
0547	657508	V19-69	7-54S	81-25E	-5229	0.58	1.76	1.02	1	1 65
0548	657507	V19-70	7-04S	80-46E	-5045	0.77	1.79	1.38	1	1 65
0549	687507	V19-72	7-07N	76-33E	-1770	0.49	2.22	1.09	1	1 65
0550	667508	V19-73	7-35N	74-13E	-2769	0.80	2.15	1.72	1	1 65
0551	667507	V19-74	8-07N	73-15E	-2186	0.71	2.32	1.65	1	1 65
0552	657508	V19-75	8-09N	70-38E	-4128	0.76	2.36	1.80	1	1 65
0553	657508	V19-76	8-09N	69-15E	-4650	0.90	2.11	1.90	1	1 65
0554	667508	V19-78	8-07N	62-47E	-4325	0.49	2.32	1.13	1	1 65
0555	667508	V19-79	7-26N	61-04E	-3605	1.19	2.50	2.98	1	1 65
0556	667507	V19-80	6-42N	59-20E	-2857	0.28	2.30	0.64	1	1 65
0557	667508	V19-82	7-04N	60-55E	-2680	0.61	2.02	1.23	1	1 65
0558	667507	V19-83	6-52N	60-42E	-3356	0.25	2.41	0.61	1	1 65
0559	667508	V19-84	6-37N	59-48E	-2923	0.91	2.33	2.12	1	1 65
0560	667507	V19-85	6-10N	57-10E	-4128	0.50	2.31	1.16	1	1 65
0561	657508	V19-87	4-43N	52-05E	-5111	0.54	1.96	1.05	1	1 65
0562	657508	V19-88	2-29N	51-28E	-5095	0.63	1.78	1.12	1	1 65
0563	657508	V19-89	0-29S	53-41E	-4857	0.93	1.92	1.78	1	1 65

REVIEW OF HEAT FLOW DATA

175

DATA NUMBER	CODE	STATION NAME	LATI- TUDE	LONGI- TUDE	ELE./ DEPTH	VT	K	Q	NO	REF	YR
INDIAN OCEAN (CONTINUED)											
0564	657508	V19-90	2-40S	54-45E	-4186	0.74	2.30	1.71	1	1	65
0565	657908	V19-91	3-34S	51-51E	-5056	0.88	1.89	1.66	1	1	65
0566	657503	V19-92	3-24S	48-46E	-4987	0.58	1.99	1.15	1	1	65
0567	657508	V19-93	3-11S	45-49E	-4607	0.61	1.90	1.15	1	1	65
0568	657508	V19-94	3-43S	43-52E	-4089	0.56	2.32	1.30	1	1	65
0569	687508	V19-95	4-13S	41-33E	-2722	0.52	2.44	1.27	1	1	65
0570	687508	V19-96	5-20S	40-26E	-1863	0.74	2.34	1.72	1	1	65
0571	687508	V19-97	6-59S	41-11E	-3369	0.62	2.39	1.48	1	1	65
0572	687508	V19-98	9-28S	43-19E	-3643	0.69	2.18	1.50	1	1	65
0573	687508	V19-100	13-08S	44-09E	-3548	0.65	2.10	1.37	1	1	65
0574	657508	V19-101	14-53S	42-51E	-3250	0.58	2.30	1.33	1	1	65
0575	667507	V19-102	16-56S	41-06E	-2548	0.29	2.51	0.72	1	1	65
0576	687507	V19-103	17-54S	39-30E	-2314	0.50	2.23	1.12	1	1	65
0577	687507	V19-106	22-57S	42-10E	-3175	0.64	2.18	1.40	1	1	65
0578	687500	V19-107	22-58S	41-22E	-3885	-	-	-	1	1	65
0579	687508	V19-108	23-11S	39-58E	-3345	0.70	2.19	1.54	1	1	65
0580	687508	V19-109	23-22S	38-51E	-3087	0.61	2.36	1.44	1	1	65
0581	687508	V19-110	23-31S	37-51E	-2903	0.80	1.99	1.60	1	1	65
0582	687508	V19-111	25-20S	36-47E	-2203	0.56	2.34	1.32	1	1	65
0583	657508	V19-112	31-42S	38-10E	-5018	0.59	2.03	1.20	1	1	65
0584	687503	V19-114	34-24S	31-25E	-4124	0.67	2.23	1.50	1	1	65
0585	687508	V19-115	35-30S	29-57E	-4565	0.53	2.49	1.32	1	1	65
0586	687507	V19-116	35-55S	27-45E	-4656	0.63	2.67	1.68	1	1	65
0587	687608	AND-1	10-01N	93-45E	-4206	3.1	1.70	5.27	1	2	64
0588	687608	AND-2	11-01N	93-42E	-2562	1.3	1.83	2.38	1	2	64
0589	687608	AND-3	11-56N	93-22E	-1390	0.5	1.79	0.90	1	2	64
0590	687608	AND-4	12-44N	93-58E	-2151	1.1	1.76	1.94	1	2	64
0591	667607	DIS 5116	5-35N	61-57E	-3560	.663	2.02	1.34	1	88	65
0592	667608	DIS 5122	5-35N	61-56E	-3560	.642	2.01	1.29	1	88	65
0593	667608	DIS 5125	2-45N	60-15E	-4806	.265	1.70	0.45	1	88	65
0594	667608	DIS 5135	2-55N	59-53E	-4697	.412	1.77	0.73	1	88	65
0595	657608	DIS 5139	1-54N	56-10E	-4812	.728	1.73	1.26	1	88	65
0596	687607	DIS 5144	1-41S	42-13E	-2255	.700	2.00	1.40	1	88	65
0597	687608	DIS 5149	2-24S	43-24E	-3552	.643	1.96	1.26	1	88	65
0598	657608	DIS 5152	2-32S	44-56E	-4160	.618	1.86	1.15	1	88	65
0599	657608	DIS 5155	2-48S	47-03E	-4812	.610	1.77	1.08	1	88	65
0600	657608	DIS 5160	3-30S	49-40E	-5042	.723	1.77	1.28	1	88	65
0601	657608	DIS 5165	3-33S	51-29E	-5100	.418	1.70	0.71	1	88	65
0602	667600	DIS 5171	2-10S	57-25E	-4402	.221	2.26	0.50	1	88	65
0603	667608	DIS 5177	2-12S	57-20E	-4402	.519	2.12	1.10	1	88	65
0604	657608	DIS 5180	6-39S	54-16E	-3824	.748	2.06	1.54	1	88	65
0605	657608	DIS 5190	2-51S	47-00E	-4800	.659	1.82	1.20	1	88	65
0606	657608	DIS 5194	2-34S	44-53E	-4180	.597	1.91	1.14	1	88	65
0607	687607	DIS 5201	1-42S	42-15E	-2046	.613	2.04	1.25	1	88	65
0608	657607	DIS 5204	3-31S	48-23E	-4940	.761	1.80	1.37	1	88	65
0609	657608	DIS 5207	3-34S	50-29E	-5082	.710	1.83	1.30	1	88	65
0610	657907	DIS 5215	2-25S	54-45E	-4360	.750	2.00	1.50	1	88	65
0611	667608	DIS 5226	11-07N	54-03E	-4028	.745	2.09	1.55	1	88	65
0612	667608	DIS 5227	11-39N	47-50E	-1900	1.80	2.14	3.85	1	88	65
0613	667608	DIS 5229	12-29N	47-02E	-2197	2.69	2.29	6.15	1	88	65
0614	667608	DIS 5230	12-56N	46-36E	-1600	1.50	2.16	3.25	1	88	65
0615	887608	DIS 5231	15-58N	41-31E	-1735	1.81	2.31	4.18	1	88	65
0616	887608	DIS 5232	18-24N	39-47E	-1480	.404	2.62	1.06	1	88	65
0617	887600	DIS 5234	20-27N	37-55E	-0870		2.75	+	1	88	65

DATA NUMBER	CODE	STATION NAME	LATI- TUDE	LONGI- TUDE	ELE./ DEPTH	VT	K	Q	NO	REF	YR
PACIFIC OCEAN											
0618	785108	E1	38-09N	142-58E	-1710	.130	2.10	0.27	1	34	62
0619	775108	E2	37-59N	143-58E	-7345	.542	2.11	1.14	1	34	62
0620	755108	E6	38-12N	147-55E	-5631	1.05	1.95	2.05	1	34	62
0621	755007	F20	33-39N	161-39E	-5605	.681	2.00	1.36	1	18	64
0622	775108	F23	34-23N	142-15E	-7490	.630	2.21	1.39	1	18	64
0623	776107	F24	34-04N	142-56E	-5110	.598	2.07	1.24	1	18	64
0624	756107	F25	33-53N	145-26E	-5770	.549	1.81	0.99	1	18	64
0625	756107	AKK0 7	39-22N	150-03E	-5480	1.74	1.90	3.30	1	18	64
0626	785503	AKK0 8	39-30N	143-28E	-2800	.546	2.16	1.18	1	18	64
0627	786507	MYJ 1	34-32N	139-46E	-1710	.574	2.54	1.46	1	18	64
0628	755508	AKK0 11	29-53N	137-56E	-3960	.397	2.06	0.82	1	18	64
0629	756507	AKK0 12	32-35N	138-06E	-3970	1.20	2.42	2.88	1	18	64
0630	786507	G1	40-02N	142-31E	-810	.702	1.75	1.26	1	18	64
0631	775808	G12	43-26N	148-15E	-5175	.407	1.53	0.62	1	18	64
0632	786500	G202	40-28N	142-59E	-1550	.464	2.16	1.00	1	18	64
0633	775508	G*2	39-42N	145-25E	-5315	.610	1.82	1.11	1	18	64
0634	755508	G*5	40-24N	145-40E	-5215	.344	1.67	0.58	1	18	64
0635	776507	G*10	41-52N	145-09E	-4435	.356	1.80	0.64	1	18	64
0636	775508	G*11	41-02N	146-00E	-5495	.568	2.44	1.38	1	18	64
0637	755500	AKK0 M1	38-11N	133-45E	-0970	1.08	1.98	2.13	1	86	65
0638	955508	AKK0 M2	40-47N	132-04E	-3080	0.35	1.78	0.63	1	86	65
0639	955508	AKK0 M3	40-48N	134-24E	-3400	1.30	1.79	2.33	1	86	65
0640	955508	AKK0 M4	38-01N	135-57E	-2550	1.39	1.75	2.44	1	86	65
0641	955508	AKK0 M5	40-13N	136-52E	-2525	0.80	1.70	1.40	1	86	65
0642	955508	AKK0 M6	40-59N	137-24E	-3422	0.96	2.08	1.98	1	86	65
0643	955508	AKK0 M7	40-23N	139-11E	-2670	1.18	1.95	2.02	1	86	65
0644	955508	AKK0 M8	39-29N	137-59E	-2508	0.72	1.81	1.30	1	86	65
0645	985500	EN 1	39-00N	139-10E	-0720	0.83	1.67	1.4	1	86	65
0646	985500	EN 2	38-32N	139-10E	-0320	0.26	1.82	0.5	1	86	65
0647	755508	H 11	39-50N	153-52E	-5560	0.50	1.74	0.88	1	86	65
0648	755508	H 12	40-05N	152-01E	-5475	0.51	1.68	0.86	1	86	65
0649	776507	H 14A	40-02N	146-02E	-5150	0.59	1.59	0.94	1	86	65
0650	955507	MAKKO 1	37-21N	134-07E	-2440	1.45	1.83	2.66	1	86	65
0651	955507	MAKKO 2	39-10N	133-02E	-2720	1.18	1.57	1.84	1	86	65
0652	955507	SAIKO 3	40-01N	132-29E	-3330	1.36	1.65	2.24	1	86	65
0653	955507	SAIKO 4	41-01N	131-54E	-3470	1.34	1.59	2.13	1	86	65
0654	956507	SAIKO 5	41-20N	132-48E	-3600	1.21	1.56	1.89	1	86	65
0655	955507	MAKKO 3	41-34N	133-35E	-3650	1.29	1.56	2.08	1	86	65
0656	955500	MAKKO 4	39-55N	134-50E	-1450	1.09	1.65	1.80	1	86	65
0657	955507	MAKKO 5	38-58N	135-25E	-3180	1.23	1.69	2.08	1	86	65
0658	955507	MAKKO 6	38-02N	135-57E	-2740	1.35	1.65	2.23	1	86	65
0659	985500	MAKKO 7	38-13N	137-52E	-1970	1.25	1.80	2.25	1	86	65
0660	955507	MAKKO 8	39-13N	132-25E	-2340	1.06	1.96	2.07	1	86	65
0661	955507	MAKKO 9	40-08N	136-44E	-2650	1.47	1.78	2.62	1	86	65
0662	955507	MAKKO 10	41-03N	136-06E	-3450	1.25	1.55	1.95	1	86	65
0663	955507	MAKKO 11	42-00N	138-10E	-3670	1.33	1.88	2.51	1	86	65
0664	955500	MAKKO 12	41-59N	139-23E	-1480	1.41	1.92	2.70	1	86	65
0665	985500	MAKKO 13	43-32N	140-20E	-0700	1.15	1.62	1.87	1	86	65
0666	985500	MAKKO 14	43-59N	139-20E	-1710	1.22	1.80	2.19	1	86	65
0667	955507	MAKKO 15	44-31N	138-26E	-2430	1.13	1.72	1.94	1	86	65
0668	985500	MAKKO 16	44-59N	137-29E	-1630	1.34	1.73	2.32	1	86	65
0669	986507	MAKKO 17	45-00N	138-36E	-2150	0.45	1.80	0.79	1	86	65
0670	985500	MAKKO 18	45-02N	139-37E	-0885	1.00	1.92	1.92	1	86	65

REVIEW OF HEAT FLOW DATA

177

DATA NUMBER	CODE	STATION NAME	LATI- TUDE	LONGI- TUDE	ELE./ DEPTH	VT	K	Q	NO	REF	YR
PACIFIC OCEAN (CONTINUED)											
0671	986500	MAKKO 19	45-05N	140-44E	-0330	1.31	2.04	2.66	1	86	65
1140	766502	TOKKO-1	31-58N	140-29E	-	1.58	2.10	3.2	1	86	65
1141	766507	TOKKO-3	33-44N	139-34E	-	1.54	1.60	2.46	1	86	65
1142	765507	TOKKO-4	33-55N	139-14E	-	1.12	1.60	1.79	1	86	65
0672	785508	MEN-2A	33-45N	119-31W	-1900	0.72	2.00	1.43	1	19	64
0673	785508	MEN-3	33-58N	122-34W	-4200	0.30	1.89	0.57	1	19	64
0674	785508	MEN-4	34-02N	125-15W	-4640	0.60	1.81	1.08	1	19	64
0675	785508	MEN-5	36-04N	125-04W	-4450	0.50	1.87	0.94	1	19	64
0676	785508	MEN-6	38-25N	126-09W	-4230	1.70	2.03	3.45	1	19	64
0677	785508	MEN-7	39-47N	126-21W	-4140	0.96	2.04	1.96	1	19	64
0678	786507	MEN-8	40-33N	126-31W	-3150	1.89	2.06	3.9	1	19	64
0679	785508	MEN-9	40-56N	126-31W	-3120	2.35	1.96	4.60	1	19	64
0680	785508	MEN-10	41-30N	126-32W	-2960	3.06	1.89	5.79	1	19	64
0681	785508	MEN-11	40-36N	127-25W	-3280	2.84	1.96	5.56	1	19	64
0682	785508	MEN-12	40-07N	128-10W	-4510	0.98	1.92	1.88	1	19	64
0683	785508	MEN-13	40-40N	129-13W	-3220	2.01	2.05	4.12	1	19	64
0684	785508	MEN-14	40-00N	131-00W	-4520	0.60	1.90	1.14	1	19	64
0685	785508	MEN-15	42-02N	133-07W	-3870	0.40	1.87	0.75	1	19	64
0686	785508	MEN-16	40-25N	133-06W	-4070	0.36	2.00	0.72	1	19	64
0687	785508	MEN-17	39-30N	133-05W	-4750	0.17	2.07	0.35	1	19	64
0688	785508	MEN-18	41-06N	135-32W	-4060	0.48	2.08	1.00	1	19	64
0689	785508	MEN-19	41-07N	151-22W	-5100	0.91	2.03	1.84	1	19	64
0690	785508	MEN-20	39-21N	149-56W	-5500	0.19	2.04	0.39	1	19	64
0691	785508	MEN-21	40-38N	149-01W	-4840	0.91	2.07	1.88	1	19	64
0692	785508	MEN-22	40-47N	146-00W	-4720	0.50	2.11	1.05	1	19	64
0693	785508	MEN-23	40-41N	142-52W	-4730	0.61	1.96	1.19	1	19	64
0694	785508	MEN-24	40-44N	139-22W	-4520	0.91	2.06	1.88	1	19	64
0695	785508	MEN-26	38-40N	142-36W	-5290	0.63	2.02	1.27	1	19	64
0696	785508	MEN-27	39-05N	139-26W	-5290	0.87	2.05	1.78	1	19	64
0697	785508	MEN-28	38-02N	137-58W	-5380	0.86	1.97	1.69	1	19	64
0698	785907	MEN-29	39-33N	135-59W	-5140	0.49	2.00	0.98	1	19	64
0699	785508	MEN-30	38-00N	134-00W	-4810	0.85	2.02	1.72	1	19	64
0700	785508	MEN-31	39-32N	133-05W	-4740	0.05	2.07	0.10	1	19	64
0701	785508	MEN-33	39-30N	131-47W	-4510	0.23	2.02	0.46	1	19	64
0702	785508	MEN-34	40-44N	131-45W	-3640	0.49	1.95	0.95	1	19	64
0703	785907	MEN-36	39-36N	129-31W	-4540	0.59	1.90	1.12	1	19	64
0704	785907	MEN-37	38-01N	128-46W	-4750	0.83	2.03	1.68	1	19	64
0705	785508	MEN-38	32-36N	118-06W	-2010	0.99	1.97	1.96	1	19	64
0706	785508	MEN-39	32-32N	117-31W	-1240	1.1	1.83	2.03	1	19	64
0707	785907	GU-1	32-32N	117-31W	-1230	1.41	1.83	2.58	1	19	64
0708	785508	GU-2	32-29N	118-03W	-1890	1.47	1.89	2.78	1	19	64
0709	785508	GU-3	32-14N	118-27W	-1630	0.95	1.88	1.78	1	19	64
0710	785508	GU-4	32-03N	118-50W	-1480	0.95	1.99	1.89	1	19	64
0711	785508	GU-5	31-50N	119-06W	-1690	1.15	1.88	2.16	1	19	64
0712	785508	GU-6	31-37N	119-35W	-3720	0.44	1.93	0.84	1	19	64
0713	785508	GU-7	31-26N	120-04W	-3970	0.89	1.87	1.66	1	19	64
0714	785508	GU-8	31-14N	120-32W	-3840	0.87	1.88	1.64	1	19	64
0715	785508	GU-9B	31-01N	120-55W	-3970	1.30	1.98	2.58	1	19	64
0716	785508	GU-10	30-48N	121-31W	-4100	1.20	2.02	2.42	1	19	64
0717	785508	GU-11	29-03N	121-04W	-4160	0.15	2.10	0.31	1	19	64
0718	785508	GU-12	29-09N	120-35W	-3910	0.83	1.97	1.64	1	19	64
0719	785508	GU-13	29-16N	120-04W	-3830	2.30	1.93	4.43	1	19	64
0720	785508	GU-14	29-22N	119-35W	-3710	1.20	1.99	2.39	1	19	64

DATA NUMBER	STATION CODE	STATION NAME	LATI- TUDE	LONGI- TUDE	ELE./ DEPTH	VT	K	Q	NO	REF	YR	
PACIFIC OCEAN (CONTINUED)												
0721	785508	GU-15B	29-35N	118-56W	-3800	0.81	2.02	1.64	1	19	64	
0722	785508	GU-16	29-37N	118-27W	-3570	0.19	2.06	0.39	1	19	64	
0723	785508	GU-17	29-33N	117-59W	-3580	1.29	2.02	2.61	1	19	64	
0724	785508	GU-18	28-59N	117-28W	-3542	1.48	1.94	2.87	6	19	64	
	A	785508	GU-18A	28-59N	117-28W	-3570	1.37	1.94	2.66	1	19	64
	B	785508	GU-18B	28-59N	117-28W	-3570	1.31	1.94	2.55	1	19	64
	C	785508	GU-18C	28-59N	117-28W	-3570	1.43	1.94	2.77	1	19	64
	D	785508	GU-18D	28-59N	117-28W	-3570	1.35	1.94	2.62	1	19	64
	E	785508	GU-18E	28-59N	117-28W	-3530	1.27	1.94	2.46	1	19	64
	F	785508	GU-18F	28-59N	117-28W	-3440	2.14	1.94	4.15	1	19	64
0725	785907	GU-19	28-52N	117-26W	-3550	2.11	1.94	4.09	1	19	64	
0726	785907	GU-20	28-58N	117-21W	-3550	0.92	1.94	1.79	1	19	64	
0727	785907	GU-21	29-06N	117-28W	-3620	0.97	1.94	1.89	1	19	64	
0728	785508	GU-22	29-54N	117-36W	-2840	1.12	2.03	2.34	1	19	64	
0729	785508	SB-1	31-16N	117-45W	-1930	1.06	2.12	2.25	1	19	64	
0730	785508	SB-2	31-15N	117-46W	-1950	1.58	2.12	3.35	1	19	64	
0731	785508	SB-3	30-54N	117-53W	-2050	0.92	2.03	1.87	1	19	64	
0732	785508	SB-4	30-53N	117-53W	-2040	0.98	2.03	1.99	1	19	64	
0733	785508	SB-5	30-18N	117-31W	-3250	1.42	2.04	2.90	1	19	64	
0734	785508	SB-6A	29-18N	117-29W	-3950	1.58	2.03	3.20	1	19	64	
0735	785508	SB-8	28-57N	117-31W	-3480	1.14	2.07	2.37	1	19	64	
0736	785508	SB-9	29-09N	116-43W	-4060	1.29	2.08	2.69	1	19	64	
0737	785508	SB-10	29-08N	116-42W	-4070	1.33	2.08	2.77	1	19	64	
0738	785508	SB-11	30-30N	116-30W	-2840	1.50	2.04	3.07	1	19	64	
0739	785508	SB-12	30-31N	116-33W	-2840	1.39	2.04	2.84	1	19	64	
0740	785508	H-1	31-27N	120-59W	-3835	0.53	1.89	1.01	1	19	64	
0741	785907	H-2	29-41N	121-36W	-4000	0.96	1.95	1.88	1	19	64	
0742	785907	T-1	32-35N	117-31W	-1225	1.12	1.83	2.05	1	19	64	
0743	785907	T-2	32-33N	117-31W	-1220	1.08	1.83	1.98	1	19	64	
0744	785508	EHF-1	31-11N	119-16W	-3690	0.63	2.04	1.28	1	19	64	
0745	788508	MOHOLE	28-59N	117-30W	-3570	1.38	2.04	2.81	1	20	64	
0746	765508	V-1	27-08N	111-38W	-1840	1.58	1.77	2.80	1	21	63	
0747	765508	V-2	27-17N	111-22W	-1870	1.78	1.65	2.94	1	21	63	
0748	765508	V-3	27-38N	111-44W	-1775	2.55	1.64	4.19	1	21	63	
0749	765508	V-4	26-46N	111-04W	-1750	1.68	1.75	2.95	1	21	63	
0750	765508	V-5	24-09N	108-55W	-3020	2.13	1.99	4.24	1	21	63	
0751	765508	V-6	22-58N	108-04W	-2900	0.34	1.81	0.62	1	21	63	
0752	765508	V-7	21-59N	107-41W	-3055	2.96	1.86	5.51	1	21	63	
0753	765508	V-8	21-00N	107-04W	-3300	2.11	1.89	3.98	1	21	63	
0754	765508	V-9	20-55N	106-25W	-4450	1.07	2.00	2.14	1	21	63	
0755	765508	V-10	20-10N	107-43W	-3290	0.71	1.76	1.25	1	21	63	
0756	765508	V-11	19-45N	108-28W	-2600	.79	1.82	1.43	1	21	63	
0757	765508	V-12	20-48N	109-34W	-2910	1.33	1.81	2.40	1	21	63	
0758	765508	V-13	22-33N	109-29W	-2860	2.96	2.08	6.15	1	21	63	
0759	755508	D-1	1-23S	131-31W	-4450	0.06	2.29	0.14	1	22	59	
0760	755508	D-2	14-59S	136-01W	-4510	0.35	1.86	0.65	1	22	59	
0761	755508	D-3	21-40S	147-41W	-4760	0.56	1.74	0.97	1	22	59	
0762	765508	D-4	40-37S	132-52W	-5120	0.61	1.80	1.1	1	22	59	
0763	765508	D-5	42-16S	125-50W	-4620	0.08	1.71	0.14	1	22	59	
0764	765508	D-6	46-44S	123-18W	-4140	0.35	2.09	0.73	1	22	59	
0765	765508	D-7	44-27S	110-44W	-3180	0.92	2.24	2.06	1	22	59	
0766	765508	D-8	43-43S	107-33W	-3180	1.34	2.28	3.06	1	22	59	
0767	765508	D-9	43-44S	104-25W	-3850	1.03	2.03	2.09	1	22	59	

REVIEW OF HEAT FLOW DATA

179

DATA NUMBER	CODE	STATION NAME	LATI-TUDE	LONGI-TUDE	ELE./DEPTH	∇T	K	Q	NO	REF	YR
PACIFIC OCEAN (CONTINUED)											
0768	765508	D-10	42-44S	96-03W	-4580	1.48	1.55	2.30	1	22	59
0769	765508	D-11	41-06S	86-38W	-3310	0.51	2.0	1.0	1	22	59
0770	755501	D-12	23-23S	72-10W	-4110	0.49	1.82	0.89	1	22	59
0771	755508	D-13	23-28S	72-58W	-3750	0.41	1.96	0.80	1	22	59
0772	755508	D-14	21-33S	79-09W	-4550	0.89	1.82	1.62	1	22	59
0773	765508	D-15	20-49S	81-08W	-2340	0.35	2.26	0.79	1	22	59
0774	765508	D-16	20-48S	81-09W	-2400	0.68	2.26	1.54	1	22	59
0775	755508	D-17	13-35S	79-09W	-4440	0.79	1.84	1.46	1	22	59
0776	785508	D-18	12-49S	77-53W	-2260	1.35	2.02	2.72	1	22	59
0777	785508	D-19	12-54S	78-06W	-3700	0.56	1.91	1.07	1	22	59
0778	775508	D-20	12-38S	78-38W	-5950	0.08	2.09	0.17	1	22	59
0779	775508	D-21	12-59S	78-21W	-5900	0.08	1.94	0.17	1	22	59
0780	765508	D-22	18-26S	78-16W	-4220	0.14	1.86	0.26	1	22	59
0781	765508	D-23	18-20S	79-21W	-3090	0.46	2.14	0.98	1	22	59
0782	755508	D-24	19-01S	81-29W	-4230	0.55	1.86	1.02	1	22	59
0783	765508	D-25	27-04S	88-53W	-3880	1.04	2.04	2.12	1	22	59
0784	765508	D-26	28-00S	96-20W	-3200	0.10	2.25	0.23	1	22	59
0785	765508	D-27	27-55S	106-57W	-2910	2.10	2.16	4.54	1	22	59
0786	765503	D-28	23-15S	117-48W	-3500	0.92	1.90	1.76	1	22	59
0787	765508	D-29	14-44S	112-06W	-3060	3.45	2.22	7.66	1	22	59
0788	765508	D-30	13-30S	108-31W	-3580	0.43	2.34	1.01	1	22	59
0789	765508	D-31	11-39S	109-48W	-3280	3.61	2.24	8.09	1	22	59
0790	765508	D-32	9-55S	110-39W	-2840	3.90	2.04	7.95	1	22	59
0791	755508	D-33	5-56S	112-29W	-4040	0.44	2.00	0.87	1	22	59
0792	755508	D-34	3-40S	114-13W	-4330	0.94	1.82	1.71	1	22	59
0793	755508	D-35	1-28N	116-04W	-3810	0.28	1.97	0.56	1	22	59
0794	765508	D-36	4-06N	115-41W	-4200	0.20	2.13	0.43	1	22	59
0795	785508	LFG-1	33-13N	118-36W	-1300	1.00	1.8	1.8	1	23	62
0796	785508	LFG-2	36-40N	123-03W	-3320	1.1	2.0	2.2	1	23	62
0797	785508	LFG-3	36-39N	123-16W	-3470	1.10	2.1	2.3	1	23	62
0798	785907	LFG-5	36-34N	123-41W	-3770	1.10	2.1	2.3	1	23	62
0799	785508	LFG-7	44-17N	138-36W	-4220	0.45	2.2	1.0	1	23	62
0800	785507	LFG-8	48-20N	157-22W	-5220	0.25	2.0	0.5	1	23	62
0801	985508	LFG-11	52-33N	175-09W	-3240	0.59	1.7	1.0	1	23	62
0802	955508	LFG-12	54-17N	176-15W	-3740	0.60	1.5	0.9	1	23	62
0803	955508	LFG-13	55-41N	177-40W	-4160	0.81	1.6	1.3	1	23	62
0804	955508	LFG-14A	56-05N	176-10W	-3690	0.69	1.6	1.1	1	23	62
0805	955508	LFG-14B	56-13N	176-18W	-3670	0.62	1.6	1.0	1	23	62
0806	785508	LFG-16	53-23N	163-20W	-4230	0.21	1.9	0.4	1	23	62
0807	775907	LFG-17	54-08N	156-52W	-5680	1.42	1.9	2.7	1	23	62
0808	785508	LFG-19	57-11N	149-38W	-2950	0.55	2.0	1.1	1	23	62
0809	785907	LFG-20	57-34N	147-37W	-4880	0.50	2.4	1.2	1	23	62
0810	785508	LFG-22	59-05N	145-05W	-4220	0.92	2.4	2.2	1	23	62
0811	785508	LFG-24	59-07N	144-20W	-4000	0.56	2.7	1.5	1	23	62
0812	785508	LFG-25	59-09N	143-39W	-3920	0.74	2.3	1.7	1	23	62
0813	785508	LFG-27	59-14N	142-50W	-2670	0.62	2.1	1.3	1	23	62
0814	785508	LFG-28	58-11N	139-31W	-2910	0.68	2.2	1.5	1	23	62
0815	785508	LFG-29	57-42N	140-08W	-3310	0.72	1.8	1.3	1	23	62
0816	785508	LFG-30	56-58N	139-32W	-3340	0.92	2.4	2.2	1	23	62
0817	785907	LFG-35	54-27N	134-41W	-2560	1.86	2.2	4.1	1	23	62
0818	785508	LFG-37	54-13N	135-27W	-2900	1.35	2.0	2.7	1	23	62
0819	785508	LFG-38	54-07N	135-51W	-2740	1.22	1.8	2.2	1	23	62
0820	785508	LFG-39	53-07N	133-27W	-2900	0.94	1.7	1.6	1	23	62

DATA NUMBER	STATION CODE	STATION NAME	LATI- TUDE	LONGI- TUDE	ELE./ DEPTH	∇T	K	Q	NO	REF	YR
PACIFIC OCEAN (CONTINUED)											
0821	785508	LFG-40	53-15N	133-30W	-2910	0.61	1.8	1.1	1	23	62
0822	785508	LFG-41	50-04N	132-25W	-3100	0.30	2.3	0.7	1	23	62
0823	785508	LFG-42	48-19N	131-38W	-3050	0.52	2.3	1.2	1	23	62
0824	785508	LFG-43	46-15N	131-59W	-3290	0.36	2.2	0.8	1	23	62
0825	785508	LFG-44	43-51N	130-55W	-3320	1.45	2.2	3.2	1	23	62
0826	785508	LFG-45	42-19N	130-39W	-3430	0.24	2.1	0.5	1	23	62
0827	785500	LFG-46	40-36N	130-26W	-3760	0.05	2.0	0.1	1	23	62
0828	785507	LFG-47	40-35N	129-22W	-3240	1.71	2.1	3.6	1	23	62
0829	785507	LFG-48	38-35N	127-45W	-4630	.30	2.0	0.6	1	23	62
0830	785508	LFG-50	36-19N	125-56W	-4620	1.11	1.8	2.0	1	23	62
0831	785508	MSN-2	23-15N	130-46W	-4930	0.11	2.04	0.22	1	24	63
0832	785508	MSN-3	20-02N	135-11W	-5180	0.75	2.08	1.56	1	24	63
0833	755508	MSN-64	10-34S	151-05W	-5070	0.73	1.62	1.18	1	24	63
0834	755508	MSN-65	8-17S	151-36W	-5190	0.87	1.65	1.44	1	24	63
0835	755508	MSN-66	5-55S	149-39W	-5160	0.47	1.59	0.75	1	24	63
0836	755508	MSN-67	4-22S	149-29W	-4600	0.44	1.69	0.74	1	24	63
0837	755508	MSN-68	5-20N	146-13W	-5090	0.64	1.62	1.03	1	24	63
0838	755508	MSN-69	7-02N	145-38W	-5100	0.91	1.66	1.51	1	24	63
0839	755508	MSN-70	8-07N	145-24W	-5000	0.80	1.67	1.34	1	24	63
0840	755508	MSN-71	9-06N	145-18W	-5300	0.79	1.77	1.40	1	24	63
0841	755907	MSN-72	10-59N	142-37W	-4890	2.77	1.61	4.46	1	24	63
0842	755508	MSN-73	11-03N	142-28W	-5000	0.66	1.61	1.06	1	24	63
0843	765508	MSN-74	13-04N	138-59W	-5000	0.41	1.58	0.64	1	24	63
0844	765508	MSN-75	15-11N	136-52W	-4990	0.70	1.83	1.28	1	24	63
0845	785508	MSN-76	24-18N	126-30W	-4750	0.43	2.10	0.90	1	24	63
0846	785508	MSN-77	29-07N	121-03W	-4080	0.10	2.00	0.19	1	24	63
0847	785508	MSN-78	31-01N	119-04W	-3620	1.43	1.91	2.73	1	24	63
0848	785508	RIS-1	28-02N	117-12W	-3900	1.22	2.07	2.52	1	24	63
0849	785508	RIS-2	26-11N	117-18W	-4000	0.91	2.14	1.95	1	24	63
0850	785508	RIS-3	24-12N	117-23W	-3935	0.62	2.02	1.26	1	24	63
0851	785508	RIS-4	22-13N	117-21W	-3890	1.29	2.08	2.69	1	24	63
0852	785508	RIS-5	20-18N	117-27W	-4010	0.33	1.83	0.60	1	24	63
0853	785508	RIS-6	18-46N	117-14W	-4090	1.20	1.80	2.16	1	24	63
0854	765508	RIS-8	14-26N	117-12W	-4110	1.60	1.76	2.82	1	24	63
0855	765508	RIS-9	12-54N	117-24W	-4230	0.24	1.69	0.41	1	24	63
0856	765508	RIS-10	11-28N	117-38W	-4310	0.52	1.90	0.99	1	24	63
0857	765508	RIS-11	9-43N	117-32W	-4230	0.33	1.63	0.54	1	24	63
0858	765508	RIS-12	8-06N	117-51W	-3880	0.59	1.95	1.15	1	24	63
0859	765508	RIS-13	6-45N	117-51W	-4000	0.41	1.87	0.76	1	24	63
0860	765508	RIS-14	5-20N	117-52W	-4355	0.38	1.88	0.71	1	24	63
0861	765508	RIS-15	3-54N	118-08W	-4110	0.35	1.99	0.69	1	24	63
0862	765907	RIS-16	4-03N	117-01W	-4160	0.46	1.99	0.91	1	24	63
0863	765907	RIS-17	4-03N	115-53W	-4120	0.78	2.13	1.66	1	24	63
0864	765907	RIS-18	4-03N	115-36W	-4170	0.19	2.13	0.40	1	24	63
0865	765907	RIS-19	4-13N	114-58W	-4210	0.34	2.06	0.70	1	24	63
0866	765508	RIS-20	4-25N	113-41W	-3980	0.30	1.98	0.60	1	24	63
0867	765907	RIS-21	4-34N	112-31W	-3950	0.54	1.98	1.07	1	24	63
0868	765508	RIS-22	4-44N	111-33W	-4060	0.65	1.87	1.21	1	24	63
0869	765508	RIS-24B	5-04N	109-11W	-3980	1.25	2.06	2.57	1	24	63
0870	765907	RIS-25	5-13N	107-59W	-3760	0.98	2.04	1.99	1	24	63
0871	765508	RIS-26	5-14N	106-33W	-3820	1.15	2.02	2.32	1	24	63
0872	765907	RIS-27	5-24N	105-41W	-3645	0.79	1.95	1.55	1	24	63
0873	765508	RIS-28	5-37N	104-27W	-3570	0.86	1.87	1.61	1	24	63

REVIEW OF HEAT FLOW DATA

181

DATA NUMBER	CODE	STATION NAME	LATI- TUDE	LONGI- TUDE	ELE./ DEPTH	VT	K	Q	NO	REF	YR
PACIFIC OCEAN (CONTINUED)											
0874	765907	RIS-29	5-43N	103-29W	-3305	2.26	1.76	3.98	1	24	63
0875	765907	RIS-30	5-37N	104-03W	-3400	0.87	1.87	1.63	1	24	63
0876	765508	RIS-31	5-34N	103-08W	-3300	0.90	1.76	1.58	1	24	63
0877	765907	RIS-32B	5-41N	102-36W	-3130	2.76	1.76	4.86	1	24	63
0878	765508	RIS-33	5-39N	102-06W	-3175	4.24	1.75	7.42	1	24	63
0879	765907	RIS-34B	5-42N	101-43W	-3440	0.36	1.84	0.67	1	24	63
0880	765508	RIS-35	5-36N	101-09W	-3250	0.92	1.93	1.78	1	24	63
0881	765907	RIS-36	5-41N	100-50W	-3405	0.64	1.94	1.25	1	24	63
0882	765907	RIS-37	5-44N	101-56W	-3285	0.69	1.75	1.20	1	24	63
0883	765508	RIS-38	5-43N	99-55W	-3420	0.58	1.94	1.12	1	24	63
0884	765907	RIS-39	6-05N	98-47W	-3470	0.54	1.74	0.94	1	24	63
0885	765508	RIS-40	6-41N	97-25W	-3520	0.21	1.74	0.37	1	24	63
0886	785907	RIS-41	6-58N	96-06W	-3785	0.05	1.67	0.08	1	24	63
0887	785508	RIS-42	6-57N	94-58W	-3740	0.73	1.60	1.17	1	24	63
0888	785907	RIS-43	5-05N	93-56W	-3540	0.66	1.72	1.13	1	24	63
0889	785508	RIS-44	4-07N	92-09W	-3150	0.28	1.95	0.55	1	24	63
0890	785907	RIS-45	3-16N	90-42W	-2360	0.44	2.00	0.87	1	24	63
0891	785508	RIS-46	2-17N	89-28W	-2160	0.24	2.09	0.51	1	24	63
0892	785508	RIS-47B	1-13N	88-32W	-2480	2.79	1.89	5.27	1	24	63
0893	785907	RIS-48B	0-15N	86-23W	-2760	2.52	1.85	4.66	1	24	63
0894	785508	RIS-49	0-09S	85-58W	-2750	0.36	1.81	0.65	1	24	63
0895	785907	RIS-50	1-41S	85-33W	-2440	3.11	1.91	5.94	1	24	63
0896	785907	RIS-51	1-45S	85-31W	-2385	1.00	1.98	1.98	1	24	63
0897	785508	RIS-52	2-44S	85-29W	-3220	1.53	1.98	3.03	1	24	63
0898	785907	RIS-53	3-52S	84-50W	-3395	1.22	1.98	2.42	1	24	63
0899	775508	RIS-54	9-07S	81-33W	-4700	0.50	1.75	0.87	1	24	63
0900	775907	RIS-55	8-51S	80-53W	-6280	0.46	2.00	0.91	1	24	63
0901	775907	RIS-56	8-47S	80-35W	-2975	0.54	2.00	1.07	1	24	63
0902	775907	RIS-57	12-34S	78-35W	-5940	0.12	2.09	0.26	1	24	63
0903	785907	RIS-58	12-46S	80-00W	-4630	0.64	1.79	1.14	1	24	63
0904	785508	RIS-59	12-59S	81-32W	-4800	1.21	1.68	2.04	1	24	63
0905	785907	RIS-60	13-04S	82-58W	-4990	1.51	1.70	2.56	1	24	63
0906	785508	RIS-61	13-11S	84-25W	-4740	0.86	1.72	1.48	1	24	63
0907	785907	RIS-62B	13-24S	86-15W	-4500	0.21	1.69	0.36	1	24	63
0908	785508	RIS-63	13-32S	87-26W	-4240	0.29	1.66	0.48	1	24	63
0909	785907	RIS-64	13-33S	89-05W	-4080	0.58	1.80	1.05	1	24	63
0910	785508	RIS-65	13-43S	90-30W	-3900	0.08	1.93	0.15	1	24	63
0911	785907	RIS-66	13-40S	92-00W	-3830	0.78	2.01	1.57	1	24	63
0912	785508	RIS-67	13-35S	93-28W	-3880	1.55	2.08	3.22	1	24	63
0913	785907	RIS-68	13-37S	94-58W	-3720	1.00	2.08	2.08	1	24	63
0914	785508	RIS-69	13-37S	96-44W	-4150	1.10	1.86	2.04	1	24	63
0915	785508	RIS-70	13-32S	97-48W	-3740	0.62	2.05	1.28	1	24	63
0916	785907	RIS-71	13-26S	99-11W	-3950	0.87	1.91	1.66	1	24	63
0917	785508	RIS-72	13-23S	100-30W	-4210	0.22	1.77	0.39	1	24	63
0918	785907	RIS-73	13-16S	101-24W	-4300	1.74	1.80	3.14	1	24	63
0919	765508	RIS-74B	13-18S	102-18W	-4430	0.79	2.22	1.75	1	24	63
0920	765907	RIS-75	13-11S	103-30W	-4170	0.78	2.10	1.63	1	24	63
0921	765508	RIS-76	13-03S	104-41W	-3720	0.40	1.98	0.79	1	24	63
0922	765907	RIS-77	12-59S	105-31W	-3910	0.64	2.13	1.37	1	24	63
0923	765508	RIS-78	12-54S	106-29W	-3720	1.33	2.27	3.02	1	24	63
0924	765907	RIS-79	12-50S	107-31W	-3710	0.41	2.22	0.92	1	24	63
0925	765508	RIS-80	12-48S	107-59W	-3550	0.50	2.16	1.09	1	24	63
0926	765907	RIS-81	12-43S	108-32W	-3550	0.98	2.17	2.13	1	24	63

DATA NUMBER	STATION CODE	STATION NAME	LATI- TUDE	LONGI- TUDE	ELE./ DEPTH	∇T	K	Q	NO	REF	YR
PACIFIC OCEAN (CONTINUED)											
0927	765907	RIS-82	12-44S	109-02W	-3415	0.91	2.17	1.97	1	24	63
0928	765907	RIS-83	12-40S	109-30W	-3405	1.06	2.17	2.31	1	24	63
0929	765508	RIS-84	12-39S	110-01W	-3255	1.34	2.18	2.93	1	24	63
0930	765907	RIS-85	12-35S	110-29W	-3180	2.17	2.18	4.74	1	24	63
0931	765907	RIS-86	12-35S	110-15W	-3165	1.36	2.18	2.96	1	24	63
0932	765907	RIS-87	12-33S	110-47W	-3010	1.20	1.82	2.18	1	24	63
0933	765508	RIS-88B	12-33S	111-13W	-3105	1.52	1.82	2.76	1	24	63
0934	765907	RIS-89	12-32S	111-29W	-3030	1.64	1.88	3.08	1	24	63
0935	765907	RIS-90	12-33S	112-01W	-3075	3.27	1.94	6.35	1	24	63
0936	765907	RIS-91	12-32S	112-16W	-3175	1.75	2.00	3.50	1	24	63
0937	765508	RIS-92	12-30S	112-37W	-3170	0.98	2.05	2.00	1	24	63
0938	765907	RIS-93	12-26S	113-05W	-3230	1.43	2.05	2.94	1	24	63
0939	765907	RIS-94	12-25S	113-31W	-3325	0.87	2.05	1.79	1	24	63
0940	765907	RIS-95	13-02S	113-17W	-3240	2.10	1.90	4.00	1	24	63
0941	765508	RIS-96	13-36S	112-42W	-3025	1.85	1.75	3.24	1	24	63
0942	765907	RIS-97	14-02S	112-20W	-2960	1.48	1.75	2.59	1	24	63
0943	765907	RIS-98	14-47S	112-32W	-3020	0.69	2.22	1.34	1	24	63
0944	765907	RIS-99	14-47S	112-54W	-3065	0.92	2.09	1.93	1	24	63
0945	765508	RIS-100	14-41S	113-30W	-3010	3.62	1.96	7.10	1	24	63
0946	765907	RIS-101	14-40S	113-45W	-3170	4.10	1.96	8.04	1	24	63
0947	765907	RIS-102	14-38S	114-02W	-2975	2.38	1.95	4.65	1	24	63
0948	765907	RIS-103	14-15S	113-11W	-3045	3.14	1.85	5.80	1	24	63
0949	765907	RIS-104	14-15S	113-33W	-3020	2.07	1.95	4.03	1	24	63
0950	765508	RIS-105	14-15S	113-50W	-3045	0.43	1.94	0.84	1	24	63
0951	765907	RIS-106	14-15S	114-09W	-3015	1.69	1.94	3.27	1	24	63
0952	765907	RIS-107	14-17S	114-32W	-3120	0.96	1.94	1.87	1	24	63
0953	765907	RIS-108	14-17S	114-59W	-3210	0.57	2.04	1.17	1	24	63
0954	765508	RIS-109	14-18S	115-37W	-3440	0.45	2.14	0.97	1	24	63
0955	765907	RIS-110	14-15S	116-23W	-3280	0.79	2.17	1.72	1	24	63
0956	765508	RIS-111	14-14S	117-35W	-3440	0.45	2.20	1.00	1	24	63
0957	765907	RIS-112	13-59S	118-33W	-3380	0.32	2.19	0.70	1	24	63
0958	765508	RIS-113	14-00S	119-39W	-3270	0.06	2.19	0.13	1	24	63
0959	765907	RIS-114B	14-04S	120-16W	-3600	0.69	2.13	1.48	1	24	63
0960	765907	RIS-115	14-03S	121-17W	-3680	0.31	2.13	0.67	1	24	63
0961	765508	RIS-116	14-01S	122-28W	-3935	0.03	2.07	0.07	1	24	63
0962	765907	RIS-117	14-07S	123-47W	-3860	0.67	2.07	1.39	1	24	63
0963	765907	RIS-118	13-33S	121-48W	-3640	0.75	2.13	1.60	1	24	63
0964	765907	RIS-119	13-33S	121-50W	-3665	0.12	2.13	0.25	1	24	63
0965	765508	RIS-120	13-52S	125-20W	-3680	0.47	2.20	1.04	1	24	63
0966	765907	RIS-121	14-02S	127-07W	-3930	0.09	2.05	0.18	1	24	63
0967	765508	RIS-122	14-02S	128-25W	-3995	0.54	1.90	1.02	1	24	63
0968	755907	RIS-123	14-02S	129-48W	-4120	1.49	1.74	2.60	1	24	63
0969	755907	RIS-124	14-03S	130-18W	-4090	0.47	1.74	0.82	1	24	63
0970	755508	RIS-125	14-03S	131-44W	-4010	0.30	1.58	0.48	1	24	63
0971	755907	RIS-127	14-02S	133-45W	-4290	0.50	1.57	0.79	1	24	63
0972	755508	RIS-128	14-02S	134-55W	-4220	0.75	1.56	1.17	1	24	63
0973	755907	RIS-129	14-03S	136-34W	-4290	0.36	1.56	0.57	1	24	63
0974	755508	RIS-130	14-09S	138-06W	-4040	1.10	1.55	1.70	1	24	63
0975	755508	RIS-131	14-03S	139-35W	-3925	0.86	1.94	1.67	1	24	63
0976	785907	RIS-132	14-55S	141-34W	-2610	0.84	2.15	1.8	1	24	63
0977	785508	RIS-133	15-15S	142-26W	-3725	0.52	2.15	1.12	1	24	63
0978	785503	RIS-134	16-30S	145-07W	-1440	0.79	2.14	1.70	1	24	63
0979	785508	RIS-135	16-52S	145-49W	-2750	0.66	2.05	1.35	1	24	63

REVIEW OF HEAT FLOW DATA

183

DATA NUMBER	CODE	STATION NAME	LATI- TUDE	LONGI- TUDE	ELE./ DEPTH	T	K	Q	NO	REF	YR.
PACIFIC OCEAN (CONTINUED)											
0980	785508	RIS-136	17-05S	147-13W	-4190	0.12	1.72	0.21	1	24	63
0981	785907	RIS-137	16-46S	148-52W	-4200	0.09	1.75	0.16	1	24	63
0982	785508	RIS-138	16-34S	148-30W	-4250	0.65	1.75	1.13	1	24	63
0983	785508	RIS-140	14-43S	145-40W	-2770	0.54	2.20	1.20	1	24	63
0984	785508	RIS-141	13-37S	145-03W	-4390	0.17	1.72	0.29	1	24	63
0985	755508	RIS-142	13-03S	144-03W	-4960	0.58	2.24	1.29	1	24	63
0986	755907	RIS-143	12-46S	143-34W	-4480	0.64	1.71	1.10	1	24	63
0987	755508	RIS-144	11-58S	142-27W	-4520	0.73	1.62	1.19	1	24	63
0988	755907	RIS-145	11-05S	140-57W	-4270	0.22	2.11	0.46	1	24	63
0989	785508	RIS-146	10-30S	139-59W	-4140	0.18	2.11	0.37	1	24	63
0990	785508	RIS-147	8-38S	138-18W	-4030	0.83	2.01	1.67	1	24	63
0991	755903	RIS-148	7-27S	137-11W	-4400	0.43	1.82	0.78	1	24	63
0992	755508	RIS-149	6-23S	136-11W	-4350	0.80	1.64	1.31	1	24	63
0993	755508	RIS-151	4-06S	133-59W	-4445	0.63	1.95	1.22	1	24	63
0994	755907	RIS-152	2-46S	132-58W	-4350	0.82	1.98	1.63	1	24	63
0995	755508	RIS-153	1-40S	131-52W	-4345	0.31	2.01	0.63	1	24	63
0996	755907	RIS-154	1-21S	131-31W	-4510	0.11	2.01	0.23	1	24	63
0997	755907	RIS-155	1-25S	131-04W	-4480	0.37	2.01	0.74	1	24	63
0998	755907	RIS-156	1-27S	130-34W	-4580	0.20	2.01	0.40	1	24	63
0999	755907	RIS-157	0-47S	131-42W	-4425	0.39	2.01	0.78	1	24	63
1000	755907	RIS-158	0-18N	132-00W	-4410	0.41	1.96	0.80	1	24	63
1001	755508	RIS-159	2-04N	132-32W	-4305	0.22	1.91	0.42	1	24	63
1002	755900	RIS-160	3-36N	133-00W	-4375	0.00	2.00	-0.01	1	24	63
1003	755907	RIS-161	3-58N	133-09W	-4375	0.10	2.00	0.19	1	24	63
1004	755508	RIS-162	5-38N	133-26W	-4390	0.21	2.08	0.44	1	24	63
1005	765907	RIS-163	7-14N	133-47W	-4410	0.82	2.08	1.7	1	24	63
1006	765508	RIS-164	9-03N	133-40W	-4980	1.08	1.67	1.80	1	24	63
1007	765907	RIS-165	10-57N	133-56W	-4910	0.85	1.67	1.42	1	24	63
1008	765907	RIS-166	12-56N	133-36W	-4810	0.64	1.67	1.07	1	24	63
1009	765508	RIS-167	14-58N	133-42W	-4775	0.74	1.82	1.34	1	24	63
1010	785508	RIS-169	18-15N	133-06W	-5190	1.05	1.91	2.00	1	24	63
1011	785907	RIS-170	19-59N	133-03W	-5060	0.64	1.91	1.23	1	24	63
1012	785907	RIS-172	23-30N	132-43W	-4880	0.61	2.02	1.23	1	24	63
1013	785508	RIS-173	25-19N	132-37W	-4530	0.38	2.13	0.80	1	24	63
1014	785907	RIS-174	27-15N	132-28W	-4815	0.49	2.10	1.02	1	24	63
1015	785508	RIS-175	28-26N	135-54W	-4740	0.77	2.07	1.59	1	24	63
1016	785907	RIS-176	28-29N	134-35W	-4660	0.36	2.00	0.71	1	24	63
1017	785508	RIS-177	28-18N	133-21W	-4385	0.74	1.92	1.43	1	24	63
1018	785907	RIS-178	27-54N	132-37W	-3700	0.51	1.92	0.98	1	24	63
1019	785907	RIS-180	28-10N	131-04W	-4550	1.10	1.96	2.16	1	24	63
1020	785508	RIS-181	28-17N	129-36W	-4740	0.52	2.00	1.05	1	24	63
1021	785907	RIS-182	28-21N	127-59W	-4660	0.97	1.98	1.92	1	24	63
1022	785508	RIS-183	28-27N	126-37W	-4500	0.88	1.96	1.73	1	24	63
1023	785907	RIS-184	28-35N	125-00W	-4445	1.13	1.96	2.22	1	24	63
1024	785508	RIS-185	28-47N	123-37W	-4370	0.94	1.77	1.66	1	24	63
1025	785907	RIS-186	28-56N	122-27W	-4220	1.10	1.96	2.16	1	24	63
1026	785907	RIS-187	29-33N	121-44W	-4005	1.15	2.05	2.36	1	24	63
1027	755108	MP-21	20-48N	159-42W	-4500	0.65	1.79	1.16	1	25	58
1028	755108	MP-32	18-18N	173-23W	-3900	0.35	2.05	0.72	1	25	58
1029	755108	MP-35-2	19-28N	174-35W	-4900	0.62	2.07	1.29	1	25	58
1030	755108	MP-36	16-45N	176-24W	-5040	0.66	1.80	1.19	1	25	58
1031	755108	MP-38	19-02N	177-19W	-4750	0.69	1.57	1.09	1	25	58
1032	785007	STN-1	32-35N	122-30W	-4000	0.67	1.90	1.27	1	25	58
1033	755108	CAP-2B	0-40N	169-17E	-4310	0.76	2.48	1.88	1	25	58

DATA NUMBER	CODE	STATION NAME	LATI-TUDE	LONGI-TUDE	ELE./DEPTH	∇T	K	Q	NO	REF	YR
PACIFIC OCEAN (CONTINUED)											
1034	785108	CAP-5B	9-04S	174-51E	-5000	0.72	1.87	1.35	1	25	58
1035	785108	CAP-9B	18-59S	177-36E	-2700	0.63	2.40	1.51	1	25	58
1036	785108	CAP-10B	21-56S	178-33E	-3900	1.25	2.07	2.58	1	25	58
1037	755108	CAP-31B	17-28S	158-40W	-4880	0.86	1.83	1.58	1	25	58
1038	755108	CAP-33B	12-48S	143-33W	-4300	0.21	1.71	0.36	1	25	58
1039	765108	CAP-40B	14-45S	112-11W	-3020	2.15	2.44	5.25	1	25	58
1040	765108	CAP48B	5-52N	123-55W	-4100	0.73	2.26	1.65	1	25	58
1041	765108	CAP-50B	14-59N	124-12W	-4350	1.24	1.96	2.43	1	25	58
1042	775108	ACA-B5-1	13-08N	91-57W	-6170	0.24	1.92	0.47	1	25	58
1043	785108	ACA-B6	11-55N	91-37W	-3600	0.46	1.67	0.76	1	25	58
1044	785108	ACA-B8	9-49N	93-02W	-3730	0.14	1.76	0.25	1	25	58
1045	765108	ACA-B9	12-14N	98-44W	-3500	0.40	1.72	0.69	1	25	58
1046	765101	ACA-B11	10-52N	105-04W	-3300	1.83	1.95	3.57	1	25	58
1047	765907	ACA-B11B	10-54N	104-25W	-2950	1.40	1.95	2.73	1	25	58
1048	765007	ACA-B13	12-12N	111-04W	-3600	0.48	1.95	0.93	1	25	58
1049	785108	ACA-B13A	20-44N	115-42W	-3910	0.59	2.02	1.19	1	25	58
1050	785108	GUA-P6	25-01N	123-04W	-4300	0.48	2.30	1.11	1	25	58
1051	785108	GUA-P7	24-54N	123-05W	-4200	0.49	2.30	1.13	1	25	58
1052	757508	V18-100	09-42S	136-28W	-4329	0.96	1.72	1.65	1	28	65
1053	757508	V18-101	08-00S	133-30W	-4696	1.24	1.56	1.93	1	28	65
1054	757508	V18-102	07-20S	133-03W	-4477	0.99	1.52	1.50	1	28	65
1055	757508	V18-105	05-19S	130-22W	-4661	0.57	1.65	0.94	1	28	65
1056	757508	V18-107	03-37S	127-41W	-4564	0.23	1.66	0.38	1	28	65
1057	757507	V18-108	02-51S	126-12W	-4612	0.36	1.78	0.59	1	28	65
1139	757507	V18-109	01-06S	124-37W	-4550	0.28	2.16	0.60	1	28	65
1058	767508	V18-110	01-14S	122-55W	-4389	0.48	2.33	1.12	1	28	65
1059	767508	V18-111	01-03N	120-46W	-4371	0.36	2.31	0.83	1	28	65
1060	767907	V18-112	02-12N	119-40W	-4332	1.52	2.30	3.50	1	28	65
1061	767508	V18-113	03-10N	118-28W	-4217	0.71	2.13	1.51	1	28	65
1062	765508	V18-114	04-14N	117-00W	-4161	0.42	2.19	0.82	1	28	65
1063	765508	V18-116	06-23N	113-32W	-4104	0.15	1.85	0.28	1	28	65
1064	765508	V18-118	08-01N	109-18W	-4065	1.92	1.67	3.21	1	28	65
1065	765508	V18-119	08-46N	107-09W	-3488	1.74	1.83	3.18	1	28	65
1066	765508	V18-122	10-16N	103-05W	-3190	1.91	1.55	2.96	1	28	65
1067	765507	V18-125	11-54N	100-44W	-3360	1.22	1.65	2.01	1	28	65
1068	765508	V18-126	12-38N	99-27W	-3426	1.78	1.64	2.62	1	28	65
1069	765907	V18-127	12-54N	98-52W	-3342	0.96	1.80	1.73	1	28	65
1070	765507	V18-128	12-49N	97-47W	-3720	0.42	1.72	0.46	1	28	65
1071	765907	V18-129	13-09N	97-07W	-3590	0.64	1.80	1.15	1	28	65
1072	765500	V18-130	13-19N	96-51W	-2757	5.78	1.85	10.	1	28	65
1073	765508	V18-131	14-31N	96-18W	-3890	1.55	1.91	2.96	1	28	65
1074	765508	V18-134	12-47N	96-17W	-3987	0.76	1.82	1.38	1	28	65
1075	765508	V18-135	08-49N	97-16W	-3793	0.66	1.61	1.06	1	28	65
1076	785508	V18-140	06-37N	88-24W	-3247	1.91	1.60	3.06	1	28	65
1077	785508	V18-141	06-44N	86-30W	-2892	0.56	1.82	1.02	1	28	65
1078	785508	V18-142	06-04N	85-43W	-1819	1.53	1.97	3.01	1	28	65
1079	785507	V18-143	05-42N	85-16W	-1840	1.41	2.15	3.03	1	28	65
1080	785508	V18-144	05-18N	84-45W	-3005	1.40	1.78	2.50	1	28	65
1081	785508	V18-145	05-34N	83-24W	-3064	1.95	1.76	3.43	1	28	65
1082	785907	V18-146	06-06N	82-05W	-3031	1.91	1.80	3.44	1	28	65
1083	785907	V18-148	06-42N	80-42W	-3424	1.70	1.80	3.06	1	28	65
1084	785508	V19-8	07-04N	78-59W	-3345	1.63	1.69	2.75	1	28	65
1085	785508	V19-9	04-56N	78-16W	-3819	2.83	2.16	6.11	1	28	65
1086	785508	V19-10	03-12N	80-08W	-1711	0.91	2.08	1.89	1	28	65

REVIEW OF HEAT FLOW DATA

185

DATA NUMBER	CODE	STATION NAME	LATI-TUDE	LONGI-TUDE	ELE./DEPTH	VT	K	Q	NO	REF	YR
PACIFIC OCEAN (CONTINUED)											
1087	785508	V19-11	02-28N	81-42W	-2398	1.12	1.79	2.00	1	28	65
1088	785508	V19-14	02-22S	84-39W	-2724	0.07	1.78	0.12	1	28	65
1089	785508	V19-15	03-35S	83-56W	-3153	1.17	1.67	1.95	1	28	65
1090	785508	V19-19	11-59S	81-31W	-4749	1.21	1.53	1.85	1	28	65
1091	785508	V19-23	13-13S	92-53W	-3647	0.83	2.19	1.82	1	28	65
1092	765507	V19-26	16-21S	104-48W	-4199	0.78	2.42	1.8	1	28	65
1093	765507	V19-27	17-01S	108-52W	-3624	0.76	2.49	1.9	1	28	65
1094	765907	V19-28	17-01S	110-23W	-3449	0.71	2.1	1.5	1	28	65
1095	765507	V19-29	17-00S	110-51W	-3438	0.58	2.23	1.3	1	28	65
1096	765507	V19-30	17-00S	111-12W	-3537	0.44	2.06	0.9	1	28	65
1097	765907	V19-31	17-01S	111-33W	-3320	0.57	2.1	1.2	1	28	65
1098	765907	V19-32	17-02S	111-53W	-3256	0.67	2.1	1.4	1	28	65
1099	765907	V19-33	17-02S	112-12W	-3184	1.57	2.1	3.3	1	28	65
1100	765907	V19-34	17-01S	112-34W	-2981	1.10	2.1	2.3	1	28	65
1101	765907	V19-35	17-01S	112-55W	-3175	0.81	2.1	1.7	1	28	65
1102	765907	V19-36	17-01S	113-31W	-3056	0.86	2.1	1.8	1	28	65
1103	765907	V19-37	17-02S	113-54W	-2830	1.67	2.1	3.5	1	28	65
1104	765907	V19-38	17-00S	114-11W	-3177	0.76	2.1	1.6	1	28	65
1105	765907	V19-39	17-00S	114-32W	-3139	1.00	2.1	2.1	1	28	65
1106	765907	V19-40	17-00S	114-53W	-3157	0.76	2.1	1.6	1	28	65
1107	765907	V19-41	16-58S	115-12W	-3270	0.24	2.1	0.5	1	28	65
1108	765907	V19-42	16-58S	115-33W	-3300	3.38	2.1	7.1	1	28	65
1109	765907	V19-43	16-58S	115-56W	-3336	1.00	2.1	2.1	1	28	65
1110	765907	V19-44	16-57S	116-18W	-3407	0.71	2.1	1.4	1	28	65
1111	765907	V19-45	16-58S	116-48W	-3374	1.05	2.1	2.2	1	28	65
1112	765907	V19-46	16-59S	117-53W	-3422	0.76	2.1	1.6	1	28	65
1113	765907	V19-48	16-39S	124-23W	-3760	0.43	2.1	0.9	1	28	65
1114	785508	H-4	28-14N	127-38W	-4580	.710	2.07	1.47	1	29	64
1115	785508	H-5	24-46N	134-30W	-4530	.632	1.97	1.25	2	29	64
A	785508	H-5A	24-46N	134-28W	-4530	.452	1.97	0.89	1	29	64
B	786507	H-5B	24-46N	134-31W	-4530	.812	1.97	1.6	1	29	64
1116	785907	H-7	23-03N	137-55W	-5295	.935	2.00	1.87	1	29	64
1117	785508	H-8	23-00N	143-58W	-4850	1.32	2.10	2.78	1	29	64
1118	785907	H-9	22-58N	148-24W	-5470	.726	1.90	1.38	1	29	64
1119	785508	H-10	23-00N	150-38W	-5580	.763	1.86	1.42	1	29	64
1120	756507	H-11	22-59N	152-59W	-5060	.860	1.86	1.6	1	29	64
1121	756900	H-12	22-29N	154-26W	-4390	.758	1.98	1.5	1	29	64
1122	756507	H-15	19-08N	157-20W	-4610	1.04	1.68	1.74	1	29	64
1123	755508	H-17	23-36N	156-07W	-4260	.695	1.87	1.30	1	29	64
1124	755508	H-18	21-56N	154-48W	-4660	.353	2.01	0.71	1	29	64
1125	755508	H-19	23-07N	156-07W	-4260	.742	1.90	1.41	1	29	64
1126	756507	LSDH-68	20-15N	154-13W	-5480	.527	1.67	0.88	1	29	64
1127	755508	LSDH-69	19-59N	151-09W	-5305	.773	1.85	1.43	1	29	64
1128	755508	LSDH-70	20-06N	145-16W	-5410	.774	1.90	1.47	1	29	64
1129	785508	LSDH-71	21-26N	140-23W	-5200	.672	2.04	1.37	1	29	64
1130	785508	LSDH-72	22-12N	138-57W	-5100	.721	2.08	1.50	2	29	64
A	755508	LSDH-72A	22-12N	138-57W	-5100	.688	2.08	1.43	1	29	64
B	755508	LSDH-72B	22-12N	138-57W	-5100	.750	2.08	1.56	1	29	64
1131	755508	LSDH-73	23-10N	130-58W	-4870	.659	2.07	1.36	2	29	64
A	755508	LSDH-73A	23-11N	130-58W	-4860	.816	2.07	1.69	1	29	64
B	755508	LSDH-73B	23-11N	130-58W	-4860	.816	2.07	1.69	1	29	64
1132	755508	LSDH-73C	23-10N	130-57W	-4880	.502	2.07	1.04	1	29	64
1133	785508	LSDH-74	27-30N	125-47W	-4483	.441	2.02	0.89	2	29	64
A	755508	LSDH-74A	27-30N	125-47W	-4450	.396	2.02	0.80	1	29	64
B	755508	LSDH-74B	27-30N	125-47W	-4515	.480	2.02	0.97	1	29	64

DATA NUMBER	CODE	STATION NAME	LATI-TUDE	LONGI-TUDE	ELE./DEPTH	∇T	K	Q	NO	REF	YR
ARCTIC OCEAN											
1143	457508	FL-1	82-30N	156-26W	-3747	.683	2.13	1.45	1	35	65
1144	457508	FL-2	82-12N	156-24W	-3742	.674	2.07	1.40	1	35	65
1145	457508	FL-3	82-31N	156-54W	-3741	.672	2.20	1.48	1	35	65
1146	457508	FL-6	82-42N	158-04W	-3740	.625	2.11	1.32	1	35	65
1147	457508	FL-8	82-39N	157-28W	-3742	.665	2.19	1.46	1	35	65
1148	457508	FL-9	82-46N	156-51W	-3743	.634	2.16	1.37	1	35	65
1149	467508	FL-10	82-57N	155-54W	-3507	.496	2.72	1.35	1	35	65
1150	467508	FL-11	83-00N	156-07W	-3520	.547	2.60	1.42	1	35	65
1151	467508	FL-12	83-06N	156-01W	-3473	.552	2.67	1.47	1	35	65
1152	467508	FL-13	83-08N	156-47W	-3577	.540	2.60	1.40	1	35	65
1153	467508	FL-14	83-08N	157-18W	-3216	.394	2.76	1.09	1	35	65
1154	467508	FL-15	82-60N	158-16W	-3137	.295	2.63	0.78	1	35	65
1155	467508	FL-16	83-01N	159-03W	-2247	.338	2.68	0.91	1	35	65
1156	467508	FL-17	82-60N	159-02W	-2215	.296	2.61	0.77	1	35	65
1157	467508	FL-19	83-03N	162-52W	-3417	.440	2.43	1.07	1	35	65
1158	467508	FL-21	83-01N	163-37W	-3494	.478	2.66	1.27	1	35	65
1159	457508	FL-22	82-53N	163-17W	-3750	.666	2.14	1.43	1	35	65
1160	457508	FL-23	82-39N	162-49W	-3748	.676	2.18	1.47	1	35	65
1161	457508	FL-24	82-22N	162-07W	-3743	.570	2.52	1.44	1	35	65
1162	457508	FL-25	82-26N	160-40W	-3760	.631	2.10	1.32	1	35	65

Acknowledgments. We thank H. W. Menard for supplying his oceanic geological data before publication and F. S. Birch, W. H. Diment, P. Grim, A. H. Lachenbruch, M. G. Langseth, T. S. Lovering, B. V. Marshall, J. Selater, V. Vacquier, R. K. Verma, R. P. Von Herzen, T. Watanabe, and M. Yasui for making their heat flow data available to us in advance of publication. We are indebted to W. Hamilton, W. M. Kaula, G. Oertel, J. Verhoogen, and R. P. Von Herzen for their critical comments and to S. C. Calvert, A. Cox, C. S. Cox, J. W. Elder, D. I. Gough, A. H. Lachenbruch, T. S. Lovering, C. A. Nelson, P. Taylor, and G. A. Thompson for their valuable suggestions. We also thank C. E. Corbato and M. C. Gilbert for advice on geologic maps and S. Mak for processing the data.

This work was supported by grants from the National Aeronautics and Space Administration (NsG 216-62) and by the Computing Facility, University of California, Los Angeles. It was carried out while one of us (Uyeda) held a visiting professorship at the Department of Geophysics, Stanford University, on a National Science Foundation Senior Foreign Scientist Fellowship.

REFERENCES

- Alexander, H. W., *Elements of Mathematical Statistics*, John Wiley & Sons, New York, 1961.
- Anderson, E. M., The loss of heat by conduction from the Earth's crust in Britain, *Proc. Roy. Soc. Edinburgh*, 60, 192-209, 1940.
- Beck, A. E., The measurement of the flow of heat through the crust of the Earth, Ph.D. Thesis, Australian National University, 1956.
- Beck, A. E., Terrestrial flow of heat near Flin Flon, Manitoba, *Nature*, 195, 368-369, 1962.
- Beck, A. E., and Z. Logis, Terrestrial flow of heat in the Brent Crater, *Nature*, 201, 383, 1963.
- Benfield, A. E., Terrestrial heat flow in Great Britain, *Proc. Roy. Soc. London, A*, 173, 428-450, 1939.
- Benfield, A. E., A heat flow value for a well in California, *Am. J. Sci.*, 245, 1-18, 1947.
- Birch, F., Temperature and heat flow in a well near Colorado Springs, *Am. J. Sci.*, 245, 733-753, 1947a.
- Birch, F., Crustal structure and surface heat flow near the Colorado Front Range, *Trans. Am. Geophys. Union*, 28, 792-797, 1947b.
- Birch, F., Flow of heat in the Front Range, Colorado, *Bull. Geol. Soc. Am.*, 61, 567-630, 1950.
- Birch, F., Thermal conductivity, climatic variation, and heat flow near Calumet, Michigan, *Am. J. Sci.*, 252, 1-25, 1954a.
- Birch, F., Heat from radioactivity, in *Nuclear Geology*, edited by H. Faul, pp. 148-174, John Wiley & Sons, New York, 1954b.
- Birch, F., The present state of geothermal investigation, *Geophysics*, 19, 645-659, 1954c.
- Birch, F., Heat flow at Eniwetok Atoll, *Bull. Geol. Soc. Am.*, 67, 941-942, 1956.
- Birch, F., and H. Clark, An estimate of the surface flow of heat in the West Texas Permian Basin, *Am. J. Sci.*, 243A, 69-74, 1945.
- Birch, F. S., Some heat flow measurements in the Atlantic Ocean, M.S. thesis, University of Wisconsin, 1964.
- Bodvarsson, G., Terrestrial heat balance in Iceland, *Timarit Verkfræðingafélags Islands*, 39, 1-8, 1955.

- Bodvarsson, G., and G. P. L. Walker, Crustal drift in Iceland, *Geophys. J.*, 8, 285-300, 1964.
- Boldizsar, T., Terrestrial heat-flow in Hungary, *Nature*, 178, 35, 1956a.
- Boldizsar, T., Terrestrial heat flow in Hungary, *Geofis. Pura Appl.*, 34, 66-70, 1956b.
- Boldizsar, T., Measurement of terrestrial heat flow in the coal mining district of Komlo, *Acta Tech. Acad. Sci. Hung.*, 15, 219-227, 1956c.
- Boldizsar, T., New terrestrial heat flow values from Hungary, *Geofis. Pura Appl.*, 39, 120-125, 1958a.
- Boldizsar, T., Geothermic investigations in the Hungarian plain, *Acta Geol.*, 5, 245-254, 1958b.
- Boldizsar, T., Terrestrial heat flow in the Nagylengyel oilfield, *Publ. Fac. Mining Sopron*, 20, 27-34, 1959.
- Boldizsar, T., Terrestrial heat flow in the natural steam field at Larderello, *Geofis. Pura Appl.*, 56, 115-122, 1963.
- Boldizsar, T., Heat flow in the Hungarian basin, *Nature*, 202, 1278-1280, 1964a.
- Boldizsar, T., Geothermal measurements in the twin shafts of Hosszuheteny, *Acta Tech. Acad. Sci. Hung.*, 47, 293-308, 1964b.
- Boldizsar, T., Terrestrial heat flow in the Carpathians, *J. Geophys. Res.*, 69, 5269-5276, 1964c.
- Boldizsar, T., and J. Gozon, The geothermic flow at Komlo-Zobak (in Russian), *Acta Tech. Acad. Sci. Hung.*, 43, 467-476, 1963.
- Bullard, E. C., Heat flow in South Africa, *Proc. Roy. Soc. London, A*, 173, 474-502, 1939.
- Bullard, E. C., Warmefluss aus der Erdkruste, *Landolt-Bornstein*, 3, 385-386, 1952.
- Bullard, E., The flow of heat through the floor of the Atlantic Ocean, *Proc. Roy. Soc. London, A*, 222, 408-429, 1954.
- Bullard, E. C., The flow of heat through the floor of the ocean, in *The Sea*, edited by M. N. Hill, vol. 3, pp. 218-232, Interscience Publishers, New York, 1963.
- Bullard, E. C., The flow of heat through the Earth, *ICSU Rev. World Sci.*, 6, 78-83, 1964.
- Bullard, E. C., and A. Day, The flow of heat through the floor of the Atlantic Ocean, *Geophys. J.*, 4, 282-292, 1961.
- Bullard, E. C., A. E. Maxwell, and R. Revelle, Heat flow through the deep sea floor, *Advan. Geophys.*, 3, 153-181, 1956.
- Bullard, E. C., and E. R. Niblett, Terrestrial heat flow in England, *Monthly Notices Roy. Astron. Soc., Geophys. Suppl.*, 6, 222-238, 1951.
- Burns, R. E., Sea bottom heat-flow measurements in the Andaman Sea, *J. Geophys. Res.*, 69, 4918-4919, 1964.
- Carte, A. E., Heat flow in the Transvaal and Orange Free State, *Proc. Phys. Soc. B*, 67, 664-672, 1954.
- Chadwick, P., Heat-flow from the Earth at Cambridge, *Nature*, 178, 105-106, 1956.
- Clark, S. P., Jr., Heat flow at Grass Valley, California, *Trans. Am. Geophys. Union*, 38, 239-244, 1957.
- Clark, S. P., Jr., Heat flow in the Austrian Alps, *Geophys. J.*, 6, 45-63, 1961.
- Clark, S. P., Jr., and E. R. Niblett, Terrestrial heat flow in the Swiss Alps, *Monthly Notices Roy. Astron. Soc., Geophys. Suppl.*, 7, 176-195, 1956.
- Clark, S. P., Jr., and A. E. Ringwood, Density distribution and constitution of the mantle, *Rev. Geophys.*, 2, 35-88, 1964.
- Cochran, W. G., *Sampling Techniques*, John Wiley & Sons, New York, 1953.
- Coster, H. P., Terrestrial heat flow in Persia, *Monthly Notices Roy. Astron. Soc., Geophys. Suppl.*, 5, 131-145, 1947.
- Creutzburg, H., *Investigation of the Heat Flow of the Earth in West Germany* (in German), vol. 4, part 3, pp. 73-108, Kali und Steinsalz, Hanover, 1964.
- Crow, E. L., F. A. Davis, and M. W. Maxfield, *Statistical Manual*, Dover Publications, New York, 1960.
- Diment, W. H., Comments on paper by E. A. Lubimova, 'Heat flow in the Ukrainian Shield in relation to recent tectonic movements,' *J. Geophys. Res.*, 70, 2466-2467, 1965.
- Diment, W. H., I. W. Marine, J. Neiheisel, and G. E. Siple, Subsurface temperatures, thermal conductivity, and heat flow near Aiken, South Carolina, *J. Geophys. Res.*, 70, in press, 1965a.
- Diment, W. H., R. Raspet, M. A. Mayhew, and R. W. Werre, Terrestrial heat flow near Alberta, Virginia, *J. Geophys. Res.*, 70, 923-930, 1965b.
- Diment, W. H., and E. C. Robertson, Temperature, thermal conductivity, and heat flow in a drilled hole near Oak Ridge, Tennessee, *J. Geophys. Res.*, 68, 5035-5047, 1963.
- Diment, W. H., and J. D. Weaver, Preliminary analysis of subsurface temperatures and heat flow in a hole near Mayaguez, Puerto Rico, in A study of serpentinite: The AMSOC core hole near Mayaguez, Puerto Rico, *NAS-NRC Pub. 1188*, 75-91, 1964.
- Diment, W. H., and R. W. Werre, Terrestrial heat flow near Washington, D. C., *J. Geophys. Res.*, 69, 2143-2149, 1964.
- Engel, A. E. J., Geologic evolution of North America, *Science*, 140, 143-152, 1963.
- Fisher, R. L., and H. H. Hess, Trenches, in *The Sea*, edited by M. N. Hill, vol. 3, pp. 411-436, Interscience Publishers, New York, 1963.
- Foster, T. D., Heat-flow measurements in the northeast Pacific and in the Bering Sea, *J. Geophys. Res.*, 67, 2991-2993, 1962.
- Garland, G. D., and D. H. Lennox, Heat flow in western Canada, *Geophys. J.*, 6, 245-262, 1962.
- Gerard, R., M. G. Langseth, Jr., and M. Ewing, Thermal gradient measurements in the water and bottom sediment of the western Atlantic, *J. Geophys. Res.*, 67, 785-803, 1962.
- Gough, D. I., Heat flow in the southern Karroo, *Proc. Roy. Soc. London, A*, 272, 207-230, 1963.
- Grim, P., private communication, 1964.
- Guier, W. H., Recent progress in satellite geodesy,

- Johns Hopkins Univ., Appl. Phys. Lab., preprint, 24 pp., 1965.
- Gutenberg, B., *Physics of the Earth's Interior*, pp. 121-148, Academic Press, New York, 1959.
- Heezen, B. C., The deep-sea floor, in *Continental Drift*, edited by S. K. Runcorn, pp. 235-288, Academic Press, New York, 1962.
- Heezen, B. C., and M. Ewing, The mid-oceanic ridge, in *The Sea*, edited by M. N. Hill, vol. 3, pp. 388-410, Interscience Publishers, New York, 1963.
- Heezen, B. C., and H. W. Menard, Topography of the deep-sea floor, in *The Sea*, edited by M. N. Hill, vol. 3, pp. 233-280, Interscience Publishers, New York, 1963.
- Heiskanen, W. A., and F. A. Vening-Meinesz, *The Earth and Its Gravity Field*, McGraw-Hill Book Company, New York, 1958.
- Herrin, E., and S. P. Clark, Jr., Heat flow in West Texas and eastern New Mexico, *Geophysics*, 21, 1087-1099, 1956.
- Hess, H. H., History of ocean basins, in *Petrologic Studies: A Volume to Honor A. F. Buddington*, edited by A. Engel, H. James, and B. Leonard, pp. 599-620, Geological Society of America, New York, 1962.
- Horai, K., Studies of the thermal state of the Earth, 3, Terrestrial heat flow at Hitachi, Ibaraki Prefecture, Japan, *Bull. Earthquake Res. Inst. Tokyo Univ.*, 37, 571-592, 1959.
- Horai, K., Studies of the thermal state of the Earth, 10, Terrestrial heat flow measurements in Tohoku District, Japan, *Bull. Earthquake Res. Inst. Tokyo Univ.*, 41, 137-147, 1963a.
- Horai, K., Studies of the thermal state of the Earth, 11, Terrestrial heat flow measurements in Kyushu District, Japan, *Bull. Earthquake Res. Inst. Tokyo Univ.*, 41, 149-165, 1963b.
- Horai, K., Studies of the thermal state of the Earth, 12, Terrestrial heat flow measurements in Hokkaido District, Japan, *Bull. Earthquake Res. Inst. Tokyo Univ.*, 41, 167-184, 1963c.
- Horai, K., Studies of the thermal state of the Earth, 13, Terrestrial heat flow in Japan (a summary of terrestrial heat flow measurements in Japan up to December, 1962), *Bull. Earthquake Res. Inst.*, 42, 94-132, 1964.
- Horai, K., and S. Uyeda, Terrestrial heat flow in Japan, *Nature*, 199, 364-365, 1963.
- Howard, L. E., and J. H. Sass, Terrestrial heat flow in Australia, *J. Geophys. Res.*, 69, 1617-1625, 1964.
- Izsak, I. G., Tesseral harmonics in the geopotential and corrections to station coordinates, *J. Geophys. Res.*, 69, 2621-2630, 1964.
- Jaeger, J. C., and J. H. Sass, Lees' topographic correction in heat flow and the geothermal flux in Tasmania, *Geofis. Pura Appl.*, 54, 53-63, 1963.
- Joyner, W. B., Heat flow in Pennsylvania and West Virginia, *Geophysics*, 25, 1229-1241, 1960.
- Kaula, W. M., Global harmonic and statistical analysis of gravimetry, *Proc. IAG Symp. on Extrapolation of Gravity Anomalies to Unsurveyed Areas, Columbus, Ohio*, Nov. 16-18, 1964, Publ. Inst. Geod. Photogr. and Cart., in press, 1965.
- Kennedy, G. C., The origin of continents, mountain ranges, and ocean basins, in *Study of the Earth*, edited by J. F. White, pp. 349-362, Prentice-Hall, Englewood Cliffs, 1962.
- Kraskovski, S. A., On the thermal field in Old Shields (English translation), *Izv. Akad. Nauk SSSR, Ser. Geofiz.*, 1961, 247-250, 1961.
- Lachenbruch, A. H., Thermal effects of the ocean on permafrost, *Bull. Geol. Soc. Am.*, 68, 1515-1530, 1957.
- Lachenbruch, A. H., G. W. Greene, and B. V. Marshall, Permafrost and the geothermal regime, in *Bioenvironmental Features of the Ogotoruk Creek Area, Cape Thompson, Alaska*, in press, 1965.
- Lachenbruch, A. H., and B. V. Marshall, Heat flux from the Arctic Ocean Basin, preliminary results (abstract), *Trans. Am. Geophys. Union*, 45, 123, 1964.
- Langseth, M. G., private communication, 1964.
- Langseth, M. G., and P. J. Grim, New heat-flow measurements in the Caribbean and Western Atlantic, *J. Geophys. Res.*, 69, 4916-4917, 1964.
- Langseth, M. G., P. J. Grim, and M. Ewing, Heat flow measurements in the east Pacific Ocean, *J. Geophys. Res.*, 70, 367-380, 1965.
- Law, L. K., W. S. B. Patterson, and K. Whitham, Heat flow determination in the Canadian Arctic Archipelago, *Can. J. Earth Sci.*, 2, 59-71, 1965.
- Lee, W. H. K., Heat flow data analysis, *Rev. Geophys.*, 1, 449-479, 1963.
- Lee, W. H. K., Results of heat flow measurements, in *International Dictionary of Geophysics*, edited by S. K. Runcorn, Pergamon Press, New York, in press, 1965.
- Lee, W. H. K., and G. J. F. MacDonald, The global variation of terrestrial heat flow, *J. Geophys. Res.*, 68, 6481-6492, 1963.
- Leith, T. H., Heat flow at Kirkland Lake, *Trans. Am. Geophys. Union*, 33, 435-443, 1952.
- Le Marné, A. E., and J. H. Sass, Heat flow at Cobar, New South Wales, *J. Geophys. Res.*, 67, 3981-3983, 1962.
- Le Pichon, X., R. E. Houtz, C. L. Drake, and J. E. Nafe, Crustal structure of mid-ocean ridges, 1, Seismic refraction measurements, *J. Geophys. Res.*, 70, 319-339, 1965.
- Lister, C. R. B., Heat flow through the ocean floor, Ph.D. Thesis, Cambridge University, 1962.
- Lister, C. R. B., A close group of heat-flow stations, *J. Geophys. Res.*, 68, 5569-5573, 1963a.
- Lister, C. R. B., Geothermal gradient measurement using a deep sea corer, *Geophys. J.*, 7, 571-583, 1963b.
- Lister, C. R. B., and J. S. Reitzel, Some measurements of heat flow through the floor of the north Atlantic, *J. Geophys. Res.*, 69, 2151-2154, 1964.
- Lotze, F., Die Joly'sche Radioaktivitäts-hypothese zur Erklärung der Gebirgsbildungen, *Nachr. Ges. Wiss. Göttingen Math. Physik Kl.*, 1927, 75-114, 1927.

- Lovering, T. S., Geothermal gradients, recent climatic changes, and rate of sulfide oxidation in the San Manuel District, Arizona, *Econ. Geol.*, **43**, 1-20, 1948.
- Lubimova, E. A., Heat flow in the Ukrainian Shield in relation to recent tectonic movements, *J. Geophys. Res.*, **69**, 5277-5284, 1964.
- Lubimova, E. A., L. M. Lusova, F. V. Firsov, G. N. Starikova, and A. P. Shushpanov, Determination of surface heat flow in Mazesta (USSR), *Ann. Geofis.*, **14**, 157-167, 1961.
- Lubimova, E. A., L. M. Lusova, and F. V. Firsov, Determination of heat flow from the Earth's interior and some results of the measurements, in *Geothermal Research*, edited by E. A. Lubimova (Russian edition), pp. 5-104, USSR Academy of Sciences, Moscow, 1964.
- MacDonald G. J. F., The deep structure of continents, *Science*, **143**, 921-929, 1964.
- Maxwell, A. E., The outflow of heat under the Pacific Ocean, Ph.D. thesis, University of California, 1958.
- Maxwell, A. E., and R. Revelle, Heat flow through the Pacific Ocean Basin, *Publ. Bur. Cent. Seism. Intern. Trav. Sci.*, **19**, 395-405, 1956.
- McBirney, A. R., Conductivity variations and terrestrial heat flow distribution, *J. Geophys. Res.*, **68**, 6323-6329, 1963.
- Menard, H. W., The East Pacific Rise, *Science*, **132**, 1737-1746, 1960.
- Menard, H. W., *Marine Geology of the Pacific*, McGraw-Hill Book Company, New York, 1964.
- Menard, H. W., Sea floor relief and mantle convection, in *Physics and Chemistry of the Earth*, edited by L. H. Ahrens et al., vol. 6, Pergamon Press, London, in press, 1965.
- Misener, A. D., Heat flow and depth of permafrost at Resolute Bay, Cornwallis Island, N.W.T., Canada, *Trans. Am. Geophys. Union*, **36**, 1055-1060, 1955.
- Misener, A. D., L. G. D. Thompson, and R. J. Uffen, Terrestrial heat flow in Ontario and Quebec, *Trans. Am. Geophys. Union*, **32**, 729-738, 1951.
- Mullins, R., and F. B. Hinsley, Measurement of geothermic gradients in boreholes, *Trans. Inst. Mining Engr.*, **117**, 379-393, 1957-1958.
- Nason, R. D., and W. H. K. Lee, Preliminary heat-flow profile across the Atlantic, *Nature*, **196**, 975, 1962.
- Nason, R. D., and W. H. K. Lee, Heat flow measurements in the north Atlantic, Caribbean, and Mediterranean, *J. Geophys. Res.*, **69**, 4875-4883, 1964.
- Newstead, G., and A. Beck, Borehole temperature measuring equipment and the geothermal flux in Tasmania, *Australian J. Phys.*, **6**, 480-489, 1953.
- Ramberg, H., A model for the evolution of continents, oceans and orogens, *Tectonophysics*, **1**, 159-174, 1964.
- Reitzel, J., Some heat-flow measurements in the north Atlantic, *J. Geophys. Res.*, **66**, 2267-2268, 1961a.
- Reitzel, J., Studies of heat flow at sea, Ph.D. thesis, Harvard University, 1961b.
- Reitzel, J., A region of uniform heat flow in the north Atlantic, *J. Geophys. Res.*, **68**, 5191-5196, 1963.
- Revelle, R., and A. E. Maxwell, Heat flow through the floor of the Eastern North Pacific Ocean, *Nature*, **170**, 199-200, 1952.
- Rhea, K., J. Northrop, and R. P. Von Herzen, Heat-flow measurements between North America and the Hawaiian Islands, *Marine Geol.*, **1**, 220-224, 1964.
- Roy, R. F., Heat flow measurements in the United States, Ph.D. thesis, Harvard University, 1963.
- Runcorn, S. K., editor, *Continental Drift*, Academic Press, New York, 1962.
- Sass, J. H., Heat-flow values from the Precambrian shield of Western Australia, *J. Geophys. Res.*, **69**, 299-308, 1964a.
- Sass, J. H., Heat-flow values from eastern Australia, *J. Geophys. Res.*, **69**, 3889-3894, 1964b.
- Sass, J. H., and A. E. LeMarne, Heat flow at Broken Hill, New South Wales, *Geophys. J.*, **7**, 477-489, 1963.
- Saull, V. A., T. H. Clark, R. P. Doig, and R. B. Butler, Terrestrial heat flow in the St. Lawrence lowland of Quebec, *Can. Mining Met. Bull.*, **65**, 63-66, 1962.
- Scheffer, V., The regional values of the geothermic gradient in the area of the Carpathian Basins, *Acta Tech. Acad. Sci. Hung.*, **43**, 429-436, 1963.
- Scheffer, V., The European values of terrestrial heat flow, *Geofis. Meteorol.*, **13**, 99-103, 1964.
- Schmucker, U., Anomalies of geomagnetic variations in the southwestern United States, *J. Geomag. Geoelec.*, **15**, 193-221, 1964.
- Schossler, K., and J. Schwarzlose, Geophysical heat flow measurements (principles and results) (in German), *Freiberger Forschungsh.*, **C**, **75**, *Geophysik*, 120 pp., 1959.
- Sclater, J., private communication, 1964.
- Sisoev, N. N., Geothermal measurement in sediments of the bottom of oceans and seas (in Russian), *Okeanologiya*, **1**, 886-887, 1961.
- Slichter, L. B., Cooling of the Earth, *Bull. Geol. Soc. Am.*, **52**, 561-600, 1941.
- Spicer, H. C., Geothermal gradient at Grass Valley, Calif.: A revision with a note on the flow of heat, *J. Wash. Acad. Sci.*, **31**, 495-501, 1941.
- Spicer, H. C., Observed temperatures in the Earth's crust, *Geol. Soc. Am. Spec. Papers*, **36**, 281-292, 1942.
- Spicer, H. C., Geothermal gradients and heat flow in the Salt Valley anticline, Utah, *Boll. Geofis. Teorica Appl.*, **6**, 263-282, 1964.
- Stenz, E., Deep-well temperatures and geothermal gradient at Ciechocinek, *Geophys. Polon.*, **2**, 159-168, 1954.
- Stocks, T., Für Bodengestalt des Indischen Ozeans, *Erdkunde*, **14**, 161-170, 1960.
- Swartz, J. H., Geothermal measurement on Eni-

- wetok and Bikini Atolls, *Geol. Surv. Prof. Paper* 260-U, 1958.
- Talwani, M., X. Le Pichon, and M. Ewing, Crustal structure of mid-ocean ridges, 2, Computed model from gravity and seismic refraction data, *J. Geophys. Res.*, **70**, 341-352, 1965.
- Uyeda, S., and K. Horai, Studies of the thermal state of the Earth, 6, Terrestrial heat flow at Innai Oil field, Akita Prefecture and at three localities in Kanto-District, Japan, *Bull. Earthquake Res. Inst. Tokyo Univ.*, **38**, 421-436, 1960.
- Uyeda, S., and K. Horai, Studies of the thermal state of the Earth, 7, Terrestrial heat flow measurements in Kanto and Chubu Districts, Japan, *Bull. Earthquake Res. Inst. Tokyo Univ.*, **41**, 83-107, 1963a.
- Uyeda, S., and K. Horai, Studies of the thermal state of the Earth, 8, Terrestrial heat flow measurements in Kinki, Chugoku, and Shikoku Districts, Japan, *Bull. Earthquake Res. Inst. Tokyo Univ.*, **41**, 109-135, 1963b.
- Uyeda, S., and K. Horai, Terrestrial heat flow in Japan, *J. Geophys. Res.*, **69**, 2121-2141, 1964.
- Uyeda, S., K. Horai, M. Yasui, and H. Akamatsu, Heat-flow measurements over the Japan trench, *J. Geophys. Res.*, **67**, 1186-1188, 1962.
- Uyeda, S., T. Yukutake, and I. Tanaoka, Studies of the thermal state of the Earth, 1, Preliminary report of terrestrial heat flow in Japan, *Bull. Earthquake Res. Inst. Tokyo Univ.*, **36**, 251-273, 1958.
- Vacquier, V., and P. T. Taylor, Heat flow and magnetic measurements off Sumatra, in press, 1965.
- Vacquier, V., and R. P. Von Herzen, Evidence for connection between heat flow and the mid-Atlantic ridge magnetic anomaly, *J. Geophys. Res.*, **69**, 1093-1101, 1964.
- Verhoogen, J., Volcanic heat, *Am. J. Sci.*, **244**, 745-771, 1946.
- Verma, R. K., and R. U. M. Rao, Terrestrial heat flow in Kolar gold field, India, *J. Geophys. Res.*, **70**, 1353-1356, 1965.
- Von Herzen, R., Heat-flow values from the south-eastern Pacific, *Nature*, **183**, 882-883, 1959.
- Von Herzen, R. P., Pacific Ocean floor heat flow measurements, their interpretation and geophysical implications, Ph.D. thesis, University of California, 1960.
- Von Herzen, R. P., Geothermal heat flow in the Gulfs of California and Aden, *Science*, **140**, 1207-1208, 1963.
- Von Herzen, R. P., Ocean-floor heat-flow measurements west of the United States and Baja California, *Marine Geol.*, **1**, 225-239, 1964a.
- Von Herzen, R. P., private communication, 1964b.
- Von Herzen, R. P., and M. G. Langseth, Present status of oceanic heat-flow measurements, in *Physics and Chemistry of the Earth*, edited by L. H. Ahrens et al., vol. 6, Pergamon Press, London, in press, 1965.
- Von Herzen, R. P., and A. E. Maxwell, Measurements of heat flow at the preliminary Mohole site off Mexico, *J. Geophys. Res.*, **69**, 741-748, 1964.
- Von Herzen, R. P., and S. Uyeda, Heat flow through the eastern Pacific Ocean floor, *J. Geophys. Res.*, **68**, 4219-4250, 1963.
- Von Herzen, R. P., and V. Vacquier, Heat flow on the Mid-Indian Ocean, *Proc. Roy. Soc. London*, in press, 1965.
- Wang, C., On the distribution of surface heat flows and the second order variations in the external gravitational field, *Res. Space Sci., Spec. Rept.*, **134**, 1-13, Smithsonian Institute Astrophysical Observatory, 1963.
- Wang, C., Figure of the Earth as obtained from satellite data and its geophysical implications, Ph.D. thesis, Harvard University, 1964.
- Wasserburg, G. J., G. J. F. MacDonald, F. Hoyle, and W. A. Fowler, Relative contributions of uranium, thorium, and potassium to heat production in the Earth, *Science*, **143**, 465-467, 1964.
- Wilson, A. F., W. Compston, P. M. Jeffery, and G. H. Riley, Radioactive ages from the Precambrian rocks in Australia, *J. Geol. Soc. Australia*, **6**, 179-195, 1960-1961.
- Yasui, M., K. Horai, S. Uyeda, and H. Akamatsu, Heat flow measurement in the western Pacific during the JEDS-5 and other cruises in 1962 aboard M/S *Ryofu Maru*, *Oceanog. Mag.*, **14**, 147-156, 1963.
- Yasui, M., and T. Watanabe, Studies of the thermal state of the Earth, 16, Terrestrial heat flow in the Japan Sea (I), *Bull. Earthquake Res. Inst. Tokyo Univ.*, **43**, in press, 1965.

(Manuscript received January 25, 1965; revised March 5, 1965.)